Final Programme &
Abstract Book

1st Mars Express
Science Conference

21 - 25 February 2005

European Space Research and Technology Centre
(ESTEC)
Noordwijk, The Netherlands

Scientific Committee

R. Amils, CAB, Madrid (ES)
A. Basilevsky, Vernadsky Inst., Moscow (RU)
J-L. Bertaux, CNRS, Verrieres (FR)
J-P. Bibring, IAS, Orsay (FR)
A. Chicarro, ESA-ESTEC, Noordwijk (NL)
T. Duxbury, JPL, Pasadena (US)
F. Forget, CNRS, Paris (FR)
V. Formisano, IFSI-CNR, Rome (IT)
E. Gibson, JSC, Houston (US)
H. Hayakawa, ISAS-JAXA (JP)
B. Ivanov, Earth Physics Inst., Moscow (RU)
R. Jaumann, DLR, Berlin (DE)
Y. Langevin, IAS, Orsay (FR)
R. Lundin, SISP, Kiruna (SE)
K. Maezawa, ISAS-JAXA (JP)
G. Neukum, Freie Univ., Berlin (DE)
G-G. Ori, Univ. Annunzio, Pescara (IT)
M. Paetzold, Univ. Koeln (DE)
G. Picardi, Univ. Rome (IT)
C. Pillinger, Open Univ. (UK)
J. Plaut, JPL, Pasadena (US)
D. Pullan, Univ. Leicester (UK)
S. Saunders, NASA, Washington DC (US)
Yu. Schkuratov, Univ. Kharkov (UA)

Local Organizing Committee

C. Bingham, Clare.Bingham@rssd.esa.int
C. Villien, Christine.Villien@esa.int
A. Chicarro, Agustin.Chicarro@esa.int
P. Martin, Patrick.Martin@rssd.esa.int

Secretariat

ESA Conference Bureau
P.O.Box 299
2200 AG Noordwijk
The Netherlands

Tel.: +31 71 5655005
Telefax: +31 71 5655658
E-mail: esa.conference.bureau@esa.int

Monday 21 February 2005

08:30 Bus service from Noordwijk to ESTEC

Opening Session

10:00 Welcome, *Gimenez, A.*

10:15 Introduction (video), *Southwood, D.*

10:20 Logistics, *Chicarro, A.*

Session 1: **Historical Perspective**

11:15 The Development of Mars Express (invited)
Schmidt, R.

11:30 Status of Mars Express in Orbit (invited)
Jansen, F.

Session 2: **The Martian Interior & Subsurface**

13:00 Lunch Break

Session 3: **The Martian Geology & Mineralogy (1)**

14:00 Key Issues in Mars Geology & Mineralogy (invited)
Ori, G-G.

Session 4: **Tutorial Evening Session**

20:30 End of Day 1, Bus service to Noordwijk

Tuesday 22 February 2005

08:15 Bus service from Noordwijk to ESTEC

Session 5: **The Martian Geology & Mineralogy (2)**

11 :00 Coffee break

Session 6: **Surface Chemistry from Orbit and In-situ**

Session 7: **The Martian Polar Regions**

Session 8: **Surface Atmosphere Interactions**

18:45 End of oral presentations

Posters on the Mars Interior, Mars Geology & Mineralogy on display all day

18:45 Poster Authors in Attendance; drinks and snacks will be served
20:00 End of Day 2- Bus-service to Noordwijk

Wednesday 23 February 2005

08:15 Bus Service from Noordwijk to ESTEC

Session 9: **The Martian Atmosphere & Climate (1)**

09:00 Key Issues in Mars' Atmosphere & Climate (invited)
Forget, F.

09:15 The Planetary Fourier Spectrometer Results at Mars (invited) 70
Formisano, V.

09:45 Seasonal Variation of Structure of Martian Atmosphere in Polar Regions 71
from LWC PFS Data
Zasova, L.V.; Grassi, D.; Ignatiev, N.I.; Formisano, V.; Giuranna, M.; Khatuntsev, I.V.

10:00 Water Vapour in the Martian Atmosphere from PFS/Mars Express Data 72
Ignatiev, N.; Titov, D.; Formisano, V.; Lellouch, E.; Grassi, D.; Encrenaz, T.; Tschimmel, M.; Fouchet, T. ; Giuranna, M.

10:15 Observations of CO in the Atmosphere of Mars with PFS onboard MarsExpress 73
Billebaud, F.; Lellouch, E.; Fouchet, T.; Encrenaz, T.; Formisano, V.; Grassi, D.; Brillet, J.; Ignatiev, N.; Titov, D.; Giuranna, M.; Maturilli, A.; Atreya, S.

10:30 Martian Morning Atmosphere during Northern Spring from the Planetary 74
Fourier Spectrometer (PFS) Measurements
Grassi, D.; Ignatiev, N.; Zasova, L.V.; Maturilli, A.; Formisano, V.; Giuranna, M.

10:45 The Loss of the Early Martian Atmosphere ans it Water Inventory 75
Lammer, H.

11:00 Coffee Break

11:15 Cloud-Tracked Martian Winds as seen from HST in Opposition 2003 76
Kaydash, V.; Shkuratov, Y.; Kreslavsky, M.; Videen, G.; Wolff, M.; Bell III, J.

11:30 Modeling of the Atmospheric CO_2 Emissions at 4.3μm under non-LTE 77
Conditions as Observed by PFS and OMEGA / Mars Express
Lopez-Valverde, M.A.; Garcia-Comas, M. ; Lopez-Puertas, M.; Lopez-Moreno, J.J.; Formisano, V.; Drossart, P.; Fouchet, T.; Bibring, J-P.

11:45 OMEGA Observations of the Mars Atmosphere 78
Drossart, P.; Combes, M.; Encrenaz, T.; Fouchet, T.; Melchiorri, R.; Bibring, J-P.; Langevin, Y.; Gondet, B.; Forget, F.; Ignatiev, N.; Lopez-Valverde, M. A.; Garcia-Comas, M.

12:00 OMEGA Observations of Atmospheric Water Vapour on Mars 79
Titov, D.; Drossart, P.; Melchiorri, R.; Encrenaz, T.; Fouchet, T.; Combes, M.; Ignatiev, N.; Bibring, J-P.; Erard, S.; Langevin, Y.; Gondet, B.

12:15. Evolution of Seasonal Water Ice Clouds as Observed by OMEGA 80
Gondet, B.

12:30 Atmospheric Sounding of Mras from Ground-based and MEX Observations 81
Encrenaz, T.

12:45 Pressure Variations in OMEGA Observations; Possible Detection of Lee Waves 82
Melchiorri, R.; Drossart, P.; Vintanier, S.; Forget, F.; Altieri, F.; Bibring, J-P.

13:00 Lunch Break

Session 10: **The Martian Atmosphere & Climate (2)**

Thursday 24 February 2005

08:15 Bus service from Noordwijk to ESTEC

Session 11: **The Space Environment of Mars**

Session 12: **The Martian Moons**

13 :00 Lunch Break

Session 13: **Exobiology on Mars**

16:00 Coffee Break

16:15 Discussion of all Exobiology Papers

Session 14: **Upcoming American Mars missions**

17:30 The NASA Mars Exploration Program (invited) 119
McCuistion, D.

17:50 The Mars Reconaissance Orbiter 2005 Mission (invited) 120
Saunders, S.

18 :10 The Mars Surface Laboratory Mission (invited)
Meyer, M.

18:30 Mars Phoenix Mission Landing Site Characterization Studies 121
Arvidson, R.; Deal, K.; Seelos, F.; Bibring, J-P.; Boynton, W.; Golombek, M.; Hays, L; Marlow, J.; Smith, P.; Tamppari, L.; Poulet, F.; Mellon, M.

18:45 End of oral presentations

Poster Session 3 213

Posters on the Space Environment, Martian Moons, Methods, Archiving Instruments & Future Missions on display all day

18:45 Poster Authors in Attendance; drinks and snacks will be served
20:00 End of Day 4- Bus-service to Noordwijk

Friday 25 February 2005

Session 15: **Future Mars Exploration in Europe**

09:00 This session is being co-ordinated by ESA Headquarters and sponsored by three ESA Directorates (Science, Human Space Flight and Technology)

13:00 Lunch Break

Session 16: **Conference Wrap-up and Media Briefing**

14:00 The Mars Express media briefing is being co-ordinated by Science Communications. A summary wrap-up of Mars Express scientific results after one year of operations around Mars will be presented by each PI for the benefit of the conference attendees and the media, and ESA staff.

Public Outreach (Parallel Session)

14:00 Public Outreach and Education Activities (demo's)
Brumfitt, A.

16:00 Adjourn

The History of Mars Exploration

Masson, Ph.L.

Mars has always held a fascination for the mankind. Since the first telescope observations of Mars in the early 1600s, the Red Planet was suspected to be more Earth-like than any other planet. Since the late 1960s when NASA's Mariner 6 and 7 spacecraft flew past the planet and sent back images of a fascinating landscape, our knowledge about Mars has grown dramatically with every subsequent visit by a successful space mission. Just three or four decades of space-based observation have produced more information and knowledge than earlier astronomers with Earth-bound telescopes could have imagined.

The dramatic saga of Mars exploration began in 1960 with the first attempts by USSR to launch two spacecraft which were designed for Mars flybys but failed to reach Earth orbit. Since then, more than 30 space missions to Mars were undertaken by USSR, USA, Europe and Japan. 50 per cent of these missions performed successfully and gathered a great wealth of scientific data. Mariner 9 (1971), Viking Orbiters and Landers (1975), Mars Pathfinder (1996), Mars Global Surveyor (1996), Mars Odyssey (2001), Mars Express (2003), and Mars Exploration Rovers (2003) missions were the major steps of Mars exploration. Their dramatic achievements paved the way for the future international exploration of the Red Planet.

The Mars Express Mission and its Main Scientific Results from Orbit (invited)

Chicarro, A.

The ESA Mars Express mission was successfully launched on 02 June 2003 from Baikonur, Ka-zakhstan, onboard a Russian Soyuz rocket with a Fregat upper stage. The mission comprises an or-biter spacecraft, which has been placed in a polar martian orbit, and the small Beagle-2 lander, due to land in Isidis Planitia but whose fate remains unknown. In addition to global studies of the surface, subsurface and atmosphere of Mars, with an unprecedented spatial and spectral resolution, the unifying theme of the mission is the search for water in its various states everywhere on the planet.

Following the Mars Express spacecraft commissioning in January 2004, most experiments on-board began their own calibration and testing phase already acquiring scientific data. This phase will last until June when all the instruments will start their routine operations. The MARSIS radar anten-nas, however, will only be deployed in early May in order to maximise daylight operations of the other instruments before the pericentre natural drift to the Southern latitudes, which coincides with nightime conditions required for subsurface sounding. Initial science results are summarised below.

The High-Resolution Stereo Colour Imager (HRSC) has shown breathtaking views of the planet, in particular of karstic regions near the Valles Marineris canyon (pointing to liquid water as the erosional agent responsible for modifying tectonic and impact features in the area) and of several large volcanoes (Olympus Mons caldera and glaciation features surrounding Hecates Tholus). The IR Mineralogical Mapping Spectrometer (OMEGA) has provided unprecedented maps of water ice and CO2 ice occurrence in the South pole, showing where the two ices mix and where they do not. The Planetary Fourier Spectrometer (PFS) has confirmed the presence of methane for the first time from or-bit, which would indicate current volcanic activity and/or biological processes. The UV and IR Atmospheric Spectrometer (SPICAM) has provided the first complete vertical profile of CO2 density and temperature, and has simultaneously measured the distribution of water vapour and ozone. The Energetic Neutral Atoms Analyser (ASPERA) has identified the solar wind interaction with the upper atmosphere and has measured the properties of the planetary wind in the Marstail. Finally, the Radio Science Experiment (MaRS) has studied for the first time the surface roughness by pointing the spacecraft high-gain antenna to the Martian surface, which reflects the signal before sending it to Earth. Also, the martian interior has been probed by studying the gravity anomalies affecting the or-bit due to mass variations of the crust.

Water is the unifying theme of the mis sion to be studied by all instruments using different techniques. Geological evidence, such as dry riverbeds, sediments and eroded features, indicates that water has played a major role in the early history of the planet. It is assumed that liquid water was present on the surface of Mars up to about 3.8 billion years (from crater counting relative ages), when the planet had a thicker atmosphere and a warmer climate. Afterwards, the atmosphere became much thinner and the climate much colder, the planet loosing much of its water in the process as liquid water cannot be sustained on the surface under present conditions. Mars Express aims to know why this drastic change occurred and where the water went. A precise inventory of existing water on the planet (in ice or liquid form mostly below ground) is important given its implications on the potential evolution of life on Mars, as the 3.8 b.y. age is precisely when life appeared on our own planet, which harboured similar conditions to Mars at that time. Thus, it is not unreasonable to imagine that life may also have emerged on Mars and possibly survive the intense UV solar radiation by remaining underground. The discovery of methane in the atmosphere could indicate just that or the presence of active volcanism. Fro m previous orbital imagery, volcanoes on Mars were assumed to have been dormant for hundreds of millions of years. This idea needs a fresh look as the implications of currently active volcanism are profound in terms of thermal vents providing niches for potential eco-systems, as well as for the thermal history of the planet with the largest volcanoes in the Solar Sys-tem. Mars Express is already hinting at a quantum leap in our understanding of the planet's geological evolution, to be complemented by the ground truth being provided by the American MER rovers.

The nominal lifetime of the orbiter spacecraft is of one Martian year (687 days), potentially to be extended by another Martian year to complete global coverage and observe all seasons twice. Mars Expre ss is the first European mission to another planet. For details: http://sci.esa.int/marsexpress/

Interior Structure, Activity, and Composition of Mars

Tilman Spohn

DLR Institute of Planetary Research, Berlin, Germany

Conventional wisdom has it that Mars has an iron-rich core (with about 15 weight-% sulfur) of about half a planetary radius, a basaltic crust of about 50km average thickness and a thick lithosphere extending to some hundred kilometres depth. This structure has been derived from geophysical data such as topography and gravity, from SNC meteorite compositional data, meteorites commonly believed to be Martian in origin, and from the results of model calculations of the thermal history of the planet. The Viking-data based geological history of the surface called for early wide-spread volcanism that within the first billion year of evolution retreated to Tharsis and Elysium. The volcanic activity decreased over time to become mostly insignificant in the Amazonian, the most recent stratigraphical epoch. The SNC data further suggest the early formation of three distinct geochemical reservoirs (enriched, depleted, and primordial) that remained separated for the remainder of the planet's evolution. Some have taken this evidence to suggest that the Martian mantle ceased to convect early on.

The new data from the Mars Express mission have cast some doubt as to whether this view of Mars can be upheld or whether we are in for some significant revision of our understanding of the planet. The HRSC data suggest that volcanic activity extended up to the most recent past, a few million years before present. This activity did not occur just locally e.g., at the bottom of Valles Marineris, but included the Tharsis volcanoes. At this point in time this volcanic activity is still to be quantified but the evidence suggests that it was far from being negligible. Moreover, the HRSC data suggest that glacial activity also extended to the recent past, a few 10 million years before present. This glacial activity suggests precipitation in an atmosphere possibly sustained by degassing of the interior in volcanic eruptions. This talk will review our knowledge of Mars and our present models of the planet and confront these with the new evidence.

Origin of Recent Volcanism due to a Global Partial Melt Zone?

Breuer, D.; Schumacher, S.

The detection of recent volcanism (> 2 – 100 Ma) in the areas of Tharsis and Elysium confirms the idea that the edifices are constructed over billion of years and are possibly active until today. The origin of this volcanic activity is unknown and strongly debated. In the past, it has been suggested that a small planet like Mars, which is only about half the size of the Earth, cools very fast associated with a rapid disappearance of its volcanic activity. Recent thermal evolution models show that the interior of a small planet cools more slowly than previously thought if a stagnant lid is located on top of the convecting mantle; the heat transport through that stagnant lid is very inefficient. However, even these models predict that the volcanism may have ceased at least one billion years ago. In the present study, the influence of a temperature- and pressure-dependent thermal conductivity in the mantle as well as the influence of the basaltic Martian crust with varying thermal conductivities will be examined on the thermal and crustal evolution of the planet. We will show that the appropriate choice of the thermal conductivity with 2 W/mK for basaltic material (instead of 4 W/mK, a value usually used in earlier thermal evolution models) can change significantly the thermal evolution of Mars. In particular, the existence of a recent or even present-day global melting zone below the lithosphere is observed. This global melt zone may be the source region for the recent volcanism instead of plume volcanism as suggested by others. Plumes, which originate at the thermal core-mantle boundary layer, disappear rapidly in the first few hundred million years due to the cooling core and are not likely to explain recent activity.

Mars Advanced Radar for Subsurface and Ionosphere Sounding (MARSIS) experiment

ABSTRACT

According to the Mars Express mission , the MARSIS primary *scientific objectives* are to *map the distribution of water, both liquid and solid, in the upper portions of the crust of Mars*. Detection of such reservoirs of water will address key issues in the hydrologic, geologic, climatic and possible biologic evolution of Mars, including the current and past global inventory of water, mechanisms of transport and storage of water.

Three *secondary objectives* are defined for the MARSIS experiment: *subsurface geologic probing, surface characterization,* and *ionosphere sounding*.

The basic principle of operation of the radar sounder MARSIS is based on the electromagnetic wave transmission by the antenna impinging on the top of the Mars surface producing a first reflection echo which propagates backward to the radar. However, thanks to the long wavelengths employed, a significant fraction of the e.m. energy impinging on the surface is transmitted into the crust and propagates downward. Additional reflections, due to the subsurface dielectric discontinuities (due to water or ice), would occur and the relevant echoes would propagate backward through the first layer medium and then to the radar generating further echo signals, much weaker than the front surface signal. As consequence time domain analysis of the strong surface return, eventually after multi-look non-coherent integration, will allow estimation of surface roughness, reflectivity and mean distance, just like in classical pulse limited surface radar altimeters. The presence of weaker signals after the first strong surface return will enable the detection of subsurface interfaces, while the estimation of their time delay from the first surface signal will allow the measurement of the depth of the detected interfaces. Moreover the detection performance will be limited by two main factors, namely the surface clutter echoes and the noise floor entering the receiver. The Mars surface geometric structure has been defined in terms of a large-scale morphology on which a small-scale geometric structure is superimposed, the first one results from gentle geometrical undulations of the surface on a scale of many hundreds to thousands meters whereas the second gives reason of the fast slight variations of the surface height, due to rocks, over an horizontal scale of some tenths of meters. From the statistical point of view, the surface height has been then modeled as a Gaussian random process. Recently attempts have be made to describe the structure of the planets surface by means of fractals, and this appears to be fruitful both as means of describing the surface, and for tying the radar results to physical models of the surface.

In this paper MARSIS performance will be analyzed in terms of sounding depth vs. layer composition and surface structure, taking into account new parameters obtained processing data from MOLA (Mars Orbiter Laser Altimeter) from current Mars Global Surveyor Mission.

The surface clutter and consequently the depth of subsurface interfaces detection will analyzed by considering the new model and new parameters as input, in order to predict the strength of the clutter signal.

The MARSIS Science Mission (invited)

Plaut, J.; Picardi, G.

The Mars Advanced Radar for Subsurface and Ionospheric Sounding (MARSIS) is an integral component of the Mars Express mission. A low-frequency sounding radar was carried on the Russian Mars 96 spacecraft, and in keeping with the concept of re-flying the science experiments lost on that mission, a call for a radar sounder was part of the Announcement of Opportunity for the 2003 ESA Mars Express mission. MARSIS is the only totally new instrument on Mars Express. The instrument was developed, delivered and operated as a joint effort between the Italian Space Agency and the U.S space agency NASA. The MARSIS science mission has been delayed due to concerns about the safety of the antenna deployment.

As a testament to the importance placed on the MARSIS experiment by ESA and the Mars Express project, the mission was designed to include several phases in which the solar illumination was favorable for low frequency penetration through the night side ionosphere. The first of these phases occurred in 2004. The second is from March through May, 2005. This night side phase in 2005 combines favorable illumination, extensive coverage of the northern hemisphere, and high downlink data rates. MARSIS observations during this period will address key questions on Mars polar deposits, the nature of the northern plains (are they remnants of an ocean?), outflow deposits, and the crustal dichotomy boundary. As solar elevation angles increase later in 2005, MARSIS will focus on ionospheric measurements. Early in the proposed extended mission, MARSIS will have the opportunity to observe the southern hemisphere, including the polar region, on the night side.

MARSIS is unique among instruments on Mars Express; it is the only instrument capable of probing the subsurface of Mars to significant depth. The experiment has the potential to revolutionize concepts about water, climate and the geologic evolution of the planet.

The High Resolution Stereo Camera (HRSC) experiment: Results after one year in orbit around Mars

G. Neukum (1) and the HRSC Co-Investigator Team
(1) Freie Universitaet Berlin, Germany

The HRSC experiment is a pushbroom scanning instrument with 9 CCD line detectors mounted in parallel on the focal plane. Its unique feature is the ability to nearly simultaneously obtain imaging data of a specific site at high resolution, with along-track triple stereo, with four colours, and at five different phase angles, thus avoiding any time-dependent variations of the observing conditions. An additional Super-Resolution Channel (HRSC-SRC) - a framing device - will yield nested-in images in the meter-range thus serving as the sharpening eye for detailed photogeologic studies. The spatial resolution from the nominal periapsis altitude of 250 km will be 10 m/pixel for the HRSC proper and 2.3 m/pixel for the HSRC. During the nominal operational lifetime of the mission of 1 Martian year, it will be possible to probably cover nearly 50% of the Martian surface at a spatial resolution of better than 20 m/pixel. The HRSC will make major contributions to the areas of geosciences, atmospheric sciences, photogrammetry/cartography, and spectrophotometry of Mars. The instrument will obtain images containing morphologic and topographic information at high spatial and vertical resolution of unique photogrammetric quality allowing the improvement of the Martian cartographic data base down to scales of 1:50,000. By the time of the conference we will show high-resolution color stereo products (3D and perspective views, digital terrain models, video animations) and first results from the scientific analysis of the data by the joint work of the international co-investigator team. By December 2004, nearly 20% of the martian surface were covered at a resolution of 10 m – 40 m per pixel in stereo and color. The major volcanoes and structures which show the signs of fluvial, hydrothermal, and glacial activity have been investigated in detail, the atmospheric properties over the areas imaged have been analysed, color properties of the surface materials have been assessed and all data have been reduced to geometrically and radiometrically calibrated image swaths, which in most cases have been map – projected and processed to extract digital terrain information. All data obtained over the first six months of the orbital phase have been put in final archival form for distribution to the general community through the ESA and NASA science data archives.

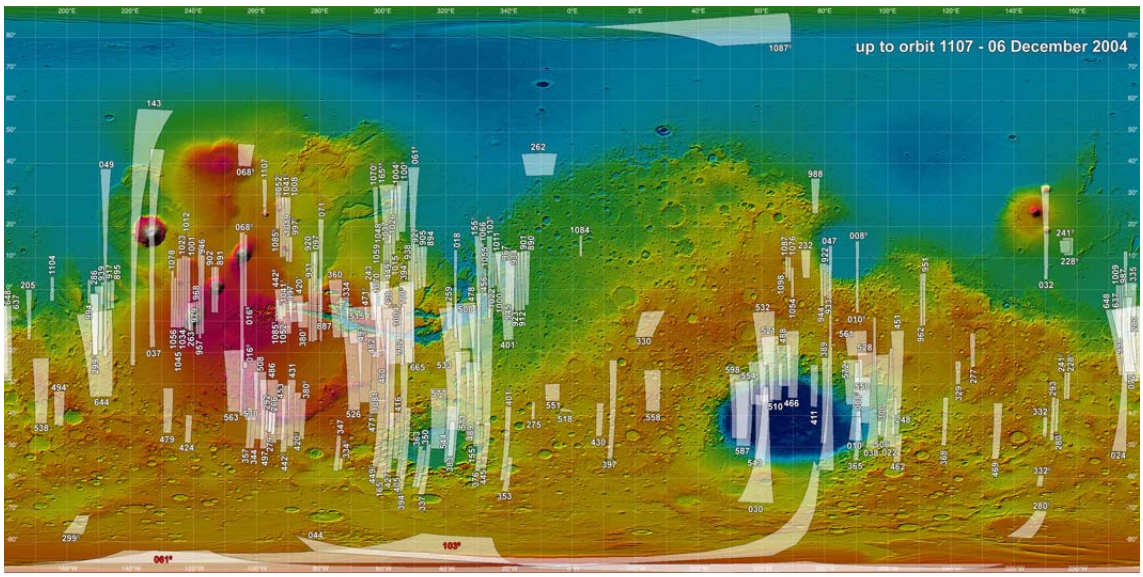

High-Resolution Digital Terrain Models from Mars Express HRSC Data

Gwinner, K.; Scholten, F.; Spiegel, M.; Schmidt, R.; Giese, B.; Oberst, J.; Jaumann, R.; Neukum, G.; HRSC Co-Investigator, Team

The High Resolution Stereo Camera (HRSC) experiment onboard the European Mars Express Mission has been specifically designed for 3D mapping purposes (Neukum et al., 2004). The multiline pushbroom stereo scanner features 5 (panchromatic) stereo and 4 multi-spectral channels, all of which are operated simultaneously. For the stereophotogrammetric analysis of HRSC data, a comprehensive software system comprising procedures for image correlation, object point determination, DTM interpolation and map projection has been developed at DLR. Additional tools, e.g. for orbit adjustment, have been developed within the HRSC Co-Investigator team. Automated procedures using a standard set of processing parameters are applied to derive first photogrammetric products soon after data acquisition and on a regular base, including digital
terrain models (DTM) on a 200 m grid (Scholten et al., 2005).

However, the results of surface reconstruction strongly depend on variable parameters such as ground resolution, data compression, scene contrast, the quality of the orbit and pointing information, and variation of image texture – particularly the occurrence of weakly textured regions
and high optical depths. Hence, the processing by fixed standard processing parameters may often fall short of the expected "optimum" data products.

This contribution focuses on the dedicated stereophotogrammetric analysis of Mars Express HRSC data at full spatial resolution. The work involves experimental procedure setups, including also additional pre-processing steps, and validation studies. Nevertheless, data processing is still based on widely automated processes and can typically be performed within days or few weeks for individual orbits. Validation has been focused on the interior accuracy of the DTM by assessing quantitative quality indicators relevant to the spatial resolution of the derived data product, and by comparison with external data sources. Mars Express HRSC has begun its imaging campaign on January 9, 2004. Since then, we analyzed more than 30 selected orbits at high resolution, and we obtained DTM with mean point accuracy from intersections of up to 10 m (i.e. in the sub-pixel domain) and lateral resolutions of 50-100 m. The role of different factors affecting DTM reconstruction will be discussed.

F. SCHOLTEN, K. GWINNER, T. ROATSCH, K.-D. MATZ, M. WÄHLISCH, B. GIESE, J. OBERST, R. JAUMANN, G. NEUKUM, and the HRSC Co-Investigator Team, Mars Express HRSC Data Processing – Methods and Operational Aspects. Photogrammetric Engineerng and Remote Sensing, submitted, 2005.
NEUKUM, G., JAUMANN, R. AND THE HRSC CO-INVESTIGATOR TEAM, 2004. HRSC: The High Resolution Stereo Camera of Mars Express. ESA Special Publications SP-1240.

Mars Surface Compositional Units: Number and Type Present from Spectrophotometric Analysis using the Mars Express High Resolution Stereo Camera (HRSC)

McCord, T.; Adams, J.; Jaumann, R.; Hansen, G.; Hoffmann, H.; Poulet, F.; Bellucci, G.; Pinet, P.; Neukum, G.

The type and distribution of compositional units on the Mars surface are critical information for understanding the geology and evolution of Mars. We are using multispectral images from the High Resolution Stereo Camera (HRSC) on the Mars Express Mission to identify and map these units. This work requires investigating the spectrophotometric properties of the HRSC data, the calibration of the data, and the effects of the atmosphere on the incident and reflected light from the surface. Four of the HRSC detector channels are equipped with color filters in the wavelength ranges blue (440 ± 45 nm), green (530 ± 45 nm), red (750 ± 20 nm) and infrared (970 ± 45 nm). The remaining channels are equipped with a 675 ± 90 nm filter. According to the push broom technique, all color channels are expose simultaneously but for different look angles and different areas of Mars (associated with the separation of the arrays in the focal plane) as the image of the surface sweeps across the focal plane and the lines of detectors. The basic color mode of the camera is with 2x2 pixel binning, resulting in about 20 m or less spatial resolution. We have explored the color channel calibration and the effects of the atmosphere in an attempt to obtain accurate reflectances for surface materials. We are analyzing selected scenes to detect and describe the fundamental compositional units present and to associate these with geologic features and specific materials. So far, we find only a limited number of compositionally different materials but the color analysis nevertheless yields distinct and unique geological information in most scenes. For example in several scenes we detect only two fundamental compositional units: bright red and dark less-red material, with the dark material present in varying degrees of roughness. In another scene a third, bight and gray compositional unit seems to be present. We are able to map the extent of these units and their mixtures using spectral mixing analysis. Using the assumption that the dark unit is basalt and laboratory spectra of this material allows us to calculation reflectance spectra that appear reasonable for the other units, thus providing a calibration source at the ground level.

Orbital Imaging Photometry and Surface Geologic Processes at Mars

Pinet, P.; Daydou, Y.; Jehl, A.; Baratoux, D.; Vaucher, J.; Chevrel, S.; Cord, A.; Martin, P.; Greeley, R.; Williams, D. Hoekzema, N.; Inada, A.; Kreslavsky, M.; Bondarenko, N.; Raitala, J.; Hoffmann, H.; Roatsch, T.; Gwinner, K.; Scholten, F.; Jaumann, R.; Neukum, G.; and HRSC team,

Access to the particle size and rock abundances from the sub-meter down to the microscale range is critical for the determination of geological processes that affect the planetary surfaces. Indeed, the geological processes controlling the size or being controlled by the size of particles include the volcanic processes, the surface features driven by the fluvial, aeolian or glacial activity, the landslides, the impact cratering and formation and emplacement of ejecta, and, last but not least, coating processes. Reflectance measurements of selected rocks and soils over a wide range of illumination geometries have been obtained by the Viking Lander, Mars Pathfinder and MER multispectral imaging facilities and provide local constraints on the interpretations of the physical and mineralogical nature of the martian surface materials. One of the new investigations from orbit that can be addressed with the multi-angular HRSC dataset generated with the nadir-looking, stereo and photometric channels, is to derive the surface photometric characteristics for mapping the variation of the soil/bedrock physical properties of Mars, and to relate them to the spectroscopic and thermal observations produced by OMEGA, TES and THEMIS instruments. For this purpose, an inverse method optimizing the determination of the global set of Hapke parameters, developed and tested on experimental data produced with a laboratory wide-field multispectral imaging facility, is implemented on the HRSC orbital dataset (see also related talk by Cord et al.). The results produced so far for the Gusev crater, Hecates Tholus, Cerberus and Hesperia Planum regions demonstrate that this orbital information can be used for characterizing the martian surface photometric behavior, as they reveal significant variations of the surface roughness and texture in relation to the various investigated geologic surfaces and agree with the photometric observations available from in situ observations.

Fluvial Erosion and Surface Run-off in the Lybia Montes and Xanthe Terra Regions

R. Jaumann[1], D. Reiss[1], S. Frei[1], F. Scholten[1], K. Gwinner[1], T. Roatsch[1], K.-D. Matz[1], E. Hauber[1], V. Mertens[1], H. Hoffmann[1] J. W. Head[2], H. Hiesinger[2], M. Carr[3], G. Neukum[4], and the HRSC Co-Investigator Team
[1] Institute of Planetary Research, German Aerospace Center (DLR), Berlin, Germany.
[2] Department of Geological Sciences, Brown University, Providence, USA.
[3] U. S. Geological Survey, Menlo Park, USA.
[4] Remote Sensing of the Earth and Planets, Freie Universitaet Berlin, Germany.

Internal structures within valleys like channels, terraces, slip-off and undercut slopes are associated with a fluvial origin. So far only a of such inner structures have been recognized in valleys. In High Resolution Stereo Camera (HRSC) (1) images of the Mars Express Mission a 130 km long inner channel is identified within a 400 km long valley in the Lybia Montes (Figure 1, left). As HRSC provides stereo information we were able to determine the depth of this inner structure and thus we could estimate the discharge in the inner channel. With maximum rates of 10^4 m^3/s it is comparable to terrestrial rivers like the Mississippi and Amazon rivers. Using the valley depth in connection with the ages of the floor, as derived from crater statistics, an average erosion rate of 1µm/a can be deduced. The development of the valley began 3.7 Ga ago and lasted 350 Myr. However it is unclear, whether it was formed continuously or through isolated flooding events. The eroded valley volume amounts to 460 km^3. Taking the maximum discharge it would require 4 x 10^4 days to erode the valley, which would be consistent with a flooding event every 3800 years. On the other side if we expect a continuous discharge over the erosianal period, the water depth of the inner channel has been as low as 1 m. These considerations demonstrate that periodic flooding as well as sustained flow were able to dig the valley within the given erosion time. Also Nanedi Vallis, Xanthe Terra Region, contains a series of features interpreted to have formed by surface flow of water. Slip-off and undercut slopes as develop in the meanders (Figure 1, right) are therefore good examples.

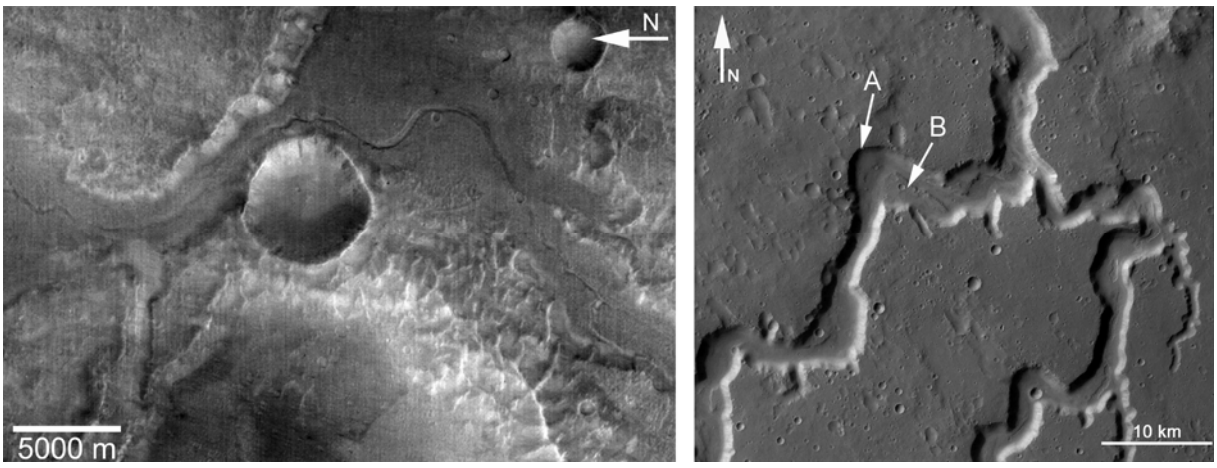

Figure 1. (Left): Part of the inner channel in the Lybia Montes (Orbit 47). **(Right):** Part of the Nanedi Vallis in the Xanthe Terra Region (Orbit 905). Slip-off (B) and undercut slopes (A) are marked.

(1) Neukum, G., Jaumann, R. and the HRSC Co-Investigator Team, 2004. HRSC: The High Resolution Stereo Camera of Mars Express. ESA Special Publications SP-1240.

Evolution of the Holden-Ladon Fluvio-lacustrine System

Marinangeli, L.; Ori, G.G.; Pondrelli, M.; Rossi, A.P.; Di Lorenzo, S.; Baliva, A.;

The Holden-Ladon fluvio-lacustrine system is part of a large outflow channels network of the Margaritifer Sinus region, located on the easternmost side of Valles Marineris. The well-preserved drainage system debouching in the Chryse Planitia basin, suggests a complex evolution of the water-related environments starting from the late Noachian [1, 2]. The largest outflow channels (Uzboi-Ladon-Margaritifer Valles) eroded and deposited material in the ancient multiringed impact basins which include the Ladon crater. A few orders of terraces are well preserved in Ladon Valles, testifying a fluctuation of the water discharge with reactivation of pre-existing valleys. The last phase of fluvial activity of the Ladon Vallis appears to be related to a chaotic process occurring in the lower drainage area. Minor valley networks lies on the higher plateau. This drainage system seems to not be connected to the main Uzboi-Ladon-Margaritifer Valles one. A few impact craters nearby the main channels system show evidence for lacustrine environment, even in geologically recent time. Recent studies on the deposits recognized in the Holden crater [3, 4] suggest that paleolacustrine system may have been active during the Amazonian period as well. The numerous alluvial fans and deltas observed in the Holden-Ladon region from MOC and THEMIS [3, 4, 5] images describe the variety of the fluvial systems occurring over a large span of time. The richness of water-related landforms and the complex interaction of the fluvial and lacustrine activities make the Holden-Ladon area an interesting site to understand the evolution of the water cycle on Mars.
We used the High Resolution Stereo Camera (HRSC) imagery and HRSC-derived Digital Elevation Model (orbits H0478, H0489 and H0511) to study the geological evolution of the Holden-Ladon system and the variation of the depositional environments and their stratigraphic relationships. The detailed topography derived from HRSC data allows a better estimation of the width, depth and terraces height of the channels, resulting in more defined calculations of the water transport, storage and discharge. Crater counting of main geological units will be performed on the HRSC images to understand the overall temporal evolution of the study area.

[1] Grant J.A., 2000. Geology, 28,223-226 [2] Grant J.A. & Parker T.J., 2002. JGR, 107, E9. [3] Pondrelli et al., 2004. Lunar and Planetary Science XXXV, Abstract #1249 [4] Pondrelli et al., JGR, under revision
[5] Malin, M.C. and K.S. Edgett, 2003. Science, 302, 1931-1934.

Mars: Recent and Episodic Volcanic and Glacial Activity as Revealed by the High Resolution Stereo Camera

Neukum, G.; Jaumann, R.; Hoffmann, H.; Hauber, E.; Head, J. W.; Basilevsky, A. T.; Ivanov, B. A.; Werner, S. C.; van Gasselt, S.; Murray, J. B.; McCord, T.; HRSC Co-I, Team

The large-area coverage at 10-20 meters per pixel resolution in colour and 3D of the High-Resolution Stereo Camera Experiment (HRSC) on the ESA Mars Express Mission has made it possible to study the time-stratigraphic relationships of volcanic and glacial structures and processes on Mars in unprecedented detail and give new insight into its geologic evolution. Here we show that calderas on five major volcanoes on Mars have undergone repeated activation and resurfacing during the last 20% of Martian history, with phases of activity as young as 2 Million years, suggesting the volcanoes are potentially still active today. Glacial deposits at the base of the Olympus Mons escarpment show evidence for repeated phases of activity as recently as ~4 Million years ago. Morphological evidence is found that snow/ice deposition on the Olympus construct at elevations of more than 7000 m led to episode(s) of glacial activity at this height. Even now, water ice protected by an insulating layer of dust may be present at high altitudes at Olympus Mons.

Insights into the Evolutionary History of the Martian Volcanic Constructs as Seen by HRSC

Werner, S.C.; Neukum, G.; HRSC Co-Investigator Team

The High-Resolution Stereo Camera experiment on the ESA Mars Express mission has covered most of the major volcanic constructs during its first year in orbit. The ability to image in colour and stereo simultaneously gives us new opportunity to better characterize most of the volcanoes in the Tharsis and Elysium region and some highland volcanoes geomorphologically and chrono-stratigraphically. We have remapped major parts of the volcanic shields and calderas on the basis of the high-resolution (as good as 10 m/pixel) HRSC imagery in colour and stereo and in combination with nested MOC imagery and the Super Resolution Channel (SRC) (as good as 2.5 m/pixel) of the HRSC. We measured crater size-frequencies and determined surface ages the imaged volcanic constructs. They are compared to earlier measurements and discussed. The new crater size-frequency measurements confirm that the large-size Tharsis and Elysium edifices have been constructed over billions of years and are characterized by episodically repeated phases of activity continuing almost to the present. The youngest ages determined by the crater size-frequency measurements are about 2 Ma suggesting that the volcanoes are potentially still active today. A number of caldera floor ages cluster around 150 Ma indicating a relatively recent peak activity period and practically coinciding in age with radiometrically measured crystallization ages of a group of basaltic meteorites from Mars (SNC meteorites). It also has been reconfirmed that the smaller-size volcanic edifices on Tharsis (Tholi and Paterae) were active very early in Mars history (> 3.5 Ga ago) and do not show any strong signs of more recent volcanic activity, although recent volcanic activity has been measured on surrounding plains unit. This appears as an indication that the volcanically active centers shifted geographically.

Erosion by Flowing Martian Lavas: Insights from Modeling Constrained by Mars Express and MER Data

Williams, D.; Greeley, R.; Hauber, E.; Gwinner, K.; Neukum, G.

Low-viscosity lava flows, particularly mafic and ultramafic lavas, have a great potential to degrade underlying substrates by thermo-mechanical erosion during tube- or channel-fed flow emplacement. We used data returned by the recent Mars Exploration Rovers (MER) and Mars Express missions to provide new constraints to evaluate the potential of Martian lavas to form lava tubes and channels by erosion of flowing lava. Recently published geochemical information on basaltic rocks at Gusev Crater from the Mars rover Spirit indicates that the dust- and coating-free interiors of the rocks Adirondack, Humphrey, and Mazatzal are primitive, high-Mg basalts (MgO = 11.6-12.8 wt%: McSween et al., 2004). Liquidus temperatures of silicate liquids of these compositions would have been ~1270?C, and liquid dynamic viscosities would have been ~2.3 Pa s (similar to glycerin), suggesting that Martian lavas had the potential for turbulent flow emplacement. From the HRSC experiment on the Mars Express orbiter comes high-resolution stereo data of Martian lava flows and channels, which provide information on slopes, channel depths, and flow thicknesses at better spatial resolutions than previously available from MOLA data. We have adapted the lava erosion model of Williams et al. (1998) to Martian conditions and used the MER-based compositions to assess the erosional potential of Martian lava flows. Our first test case is a long lava channel on Hecates Tholus in Elysium Planitia, in which HRSC data show is >66 km long (from caldera top to base of volcano), is ~100-30 m deep over the first 20 km with depth decreasing downstream, and was emplaced on slopes between 2-8?. Our computer modeling results suggest turbulent emplacement was likely (assuming initially 7.5 m thick flows), with maximum erosion rates of tens to hundreds cm/day, depending upon the ice content of the basaltic substrate. Eruption durations required to erode the measured depths (20 days to 5 months) are consistent with those of terrestrial basaltic lavas. Further study and application will provide a better understanding of lava emplacement processes on Mars.

Tropical to Mid-Latitude Glaciation in Mars Express HRSC Data

Head, J.; Murray, J.B.; Muller, J-P.; Neukum, G.; Werner, S.; Hauber, E.; Markiewicz, W.; Head III, J.W.; Foing, B.H.; Page, D.; Mitchell, K.L.; Portyankina, G.; HRSC Co-Investigator, Team

Mars Express HRSC (High-Resolution Stereo Camera) image data of debris aprons at the base of massifs in eastern Hellas reveal numerous concentrically ridged lobate and pitted features and related evidence of extremely ice-rich glacier-like viscous flow and sublimation. Together with new evidence for recent ice-rich rock glaciers at the base of the Olympus Mons scarp superposed on larger

Late Amazonian debris-covered piedmont glaciers, these deposits are interpreted as evidence for geologically recent and recurring glacial activity in tropical and mid-latitude regions of Mars during periods of increased spin-axis obliquity when polar ice was mobilized and redeposited in microenvironments at lower latitudes. The data indicate that abundant residual ice likely remains in these deposits and that these records of geologically recent climate changes are accessible to future automated and human surface exploration.

Evidence from the Mars Express High Resolution Stereo Camera for a Frozen Sea Close to Mars' Equator

Murray, J.B.; Muller, J-P.; Neukum, G.; Werner, S.; Hauber, E.; Markiewics, W.; Head II, J.W.; Foing, B.; Page, D.; Mitchell, K.L.; Portyankina, G.; HRSC Co-InvestigatorTeam

The Cerberus Fossae fissures on Mars are the source of both lava and water floods 2-10 million years old . Evidence for resulting lava plains has been identified in eastern Elysium, but seas and lakes from these fissures and previous flooding events were presumed to have evaporated and sublimed away. HRSC images from the ESA Mars Express spacecraft indicate that they may still be there. We have found evidence consistent with a presently-existing frozen body of water, with surface pack-ice,
around +5º latitude and 150º east longitude in southern Elysium. It measures about 800 km x 900 km and averages up to 45 metres deep: similar in size and depth to the North Sea. It has probably been protected from complete sublimation by a surface sublimation lag formed from suspended sediment exposed by early loss of the surface ice. Its age from crater counts is 5 ±2 Ma. If our interpretation is confirmed, this is one place that might preserve evidence of primitive life, if it has ever developed on Mars.

Delta-like deposits in Xanthe Terra as seen by the High Resolution Stereo Camera (HRSC)

Hauber, E.; Gwinner, K.;, Scholten, F.; Reiss, D.; Michael, G.; Frei, S.; Jaumann, R.; Ori, G.G.; Marinangeli, L.; Neukum, G.; and the HRSC Co-Investigator Team

HRSC images taken in MEX orbits 894, 905, and 927 show several fans and delta-like deposits both at the mouths of channels debouching into impact craters and within the valleys incised into the Xanthe Terra highlands. These fluvial and possibly lacustrine deposits may contain important information about the hydrologic and climatic conditions at the time of their formation. We constructed Digital Elevation Models (DEM) and multispectral orthoimages from HRSC stereo data, DEM from Mars Orbiter Laser Altimeter (MOLA) data, and mosaics from Themis-IR nighttime images and Mars Orbiter Camera (MOC) images. We concentrate on two deposits in impact craters (a larger one at 11.75°N/313.16°E and a small one 8.5°N/312°E). The larger deposit is situated at the mouth of Sabrina Vallis. Using HRSC stereo data, we calculated a surface area of ~220 km^2 and a volume of >6 km^3 (as compared to a size of 115 km^2 and a volume of <6 km^3 of the fan-deposit described by *Malin & Edgett* [2003]). MOC images show that at least the lower distal parts of the deposit displays a fine-scale layering at the limit of the MOC image resolution (~few meters per pixel). The smaller deposit is situated inside a small, ~6 km-diameter impact crater. The most distal portion of the Nanedi Valles system breaches the wall of this crater at its southern rim. The deposit is clearly made of material transported down Nanedi Valles. Its surface shows a distributary pattern similar to the system of conduits on terrestrial birdfoot deltas. The small crater also has a possible outlet at its eastern rim, which connects to the Hypanis Valles system in the north. The assemblage of landforms here might be indicative of a standing body of water. From the morphology and morphometry of these deposits (see also *Di Achille et al.*, this conference), and from the analyses of the transport processes inside Nanedi Vallis (see *Jaumann et al.*, this conference), we will try to put constraints on the hydrological and climatic evolution of the Xanthe Terra region.

Erosional Processes, Ages and Stratigraphic Sequence in the Hydraotes Chaos Region, Mars: Observations of the HRSC camera aboard Mars Express

Wagner, R.

Observations of the High Resolution Stereo Camera (HRSC) aboard Mars Express in the Hydraotes Chaos region, eastern Valles Marineris, and of similar areas of so-called chaotic terrain show a wide range of high- and lowland morphologies. Characteristic surface features are small buttes, angular mesas and debris aprons at various elevation levels (Fig. 1, left). Crater size-frequency distributions were measured in order to determine crater retention ages of highlands, mesas, and valley floors. Height measurements were carried out by using HRSC stereo imagery. The major goal of this study is to constrain (1) the main erosional processes, (2) the evolution of the characteristic terrains, and (3) to understand the subsurface structure of the area.

Method: Heights of distinct mesas were obtained by measuring parallaxes between HRSC's high resolution nadir and a stereo channel with a stereo comparator. In order to derive height information, parallax shifts have been calibrated using the MOLA DTM. Crater size-frequency distributions have been measured at three different height levels in Hydraotes Chaos. Then, the cratering chronology model by Hartmann & Neukum [1] was applied in order to obtain absolute cratering model ages.

Results: Heights derived from parallax measurements range from -5100 m (valley floors) to 2500 m (top level). Basaltic plains at the top level (Xanthe Terra) were eroded down to different levels in several episodes over a long period of time, starting 3.7 Ga ago (Fig. 1, right, red data points). and ending sometime between 400 and 200 Ma ago (Fig. 1, right, blue data points). By then, most of the former mesas and highland units were eroded more or less down to the valley floor level. The valley area of Hydraotes Chaos first was formed by the action of flowing water because the morphology as now seen in the images at high resolution, colour and 3D, cannot be explained by any other process. The different mesa levels and erosional epochs showing up in the age measurements suggest that there have been at least three extended episodes of erosional activity.

References: [1] Hartmann, W. K. and Neukum, G. (2001) Sci. Rev. 96, 165-194. [2] Ivanov, B. A. (2001) Sci. Rev. 96, 87-104.

Analysis of regional differences in gully occurrence of the Hale and Bond craters on Mars

D. Reiss[1], K. Stephan[1], S. van Gasselt[2], E. Hauber[1], R. Jaumann[1], G. Neukum[2] and the HRSC Co-Investigator Team

[1]Institute of Planetary Science, German Aerospace Center, Berlin, Germany
[2]Remote Sensing of the Earth and Planets, Freie Universitaet, Berlin, Germany

Gullies on Mars indicate liquid water in the recent past. The strong latitude-dependence suggests a climatic control on their formation. However, in some regions many gullies occur in one crater and do not in another crater nearby. This is the case for the Hale (gullies) and Bond (no gullies) crater, respectively. These regional differences have been interpreted as an argument against climatically controlled deposition and melting of volatiles. The formation of gullies on Earth depends on rainfall and/or melting of snow as well as on several parameters such as (1) the presence of steep slopes, (2) sufficient amounts of fines/debris and (3) low or no vegetation. We investigated the Hale/Bond region (325°E and 35°S) with *High Resolution Stereo Camera (HRSC)* images, which covers this region with a resolution of ~25 m/pxl in the nadir channel, 100 m/pxl in color (blue, green, red, near infrared) and HRSC stereo data (100 m/pxl). The color images and derived products show regional variances in surface reflectance, which correlate well with differences in the thermophysical surface properties derived from *nighttime THEMIS-IR* images. The gully regions in the Hale crater show low nighttime temperatures (unconsolidated material), while higher temperature slopes (consolidated material) occur in the Bond Crater. These different surface properties of unconsolidated (gullies) and consolidated (no gullies) material is confirmed by the morphology as analyzed in *MOC*–images. The morphology indicates debris slopes in the Hale crater in contrast to Bond crater where the material seems to consist of cemented mantle deposits. Furthermore, the Bond crater is highly degraded and the rim slopes derived from *HRSC stereo data* vary between 10° to 20° in contrast to the more pristine Hale crater with slopes in the range of 20° to 30°. We conclude that the occurrence of gullies in the Hale/Bond region depends on the distribution of unconsolidated material and/or steep slopes. The regional and local gully distribution is likely to vary because of differences in topography and surface material composition.

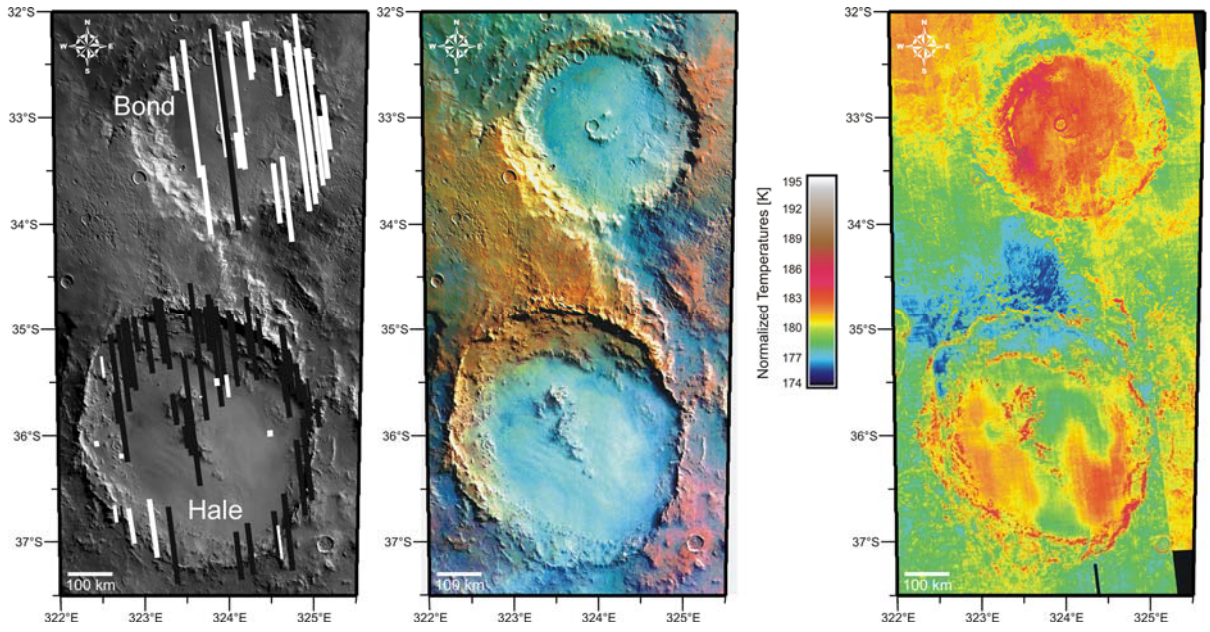

Figure 1: **(left):** HRSC mosaic of Orbit 511 and 533 with MOC-NA footprints. Black filled MOC-NA show gullies and white filled show no gullies. (middle) HSV saturation stretch of the blue, green and infrared channel of HRSC orbits 511 and 533. **(right):** THEMIS-IR Band 9 nighttime image mosaic with normalized temperatures. Blue colours indicate fine grained material and red colours consolidated material.

Lobate Debris Aprons of the Southern Hemisphere of Mars

van Gasselt, S.; Hauber, E.; Reiss, D.; Scholten, F.; Neukum, G.; HRSC Co-I, Team

Lobate Debris Aprons (LDA) have been observed on Mars at the northern hemispheric dichotomy boundary and in the vicinity of the large southern hemispheric impact basins Argyre and Hellas Planitiae [Squyres, 1978]. Their formation has been attributed to the creep and viscous deformation of ice and rock material,similar to terrestrial rock glaciers [Sqyures, 1978, 1979]. Thorough work on the distribution and inventory of Argyre Planitia LDAs is missing although the LDAs of the dichotomy boundary and the Hellas impact basin have been analysed in detail by a variety of authors.The Hellas and Argyre Planitiae populations of LDA and similar landforms, such as concentric crater fill and lineated valley fill, have been analyzed with a focus on the textural properties as well as the stratigraphic relationships as identified in High Resolution Stereo Camera (HRSC) and Mars Orbiter Camera (MOC) image data.LDA landforms are considered to be composed of ice and rock material as characteristic surface features such as flow lobes, ridge and furrow patterns as well as a highly convex-shaped cross profile have been identifed in early orbiter imagery.HRSC image data show, however, varieties of landforms which are connected to a variety of mass movement processes, such as debris flows, rock and debris avalanches, lobate flows of unknown origin as well as dry high-velocity landslides.
It is suggested, that the source of LDA material is connected to these different input systems and that LDAs must be considered as large accumulation zones of a variety of smaller-scaled slope processes.
The textural differences of individual LDA units as identified in MOC imagery has been nested into HRSC context data in order to compile maps of the geomorphologic and geologic inventory of selected regions.High-resolution digital terrain models of selected areas with a resolution of 50 metres per pixel have been utilized to determine flow thicknesses and basic physical properties of the debris apron contruct.
The distribution of LDA in the circum-Argyre basin compare well with the eastern Hellas debris aprons in terms of sizes, shape as well as the morphologic inventory of individual mass movement features. As far as possible, first results concerning the relative and absolute ages will be presented during the meeting.

References: S. Squyres, Martian fretted terrain - Flow of erosional debris, Icarus, 34, 1978; Squyres, The distribution of lobate debris aprons and similar flows on Mars, J. Geophys.
Res., 84, 1979.

Water-related Processes of Martian Impact Crater Ejecta Blanket Emplacement: New Results from the Mars Express High Resolution Stereo Camera

Komatsu, G.; Ori, G.G.; Di Lorenzo, S.

We utilized images and stereo-derived topographic data acquired by the HRSC (High Resolution Stereo Camera) onboard Mars Express in order to study geology of Martian impact crater ejecta blankets. We examined more than a dozen impact craters with possible evidence for water involvement during the formation by constructing 3-dimensional views and deriving various parameters. The high precisions of the HRSC data set ensure quantitative analyses of such impact craters better than previously possible. The ejecta geomorphology and morphometric properties indicate the origin as water-related ejecta emplacement and liquefaction/fluidization. The ejecta radius has a strong correlation with crater cavity radius and volume, implying that the ejecta formation is primarily a function of impact energy. However, the thickness of ejecta appears to be a function of rim height, implying a gravity-driven process that contributed to the ejecta material movement together with the excavation-derived momentum.

Geological Mapping and Structural Analysis of Gusev Area: a Record of 4 Ga of Martian History

Zegers, T.; Foing, B.; van Kan, M.; Pischel, R.; Martin, P.; Jaumann, R.; Pinet, P.; Jehl, A.; Werner, S.; Neukum, G.; HRSC Co-Investigator, Team

The Gusev crater and surrounding terrains contain the geological record of Martian processes from approximately 3.9 Ga to present. This record includes the Noachian evolution of the Martian Highlands, fluvial processes in the Hesperian, and most recent aeolian processes.
Using Themis IR and visual images, combined with narrow angle MOC images and recent HRSC data, we mapped the wider region of the Gusev crater (172° E to 179° E by 10° S to 18° S), focussing on the geological units and their geometrical relationships.
In addition to the image data, the stereo data from HRSC were used to study the three dimensional geometry of units and structures. To this end a number of geological cross sections were constructed, based on HRSC digital elevation models. The cross-section were used to establish the thickness of various geological units and their relative age relationship.

The geological map and geometrical analysis show that the Gusev area can be divided into three terrains formed at different times by different processes : The Noachian Gusev Highlands, the Gusev crater fill units, and the units situated north of the dichotomy boundary.
The highlands consist mainly of a thick unit called the Gusev Highland Formation. This unit most likely consists of a mix of mafic volcanic rocks and impact ejecta. The oldest unit found in the highlands occurs in areas of highest topography. These 'mountains' consist of tilted rock units, which have been eroded on the flanks prior to deposition of the blanketing Gusev Highland Formation. The process by which these units were tilted remains uncertain, but it may be an indication of a more dynamic early evolution of Mars.
In Gusev crater 5 different units have been mapped. From Spirit we know that what has been mapped as Gusev Crivitz Formation is not, as anticipated, a sedimentary unit, but a picritic (high-Mg) basalt. From our geological cross sections it appears that the sediments transported to Gusev crater by Ma'adim Vallis are covered by the Gusev Crivitz Formation.
The northern part of Gusev area consists of several thick units, which have been locally deposited. Apart from the volcanic shield deposits of Apollinaris Patera it is not yet clear where these units originated and what their composition is.

The surface ages of the mapped units have been determined by crater counts, placing absolute time constraints on the relative timescale from superposition and geometrical analysis.

Geoscientific mapping using HRSC and other Martian datasets

Ori G.G.[1], A.P. Rossi[1], S. Di Lorenzo[1], G. Di Achille[1], L. Marinangeli[1], Neukum G.[2] and the HRSC Co-Investigator Team

[1]International Research School of Planetary Sciences (ggori@irsps.unich.it), Università d'Annunzio, Italy, [2]Freie Universität Berlin, Germany.

The interpretation of planetary geoscientific data is nowadays based on the combination and fusion of several data sets and their integration in a single set of data. The creation of coregistered digital thematic maps in a GIS environment and the development of visualizations procedures for the integrated analysis of Mars Express data are critical issues to enhance the overall scientific return and, particularly, the geological mapping which is one of the most important outcomes of planetary missions. The advantages of a GIS approach is to have several information from different planetary missions visualized simultaneously with the same spatial reference system where multiple scalar (raster) and vector attributes define the digital map.

A demonstrative Planetary Geosciences Information System for Mars (MEGIS) has been built up at IRSPS using data from Viking, Mars Global Surveyor and Mars Odyssey missions under an Italian Space Agency (ASI) grant. The ingestion of the HRSC images and topography in this GIS system provides a unique opportunity to perform comprehensive study with multi-resolution quality the surface of a planet. A few examples of geological mapping based on this digital system of Eastern Hellas, Ares Vallis and Kasei Vallis will be shown.

Mars Express Science Planning and Operations and their Accuracy

Pischel, R.; Hoffmann, H.; Companys, V.; Rabenau, E.; Zegers, T.; Ricketts, M.; Lauer, M.; Roatsch, T.

The planning of science operations for the ESA Mars Express puts challenging demands in terms of complexity, reliability, and flexibility. Since the beginning of payload operations in January 2004 the Mars Express spacecraft has been orbiting around Mars more than 1200 times conducting more than 500 science observations.

The paper describes the complex process of science planning for Mars Express and gives an overview about one year of science operations. The planning process is explained using the example of the High Resolution Stereo Camera (HRSC). The paper shows in particular, how observations are planned with emphasis on the accuracy of the information used in the planning cycle. It describes which "targeting" accuracy has been actually achieved by analyzing HRSC images.

In addition, the implementation of key planning elements as the "frozen orbit" concept will be assessed. This concept warrants a highly accurate long-term orbit predict and thus a detailed long- to mid-term planning cycle. Other driving elements for the planning process like the link between mid-term planning and the overall mission science objectives will also be discussed.

Accessing and Using Mars Express SPICE Observation Geometry Data

Acton, C.

The Mars Express Project Science Team of the Research and Scientific Support Department of ESA, located at ESTEC, offeres MEX science teams two means for determining the observation geometry needed to analyze instrument data, and to readily correlate science data obtained from multiple instruments. In particular, NASA's "SPICE" ancillary information system is offered as an ancillary information system that is secondary to the products provided by ESA's Flight Dynamics Facility, located in Darmstadt, Germany.

The SPICE system comprises a suite of elemental data files, and a software library containing modules needed to read those data files and to compute many derived quantities needed in scientific research. The data files provide spacecraft location and orientation, Mars location, size, shape and orientation, instrument mounting alignment and orientation, reference frame specifications, and time conversion information.

The SPICE data and allied software are portable to all popular computing environments. Dissemination of these is not restricted under U.S. export regulations.

SPICE is used on NASA's mars missions as well, so scientists can use a single means of determining and comparing positions, orientations and related geometric aspects of internationally available mars science data sets.

As the SPICE information system offers a great deal of capability, there is consequently a good deal to learn in order that a scientist can best utilize its capabilities. This paper provides an introduction to and starting point for those interested in learning how to obtain and fully utilize the Mars Express SPICE ancillary data.

This paper will be supplemented with demonstration of SPICE data access and usage for MEX and other mars missions during the half-day MEX archive access demonstration associated with the conference.

Science Data Archive Demonstration

J. Zender (1), D. Heather (1), J. Diaz del Rio (1), P.D. Martin (1), I. Ortiz (2), J. Dowson (2), A. Venet (2), C. Arviset (2)

1) European Space Agency, ESTEC, Keplerlaan 1, 2201 AZ Noordwijk, The Netherlands, Joe.Zender@rssd.esa.int
(2) European Space Agency, ESAC, Villafranca del Castillo, 28080 Madrid, Spain

The scientific data from ESA's planetary missions are made accessible to the world-wide scientific community via the Planetary Science Archive (PSA). The PSA consists of web-based services incorporating search, preview, download, notification and shopping basket functionality. Scientific data from all Mars Express instruments as well as auxiliary data sets are distributed via the PSA to the scientific community. The demonstration will introduce the concept of the different services offered on the PSA. Several search strategies will be shown supplemented by a full cycle from data query to data download.
Individual instrument query panels, geometry query panels and data set query panels will be discussed in detail and their combined usage will be shown.
The PSA contains data sets and products conform to the PDS Standard. This is reflected in the user interface, especially in the data download options. The PSA combines latest software technologies with the advantages of a well-known standard ensuring the preservation of engineering and scientific data from planetary missions on the long-term.

Mars Surface Diversity as indicated by the OMEGA Observations

Bibring, J.-P.

The OMEGA observations acquired after one terrestrial year have enabled to map most units from medium (2 to 4 km) to high resolution (< 500 m), at all latitudes. We have thus identified the major constituents of both perennial polar caps, the mafic rocks of the cratered terrains, the hydrated minerals in a few areas, including salts. We will discuss the overall picture of the Mars evolution we can derive from the identifications and mappings obtained so far, and present the future observations we plan to conduct within the nominal - and possibly extended - Mars Express mission.

OMEGA Analysis of Mafic and Hydrated Minerals Associated with the Syrtis Major Region of Mars

Mustard, J.; Gendrin, A.; Poulet, F.; Bibring, J.P.; Langevin, Y.; Erard, S.; Pelkey, S.; Milliken, R.; Kanner, L.

Syrtis Major is a large, Hesperian-aged low-relief volcanic region on the western rim of the Isidis Basin along the dichotomy boundary between the southern highlands and the northern plains. It has long been studied with remotely sensed visible-near infrared reflectance and thermal emission data because of the good exposure of volcanic materials. OMEGA observations of this region range in spatial resolution from several hundred meters to 4.8 km/pixel. The volcanic plains are dominated by a two-pyroxene composition, with high-Ca pyroxene apparently more abundant than low-Ca pyroxene (LCP). The central caldera complex exhibits more mineralogic diversity, with the presence of olivine-bearing volcanics. Outcrops of nearly pure LCP and olivine are observed in the Noachian-aged regions to the north and east of Syrtis Major.

In this same region, hydrated minerals are observed with clays positively identified. Within the boundaries of Syrtis Major some older knobs and massifs as well as interior deposits and ejecta blankets of several large impact craters that predate the volcanism exhibit hydrated minerals. The history of Syrtis Major has involved the interaction of volcanism with hydrated minerals and perhaps ancient ice deposits.

Identification and mapping of sulfates by OMEGA/Mars Express

Gendrin, A.; Mangold, N.; Bibring, J-P.; Langevin, Y.; Gondet, B.; Poulet, F.; Quantin, C.; Bonello, G.; Mustard, J. ; Arvidson, R.; Le Mouelic, S.; and the, OMEGA team

The imaging spectrometer OMEGA onboard Mars Express allowed for the first timemthe identification of several hydrated sulfate minerals associated with layered deposits. The mineral kieserite (monohydrated magnesium sulfate) was unambiguously identified. A polyhydrated sulfate signature is also present. Finally, a third type of spectrum is interpreted to be due to gypsum. The entire dataset has been searched, which covers almost 50% of the surface, and sulfate deposits were identified inside Valles Marineris, the chaotic terrains, and Terra Meridiani. Numerous deposits are found in Candor, Melas, Hebes, Juventae and Capri chasma. In addition, Iani and Aram chaos have spectra indicative of a very diverse sulfate mineralogy. Finally, kieserite and polyhydrated sulfates are inferred to be present in the etched terrains of Terra Meridiani. We will discuss the location and main spectral characteristics of each of these deposits.

Variation of the 3 Micron Absorption Feature on Mars

Poulet, F.; Mustard, J.; Langevin, Y.; Bibring, J.-P.; Gendrin, A.; Gondet, B.; Gomez, C.

Characteristic water and hydroxyl absorptions in the 1.9, 2.2-2.5, and3 µm ranges have been detected on Mars by OMEGA. Laboratory measurementshave shown that these bands depend on the composition, grain size. OnMars, a dependence on other surface physical properties (thermal inertia) aswell as water in exchange with the atmopshere is also expected.Using a similar method defined by Calvin et al. (1997) to measure the 3 µm band,we will study the variation of this broad water band at different locationson Mars and at different time. The relation with albedo, temperature and1.9 µm feature will be also presented.

A New View of the Geology of Valles Marineris Interior Deposits with OMEGA Spectral Data

Mangold, N.; Gendrin, A.; Quantin, C.; Poulet, F.; Bibring, J-P.; Gondet, B.; Mustard, J.F

Valles Marineris interior deposits were the subject of intense debates since Viking data shown that these deposits are layered. The composition of these layers is important to understand the past martian environment despite their origin is still unknown among eolian, volcanic or fluviolacustrine processes. OMEGA data gives new insights in the understanding of the evolution of Valles Marineris with the identification of Magnesium or Calcium sulphates over the deposits of Hebes, Ius, Melas, Candor and Juventae Chasmata. Sulphates tell us that water was involved in the formation or in the weathering of these layered deposits. We show preliminary results of a detailed correlation between the spectral data and the geometry of layers from visible images and topography.

New Insights on Geology of Melas Chasma from OMEGA Data

Quantin, C.; Gendrin, A.; Mangold, N.; Bibring, J-P.; Poulet, F.; Allemand, P.; Delacourt, C.; Omega Team

Melas Chasma, the central part of Valles Marineris displays many sedimentary landforms like interior layered deposits or paleo-valley networks. The area is covered by multiple remote sensing data from MGS, Mars Odyssey and more recently from Mars Express. The different stripes acquired by OMEGA/MarsExpress instrument until today allow to map the mineralogy of Melas Chasma. Here, we report a geological study of the spectral signatures revealed by OMEGA data in Melas Chasma. In particular, spectrums of sulfates have been identified in this area. We studied their spatial distribution and their morphological signature. The mineralogy determined from OMEGA data provides new insights into the sedimentary history in Valles Marineris.

Hydrated Minerals in the Circumpolar Regions: Implications for Aqueous Alteration Episodes

Langevin, Y.; Poulet, F.; Bibring, J-P.; Gondet, B.

The OMEGA VIS/IR imaging spectrometer has observed the North polar regions of Mars at resolutions of a few km since science operations resumed after the conjunction in late September. The 3 µm OH band is observed with varying intensity for all Mars terrains. It is strongest in bright regions covered by dust deposits. By contrast, the 1.9 µm OH overtone feature, which is characteristic of hydrated minerals (clays, sulfates, carbonates), had until September only be observed in a small fraction of ancient terrains, with interesting implications for episodes of aqueous alteration very early in the geological history of the planet. We will present evidence that such hydration features are also found in circumpolar regions. We will discuss the possible interpretation in terms of the climatic history of the planet.

Mars Express OMEGA Observations over Meridiani Planum

Arvidson, R.; Gendrin, A.; Bibring, J-P.; Poulet, F.; Langevin, Y.; Wolff, M.; Mustard, J.; Morris, R.

The OMEGA hyperspectral imager (0.35 to 5.1 micrometers) covered the hematite-bearing plains and underlying etched terrains of Meridiani Planum during orbits 171, 314, 430, 485, 518, and 529, with spatial resolutions ranging from several hundred meters to approximately a kilometer. In addition, the Opportunity rover acquired Pancam and Mini-TES observations of the surface and atmosphere during the times when OMEGA acquired its data. Using a radiative transfer modeling approach (DISORT) that combines surface and orbital observations we extracted surface reflectance spectra from OMEGA for the approximately 864,000 square kilometers surrounding the Opportunity site. OMEGA spectra show significant variation within the hematite-bearing plains, in part associated with a 1 micrometer feature that deepens from northwest to southeast and assigned to ferrous silicates. The etched terrains that underlie the hematite bearing plains show significant spectral variability that is associated with stratigraphic position within the 300 m thick stack of layered materials. Significant features include a prominent 1.92 micrometer absorption in some deposits (associated with hydrated phases and/or molecular water) and absorptions in the 2.2 to 2.5 micrometer region associated with cation-hydroxl vibrations. Finally, the 3 micrometer water band also shows high absorption values for the etched terrain materials (as compared to the underlying cratered terrain), consistent with an abundance of hydrated phases and/or molecular water in the layered deposits. We are currently exploring direct evidence for hydrated sulfate minerals using cation-hydroxl features from 1 to 2.5 micrometers and 3 to 5 micrometer features directly related to vibrational modes of sulfate ions. OMEGA data, calibrated using ground truth observations from Opportunity, will allow us to extend to rover-based observations to regional scales and thus provide the overall geologic context and environments of deposition for the sedimentary rocks explored by the rover since January 2004.

Mars Photometry from OMEGA Observations

Erard, S. ; Pinet, P.; Daydou, Y.; Drossart, P.; Melchiorri, R.; Fouchet, T.; Forni, O.; Bellucci, G.; Altieri, F.; Bibring, J-P.; Langevin, Y.; OMEGA Science team

The wide diversity of viewing geometries available in the OMEGA data set allows to study photometric properties of both the surface and the atmosphere of Mars. Selected observations are used to constrain a previous spectro-photometric model of Mars (Erard, 2001), which in turn will permit to correct these geometrical variations in the data set, and to evidence specific behaviors. Key issues are related to: 1) Absolute accuracy of the measured flux, from comparison with older data (e.g. Klassen and Bell 2003); 2) Contribution from aerosols scattering to the spectra; 3) First derivation of surface reflectance in the 3-5 µm range, and systematics of thermal/reflected flux combination; 4) Surface properties inferred from EPF sequences (see also Pinet et al. in this conference).

Science Results from Mars Odyssey

J. J. Plaut
Jet Propulsion Laboratory, 4800 Oak Grove Dr., Pasadena, CA 91109.
plaut@jpl.nasa.gov

The Mars Odyssey mission has collected science data for over one Mars year. Observations are obtained by three science instrument packages: (1) the Gamma Ray Spectrometer suite (GRS), which is composed of the Gamma Sensor Subsystem (GSS), the Neutron Spectrometer (NS) and the High Energy Neutron Detector (HEND), (2) the Thermal Emission Imaging System (THEMIS), and (3) the Martian Radiation Environment Experiment (MARIE). Currently, two of the three science investigations are returning data. The MARIE instrument was disabled during intense solar activity in October of 2003 and is in a powered off state. The Odyssey mission has added significantly to our understanding of Mars. Gamma and neutron observations of the high latitudes have been used to identify water-ice-rich soil to 1-m depth at latitudes poleward of 60° north and south along with identifying enigmatic deposits of hydrogen in mid-latitudes. The THEMIS instrument has provided daytime and nighttime infrared imaging over 92% and 96% of the planet respectively. These data show diverse temperature signatures, implying surface properties ranging from bedrock outcrops to areas with extensive dust coverage. Visible imaging campaigns have provided comprehensive views of the polar regions, allowing assessment of surface variations as a function of season. The MARIE instrument has detected radiation signatures from solar activity during its 18 months of operation, including events with significantly different signatures at Mars and Earth. The orbiter has played a key role as a data relay platform for the Mars Exploration Rovers. Coordinated observations between the rovers and Odyssey provide ground truthing of the orbital data. The Odyssey prime mission was completed in August 2004. In the extended mission, activity will focus on inter-annual comparative observations, global high-resolution mapping by the THEMIS visible camera and synergistic science and operations support for other Mars missions.

Chemical Composition of the Martian Surface derived by the Mars Odyssey Gamma-Ray Spectrometer

Brückner, J.; Boynton, W.; Taylor, G.J.; Wänke, H.; Dreibus, G.; Reedy, R. C.; Evans, L.; Starr, R.; Squyres, S.; Kerry, K.; Janes, B.; Gasnault, O.; d'Uston, C.; Kim, K.; Drake, D.; GRS Team

The Gamma-Ray Spectrometer (GRS) of the Mars Odyssey spacecraft is providing data on the chemical composition of the Martian surface. Cosmic-ray induced and natural gamma-rays are emitted by the surface and measured in orbit. Due to the low gamma-ray flux long integration times are required. After two years of global measurements, elemental concentration maps could be obtained with sufficiently good counting statistics. For H, Si, Cl, and Fe, maps from a latitude range of approximately +45 to 45 degrees are reported, while for K and Th the latitude band covers +75 to -75 degrees. The Si concentration distribution in the latitude band varies mostly in the range expected from Martian (SNC) meteorites. However, in the Tharsis Montes the Si content is well below this range pointing to a mechanism depleting Si-bearing minerals. Fe concentrations are somewhat lower than SNC values in this mountain area as well as in the southern highlands, while north of the equator Fe falls in the expected range of SNCs. Mars (bulk and surface) is enriched in Fe compared to Earth. Chlorine is generally enriched on the surface having the highest content west of Tharsis Montes, which could be originating either from volcanic exhalations or special surface processes. Sulphur contents can only be determined over large areas, but a strong correlation with Cl in these areas is observed. High contents of S were observed with in-situ measurements at the five landing sites, and good correlations between S and Cl exist. K and Th are not evenly distributed on the surface, as one might expect. K reveals concentrations either at the high side of SNC data mostly in the southern hemisphere or exceeding them up to a factor of 2 in large areas mostly in the northern lowlands. K and Th show a correlation in the maps with K/Th ratios between 5000 and 6000, compatible to predicted Mars bulk ratios. The high Th areas are somewhat larger than those of K, which could point to higher solubility of Th in acid waters of a once wet Mars. Hydrogen, reported as water-equivalent content, can be directly measured by the GRS. Besides the discoveries of huge amounts of H2O ice in the polar regions (covered elsewhere), high to very high concentrations are found in large equatorial areas. Since water ice is thermodynamically not stable in these latitudes over long periods of time, H could be bound in hydrated minerals or compounds with good adsorption potential. In summary, Mars is revealing a surface, which is slowly varying in Si, rich in Fe, strongly enriched in Cl, K, and Th, and high in H.

The Mars Exploration Rover Mission

Arvidson, R.E.

The two Mars Exploration Rovers, Spirit and Opportunity, landed on opposite sides of the planet in January 2004 and have been operating since then. Spirit has traversed over 4 km on the floor of Gusev Crater and onto the older Columbia Hills. Spirit has found evidence of continuing interaction of water vapor and perhaps ice and thin films of water with surface rocks and soils, in addition to indications that older rocks in the Columbia Hills have been highly modified by corrosive ground water. Opportunity, on the plains of Meridiani, has discovered layered rocks dominated by evaporate minerals. These rocks are also cross-bedded and formed in an ancient, open body of water. More recently, Opportunity has explored the MER heat shield impact site and is now driving south to vast exposures of bright etched terrains. The two rovers will continue to explore the terrains and materials at the two landing sites, in addition to tracking the dynamics of the atmosphere of Mars as seasons change

MER Mössbauer Investigations of the Mineralogy of Soils and Rocks at Meridiani Planum and Gusev Crater on Mars

Klingelhöfer, G.; Morris, R.; Rodionov, D.; Schröder, C.; de Souza, P.; Bernhardt, B.; Bonnes, U.; Evlanov, E.; Foh, J.; Gellert, R.; Gütlich, P.; Fleischer, I.; Kankeleit, E.; Ming, D.; Renz, F.; Squyres, S.; Wdowiak, T.; Yen, A.

The Mars-Exploration-Rovers (MER) Spirit at the Gusev Crater landing site and Opportunity at the Me-ridiani Planum landing site are both carrying the Mössbauer spectrometer MIMOS II, which is part of the Athena instrument suite consisting of remote sensing instruments [1], and the In-Situ instruments mounted on an robotic arm (IDD [2,3] The IDD instruments are used to determine in-situ the chemistry and mineralogy of rocks and soils.

The MB results on rocks and soils at the Gusev crater landing site [4] show a primarily olivine-basalt composition, but also a Fe(3+)-rich component (nanophase ferric oxide, np_Ox) has significant abun-dance in surface soils and in rock coatings.(rinds) of some rocks but not in rock interiors. The np-Ox probably is the product of oxidative alteration of Fe(2+) silicate and oxide phases in the presence of H2O. The presence of sulfur in soil and in rock coatings as determined by the APXS suggests acidic-sulfate conditions during the alteration. Generally, rocks in the Columbia Hills are significantly more altered than those in the Gusev plains.

The Meridiani Planum landing site looks very different from Gusev crater. Opportunity landed inside a shallow crater (Eagle crater), with an outcrop covering part of the crater interior close to the rim. Möss-bauer measurements [5] show that part of the outcrop material consists of the Fe-sulfate jarosite (K,Na)Fe3(SO4)2(OH)6, the Fe-oxide hematite, and a basaltic component (olivine, pyroxene). The same material was found again a couple of hundred meters away at the craters Fram and Endurance suggesting that the whole area is covered with this 'jarositic' material. The Moessbauer detection of the hydroxide sulfate jarosite is direct evidence for oxidative aqueous alteration processes at Meridiani planum, and therefore the presence of significant amounts of water at this site in the past. The plains and large portions of Eagle and Endurance crater are covered by spherules with a diameter of several mm. Mössbauer data clearly show that the composition of these spherules (called 'Blueberries') is dominated by the Fe-oxide hematite. The composition of the soil at Meridiani is found to be basaltic, dominated by olivine similar to the Gusev site. An isolated rock close to Eagle crater (called Bounce rock) was determined by MB to be completely composed of Fe(2+) pyroxene. The data look very similar to some of the SNC me-teorites. These results are supported by the APXS data [6].
This work is funded by the German Space Agency DLR and NASA, USA.

Reference: [1] Squyres S. W. et al. (2003), J.Geophys Res., 108(E12), 8062, doi:10.1029/2003JE002121. [2] Klingelhöfer et al. J. Geophys. Res., 108(E12), 8067, doi: 10.1029 /2003 JE 002138, 2003. [3] Rieder et al. J. Geophys. Res., 108(E12), 8066, doi:10.1029/2003JE002150. [4]R.V.Morris, G.Klingelhöfer, et al., Science, Vol.305, no.5685, 6.August2004,pp.833-836. [5] G.Klingelhöfer, R.V.Morris, et al., Science, December 2004 in print. [6] Zipfel J. et al., Meteoritics and Planetary Science, vol.39, suppl.(2004)A118.

Inferences of Strength of Soil Deposits along MER Rover Traverses and Comparisons with remotely-sensed Surface Properties

Richter, L.; Anderson, R. C.; Arvidson, R. E.; Crumpler, L.S.; Fergason, R. L.; Golombek, M.P.; Haldemann, A.H.; Li, R.

As the two Mars Exploration Rovers ‚Spirit' and ‚Opportunity' traverse terrains within Gusev crater and at Meridiani Planum, respectively, they leave behind wheel tracks that are routinely imaged by the different sets of cameras as part of the ATHENA instrument suite. Stereo observations of these tracks reveal wheel sinkages which are diagnostic of the strength of the soil-like deposits crossed by the vehicles, and observations of track morphology at different imaging scales – including that of the Microscopic Imager – allow to constrain soil grain size distributions.

This presentation will discuss results of systematic analyses of MER-A and –B wheel track observations with regard to solutions for soil bearing strength, cohesion, and friction angle which are obtained by fitting sinkage measured in rover stereo images to wheel-soil theory calibrated to the shape of the MER wheel and by consulting comparisons with terrestrial soils. Results are applicable to the top 1...5 cm of the soil deposits as this is the depth range ‚sampled' by sinkage of the wheels. The large number of wheel track observations per distance travelled enables investigations of variations of soil physical properties as a function of spatial scale, type of surface feature encountered, and local topography. This is especially relevant for ‚Spirit' as the track imaging dataset is statistically significant in the sense that mapping of soil strength along the traverse from the landing site to the ‚Columbia Hills' with extrapolations to either side of the traverse path can be attempted if correlations of physical properties with local geology are recognised and accounted for.

Exploiting relationships between soil strength and degree of soil consolidation known from lunar regolith and dry terrestrial soils allows to relate inferred soil strengths to bulk density which provides a means to ground-truth radar reflectivities obtained for the landing sites from Earth-based observations. Corresponding comparisons will be discussed. Moreover, bulk density is correlated with soil dielectric constant, being of relevance also for Mars-orbiting radars.

The obtained estimates for soil bulk density are used to determine local thermal conductivity of near-surface materials, based on correlations between the two quantities, and to subsequently estimate thermal inertia. This represents an independent method to provide ground truth to thermal inertia determined from orbital thermal measurements of the MER landing sites (MGS TES, MODY THEMIS, MEX PFS & OMEGA), in addition to that offered by thermal inertia retrievals from the Mini-TES instrument being part of the rover ATHENA payload suite.

Studies of Northern and Southern Polar Caps by HEND instrument on NASA Mars Odyssey

Mitrofanov, I.

Observational data are presented from Russian High Energy Neutron Detector (HEND) onboard NASA Odyssey orbiter, which characterize the composition of shallow subsurface of the Northern and Southern polar caps on Mars. New occultation technique is developed for the HEND data analysis, which takes into account the shadow effect of the spacecraft, as seen from the position of HEND on the Science Deck. Odyssey has practically polar circular orbit, and projection of orbital velocity on the polar region rotates in respect to the surface due to rotation of the planet. Correspondingly, the spot of shadow rotates around the pole together with the direction of velocity projection. At some phases the shadow spot of Odyssey entirely obscures the polar cap, and HEND does not detect neutrons from the cap surface. At another phases the polar cap is well seen by the instrument, and neutrons from the cap surface contributes into in the counting rate.

The occultation technique allows to increase the spatial resolution for orbital mapping of the polar regions of Mars. Separate samples of HEND data are presented for summer seasons at North and at South poles correspondingly to the phase angle of projection of Odyssey orbital velocity. Comparison of these samples allows to make more accurate estimation of the content of water ice at Northern polar cap and of the contents of carbon dioxide ice and/or water ice at Southern polar cap. These estimation are compared with the recent data from Mars Express for top surface composition of the residual polar caps.

Additional Constraints on the Distribution of Hydrogen in the Polar Regions of Mars

Boynton, W.; Janes, D.; Kerry, K.; Williams, R.; Drake, D.; Kim, K.; Reedy, R.

In previous work we have noted the high abundance of hydrogen in the polar regions of Mars and have attributed it to an ice-rich layer that is buried beneath a dry dust layer. We have had limited success in getting simultaneous firm constraints on both the thickness of the dry layer as well as the ice content of the ice-rich layer beneath it. We have been looking at other constraints on the distribution of H in order to better determine both of these parameters. We realized that the ice content of the lower layer is high enough that it will dilute the amount of the elements contained in the dusty material with which it is mixed. Thus a decrease in the intensity of gamma rays from elements other than H should be expected to decrease as the ice content increases. Silicon was chosen for this study, since it is an element that is otherwise not expected to vary much from place to place on Mars. We built several different computer models of a stratified Mars regolith with different dry-layer thicknesses and different ice contents in the deeper layer and calculated the variation in Si gamma ray flux with the Monte Carlo code MCNPX. As expected, we found that the high H content of the ice-rich layer also had a significant effect on the distribution of thermal neutrons, which are the excitation source for both H and Si gamma rays. By considering both H and Si gamma rays, we are now better able to constrain the distribution of H in the polar regions. Detailed results will be presented at the meeting, but early work suggests that the ice content of the lower layer is greater in the South than in the North, but in the North the ice-rich layer is closer to the surface.

Observations of Martian Polar Layered Deposits in the THEMIS Investigation

Ivanov, A.; Plaut, J.; Titus, T.

Martian polar regions represent the largest known reservoir of water ice on the surface of the planet. However, internal structure of the permanent ice caps, their history and processes involved in their formation are largely unknown. The goal of this presentation is to review content of existing datasets (especially THEMIS data) accumulated around the poles and available data products to enable future collaboration in studying properties of the polar regions.

The THEMIS instrument allows simultaneous observations in both Thermal IR (10 bands from 6 to 15 μm) and Visible wavelengths (5 bands from 425 to 860nm). An intensive program of polar region observations was conducted by the THEMIS Science Team. For polar observations we primarily employed IR bands 9 and 10 (12.58 μm and 14.88 μm) and VIS band 3 (650nm). High resolution, high density imaging campaigns were designed and implemented. Both North and South Polar layered deposits were imaged while covered by CO2 seasonal frost (usually at 36m/pixel) and defrosted (usually at 18m/pixel). During summer at both poles, IR images of PLDs were taken as well. THEMIS has acquired a significant number of IR and VIS image pairs. Mosaicing of high resolution VIS data taken over polar regions is currently in progress.

We will present examples of the above products and discuss their use in analysis of the structure of the Polar Layered deposits. Collaborative observations with instruments onboard Mars Express spacecraft (especially HRSC, PFS, OMEGA and SPICAM) will be discussed as well. Analysis of the polar layered deposits will benefit by fusing data from Mars Global Surveyor, Mars Odyssey and Mars Express instruments.

The Martian North Polar Cap Spirals are the Traces of an Ancient Ice Sheet Collapse

Kostrikov, A.

A hypothesis for the origin of helical structure of troughs on the surface of Martian north polar cap is proposed. It follows from the laboratory experiments and theoretical analyze that being defreezed at its bed the Martian north pole ice sheet began to transform, as a matter of fact, to an ice body resembling the ice shelf. This transformation was accompanied by drastic amplification of radial tension that came to the breaking of ice entirety, the emergence of deep crevasses all over the ice sheet. This planetary scale process was so intensive that being influenced by Coriolis force crack trajectories deviated to the right, forming spirals. After bed temperature fell down and the sheet collapse ceased, the obtained relief began to undergo a smoothing owing to the continuous slow ice spreading and mass transfer from the warm north crack slope to the shady south one. This process transformed the helical structure of crevasses to the helical structure of troughs.

Observations of the Polar Regions on Mars by the HRSC Experiment on Mars Express

Hoffmann, H.; Bischof, B.; Frisk, U.; Harri, A-M.; Makkonen, P.; van Scheele, F.; Siili, T.; Walther, S.

Already during its early commissioning phase, the HRSC experiment on Mars Express (Neukum et al., 2004, ESA-SP 1240) acquired some images of the south polar area. The observations were performed at higher altitudes away from periapsis yielding a spatial resolution of about 60 to 80 m/pixel. Special emphasis was given to obtain multispectral data at highest possible spatial resolution while stereo data were not acquired. A complete mapping campaign of the south polar region is planned at the end of the nominal mission. Because of the wide range in illumination conditions, the observation in orbit 103 (solar longitude 348) was also used as a test case for a first-order photometric correction (cf. Gwinner et al., 2004, this volume). Atmospheric phenomena detected in this orbit include a dust cloud at the edge of the polar cap and the presence of haze close to the terminator. The OMEGA imaging spectrometer onboard Mars Express identified three different units in the south polar cap (Bibring et al., 2004, Nature 428) with a CO2-ice rich unit mixed with some water ice, an H2O-ice rich unit with some CO2-ice on the scarps around the residual cap, and a unit consisting of dust mixed with H2O-ice but without CO2-ice. All three units described by OMEGA could be recognized within the HRSC image based on their differences in albedo. They could be mapped in greater detail and differentiated even further. Within the CO2-ice rich residual cap, two different terrains could be distinguished with a brighter, rough terrain and a smooth, slightly bluish terrain exhibiting the highest frequency of swiss-cheese like features. The two terrains indicate differences in their sublimation stages. A mapping campaign of the Martian north polar region has started just now in early December 2004. First results of these observations will be presented and compared with the observations the south.

Evolution of the Permanent North Polar Cap during the North Summer Season

Langevin, Y.; Schmitt, B.; Bibring, J-P.; Poulet, F.; Gondet, B.; Douté, S.

The OMEGA VIS/IR imaging spectrometer has observed the North polar cap of Mars since the spring equinox from distances of 6000 km to 8000 km, following the recess of the seasonal cap. Since science operations resumed after the conjunction in late September, the outlines of the ice rich regions have remained stable. The North polar cap appears very similar in 2004 when compared to the situation in 1976 (Viking), with only a few regions exhibiting drastic changes in ice coverage. A comprehensive coverage has been obtained typically every week for the central regions (> 80° N), with resolutions improving from ~ 4 km in October to 2 km or less in late November and December. Large albedo variations are observed in the visible range, as already reported from Viking and MGS observations. The high repeat rate of OMEGA observations show that significant changes can occur in less than one week, and that regions may exhibit decreases in albedo while others get brighter, with ice variegation at scales of less than 10 km. The unique spectrometric capability of OMEGA has made it possible to simultaneously monitor the evolution of ice grain size and that of its dust content from the intensity of the ice absorption bands between 1 and 4 µm. We show that the observed albedo variations result from a complex combination of the full range of processes previously considered as possible explanations: changes in grain size due to frost sublimation or surface ice thermal processing, dust deposition or removal during ice sublimation, increase of macroscale surface roughness by sublimation of interstitial ice. This complex evolution presents intriguing similarities with processes at work on terrestrial ice caps.

Physical State and Distribution of H_2O and CO_2 Ices and Dust on the Perennial Mars South Polar Cap from OMEGA/MEx Observations

Schmitt, B.; Douté, S.; Altieri, F.; Bellucci, G.; OMEGA Team

The determination of the physical state and composition of the ices composing the surface layer of the Mars polar caps is of prime importance for the understanding of the sublimation history of volatiles, the thermal state and the extend of the south polar cap. It is also a prerequisite for an accurate mapping of the abundance of the ices and of their physical characteristics by spectral inversion of the OMEGA observations.

Four observations covering about the whole bright south polar cap and part of the surrounding terrains have been recorded by the OMEGA imaging spectrometer before the southern autumn equinox

The statistical analyses (PCA) of the observations shows the presence of two types of CO2-rich terrains on the perennial cap : one concentrated in the cap centre and the other on the outer parts. Two types of dusty water ice terrains are also found on the border of the cap and in isolated patches at some distance from the perennial cap.

From this analysis we extracted several end-member and representative spectra of the different types of icy terrains. Then, we modelled these spectra using our radiative transfer code in layered media (Douté and Schmitt 1998) in order to determine the coexistence modes of CO2 ice, H2O ice and dust at the centimetre scale (granular mixtures, layered deposits, …) and pixel scale (geographical mixture). The relative abundances of these three components are determined.

From these results we discuss the state of volatiles in the south polar cap just before southern winter.

Composition and Spatial Distribution of the Northern Seasonal Condensates during Spring from the Statistical Analysis of OMEGA NIR Spectro-images

Doute, S.; Schmitt, B.; Bibring, J-P.; Langevin, Y.

Monitoring the exchange of CO2, H2O and dust between the atmosphere, regolith, seasonal deposits and permanent polar caps of Mars is required to study the climate of the planet and its evolution.
The imaging spectrometer OMEGA (Observatoire pour la Minéralogie, l'Eau, les Glaces et l'Activité) of Mars Express contributes to such a task by acquiring regularly spectro-images of the polar regions in the 0.35-5.09 micron range.

We have analyzed the Near Infrared segment of observations acquired at Ls from 350 to 90 (spring of the northern hemisphere) focusing on the northern circumpolar seasonal deposits. Our goal is to study the modalities of their progressive demise by metamorphism and sublimation. More precisely, we seek to determine the composition, physical state and granularity of the icy deposits as well as their dust content as a function of time for different latitudinal bands.

Here we present the results obtained after a first phase of analysis. We apply different statistical methods (PCA, MNF, etc.) to (1) classify the spectro-images into a small number of spectrally similar terrains and (2) extract endmembers (spectra with unique and extreme signatures). We carefully examine the position, depth, width and shape of characteristic absorption bands of CO2 and H2O ices at the surface by direct comparison with laboratory data. Such operations give the spatial distribution of the different types of terrains encountered and a first estimate of their composition as well as physical properties : mixing mode between CO2, H2O and dust, texture and granularity. Consequently the identification andclassification of the series of OMEGA spectro-images allows to produce compositional maps organized in a time sequence. The interpretation of these maps provides insights about the mechanisms and timing presiding to the spring sublimation of the seasonal northern polar cap.

On the Visual Colour of Martian Polar Deposits

Bellucci, G.; Altieri, F.; Schmitt, B.; Bibring, J-P.

The OMEGA imaging spectrometer provides contiguous spectral images at ~1 km spatial scale in the 0.36 – 5.2 ìm wavelength range. Since beginning of its operations in January 2004, it has mapped the Martian polar deposits several times at different seasons. In this paper we have studied the spectral characteristics of these deposits in the visual range. In particular, we report on the spectral characteris tics of the interlayer deposits which show a distinct bluer colour compared to the surrounding ice-free terrains. The implications on the deposition and nature of these deposits are discussed.

Precession-induced Exchanges of Water between the Poles on Mars

Montmessin, F.; Haberle, R.M.; Forget, F.; Clancy, T.

We have performed GCM-based simulations of Martian volatiles to study their behavior in a recent past. We focus on the specific impact of the changes in orbit precession on both the water and the dust cycles. We show that with a perihelion date coinciding with northern summer, the surface water ice reservoir currently stable at the north pole of Mars would be partially transferred to the south pole.
These results suggest that significant exchanges of water recently took place between the Martian poles, providing a believable explanation to the recent discovery of exposed water ice units in the south polar region.

Martian Variable Features: New Insight from the Mars Express Orbiter and the Mars Exploration Rover, Spirit

Greeley, R.; Foley, D.; Williams, D.; Whelley, P.; Thompson, S.; Neakrase, L.; Squyres, S.; Neukum, G.; Arivdson, R.; Haldemann, A.; HRSC Co-Investigator Team; Athena Science Team

New linear, low albedo patterns (termed variable features) formed on the floor of Gusev crater between September 2003 and February 2004, including the ~7.5 km-long streak on which the rover, Spirit, landed. Spirit Pancam images show that the rover crossed one of the newly formed features during the traverse to Bonneville crater. Spirit Microscopic Imager data reveal that sand grains within the streak are relatively free of dust, whereas grains outside the streak are mantled with dust. During the solar conjunction, Spirit remained in one location; images taken before and after the conjunction show patches of the surface beneath the rover that record a darkening, suggesting removal of bright material. Two MI mosaics taken 18 sols apart of the surface within 0.5 m of the nearest dark patch show that some of the larger (1-2 mm) particles moved about 0.7 mm. These observations support the hypothesis that some dark variable features result from the removal of fine-grained material, presumably by winds that expose a relatively lower albedo substrate. Other variable features on the Gusev floor faded between September 2003 and February 2004 and are interpreted to represent settling of dust from the atmosphere, consistent with the accumulation of dust measured on Spirit. The observation of dark variable features fading with time, while some new dark linear streaks have formed, is consistent with local wind gusts or, more likely, the passage of dust devils that locally sweep dust from the surface.

Martian Dust Devils: First Calculations of the Forward Velocity from HRSC-images

Stanzel, C.; Pätzold, M.; Wennmacher, A.; Hauber, E.; Neukum, G.

For the very first time the velocity of Martian dust devils across the surface could be obtained from images taken by the High Resolution Stereo Camera (HRSC) on board the Mars Express orbiter. Dust devils are temporal variable and moving atmospheric vortices, filled with dust. So far only the detection of dust devils as a snap-shot was possible in orbiter images. With the aid of the stereo channels of HRSC the analysis of dust devils can be extended towards the forward velocity, and therefore lead to a better understanding of their evolution, behaviour and contribution to surface-atmosphere interactions, e.g. dust transport.
Six Martian dust devils have been detected by HRSC in Arcadia Planitia. Three of them could also be recognised in an image taken approximately two minutes before. The velocity across the surface was higher than 20 m/s for these three dust devils. It is assumed that dust devils move with the ambient wind. The calculated values of the forward velocity seem to be very high, however, all three vortices had the same direction of motion and were moving approximately the same distance in the same time. This underlines the theory of movement with the ambient wind.

Wavelength Dependency and Angular Effects of Reflectance of Fog in Valles Marineris

Inada, A.; Altieri, F.; Gwinner, K.; Hoekzema, N.M.; Poulet, F.; Keller, H.U.; Markiewicz, W.J.; Neukum, G.; Bibring, J-P; Muller, J-P.; HRSC and OMEGA, Coinvestigator Teams

Fog in Valles Marineris was observed by the High Resolution Stereo Camera (HRSC) and Visible and Infrared Mineralogical Mapping Spectrometer OMEGA on board Mars Express at a solar longitude of 40 deg.. The fog appeared brighter than the surface outside of the valley and displays little contrast in brightness. HRSC has four color channels (Blue: 0.440• }0.045 micron, Green: 0.530• }0.045 micron, Red: 0.750• }0.020 micron, and Infrared: 0.970• }0.44 micron) and five panchromatic channels (0.675• }0.90 micron), while OMEGA collects spectra with the wavelength range between 0.5 and 5.2 micron. We will present the comparison of data from these two instruments in the visible wavelength. OMEGA• fs data in long wavelength will be used to determine the composition of the fog. Moreover the angular dependence of reflectance of fog is studied using HRSC• fs five stereo-panchromatic channels (the angles from nadir are 0, • }12.8, • }18.9 deg.). The reflectance shows clear emission angle dependence. The reflectance of the nadir channel is the darkest due to the shortest light path length in the bright atmospheric feature.

Martian Surface Albedo and Related Features Monitored by the Planetary Fourier Spectrometer Onboard the Mars Express Mission: First Results

Esposito, F.; Palomba, E.; Colangeli, L.; D'amore, M.; Formisano, V.

The Planetary Fourier Spectrometer (PFS) SW channel, covering the 1.2-5 micron spectral range, is well suited to study the reflectance properties of the Martian soil. These properties vary with time due to the dust dynamics in the Martian environment. Wind can locally blow off the dusty material exposing soil and fresh rocks or, conversely, can support grain mobility inducing local dust settling. We present the results of a preliminary analysis of the PFS data. For each of the observed regions a value for the albedo was retrieved in the near IR part of the SW spectrum. The results show good agreement with previous studies, although some variations are observed. Some of these albedo changes could be due to small to medium scale dust storms.

The Retrieval of Atmospheric Optical Depth and Surface Albedo of Mars from the Brightness of Surface Shadows in the HRSC Images

Markiewicz, W.; Petrova, E. V.; Hoekzema, N.M.; Inada, A.; Keller, H. U.; Gwinner, K.; the HRSC Co-Investigator Science Team; Hoffmann, H.; Neukum, G.

We present results for retrieving the optical depth of the Martian atmosphere and the albedo of the underling surface from Mars Express high-resolution images (HRSC experiment). Since the Martian atmosphere is optically thin out of dust-storms seasons, a core problem in this analysis is to separate the atmosphere and surface contributions to the observed intensity. We have developed a method that within a certain approximation separates these two components by comparing the brightness of shadowed and nearby illuminated surface regions. The required single scattering properties of atmospheric aerosols are assumed to be those derived from the analysis of the sky brightness measurements obtained by the Imager for the Mars Pathfinder. Both the Lambert and non-isotropic reflectance laws are considered for the surface. We find that (1) both the optical thickness and the surface albedo can be estimated with the shadow method; (2) this method applied to stereo channels can also serve for separating the angular functions of the surface reflectance and atmospheric scattering; (3) the shadow method is extremely easy to use for analyzing the long-wavelength images, where the contribution of the Martian atmosphere is relatively low compared to that of the surface. At the same time, the method has the following limitations: (1) the accuracy of the method is sensitive to the spatial resolution of the images and to the optical thickness itself; (2) the method is somewhat "subjective": the result depends on an accurate choice of the regions to be compared; (3) the difference in elevation between the compared regions must be taken into account.

Monitoring of Integrated Dust Content in the Martian Atmosphere from Planetary Fourier Data: Comparison of Thermal and Solar Wavelenghts

Rinaldi, G.; Grassi, D.; Cottini, V.; Formisano, V.; Ignatiev, N.; Giuranna, M.; Maturilli, A.; Zasova, L.

The data of the Planetary Fourier Spectrometer on board of the Mars Express mission have been used to retrieve the integrated dust content in the Martian atmosphere considering independently the thermal IR band centered at 1100 cm-1 and the Solar scattered radiation at the bottom of 3700 cm-1 CO2 band.
The comparison of the two sets of values among different orbits shows a consistent trend but different absolute values, indicating possibly the need of a critical revision of adopted models for dust refractive indices and size distribution.
Uncertainties related to the effects of water ice clouds and dust vertical distributions are also discussed, demonstrating the need of extensive comparison against the results of other MEX experiments (namely SPICAM).

OMEGA/Mars Express Limb Observations of Mars : The Dust Vertical Properties

Fouchet, T.; Bézard, B.; Drossart, P.; Combes, M.; Altieri, F.; Bellucci, G.; Poulet, F.; Langevin, Y.; Gondet, B.; Bibring, J-P.; Titov, D.

The OMEGA spectro-imaging system aboard the Mars Express (MEx) mission covers the 0.35-5.1 micron wavelength range at a resolving power of 200. Since MEx orbit insertion in late 2003, OMEGA has obtained several limb observations covering a wide variety of latitudes, longitudes, and seasons. We have retrieved the dust opacity and particle size as a function of altitude, as well as the dust single scattering albedo in the lower atmosphere. We unambiguously demonstrate that the mean dust particle size decreases with altitude. The dust opacity vertical profiles exhibit a wide diversity in vertical scale height, total opacity, and degree of sedimentation. We also explore the variation of the dust single scattering albedo with latitude and season.

Optical Depth Retrievals from and Atmospheric Correction of HRSC Stereo Images of Gusev Crater: Validation by Comparing with Spirit's Ground Truth

Hoekzema, N.; Inada, A.; Markiewicz, W.; Hviid, S.; Keller, H.U.; Gwinner, K.; Hoffmann, H.; Meima, J.; Neukum, G.; and the HRSC and MER, Co-investigator team

A primary task for the Mars Express orbiter is to map Mars in high-resolution and in stereo with its High Resolution Stereo Camera (HRSC). The Martian atmosphere contains variable amounts of aerosols that scatter light and influence the images. For many applications, analysis of HRSC images requires atmospheric correction. Minimum required inputs for such a correction are the optical depth of the atmosphere and the single scattering properties of the aerosols.

Optical depths can be retrieved from stereo-images with the so-called 'stereo-method'. This method estimates optical depths by analyzing how contrasts differ between stereo images. Software for using the stereo-method has been developed at the Max-Planck-Institute for Solar System Studies (MPS) in Katlenburg-Lindau, Germany. The method uses map-projected ortho-stereo-images and complementary data on the imaging geometry from photogrammetric software developed at DLR. Once an optical depth is known, and a phase function is chosen, we can correct for atmospheric effects with other programs developed at MPS, such a MPAE_ATM_DUST.

For validation, we compared optical depths retrieved from HRSC stereo images of Gusev crater taken on January 16.04 with in-situ measurements by Spirit, the rover that landed in this crater. That day Spirit measured the local optical depth at 0.87-0.89 by looking up at the Sun. From HRSC images, we estimated 0.86 ± 0.08 for a small region around the landing site, and 0.91 ± 0.04 for the full crater. Both values are in good agreement with Spirit's ground truth. Spirit landed in a region that displays considerable contrast, which improves the accuracy of the retrieval considerably. In addition, very careful consideration of topography proves crucial since the retrieved optical depths, and especially their errors, depend very strongly on altitude variations within the analyzed field.

We calculated a corrected image of a region around the landing site, using an optical depth of 0.89 and an aerosol phase function as derived from Mars Pathfinder data. We find reasonably good agreement with local measurements from Spirit.

The Planetary Fourier Spectrometer Results at Mars (invited)

Formisano, V.

PFS experiment on board MEX has now (at the time of the conference) been active for one Earth year . It has acquired a number (>110 000) of spectra at different latitudes longitudes and local times. Nadir pointing inertial and limb measurements have been performed allowing the achievements of numerous important results. The initial terrible problem of microvibrations was partially solved by switching off one laser diode (the driver of the SW channel).

We shall discuss first a complete spectrum SW + LW to identify the spectral region of major interest. From the LW channel we derive the vertical temperature profile the dust opacity at 10 microns the soil temperature and the ice opacity. The temperature fields are used to compute thermal winds. Unusual temperature profiles and winds are observed over the big volcanoes where also often are observed water ice clouds. The vertical temperature profile compared with the vertical water condensation vertical profile allows us to predict water ice clouds or fog.

Minor species results are : CO mixing ratios (900 – 1500 ppm) with an average latitudinal variation (larger concentrations on the northern winter polar region).

Water mixing ratios (10 precipitable microns) uniform and well mixed at 10-15 Km (LW channel) and non uniform with local enhancements (up to 35 40 precipitable microns) in the boundary layer (SW channel) . A correlation of these enhancements with the HEND Odyssey results points to the source of the underground permafrost.

As minor species in the atmosphere we have identified methane (11 +- 2 ppbv) . Formaldehyde has been measured to be at 130 +- 50 ppbv . Both these gases seem to vary from place to place and they vary together . In practice Formaldehyde seems to be the oxydate state of methane . The possible source of these gases is discussed elsewhere.

Three acids have been identified in the martian atmosphere : HF – HCl – HBr they all have a mixing ratio of 150 – 200 ppbv .

Non LTE emissions in the upper Martian atmosphere are normally seen in Nadir pointing in the 4.3 microns band. In the limb measurements we see also CO and CO2 (and an isotopic CO2 band) in emission at altitudes up to 120 Km. In other occasions we also see Oxygen produced by ozone breaking by UV emitting a number of lines (up to 32 lines have been counted and their intensity has been measured).

The dust opacity is measured at 3 different wavenumbers and therefore allows us to put constrains on its size distribution and mineralogic composition.

Polar cap ice composition studies fitting the measured spectra allow us to make important conclusions on the CO2 grain size on the percentage of the water ice present and on the amount of dust revealed.

Soil composition studies have also recently started.

(*) The composition of the PFS team data analysis is :V. Formisano, S. Atreya ,A. Blanco, M. I. Blecka, F. Billebaud ,L. Colangeli, T. Encrenaz, F. Esposito, S. Fonti, M.Giuranna, D. Grassi, G.Hansen, I. Khatuntsev, N. Ignatiev, A. Jurewicz, E. Lellouch, J. Lopez Moreno, A. Maturilli, V.Orofino, E. Palomba, B.Saggin, D. Titov, L. Zasova, M.L. Valverde.

Seasonal Variation of Structure of Martian Atmosphere in Polar Regions from LWC PFS Data

Zasova, L.V.; Grassi, D.; Ignatiev, N.I.; Formisano, V.; Giuranna, M.; Khatuntsev, I.V.

Longwavelength channel of PFS covers a spectral range 300 – 1500 cm-1 with spectral resolution 1.8 cm-1. Vertical temperature profiles and aerosol opacity of Martian atmosphere are retrieved from the same single spectrum obtained on the day side, when the surface temperature was rather high. At night side the temperature is low, and the spectra have to be averaged. In the polar regions we also deal with averaged spectra, so the effective field of view was increased there 2-10 times depending on the number of spectra to be averaged (40-200 km respectively). A unique orbit (N68) passed through the Northern polar region at polar night. A temperature field obtained for this orbit (Fig.1) shows position of the descending Hadley branch and its temperature structure: a temperature inversion was observed below 20km (at 50-70° N), which was not known before. The amplitude of thermal inversion reaches a maximum of 20K in the polar hood and smoothes out above the CO2 polar cap, where the temperature maxima corresponds to the altitudes not available for the observations with spectral resolution of PFS. The CO2 clouds probably exist in the atmosphere at latitudes exceeding 70° (a terminator latitude is around 80°). The next orbit over North pole was obtained at Ls = 13°. A comparison shows that the structure of the atmosphere over Northem polar region changed dramatically. The descending branch becomes not so evident, and the temperature inversion between 10-20 km disappeared, although the changes in polar hood and the CO2 cap boundary are not significant. Seasonal variations in the atmosphere in both polar regions will be demonstrated.

Fig. 1. Temperature field for orbit 68 (Ls=342°) , passing over Tharsis, Ascraeus Mons and Alba Patera

Water Vapour in the Martian Atmosphere from PFS/Mars Express Data

Ignatiev, N.; Titov, D.; Formisano, V.; Lellouch, E.; Grassi, D.; Encrenaz, T.; Tschimmel, M.; Fouchet, T. ; Giuranna, M.

Measurements of Martian atmospheric water vapour obtained with the Planetary Fourier Spectrometer during the first year of Mars Express operations are presented. Two channels of the instrument cover a number of H2O bands both in the thermal and near IR parts of the Martian spectrum. The 2.56 μm and 30-50 μm H2O bands, the most favourable in the sense of the instrument performance, are used to monitor routinely the water abundance on a global scale from pole to pole. Atmospheric parameters are obtained from the same spectra, whenever possible. The zonally averaged picture is generally consistent with previous observations: the first MEX operational period (+/-30 degrees around Martian vernal equinox) is characterized by the south-north asymmetry, with the atmospheric water maximum of 10 microns of precipitated water at the latitudes of 10-30N, and the minimum of 5 microns at 40-20S. The most "wet" regions with the abundance up to 15 prc. microns, Arabia Terra and Tharsis, coincide with those in the time-averaged MGS TES data. Atmospheric water enhancement in Arabia Terra correlates also with the subsurface water enrichment observed by HEND on Mars Odyssey. Water vapour abundances retrieved simultaneously from the two PFS channels tentatively indicates that the H2O mixing ratio tends to increase near the surface.

Observations of CO in the Atmosphere of Mars with PFS onboard MarsExpress

Billebaud, F.; Lellouch, E.; Fouchet, T.; Encrenaz, T.; Formisano, V.; Grassi, D.; Brillet, J.; Ignatiev, N.; Titov, D.; Giuranna, M.; Maturilli, A.; Atreya, S.

The SWC detector of PFS allows to observe the (1-0) infrared band of CO in the atmosphere of Mars. In order to derive informations on the CO mixing ratio, we developped an analysis procedure which uses a radiative transfer code to fit the spectra recorded along the orbits in the (1-0) (4.7 micron) wavelength range. Applying systematically this procedure to available orbits enables us to ultimately produce maps of the CO mixing ratio in the atmosphere of Mars, as a function of location.
Analyses of the dependence -or not- of this mixing ratio with several parameters such as elevation, local time, latitude and other informations derived independently from the data by other colleagues (like atmospheric water vapor content) are also done.
We will present here preliminary results we obtained on these issues.

Martian Morning Atmosphere during Northern Spring from the Planetary Fourier Spectrometer (PFS) Measurements

Grassi, D.; Ignatiev, N.; Zasova, L.V.; Maturilli, A.; Formisano, V.; Giuranna, M.

Taking advantage of the specific characteristics of Mars Express orbit, the Planetary Fourier Spectrometer (PFS) has been able to monitor the main fields of Martian atmosphere in a range of local times not covered by previous experiments.
This work presents a review of the air temperature fields measured by PFS in the middle-morning hours during early Northern spring. Extensive comparison with the expectations of LMD-AOPP-IAA Global Circulation Model is provided, highlighting the actual correspondence of several phenomena. Noteworthy, discrepancies tends to increase at higher latitudes, indicating possibly a different strength of Hadley circulation compared to model outcomes. The trend of dust load is also discussed, suggesting a relatively constant value vs. local time.
The complementary characteristics of PFS dataset with respect to other experiments (namely, the Thermal Emission Spectrometer on Mars Global Surveyor), together with the higher vertical resolution of derived T(z) fields can represent important constraints to Global Circulation Models, once fully exp loited by means of data assimilation.

The Loss of the early Martian Atmosphere and its Water Inventory

Lammer, H.

The evolution of the Martian atmosphere and the evidence of the existence of an ancient hydrosphere are of great interest in studies regarding the evolution of the planet's water inventory by the ASPERA-3 instrument on board of ESA's Mars Express. Although the Martian climate is at present too cold and the atmosphere too thin so that liquid water can not be stable on the surface, there are many indications that the situation was different in the past. Several observations of networks of valleys in crater rich areas of the southern hemisphere suggests that Mars had once a significant hydrologic activity during the first Gyr of the planets lifetime. Recent observations imply that an ancient water ocean equivalent to a global layer with the depth of about 150 m is needed for the explanation of the surface features. The evolution of the Martian atmosphere and its water inventory since the end of the magnetic dynamo at the late Noachian period about 3.5 - 3.7 Gyr ago was dominated by non-thermal atmospheric loss processes like solar wind erosion and sputtering of oxygen ions and thermal escape of hydrogen. Recent studies show that these processes could remove a global Martian ocean with a layer thickness of about 10 – 20 m, indicating that the planet should have lost the majority of its water during the first 500 Myr. The present study uses multi-wavelength observations by the ASCA, ROSAT, EUVE, FUSE and IUE satellites of Sun-like stars at various ages for the investigation of how high X-ray and EUV fluxes of the young Sun have influenced the evolution of the early Martian atmosphere. We apply a diffusive-photochemical model and investigate the heating of the Martian thermosphere by photo-dissociation, ionization energy and due to exothermic chemical reactions, as well as cooling due to CO2 IR-radiation loss. Our model yields high exospheric temperatures during the first 100 – 500 Myr, which results in blow off for hydrogen and even high loss rates for atomic oxygen and carbon. By applying a hydrodynamical model for the estimation of the atmospheric loss rates we obtain results, which indicate that the early Martian atmosphere was strongly evaporated by the young Sun and lost most of its water during the first 100 – 500 Myrs after the planets origin.

Cloud-Tracked Martian Winds as seen from HST in Opposition 2003

Kaydash, V.; Shkuratov, Y.; Kreslavsky, M.; Videen, G.; Wolff, M.; Bell III, J.

We performed synoptic wind measurements using global Hubble Space Telescope data taking an advantage of the closest Earth-Mars encounter as Mars passed within 0.372 AU of Earth. Several series of images of Mars were taken with the High-Resolution Channel of the Advanced Camera for Surveys. The image scale was about 7 km/pixel in the disk center. Images were taken close to the perihelion, on August 24 and September 5, 7, 12, and 15. The observations were timed to allow imaging of the same hemisphere of Mars at all dates (disk center at 19°S, 20-35°W). The season on Mars was summer in the southern hemisphere (the areocentric longitude of the Sun Ls = 247 – 261°). For reliable determination of transient cloud features movement we used images in two close UV-channels (filters centered at 250 and 330 nm), because of higher visibility of global and local atmospheric haze features in the UV. Time interval between consecutive images was about 7.5 minutes. Accurate transformation of images into a common projection (with calculation of the local covariance between images) and visual inspection of 250/330 nm color ratio allowed us to detect cloud shifts due to their movement relatively to the surface features and measure speed and direction of cloud movement, which we consider as a proxy for wind speed and direction. The most accurate wind determinations are for the western (morning) part of the Martian disk from 20N to 40S (region of Tharsis rise), where extensive and complicated system of clouds and hazes is observed. We confirmed domination of westward winds at low latitudes (30 S –10 N). Our measurements show wind speed varying from 10 to 90 m/s with mean values about 50 m/s. For higher southern and northern latitudes the wind direction systematically deflects poleward. We found evidence of local deviation of wind direction pattern near eastern edge of Tharsis rise. The time of our Martian observations near winter solstice is known as dust storms period. However, the HST data does not confirm increasing of atmospheric optical depth due to high dust loading. We also checked MGS TES retrievals of dust opacity index and found that there is no evidence for large dust lifting events, though during the observation period the atmosphere was relatively dusty in comparison with the aphelion season. We compared our wind measurements with predictions of the European Mars Climate Database (the global climate model available at http://www.lmd.jussieu.fr/mars.html). For this comparison we used altitude of 30-40 km, the typical altitude of water clouds condensation for the season of observation, as recently obtained from TES atmospheric measurements (M. Smith, JGR, 2002). We found that the agreement between our results and the model is satisfactory for 30-35 km altitudes of upper water cloud layer in the "MGS dust scenario". The "low dust scenario" of this model gives worse agreement in wind speed and direction for given altitudes. Synchronous HST and MeX observations of atmosphere circulation could provide important complementary measurements of Martian winds.

Modeling of the Atmospheric CO_2 Emissions at 4.3μm under non-LTE Conditions as Observed by PFS and OMEGA / Mars Express

Lopez-Valverde, M.A.; Garcia-Comas, M. ; Lopez-Puertas, M.; Lopez-Moreno, J.J.; Formisano, V.; Drossart, P.; Fouchet, T.; Bibring, J-P.

A theoretical model of the CO_2 infrared emissions in the Martian atmosphere, able to handle non-local thermodynamic equilibrium situations, is used to simulate a set of 4.3-um spectra taken by the instruments "Planetary Fourier Spectrometer" (PFS) and "Observatoire pour la Mineralogie, l'Eau, la Glace et l'Activite" (OMEGA), both on board Mars Express. We focus on PFS nadir and on OMEGA limb spectra.

With higher spectral resolution than OMEGA, PFS data show an emission feature in the center of the strong absorption 4.3um band of CO_2, with a double peak structure that can be explained by strong solar pumping in the 2.7um CO2 bands. OMEGA limb data, on the other hand, presents a high vertical sampling and its spectrally integrated profiles are used to test the non-LTE model predictions of the excitation sources. Quantitative comparisons and sensitivity analysis will be presented in order to ascertain the impact of the modelling uncertainties and our ability to understand these data sets.

The systematic observations from Mars Express in this spectral range represent an unprecedented data set to validate theoretical models like the present, and consequently, to learn about the radiative properties of the middle and upper atmosphere of Mars.

OMEGA Observations of the Mars Atmosphere

Drossart, P.; Combes, M.; Encrenaz, T.; Fouchet, T.; Melchiorri, R.; Bibring, J-P.; Langevin, Y.; Gondet, B.; Forget, F.; Ignatiev, N.; Lopez-Valverde, M. A.; Garcia-Comas, M.

Atmospheric retrieval from OMEGA/Mars Express experiment has been performed with a focussing on the following topics:

- a first order atmospheric pressure and minor constituents retrieval, in an automatic procedure to correct OMEGA IR reflectance spectra from atmospheric features
- minor constituents (CO, H2O) retrieval
- dust opacity study
- limb emission, by fluorescent emission of CO2 and CO, observed at 4.3 and 4.6 micrometers.

The first three topics are presented in separate abstracts (Encrenaz et al, Melchiorri et al, Fouchet et al). Limb fluorescent emission will be detailed here. After one year of observations, a sampling of the limb atmosphere in various conditions of latitude, illumination and dust content has been obtained, which allows us to study the variability of this emission. The CO2 and CO emission peak respectively at ~90 km and ~50 km. Some variability is observed, possibly due to atmospheric temperature profile variations. Synthetic modelling is made using complete non-LTE Martian models (Lopez-Valverde et al, JGR, 1994) to compare with OMEGA observations.

OMEGA Observations of Atmospheric Water Vapour on Mars

Titov, D.; Drossart, P.; Melchiorri, R.; Encrenaz, T.; Fouchet, T.; Combes, M.; Ignatiev, N.; Bibring, J-P.; Erard, S.; Langevin, Y.; Gondet, B.

The OMEGA instrument on board the Mars Express orbiter is an imaging spectrometer covering the wavelength range from visible to thermal infrared. Absorption bands of atmospheric water vapour at 1.86 and 2.56 micron are well pronounced in the OMEGA spectra. They are used to derive the water vapour abundance and its variability. First results are generally consistent with expected for this season water vapour abundance of 10(5) precipitable microns. However the retrieved vapour abundance often shows strong variations which are probably due to influence of surface spectral features. They are taken into account more accurately in the current work. Results of water vapour retrievals as well as their comparison with the PFS data will be presented.

Evolution of Seasonal Water Ice Clouds as Observed by OMEGA

Gondet, B.

The unambiguous identification of water ice clouds in the OMEGA data set enables to monitor their time and space evolution, over the entire Mars surface. We will present the results acquired over one terrestrial year, and discuss some climatic outcomes.

Atmospheric Sounding of Mars from Ground-based and MEx Observations

Encrenaz,T. ; Bezard, B. ; Drossart, P. ; Fouchet,T. ; Lellouch, E. ; Formisano,V. ; Bibring,J-P. and the TEXES, MEx-PFS and MEx-Omega Teams.

We will report on new infrared spectroscopic results on the martian atmosphere which have been obtained both from the ground and from Mars Express. High-resolution spectroscopic data (R = 77000) have been obtained around 8 microns, in June 2003, using the TEXES imaging spectrometer on the NASA Infrared Telescope Facility (IRTF) at Mauna Kea (Hawaii).Maps of H2O2 and H2O have been retrieved, in close agreement with the predictions of the Global Climate Model. A search for CH4 was unsuccessful, but led to upper limits consistent with the previous observations. Methane was also searched for with PFS aboard Mars Express, at 3.3 microns, in the areas where strong CH4 abundances have been previously reported. However, no methane excess was found with PFS in these regions. Finally, we have studied the CO and H2O abundances over Olympus Mons using OMEGA aboard Mars Express.
Mixing ratios were found to be consistent with previous determinations (CO = 8 10-4) or expected values from TES measurements (H2O = 1.5 10-4, Ls = 337°).

Pressure Variations in OMEGA Observations; Possible Detection of Lee Waves

Melchiorri, R.; Drossart, P.; Vintanier, S.; Forget, F.; Altieri, F.; Bibring, J-P.

The OMEGA instrument on board the Mars Express orbiter is an imaging spectrometer covering the wavelength range from visible to thermal infrared.
Given its high spatial resolution (low limit, ~400m) it is possible to observe atmospherical structures at very low scale. We report on the observation of lee waves developed around craters. A possible study is proposed using the analysis of the 2 m CO2 band depth.
This kind of structure are easily detectable in the visible when in presence with ice clouds, which follow the isobaric lines.
We have developed a line by line a model to resolve the radiative trasfer equation for the solar reflected component of the OMEGA spectrum.
Introducing the environmental parameters derived by the LMD-GCM (global Circulation Model) is possible to limit the variability of most of the parameters specific to the observation, leaving as variable for a fit only the ground pressure. With this model we propose the possibility of detection and analysis of lee waves even without the presence of clouds.

The UV Spectrometer of SPICAM : Instrument Description, In-orbit Performances and Overview of Scientific Results (invited)

Bertaux, Jean-Loup; Bertaux, Jean-Loup; Korablev, Oleg; Quemerais, Eric; Perrier, Séverine; Dimarellis, Emmanuel; Reberac, Aurelie; Fedorova, Anna; SPICAM Team, The

SPICAM, a light-weight (4.8 kg) UV-IR dual spectrometer on board Mars Express orbiter, is dedicated primarily to the study of the atmosphere of Mars. The UV imaging spectrometer (118 - 320 nm, resolution 1 nm, intensified CCD) was designed primarily to atmospheric vertical profiling by stellar occultation. The wavelength range was dictated by the strong UV absorption of CO2 (l<200 nm) and the strong Hartley ozone absorption (220-280 nm) which on Earth protects life from UV solar radiation. The optical scheme contains one parabolic off-axis mirror, a retractable dual-slit system, and a holographic grating, focusing the spectrum image of the slit on the front end of a Hamamatsu intensifier with a CsTe solar blind cathode; the phosphor side of the intensifier is connected to a Thomson CCD 7863 through a fiber optics window. This detector combination allows to change the gain, providing a large dynamic range. This allows to look at weak and bright sources: from the sun (through a dedicated lateral viewport) to very weak aeronomical emissions on the night side of Mars. At highest gain, photons are actually counted. The CCD may be read in various binning modes, allowing a great versatility of observation modes: nadir and limb viewing (both day and night), solar and stellar occultations. As an introduction to several other SPICAM presentations in this conference, we will review a number of original findings made by SPICAM during 2004:

-the first vertical profile of density/temperature of CO2 (20-150km) obtained ever from an orbiter . About 1 or 2 profiles are obtained each day, with the objective of consolidation of climatic models needed for aerocapture, aerobraking, and EDL (Entry, Descent, Landing).

- numerous vertical profiles of ozone (only one was recorded before by Phobos mission) and cloud layers.

- the systematic measurement of total vertical ozone along track on the dayside, from its UV absorption imprinted in the solar light scattered by the ground and atmosphere.

- the first simultaneous measurements of ozone and water vapour (with IR channel) from an orbiter.

- the discovery of a new population of small particles (reff<0.15µm) in the atmosphere of Mars, both from occultations and from day side limb emission.

- the discovery of nightglow NO bands in UV and implications for atmospheric transport.

-the first measurement of H2O and CO2 ices albedo spectrum

- the detection of an absorption feature in the normal reflectance of Phobos around 220 nm, mimicking the famous organic interstellar dust signature.

- a search for auroral activity near the crustal remnant magnetic field, and thorough study of the ionosphere-upper atmosphere through high-altitude aeronomical observations.

All these successes are the result of a highly capable spacecraft, and engineers and scientists dedicated to the design, building, testing of the instrument, integration on the spacecraft, and complex operations managed at ESOC. The instrument was build at Service d'Aéronomie du CNRS (France), BIRA (Belgium) and IKI (Russia).

In-flight Performances and Scientific Achievements of the SPICAM AOTF near IR Spectrometer: an Overview

Korablev, O.; Bertaux, J-L.; Fedorova, A.; Kiselev, A.; Dimarellis, E.; Perrier, S.; Reberac, A.

The near-IR channel of SPICAM experiment on Mars Express spacecraft is a 800-g acousto-optic tuneable filter (AOTF)-based spectrometer operating in the spectral range of 1-1.7 mm with resolving power of ~1700. It was originally put aboard as an auxiliary channel dedicated to nadir H2O measurements in the 1.37-mm spectral band, redundant to similar measurements of PFS. This primary scientific goal of the experiment is achieved though successful water vapour retrievals from individual spectra, resulting in spatial and seasonal distributions of H2O. Besides, well-resolved spectra in the 1-1.7 mm range allows to do a number of additional important measurements, such as ozone abundance above 15-20 km via O21D 1.27-mm emission, detection of H2O and CO2 ices and their characterisation due to signatures at 1.5 mm and throughout the spectral range, polarization and spectral description of aerosols. These results will be overviewed with the emphasis on in-flight performances and flight operations of the instrument. Prospective of SPICAM IR sun occultations, and possible synergies with PFS and OMEGA will be also discussed.

Retrieval of Vertical Distributions of CO_2, Density, Temperature, Ozone, and Dust Properties from SPICAM Solar and Stellar Occultations

Quémerais, E.; Bertaux, JL; Rannou, P.; Perrier, S; Lebrun, JC; Korablev, O.; Fedorova, A.; Tamminen, J; Kyrola, E

SPICAM is the first instrument to perform stellar occultations on Mars. The purpose is to use the spectral absorption properties of atmospheric components to retrieve their vertical distributions. The SPICAM UV spectrometer covers the wavelength range 110-30 nm, which encompass the whole CO2 absorption band (110-200 nm), and the ozone Hartley band centered at 250 nm. Dust is absorbing everywhere, but is easier to see above 200 nm, clear of the CO2 absorption. We use hot stars, which provide more UV than the sun below 200 nm, and stellar occultations may probe therefore higher altitudes than solar occultations. During one occultation, MEX is maintained in a fixed inertial direction, and the atmospheric transmission T(ƒÜ,z) (as a function of wavelength ƒÜ) is measured each second by comparing the star spectrum F0(l) recorded outside the atmosphere to the spectrum F(l,z) recorded when the line of sight goes through the atmosphere, at a tangent altitude z:

T(l,z)= F(l,z)/ F0(l)

The first step of the processing is to establish the transmission by correcting from instrumental effects (i.e., the CCD Dark Current) and some background light sometimes present at the limb.
The second step is to fit the measured transmission at each altitude by a simple forward model (spectral inversion):

Tmod(l,z)=exp(-sCO2(l)*N(CO2)- sO3(l)*N(O3)- sdust(l))

where sCO2(l), sO3(l) are respectively the cross sections of CO2 and ozone and N(CO2), N(O3) their slant density (along the line of sight), and ƒädust(ƒÜ) the optical thickness of dust, described by one, 2 or 3 parameters as a function of l. The third step is to perform the vertical inversion of the slant densities, to retrieve the local densities by a modified onion peeling technique, including Tikhonov regularization.
From the retrieved CO2 density, the vertical profile is integrated from the top to yield the pressure, and the law of perfect gases is applied to determine the temperature. The CO2 density is retrieved from about 150 km down to 10-30 km, depending on the dust load in the lower atmosphere, where the star signal disappears. For solar occultations, a lateral viewport is used, and 5 points on the sun are recorded together, allowing to retrieve 5 profiles at each occultations which can be merged together.
We will present some details of each of the three steps, both for stellar occultations and solar occultations, and some statistics on the observations which have been obtained so far with Mars Express. An expected finding is that star occultations on the deep night are preferred, because of minimal limb light background.

Analysis of the Mars Express Observations of the Atmosphere and the Polar Caps : Interpretation with a Global Climate Model

Forget, F.; Bibring, J. P.; Bertaux, J. L.; Formisano, V.; Paetzold, M.; Angelats I Coll, M.; Bottger, H.; Doute, S.; Drossart, P.; Encrenaz, T.; Federova, A.; Gonzalez-Galindo, F.; Grassi, D.; Haberle, R. M.; Hinson, D.; Korablev, O.; Langevin, Y.; Lebonnois, S.; Levrard, B.; Melchiorri, R.; Montmessin, F.; Quemerais, E.; Schmitt, B.

The Mars Express payload includes a suite of instrument which renew our view of the Mars Climate System. To make themost of these combined observations and help to interpret them in the general context of Mars Climate Science, we will compare these observations with simulations from our Global Climate Model (GCM) developped at LMD in collaboration with the University of Oxford and IAA in Granada. This model includes a state of the art parameterization of the water, CO2 and chemical cycle, and has recently been extended into the thermosphere. This talk will include the following aspects:

1) An analysis of the thermal structure as observed with the various instruments, in particular with Spicam stellar occultations, PFS inversion of the 15 microns band and MaRS radio-occultation temperature profiles.

2) An analysis of the composition of the polar caps (water, CO2, dust components, grain size) as observed by Omega in particular. The model can simulate the evolution and the stratification of these various components, and it helps to shed light on the physical process at work.

3) A comparison with the observed measurements of the water vapor. The different wavelengths observed by the Mars Express instruments can provide different values, sometime contradictory. With the help of the model we can try to reconcile these observations and possibly help to identify some new sources.

4) Tranport of tracers by the martian atmosphere. Among the surprising results from Mars Express are the observations of methane and other trace gases exhibiting spatial variations. We have performed theoretical observations with various lifetimes, sources and sinks to better constrain the nature of the processes affecting these gases.

Ozone Retrieval from SPICAM UV and Near IR Measurements: a First Global View of Ozone on Mars

Perrier, S.; Bertaux, J-L.; Quemerais, E.; Korablev, O.; Fedorova, A.; Lefèvre, F.; Lebonnois, S.

SPICAM uses four methods to measure ozone on Mars: the UV stellar occultations and solar occultations both provide unique vertical distribution, but at a limited number of points (typically 1 to 2 per day). In the nadir viewing geometry, the total vertical ozone content is measured from its broad UV absorption near 250 nm, while the emission line of O2 at 1.27 µm, produced when O3 is photo-dissociated, is a measure of ozone favoring the contribution above 20 km. Typical results from the 4 methods will be presented, in order to assess their performances. Vertical profiles, as well as along track nadir (total column) measurements, will be compared to model predictions for various seasons and latitudes. A first attempt to establish an ozone martian climatology will be presented.

Intercomparison of the SPICAM and PFS Measurements of Water Vapour in the Martian Atmosphere

Fedorova, A.; Ignatiev, N.; Formisano, V.; Bertaux, J-L.; Korablev, O.; Perrier, S.

Mars-Express mission caries out an intensive investigation of waver vapor in Martian atmosphere. The H2O measurements are performed by PFS, SPICAM, and OMEGA instruments in several spectral ranges and with various spectral and spatial resolution. The two relatively high resolution spectrometers, PFS and AOTF channel of SPICAM, have overlapping spectral ranges and comparable resolution (1.8 and 4 cm-1, respectively), which makes especially useful the joint analysis of their data to avoid the influence of calibration uncertainties on the results. The PFS measurements in the three H2O bands, 30-50, 2.56, and 1.38 um are compared with those of SPICAM in the 1.38 um band. Reasons of discrepancies are discussed.

Detection of Cloud layers with SPICAM Occultations

Quemerais, E.; Bertaux, J-L. ; Montmessin, F.; Rannou, Pascal; Korablev, O.

Whereas limb observations allow the detection of clouds on the day side of the planet, stellar occultation is the most powerful technique for night-time observation of aerosol layers.
When analyzing a SPICAM star occultation, the vertical distribution of aerosol opacity
is readily retrieved by inverting Abel's integral (with Tikhonov regularization if necessary). On many star occultations, one or more detached layers of aerosols are found in the vertical profiles of extinction. These detached layers are likely cloud particles (H2O or CO2).
A first analysis of a number of SPICAM occultations will be presented, and compared to Viking observations (Jaquin et al.,) of visible light scattered at the limb. Optical parameters of the detached layers particles will be compared to standard dust particles.

The Mars Express Orbiter Radio Science Experiment (MaRS) (invited)

Pätzold, M.; Häusler, B.; Tyler, G.L.; Asmar, S. W.; Barriot, J-P.; Dehant, V.; Hinson, D.P.; Simpson, R.A.

The Mars Express Orbiter Radio Science experiment (MaRS) relies on the observation of the phase, amplitude, polarisation and propagation times of radio signals transmitted from the spacecraft and received at ground station antennas on Earth. The radio signals are affected by the medium through which the signals propagate (atmospheres, ionospheres, interplanetary medium, solar corona), by the gravitational influence of the planet on the spacecraft and finally by the performance of the various systems involved both on the spacecraft and on ground.
The radio links of the spacecraft's TT&C subsystem between the orbiter and the Earth will be used for these investigations. A simultaneous and coherent dual-frequency downlink at X-band and S-band via the spacecraft's High Gain Antenna (HGA) is required to separate the contributions from the classical Doppler shift and the dispersive media effects caused by the motion of the spacecraft with respect to the Earth and the propagation of the signals through the dispersive media, respectively.
As part of the Mars Express Orbiter payload, the Mars Express Orbiter Radio Science experiment (MaRS) is performing the following experiments:
(a) the radio sounding of the neutral Martian atmosphere and ionosphere (occultation experiment) to derive vertical density, pressure and temperature profiles in the altitude range from the surface to about 50 km and to derive vertical ionospheric electron density profiles from 80 km to over 400 km as a function of latitude, longitude, local time and planetary season. More than 100 profiles of the atmosphere and ionosphere have been obtained during the first Earth occultation season from April to mid August 2004. More are expected during the second season starting in early December 2004. Quite a number of coordinated observations with SPICAM have been planned and performed during both seasons in order to derive a combined density and temperature profile ranging from the surface to about 150 km altitude. (b) the determination of gravity anomalies in comparison with topographic 3D models for the investigation of the structure and evolution of the Martian crust and lithosphere in selected target areas. Several of these observations have been scheduled starting from mid October 2004 over Valles Marineris, Olympus Mons and Alba Patera. (c) The determination of temporal changes of the low degree and order global gravity field caused by seasonal mass exchange between the planetary poles. This experiment will be performed continuously over the entire mission and hopefully during the proposed extended mission in order to cover several planetary seasons. (d) the determination of dielectric and scattering properties of the Martian surface in specific target areas by a bistatic radar experiment, which was performed twice in 2004 during the commission. (e) the precise determination of the mass and the low order gravity field of the moon Phobos during close flybys in order to characterize its internal structure and origin. Unfortunately, no close flyby could be scheduled for MaRS in 2004.
This presentation will give an overview of the results obtained during the first year in orbit.

Sounding of the Martian Ionosphere by the Radio Science Experiment MaRS on Mars Express

Tellmann, S.; Pätzold, M.; Häusler, B.; Tyler, G.L.; Asmar, S.W.; Carone, L.; Griebel, H.; Hinson, D.P.; Schaa, R.; Selle, J.; Simpson, R.A.; Stanzel, C.; Twicken, J.D.

The radio science experiment MaRS on Mars Express sounded the Martian atmosphere and ionosphere during the first occultation season from April to mid August 2004. More than 100 vertical profiles of the ionospheric electron density have been derived in regions ranging from the northern mid-latitudes to low southern latitudes. The local times are either early morning or late afternoon during local northern spring. Two carrier frequencies at X-band and S-band have been used simultaneously for the sounding and profiles of electron content could also be derived, carrying information on the lateral distribution of electron density. The derived electron density and content profiles have an altitude range from 80 km to more than 1000 km. The ionospheric peak density was found in altitude ranges between 130 and 140 km, and signatures of the ionopause between 350 and 400 km. Examples profiles from the first occultation season (and if already available also from the second season which starts early December 2004) will be presented and compared with models and past observations.

Combined Observations of Vertical Density and Temperature Profiles in the Neutral Martian Atmosphere from SPICAM Stellar and MaRS Earth Occultations

Pätzold, M.; Quemerais, E.; Bertaux, J-L.; Reberac, A.; Lebonnois, S.; Schaa, R.; Tellmann, S.; Dimarellis, E.; Häusler, B.; Hinson, D.P.; Tyler, G.L.; Korablev, O.

Coordinated observations of the SPICAM instrument and the MaRS radio science experiment have been planned and performed in June/July 2004 during the first Earth occultation season of the Mars Express spacecraft. The goal was to compare the retrieved vertical density and temperature profiles in the Martian neutral atmosphere for cross validation purposes.

The SPICAM vertical profiles have been obtained by stellar occultations, using CO2 UV absorption. The atmospheric transmission is measured as a function of wavelength in the range 110 – 310 nm, yielding the CO2 vertical density profile in the altitude range 30 – 140 km. The lower limit may vary from profile to profile because it is affected by dust which leads to star signal extinction. The temperature is derived from the density profile by integration assuming hydrostatic equilibrium.

The MaRS vertical profiles of density and temperature have been derived from the bending of the X-band and S-band radio carrier ray paths in the atmosphere prior to the occultation of the spacecraft by the planetary disk as seen from the Earth. The bending is due to atmospheric refractivity and the vertical density and temperature profiles are again derived assuming hydrostatic equilibrium and the ideal gas law in the altitude range from the surface to about 50 km.

Both, the SPICAM and the MaRS data sets overlap in the altitude range between 30 and 50 km. The coordinated observations have been planned for locations where the footpoint coordinates of both profiles have been within 10° in latitude and 20° in longitude. The coordinated SPICAM and MaRS observations for each location have then been performed within a maximal 60 hours time difference, sometimes in the same orbit.

Both data sets will be presented. Each data set is also compared with the Mars GCM climate model from LMD to compensate for not perfect coincidences of time and location.

Analysis of SPICAM UV and Near IR Solar Light Scattered at the Limb by Aerosols: Evidence for Vertical Variation of Particle Size Distribution

Rannou, P.; Bertaux, J-L.; Quemerais, E.; Perrier, S.; Korablev, O. Federova, A.

SPICAM has measured scattered light at the limb of Mars, in UV and IR simultaneously. The UV spectrometer channel (between 200 and 300 nm) carries valuable informations about the size and number of dust particles above 50 km up to 80 km. In particular, the radiance factor increases with altitude in UV, while the IR spectrometer (1 to 1.7 microns) shows a radiance factor decreasing with increasing altitude, demonstrating that IR data probe lower atmosphere level than UV data. Combining the two sets of data, we are able to draw a consistent picture of dust and cloud vertical profile at several locations and seasons along the martian year. Especially, the UV channel is sensitive to a high altitude small dust component which is directly detected for the first time (simultaneously with stellar occultation measurements in extinction). Such a dust component may have a strong effect on climate through its ability to trigger water condensation and produce clouds, to promote transport of water and to locally modify atmospheric thermal equilibrium. Finally, the size and number of these small aerosol particles should give constraints on the nature of this dust component.

High-altitude Aerosol Particles on Mars: Implications for Water Cycle and Thermal Regime of the Atmosphere

Rodin, A.; Bertaux, J-L.; Rannou, P.; Quemerais, E.; Korablev, O.; Rybakova, A.; Wilson, J.

The detection of the deep, rarefied, optically thin aerosol layer extending up to 50-60 km in the atmosphere of Mars from the limb and stellar occultation data of the SPICAM UV channel raises questions about its nature and impact to the state of the atmosphere. Indeed, the presence of widespread, tiny dust particles in the martian atmosphere has been presumed by early model works as a possible source of condensation nuclei for water ice clouds.Homogeneous nucleation of water ice is strictly forbidden at Martian temperatures even in high supersaturation conditions, and external particles are required to form clouds.

3D GCM simulations of the water cycle in the Martian atmosphere, taking into account microphysical processes including condensation,coagulation and sedimentation, show that the observed seasonal evolution of water suggests that cloud formation occurs in a broad altitude range, including high altitudes where the presence of submicron nucleation having sufficient lifetime of levitation is required. The absence of such condensation centers would result in significant losses of the atmospheric water onto polar caps, particularly in the equinox season, through high supersaturation at the tropopause level. Another possible effect of the fine-sized, high altitude aerosol fraction, composed of tiny dust particles and water ice crystals, is heating the atmosphere above 40 km by direct absorption of the solar shortwave radiation. Resulting temperature distribution in turn affects the conditions of water saturation and condensation in the middle atmosphere of Mars. Simulations of possible mechanisms of supply and removal of the particles from the atmosphere are presented.

Detection of Martian Nightglow NO Bands in UV and Implications for Atmospheric Transport

Bertaux, J-L.; Leblanc, F.; Perrier, S.; Quemerais, E.; Korablev, O.; Simon, P.; Dimarellis, E.; Reberac, A.; Forget, F.; Stern, S.A.; Sandel, B.

We report for the first time the detection of light emissions in the night side of the atmosphere of Mars by the SPICAM UV spectrometer. The UV spectrum of this nightglow is composed of the (expected) Hydrogen Lyman a emission (121.6 nm), and of the g and d bands of nitric oxide (NO, 190-270 nm) produced when N and O atoms combine to produce the NO (nitric oxide) molecule. N and O atoms are produced by EUV photo-dissociation of O2, CO2 and N2 in the dayside upper atmosphere, and transported to the night side. Observations were recorded at several orbits, requiring a special "limb grazing" mode to enhance signal. We found that the NO emission is brightest in the winter south polar night, which can be explained by continuous downward transport of air in this region permanently in the night at this season (Ls=74°, southern winter), and where CO2 condenses at ground level. It offers a new way to study the general circulation mechanisms by remote sensing of the upper atmosphere from Mars orbiters.

Mars Express/SPICAM UV: First Results on the Martian Upper Atmosphere

Leblanc, F.; Bertaux, J-L.; Chaufray, J.Y.; Witasse, O.; Lilensten, J.; Quemerais, E.

The first results obtained by SPICAM in the UV dayglow mode during the beginning of 2004 will be described. The different clearly identified emissions of the dayglow are the Lyman alpha, the C (156.1 and 165.7 nm) and O (130.4 and 135.6) emissions, the CO 4+ bands, the CO Cameron band, the CO2+ band at 289 nm and O (297.2 nm) emissions. Their putative origins and comparison with model will be given. The typical information on the structure and composition of the main ion and neutral species in the Martian upper atmosphere that can be deduced from zenith angle and altitude coverage will be underlined. The results for a search of auroral emission in the martian nightglow will be also described in this presentation.

Martian Water Vapor Observations with PFS-Mars Express

Lellouch, E.; Fouchet, T.; Ignatiev, N.; Titov, D.; Encrenaz, T.; Billebaud, F.; Formisano, V.; Grassi, D.; Giuranna, M.; Tschimmel, M.

The PFS instrument onboard Mars Express records several hundreds of spectra per obserbing orbit, covering the 1.2-5.5 and 6-50 micron range. Water vapor is detected in the 1.38 and 2.6 micron bands as well as in rotational lines longward of 30 micron. We will present an analysis of these data in terms of geographical, latitudinal, and temporal variations of the water abundance in the martian atmosphere. Particular emphasis will be given on the water cycle and comparisons with earlier findings.

Distribution of Argon in Mars' Atmosphere as Measured by the GRS on Mars Odyssey: Aid to Understanding Martian Meteorology

Sprague, A.; Boynton, W. V.; Kerry, K. E.; Janes, D. M.; Reedy, R. C.; Metzger, A. E.

Measurements made by the 2001 Mars Odyssey Gamma Ray Spectrometer (GRS) of 1294 keV gamma-rays resulting from the 110 minute half-life decay of 41Ar show significant variations with season and latitude. The atmosphere is enriched with Ar relative to CO2 over both the southern and northern polar regions during winter with the greater enhancement observed in the south. While the Ar concentration increases until winter solstice over the northern polar region, fluctuations in the relative amount of Ar in autumn and winter indicate periodic mixing of atmosphere from lower latitudes. In contrast, the rise in Ar concentration over the south-polar region reaches a well-defined maximum at the beginning of winter and then smoothly drops to a minimum in spring. These differences in Ar behavior indicate differences in mixing characteristics between the northern and southern polar regions. Both polar regions exhibit a significant drop in Ar concentration in late winter and spring as the polar atmosphere is mixed with pure CO2 from the subliming perimeter of the CO2 ice caps.

We acknowledge the contributions of the entire GRS team, Bob Haberle for providing great discussion and the NASA ARC MGCM output 2002.17 for analysis purposes, and funding from NASA contract no. 1228726.

Low-Altitude Ionospheric Plasma Energization at Mars – ASPERA 3-Findings

Lundin, R.

The Analyzer of Space Plasma and Energetic Atoms (ASPERA)) on-board the Mars Express spacecraft (MEX) found that the solar wind plasma and accelerated ionospheric ions may be observed all the way down to the MEX pericenter of 270 km above the dayside planetary surface. This is very deep in the ionosphere, implying a direct exposure of the martian topside atmosphere to solar wind plasma forcing. The solar wind forcing results in an energization of ionospheric plasma. The low-altitude ion energization and outflow near Mars is surprisingly similar to the ion energization and outflow over the strongly magnetized planet Earth - from narrow "monoenergetic" ion beams to beams with a broad energy distribution. The ion outflow near the planet is in the direction of the external sheath flow, i.e. the ion energization is the result of a localized and direct solar wind momentum exchange. On the other hand the distribution of the energized plasma implies similar energization processes like that over the Earth, i.e. energization in a magnetized environment by waves and/or parallel (to B) electric fields. But the boundary conditions for Martian plasma energization is different from that of the Earth - a weak local magnetic field and penetration of solar wind plasma deep into a cold and dense ionospheric plasma.
This report will be discuss results from the first year of ASPERA-3 investigations on the low-altitude energization of plasma near Mars.

Review of Energetic Neutral Atom Imaging Results from the ASPERA-3 Experiment

Barabash, S.; The ASPERA -3, team

ENAs (Energetic Neutral Atoms) at Mars result from two processes (1) charge - exchange of the solar wind and planetary plasma on the exospheric gasses, and (2) backscattering of the precipitating ions from the upper atmosphere. The ASPERA - 3 experiment on Mars Express performs ENA imaging in the energy range 0.1 - 10 keV. We review the results of the ASPERA - 3 ENA imaging at Mars with focus on the following observations (1) mapping of the solar wind precipitation onto the Martian upper atmosphere, (2) determination of the total energy influx from the solar wind into the upper atmosphere, (3) imaging of proton plasma distribution in the subsolar region, (4) exospheric sounding with ENAs. We also provide update on the detection of the unknown neutral beams of 1 keV coming from unidentified sources in the interplanetary medium.

Energetic Neutral Atom Investigations of Mars' Environment

Mura, A.; Orsini, S.; Milillo, A.; Massetti, S.; D'Amicis, R.

Issues related to the detection of Energetic Neutral Atoms (ENA) coming from Mars' environment are discussed here. ASPERA-3 data from both NPD (Neutral Particle Detector) and NPI (Neutral Particle Imager) are analysed and compared to simulated signal. Open questions, such as the search for extra ENA signals that may be related to the presence of magnetic anomalies on the surface of Mars, or related to Phobos' outgassed materials, are also discussed in this frame.

Expected Influence of Crustal Magnetic Fields on ASPERA-3 ELS Observations: Lessons from MGS

Brain, D.; Luhmann, J.; Mitchell, D.; Lin, R.

Mars lacks a global magnetic field, and therefore the solar wind interacts directly with the atmosphere over much of the planet. Over some regions, however, Mars' crustal magnetic field is strong enough to locally stand off the solar wind to altitudes >1000 km, shielding the enclosed atmosphere. Like Earth's polar cusp regions, Martian crustal fields do not act as perfect shields for the atmosphere. At times, crustal magnetic field lines connect with the interplanetary magnetic field (IMF), providing conduits for charged particle exchange between the solar wind and lower ionosphere. These open field lines have been observed using electron energy spectra and pitch angle distributions from Mars Global Surveyor (MGS). The volume of atmosphere protected by crustal magnetic fields as well as the extent and variability of open field lines has implications for atmospheric escape to space and the energetics of the upper atmosphere.

Electron and magnetic field data from the Mars Global Surveyor MAG/ER instrument provide a means of measuring the influence of crustal sources on nonthermal escape processes. The angular distribution of electrons observed by the electron reflectometer (ER) can be used to determine where and when crustal magnetic field lines are connected to the IMF. Using more than five years of data from the MGS mapping orbit, we have classified ER observations of electrons at 115 eV according to the topology of the magnetic field. This extended data set allows us to quantify the effects of a number of parameters that control magnetic field topology at 400 km. We will show where open and closed field lines are likely to occur, and how changes in solar wind pressure or the direction of the interplanetary magnetic field affect the locations of open field regions. From these results we will calculate the fraction of Mars' atmosphere that is shielded from the solar wind under different conditions, and the fraction of the lower ionosphere accessible through cusps.

The electron spectrometer (ELS) on ASPERA-3 has many observational advantages over the ER instrument on MGS. ELS provides full 3D electron distributions, ELS data can be correlated with concurrent ion observations from IMA, and the elliptical orbit of Mars Express enables lower altitude observations of the Martian cusp regions than are currently possible with MGS. One disadvantage of the ELS instrument is the lack of an onboard magnetometer. We will discuss how concurrent MGS data can be leveraged to provide information on the draping direction of the solar wind magnetic field and the upstream solar wind pressure. Additionally, models of the crustal magnetic field derived from MGS data can be used to determine the likely orientation of the ambient magnetic field when Mars Express is above strong crustal sources. This information might be used to explore pitch angle distributions and to probe weak crustal magnetic fields. Finally, we will discuss how heat flux electrons can be used to decipher the magnetic field at Mars Express, given what is known from MGS.

Observations of Magnetic Anomaly Signatures in Mars Express ASPERA-ELS Data

Soobiah, Y.; Coates, A.; Linder, D.; Winningham, D.; Frahm, R.; Lundin, R.; Barabash, S.; Holmström, M.

We present observations made by the ASPERA-3 Electron Spectrometer, near magnetic anomalies in the Martian crust. We have found local plasma near remanent magnetic fields either increases in flux to form intensified signatures or significantly reduces to form plasma voids. An initial statistical analysis show intensified signatures are mainly a dayside phenomena and voids as a feature of the night hemisphere.

Martian Ionospheric Photoelectrons: ASPERA-ELS Measurements

Coates, A.; Soobiah, Y.; Winningham, D.; Frahm, R.; Sharber, J.; Lundin, R.; Barabash, S.

The electron spectrometer (ELS), part of the ASPERA instrument on Mars Express, has made new measurements of ionospheric photoelectrons at Mars. ELS has a high energy resolution mode, especially suited for these observations. We will compare ionospheric measurements on the day and night sides of Mars, looking in particular at ionospheric photoelectrons on the day side. We find evidence for the photoelectron peak, Auger features, and the turn-on of ionospheric photoelectrons at dawn. We compare these observations with those on the night side.

3D Structure of the Solar Wind Interaction with the Mars Ionosphere

Maezawa, K.; Jin, H.; Kubota, Y.

With the triangular mesh we performed 3D global simulation of the solar wind interaction with Mars with a high spatial resolution. Some of our important findings are:
(1) On the dayside, the solar wind dynamic pressure is the principal factor controlling the total balance between the production and loss of ionospheric ions. When the solar wind dynamic pressure is low, there occurs an excess of ion production against chemical loss and ionospheric ions flow upward to withstand the solar wind at the ionopause. On the contrary, when the solar wind pressure is high, the chemical loss exceeds the production in the ionosphere, and the solar wind ions move downward to help balance the loss in the lower ionosphere.
(2) When the latter case occurs, the IMF field lines descend toward the surface slowly with the solar wind ions, picking up newly ionized particles on their way, so that there occurs a broad transition region where solar wind ions coexist with ionospheric ions. This transition layer connects smoothly to the lower ionosphere without discontinuity.
(3) On the nightside, the field tension exerted by IMF is the principal factor controlling the nightside ionospheric structure. A ridge of the ionospheric density is produced in the plane perpendicular to the IMF because of more rapid transport of dayside ionspheric ions toward nightside in this plane. In the wake of Mars, flow vortices are produced by the flow detached from the ionosphere by the field tension.
(4) The total (global) escape rate of ions from the Mars ionosphere depends strongly on solar wind parameters, being an increasing function of solar wind density, velocity, and IMF magnitude.
Based on these results, the observation results from Mars Express are discussed.

Escape of CO and $C0_2$ ions from the Martian Ionosphere

Fedorov, A.; Andrei Budnik, E.; Carlsson, E.; Barabash, S.; Sauvaud, J-A.; ASPERA Team

According to the Viking measurements and theoretical models, martian ionosphere contains non-negligable fraction of CO+ and CO2+ (up to few percent of O+ contents) ions. Due to the strong solar wind - ionosphere interaction, ionospheric ions can be accelerated, pushed antisunward, and finally escape from the planet.
The most recent Mars Express results indicate that the reservoirs of carbon containing materials on the surface and in the atmosphere are not large enough to store all amount of carbon which as believed was present in the ancient Martian atmosphere. The escape induced by the solar wind interaction may be one of the channels of carbon escape.One can assume that carbon containing accelerated ions should be observed in the martianwake along with the oxygen ions. Thus the study of the ion composition of the martian wake can help to estimate the carbon escaping rate and clarify the mechanism of carbon losses.
To obtain CO+ and CO2+ flow in the marian tail we have studied in detail the IMA (ASPERA-3) mass-analyzer data. The difficulty of this study is that CO+ peak (M/Q = 28) is rather close to the O2+ peak (M/Q = 32). Yet the weak flow of CO2+ (M/Q = 44) should be distinguished from the intense peak of O2+. This problem has been solved by accurate fitting of different species to the measured spectra. We have found that in particular cases CO2+ and C0+ can be a significant part of the outgoing ion flow. We present the statistics of appearance of these carbon containing ions in the martian tail.

The Mars Thermospheric Circulation : Recent Constraints from MGS and Odyssey Aerobraking and Mars Express (SPICAM) Measurements

Bougher, S.; Bell, J.

The thermospheric wind patterns of Earth and Venus have been constrained using an assortment of ground-based and spacecraft measurements over the past 40-years [e.g. Bougher et al., 2002]. Multi-dimensional (3-D) thermospheric general circulation models (TGCMs) have subsequently been used to investigate the underlying forcing mechanisms that maintain these circulation patterns and drive variations over various timescales (e.g. solar cycle, seasonal, diurnal, etc).

The global thermospheric wind patterns for Mars can now be investigated using new constraints from recent aerobraking and Mars Express measurements. Mars Global Surveyer (1997-1999) and Mars Odyssey (2001-2002) Accelerometer datasets obtained during aerobraking exercises provide density and temperature distributions over limited local time and latitude regions at lower thermospheric altitudes (~100-160 km) [e.g. Keating et al., 1998; 2003; Withers et al., 2003]. Latitudinal gradients of these fields (i.e. into the winter polar night) vary greatly with the changing Martian seasons. The observed winter polar warming features serve as a tracer of the strength and variability of the Martian thermospheric wind patterns during solstice conditions [Bougher et al., 2003]. Aerobraking data is also being used to estimate cross-track (zonal) wind speeds in the Mars lower thermosphere [e.g. Withers et al., 2002]; corresponding spacecraft navigation data can also be used for the same purpose. Most recently, the Mars Express SPICAM instrument discovered nitric oxide (NO) nightglow spectral features in the γ- and δ-bands from limb observations (Ls = 74º) [Bertaux et al., 2004; Stern et al., 2004]. These observed UV nightglow emissions are brightest in the winter polar night region, providing another tracer of the strength and variability of the Martian thermospheric wind system, at least during solstice conditions.

These new constraints for Martian thermospheric winds are now investigated using Mars TGCM simulations for Ls = 90º and 270º conditions appropriate to the MGS and Odyssey aerobraking datasets described above. Implications for the NO nightglow morphology and intensity will also be discussed. Lastly, these tracers of the Martian thermospheric circulation will be compared to those gleaned earlier from Venus using various Pioneer Venus Orbiter measurements [e.g. Bougher et al., 1997].

References:

Bougher, S. W., M. J. Alexander, and H. G. Mayr, Upper Atmosphere Dynamics: Global Circulation and Gravity Waves, in Venus II, pp.259-292, U. of Arizona Press, (1997).

Bougher, S. W., R. G. Roble, and T. J. Fuller-Rowell, Simulations of the Upper Atmosphere of the Terrestrial Planets, in AGU Monograph : Comparative Aeronomy in the Solar System, Eds. Mendillo, Nagy, and Waite, (2002).

Bougher, S.W., and J. R. Murphy, Polar warming in the Mars lower thermosphere: Odyssey Accelerometer data interpretation using coupled general circulation models, EOS Transactions, AGU Supplement, 84 (46), P21C-05, (2003).

Keating, G. M. et al., Science, 279, 1672-1676, 1998.

Keating, G. M., et al., Brief review on the results obtained with the MGS and Mars Odyssey 2001 Accelerometer Experiments, International Workshop: Mars Atmosphere Modelling and Observations, Granada, Spain, January 13-15, (2003).

S. A. Stern et al, Detection of Nightglow in the Upper Atmosphere of Mars by SPICAM Aboard Mars Express, DPS Meeting Abstract, Louisville, KY, (2004). Also J.-L. Bertaux et al, Science, (2004)?

Withers, P. G., S. W. Bougher, and G. M. Keating, Icarus, 164, 14-32, (2003).

Withers, P. G., S. W. Bougher, and G. M. Keating, MGS Accelerometer-derived Profiles of Upper Atmosphere Pressure and Temperatures : Similarities, Differences, and Winds, EOS Trans. AGU, 83(19), Spring Sci. Mtg Suppl., Abst. P41A-10, (2002).

Remapping Phobos using Mars Express HRSC / SRC images

Duxbury, T.;Hoffman, H.; Oberst, J.; Giese, B.; Kirk, R.; Neukum, G., and the HRSC Co-I Team

Updating the current Viking-based Phobos global control network, the geoid model, the rotational model with forced librations, the orbital model with secular acceleration, the digital terrain/image models and cartographic map products using the new Mars Express HRSC/SRC images has begun. The global control network will be increased from 320 to over 3,000 points allowing a high higher degree and order harmonic expansion to be used to define global shape. The generation of the global control network will include solving for the Phobos orbit and rotational state. The images already indicate that a 12 – 13 km orbit position correction is needed. Determining whether this is due to secular acceleration will require a few years of HRSC/SRC observation, giving complete orbital coverage. Both the combination of improved shape model (moments of inertia) and higher spatial resolution from the HRSC/SRC images over Viking will enable the amplitude of forced rotational libration, about 0.9 deg, to be determined more precisely as well. Combining all of these results will allow high-resolution digital terrain models (DTM's) and digital image models (DIM's) to be produced, useful for future sample return missions such as the Russian GRUNT mission.

HRSC/SRC Imaging Results from the Phobos and Deimos Flybys

J. Oberst, T. Duxbury, B. Giese, H. Hoffmann, K. D. Matz, T. Roatsch, G. Neukum, and the HRSC Co-I Team

From May through August 2004, Mars Express had six encounters with Phobos. The small (13x11x9 km) Martian satellite was observed at ranges from 1900 km to as close as 150 km at a large range of solar phase angles between 23° and 84°. All except the first of the flybys occurred at similar positions of Phobos during its orbit about Mars. During these flybys, the High-Resolution Stereo Camera (HRSC) on board obtained scanner-images in 5-fold stereo. Additional framing images were obtained by the HRSC's Super Resolution Channel (SRC). The high intrinsic geometrical precision of the imaging experiment permitted us to carry out astrometric observations of Phobos. Fortuitously, observations of known stars together with the Phobos limb allowed us to separate camera pointing errors from Phobos positional offsets. Analysis of data from all flybys show consistently that the satellite has advanced by ~6 sec. (corresponding to 12 km along the orbit) beyond what is predicted by its ephemeris from the Viking era. There is no appreciable offset of the predicted Phobos' orbit parameters in the radial (towards Mars) or out-of-orbit-plane direction. In the past weeks, Mars Express has returned images from Deimos for the first time – which are still awaiting analysis at the time of writing. More Martian satellite flybys and HRSC observations are expected in the coming months and through 2005.

Fig. 1: Observations of Phobos during orbit 413 (May 18, 2004) by the 5 panchromatic channels of HRSC, showing Phobos from slightly different perspectives. While the Nadir channel was operated in full resolution (center), the other channels were run with 2x2 pixel summation.

The Parallel Grooves of Phobos: New evidence on their Origin from HRSC Mars Express

Murray, J.B.; Muller, J-P.; Iliffe, J.C.; Neukum, G.; HRSC Co-Investigator, Team

The origin of the grooves of Phobos has been debated since they were first discovered, and there is as yet no consensus on their origin. Early hypotheses included faults or outgassing vents caused by tidal or drag forces during the capture of Phobos, and chains of secondary craters or fracturing associated with the Stickney impact. More recently, it has been suggested that they result from chains of secondary craters from large impacts on Mars. This last hypothesis predicts that the leading apex of Phobos should be the most heavily grooved, with families of parallel grooves crossing each other at all angles, but deciding between these various hypotheses has been hampered by the fact that only about half of Phobos has been imaged by previous missions with sufficient resolution and illumination to detect the grooves. Phobos has now been imaged on 5 passes by HRSC, and on two of them, the leading apex is visible at 48m and 50m resolution. Despite unfavourable vertical illumination, it can be seen to be heavily grooved, with orientations corresponding closely to those predicted by the last idea. This is overwhelming evidence that the grooves of Phobos were caused by debris ejected from large impact craters on Mars.

Phobos Observations with SPICAM UV and near IR Measurements

Perrier, S.; Bertaux, J-L.; Korablev, O.; Fedorova, A.; Levasseur-Regourd, A.C.; Stern, A.

The orbit of MEX provided five close encounters with Phobos, with distances ranging from 162 to 1895 km . In the UV (FOV 0.16 x 0.02° plus drift), we obtained spatially resolved spectra of the Phobos surface backscattered solar light for all encounters, while in the near IR, the 1° FOV allowed spatial resolution only for the closest approach. In the UV (110-310 nm), all spectra are alike: there is no significant spatial variation of the spectral reflectance.

The combination of all spectra allows to produce a high S/N curve of the spectral reflectance. It is very low (~0.015), and shows a distinct broad absorption feature around 220 nm, and one weaker absorption at 260-270 nm (possibly a silicate feature). The 220 nm may be fitted by organic materials produced in the lab to interpret the well known Interstellar Medium (ISM) extinction feature.

The IR albedo spectra show a noticeable slope between 1.1 and 1.7 µm. The two IR channels are probing orthogonal polarizations, and their ratio changes with the phase angle (different for each encounter, 20 to 60 °). This is consistent with the idea that Phobos? surface is composed of a powder of small particles (<1 µm), containing carbon under the form of organic materials (identified from UV data).

The Search for Life on Mars

Everett K. Gibson, Mars Express Interdiscipline Scientist, Mail Code KR, Astromaterials Research Office, NASA Johnson Space Center, Houston, TX 77058 U.S.A.

The search for life on Mars has gone on for more than a century. From the telescopic observations made famous by G. Schiaparelli and P. Lowell at the start of the 20th Century to the development of the Space Age, mankind has sought to know whether life existed on Mars in the past or is present now. There are no greater questions than: "Are we alone in our solar system?" "Is there past or present life on Mars?" The quest for answering these questions has led to more than 35 missions to the red planet. Two-thirds of the spacecraft missions to Mars, as flybys, orbiters or landers, have resulted in failures. The Soviet Union's Mars 2, 3, 5, and 6 and the United States Mariner 4, 6, 7 and 9 cracked open the secrets of the planet by providing information about the atmosphere and by showing that the surface had an abundance of craters, rift valleys, volcanoes, meandering features which appeared to be stream beds and seasonally variable polar caps. The presence of water was detected in the atmosphere along with frozen ice in the polar caps. However, the martian atmospheric surface pressure of 6 to 7 millibars would not permit liquid water to exist unless it was a salty brine. The question arose, "Where has all of the water gone which assisted with the formation of the surface features?"

The two Viking missions to Mars in 1976 carried five life detection experiments: cameras, gas chromatograph-mass spectrometers to seek presence of organic compounds, and three life detection instruments. The life-detection instruments were based upon the principle that should Martian life be present, its metabolism would be similar to the earth's. The gas release and pyrolytic experiments yielded negative results but the labelled-release experiment produced inconclusive results. With the GC-MS failing to find organic carbon concentrations above 1 ppm, the Viking results were interpreted to indicate that no life had been detected.

In the mid-1980s, it was recognized that Martian near-surface samples had been found on Earth. A suite of meteorites known as the SNCs were identified to originate on Mars. Trapped noble gases within the SNCs were identical to the Martian atmosphere measured by the Viking landers on Mars. This discovery allowed scientists to work with Martian samples in terrestrial laboratories using the most sophisticated analytical instruments. The search for life on Mars was in a dormant period until the 1996 announcement that the ALH84001 Martian meteorite possibly contained remnants of possible biogenic activity catalyzed the exploration of Mars. Subsequently, two younger SNC meteorites showed additional evidence of biogenic activity which suggested biology was active on Mars over a 3.5 Gy+ interval. The commitment by the U.S. to sent two rovers to Mars in 2004 to seek evidence of past water was made along with ESA developing the Mars Express mission with its Beagle 2 lander. The Beagle 2 lander had the proper analytical instrumentation to directly measure the nature of biogenic components present on the surface of Mars but the lander failed. The Gas Analysis Package (GAP) with its stable isotope mass spectrometer would measure the abundances, and isotopic composition of all carbon components present within the soils, rocks and atmosphere. The GAP's isotopic analysis of methane in the Martian atmosphere, detected by PFS and SPICAM, would indicate whether the methane had a biogenic or abiotic origin.

For any planet to be habitable for life, as we know it, the presence of water, potential energy sources (i.e. solar, geochemical, or hydrothermal), the presence of carbon and the renewal of nutrient and energy sources by geological activity is required. Mars has shown that it possesses the required properties to support life. The habitability of a planet such as Mars is not a static phenomenon. It changes with time as a function of the position of the planet in the habitable zone of the Solar System along with the geological and biological evolution of the planet. Once life gets started it is extremely difficult to extinguish. Mars has shown us that it meets the requirements for habitable life and it is now up to the scientific community to locate that life should it be present.

The Search for Life on Mars With PFS : Methane , Formaldehyde and Water .

V. Formisano

PFS has detected methane in martian atmosphere (10+- 5 ppbv) but it has also measured formaldehyde (130 +- 50 ppbv) . Formaldehyde seems to be strongly correlated with methane . On the other hand mapping of methane mixing ratio has brought us to the conclusion that it correlates well with the boundary layer water vapour. The map of the water vapour , on the other hand points to a strong correlation with the equatorial underground water ice identified by Odyssey – HEND experiment. Recent modelling of these results and study of Gulleys point to an acquifer layer at 200- 300 m under the surface of Mars. PFS results therefore point to three possible scenarios :

The first (the HOT chemistry) : deep underground where the temperature reaches 400 – 500 Celsius in presence of CO2 and water, CH4 can be formed. As the equatorial ice table is unstable and must be reforbushed from below , methane and water (clathrates) would be slowly moving toward the surface . Formaldehyde could be perhaps formed in methane percolating through 10 –30 cm of dry soil on top of the ice table.

The second (the COLD chemistry) : the permafrost just tens of cm below the surface in the equatorial regions of Mars is continuously bombarded by solar energetic particles and by cosmic rays. There is ,therefore , a resemblance with the cometary environment , specially if we add a daily or seasonal thermal cycling. Comets are well known to host complex chemistry with the generation of complex organic molecules , up to the point that they are considered precursors of life. Mars would be similar to comets and could have the same chemistry and eventually also more complex organic molecules.

The third (LIFE) : 200-300 meters under the surface of Mars in the acquifer region necessary to substain the overall picture resulting from PFS and HEND measurements some sort of biota could be present with methanogetic bacteria producing methane and methanothrophic bacteria oxidising methane and eventually producing formaldehyde (and other molecules?).

The likelihood and the importance of the different scenarios will be discussed with respect to the source power needed to explain the observations : 2.5 million tons of methane are needed per year . Our conclusions point to one decisive measurement to be done in the future : composition in terms of volatiles of the subsurface equatorial permafrost and its underground gradient.

Oxidant Enhancement in Martian Dust Devils and Storms: Implications for Life and Habitability

Atreya, S.; Wong, A-S.; Renno, N.; Delory, G.; Farrell, W.

The Viking Gas Chromatograph Mass Spectrometer (GCMS) found no signs of organics in the surface samples of Mars, while the Gas Exchange Experiment (GEX) showed a rapid release of O2 when nutrients and water were added to the soil. It was suggested that these seemingly contradictory results could be reconciled if the surface contained an oxidant such as hydrogen peroxide (H2O2). In 2003, H2O2 was at last detected in the martian atmosphere [1, 2]. However, the measured mixing ratio of 20-40 ppb – which agrees well with global photochemical models [3] – is too low to account for the above Viking results, even if a large fraction of hydrogen peroxide could diffuse from the atmosphere to the surface.

Here, we will discuss a new mechanism that can produce a substantially greater abundance of H2O2 in the atmosphere, as well as lead to the settling of hydrogen peroxide "dust" on to the surface of Mars. The mechanism is driven by triboelectricity generated in saltation of sand and dust particles or in the surface during martian dust devils and dust storms. Electrostatic fields up to ~25 kV/m have been estimated. Such fields result in a large production of CO/O- and OH/H- in the martian CO2-H2O atmosphere. Using an electro-photochemical model, we calculate that the abundance of H2O2 in the martian atmosphere resulting from above triboelectric fields in dust devils and storms can greatly exceed that produced by the solar UV driven photochemistry.
Even more importantly, a significant amount of H2O2 is expected to condense on dust particles and precipitate out of the atmosphere to the surface as hydrogen peroxide dust, because the atmospheric abundance of H2O2 exceeds that permitted by saturation especially for larger fields. Unlike the gas phase, the residence time of H2O2 bound to dust particles or grains in the regolith would be long, so that large quantities of H2O2 can accumulate in the martian surface. The lack of organics on the martian surface is most likely due to the presence of this powerful oxidant, hydrogen peroxide, or another superoxide processed from H2O2 in the surface of Mars. We are also investigating whether the non-uniform distribution of methane reported by the PFS on Mars Express [4] and ground-based observations [5] could be related in part to the possible non-uniform distribution of such oxidizers as H2O2 in the martian regolith.
Since aeolian processes are believed to have been prevalent throughout the martian geologic history, the associated enhancement of H2O2 in the atmosphere and the existence of H2O2 in the surface, together with the relatively large UV radiation reaching the martian surface, are expected to render the martian surface and near-surface environment antiseptic and consequently inhospitable to life.

References: [1] Encrenaz et al., Icarus 170, 424, 2004; [2] Clancy et al., Icarus 168, 116, 2004; [3] Atreya S.K., and Gu Z., JGR 99, 13133, 1994; [4] Formisano V., Atreya S., Encrenaz T., Ignatiev N., Giuranna M., Science, in press (also in Science Express, 28 October 2004); [5] Mumma et al., DPS Meeting, Louisville, KY, 2004.

Isotopes: Fingerprinting the Sources and Sinks of Martian Methane

Morgan, G.; Wright, I.; Pillinger, C.

The existence of methane in the Martian atmosphere, at the sub ppm level, is now commonly accepted. Ground-based spectroscopic measurements by Krasnopolsky and more recently by Mumma, complemented by the results reported by Formanisano, from the Planetary Fourier Spectrometer (PFS) onboard Mars Express, have all independently verified the presence of this simple, yet most interesting of hydrocarbon species.1,2,3,4

Whilst the presence of this gas is indisputable, the picture portrayed for the actual abundance levels and the global distribution of this gas is confused. The theories about the potential sources and sink processes and are equally as disparate. Krasnopolsky has proposed that methanogenic bacteria, living beneath the surface, are a plausible source of the methane whereas Mumma also considers other working hypotheses including geothermal processes and release from clathrate hydrates.3,4

Methods for monitoring the abundance of atmospheric methane on Earth and assigning origins are well established. Since the late 1970s extensive efforts have been invested in the evaluation of the terrestrial global methane budget, as it is believed to contribute about 16% of the enhanced greenhouse effect. These investigations usually take the form of direct measurements of methane flux densities from various sources which are then extrapolated to the global scale. In 1982, Stevens and Rust proposed that the global budget of methane could be constrained by measuring the stable carbon isotope composition ($\delta^{13}C$) of the methane in its sources, sinks and atmosphere.5 They reasoned that the isotopic composition of the globally averaged atmospheric methane would be the weighted sum of the individual sources corrected for the isotopic shift from the sink processes. Schoell et al. had previously shown that the isotopic composition of methane from different environments would vary because of different formation processes, specific equilibrium fractionation and chemical and biological kinetic isotope effects.6 In reality, the determination of the isotopic composition of a species enables one to derive the chemical and physical history of that compound. Further discrimination of sources have been achieved by parallel (δD) and combined ($\delta^{17}M$) studies on the isotopomers of methane.7,8,9

In situ high precision stable isotope measurements on the methane, and other species potentially involved in the carbon cycle, would constrain the source and sink processes of this most intriguing hydrocarbon on Mars.

The Gas Analysis Package (GAP) onboard Beagle2 had the capability of measuring the stable isotopic composition of host of chemical species, present both in the atmosphere and within solid samples collected by the mole. It was also designed to conduct measurements on the concentration of methane present in the atmosphere, at the landing site, and to monitor any temporal and seasonal variations. An upgraded version of the GAP instrument, utilising the existing static mass spectrometer, would potentially be capable of conducting the stable isotope measurements required to discriminate the primary source and sink processes of methane on Mars.

1) Krasnopolsky V.A., Bjoraker G.L., Mumma M.J., Jennings D.E. (1997) High resolution spectroscopy of Mars at 3.7 and 8μm: A sensitive search for H2O2, H2CO, HCl and CH4 and detection of HDO, JGR, 102 (E3), 6525-6534. 2) Krasnopolsky V.A., Maillard J-P., Owen T.C (2004) First detection of methane in the martian atmosphere: evidence of life? Geophysical Research Abstracts, EGU, Vol 6, 06169. 3) Mumma M.J., Noval R.E., DiSanti M.A., Bonev B.P. (2003) Sensitive search for methane on Mars, Abstract AAS (DPS.) 4) Formisano V., Atreya S.K., Encrenaz T., Ignatiev N, Giuranna M. (2004) Detection of methane in the atmosphere of Mars, Science Online, AAS (DSP. 5) Stevens C.M. & Rust F.E (1982) J.Geophys.Res., 87 (C7), 4879-4882. 6) Schoell M., 1980, Geochimica et Cosmochimica Acta, 44, 649-661. 7) Tyler S.C. (1992) in Isotope Effects in Gas¡VPhase Chemistry, ACS Symposium Series, Vol 502, pp 390-408. 8) Morse A.D., Morgan G.H., Butterworth A.L., Wright I.P., Pillinger C.T. (1996) Combined isotopic analysis of nanogram quantities of atmospheric methane, Rapid Communications in Mass Spectrometry, 10, 1743-1746. 9) Jackson S.M., Morgan G.H., Morse A.D., Butterworth A.L., Pillinger C.T. (1999) The use of static mass spectrometry to determine the combined stable isotopic composition of small samples of atmospheric methane, Rapid Communications in Mass Spectrometry, 13, 1329-1333.

A terrestrial Mars analog: Rio Tinto, an iron and sulfate rich mineral ground produced by microbial metabolism.

R. Amils[1,2], D. Fernández-Remolar[1], F. Gómez[1], J. Gómez-Elvira[1], A.H. Knoll [3], R.V. Morris[4],O. Prieto-Ballesteros[1], N. Rodríguez[1], E. González-Toril[1], J.L. Sanz[2],A. Aguilera[1], A.G. Fairén[2], T. Stevens[5], C. Stoker[6] and the MARTE team.[1]Centro de Astrobiología, 28850-Torrejón de Ardoz, Spain, [2] Centro de Biología Molecular, U. Autónoma de Madrid, Cantoblanco, 28049-Madrid, Spain, [3]Department of Organismic and Evolutionary Biology, Harvard University, 26 Oxford Street, Cambridge, MA 02138, USA, [4]Astromaterials Research Office, NASA Johnson Space Center, Code SR, TX 77058, USA, [5]Portlan State University, OR, [6]NASA-Ames Research Center, Code SS, Moffet Field, CA 94035, USA,

Current Mars exploration is producing a considerable amount of information which requires comparison with terrestrial analogs in order to interpret and evaluate compatibility with possible extinct and/or extant life on the planet. The first astrobiological mission specially designed to detect life on Mars, the Viking missions, thought life unlikely, considering the amount of UV radiation bathing the surface of the planet, the resulting oxidative conditions, and the lack of adequate atmospheric protection. The discovery of extremophiles on Earth widened the window of possibilities for life to develop in the universe, and as a consequence on Mars. The compilation of data produced by the ongoing missions (Mars Global Surveyor, Mars Odyssey, Mars Express and Mars Exploration Rover Opportunity) offers a completely different view: signs of an early wet Mars and rather recent volcanic activity. The discovery of important accumulations of sulfates, and the existence of iron minerals like jarosite, goethite and hematite in rocks of sedimentary origin has allowed specific terrestrial models related with this type of mineralogy to come into focus. Río Tinto (Southwestern Spain, Iberian Pyritic Belt) is an extreme acidic environment, product of the chemolithotrophic activity of microorganisms that thrive in the massive pyrite-rich deposits of the Iberian Pyritic Belt. The high concentrations of ferric iron and sulfates, products of the metabolism of pyrite, generate a collection of minerals, mainly gypsum, jarosite, goethite and hematites, all of which have been detected in different regions of Mars. The ongoing MARTE project is uncovering an interesting scenario of microbial activity associated with pyrite oxidation in the subsurface of the Iberian Pyritic Belt. A Mars drilling mission simulation demonstrating that this technology is ready for future exploratory missions to this planet is also being carried out. The detection of methane in the positive redox potentials and low pH of the Tinto River waters proves that methanogenic activities can be found associated to iron and sulfur oxidation, which gives a new slant to the recent detection, with PFS, of this compound in the martian atmosphere. In addition to this, the recent observation that in the Tinto ecosystem ferric iron can protect complex eukaryotic systems from lethal UV radiation proves the existence of alternative radiation protection mechanisms in an jarosite-producing acidic environment containing ferric iron.

Paleolakes of Southern Claritas Fossae, Mars

Raitala, J.; Korteniemi, J.; Kostama, V-P.; Hauber, E.; Kronberg, P.; Neukum, G.

In the southern Claritas Fossae area, the rugged ancient highland remnants enclose a topographic depression which has been studied using several Mars Express HRSC data sets. Claritas Fossae deforms the southern reach of the Tharsis uplift. Volcanic, tectonic, and water/ice -related events have alternated in its geologic history. Long faults and grabens cut the surface patterned by old upland remnants, lava plains, and fluvial and eolian formations. The high elevations seem to have cumulated water on their tops, most probably in the form of snow or ice. The ancient volatile material coverage was moved downhill into the adjoining lowlands. The large mountain-enclosed depression acted as a reservoir for the water in some consistency. After the meltwater arose close to the level of the lowest barrier rim valley floor it overflooded and carved a distinct flow channel. The water penetrated through a saddle valley to the west, was led through a couple of impact craters and spreaded further into the plains of Icaria Planum. The middle channel area has additional shorter sapping channels connecting into the main channel from the north. This sapping and some additional minor channels indicate the previous existence of water and groundwater supply at first into and then from the direction of the older impact crater which locates midway from the local topography high and the saddle valley bottom. The sapping groundwater finally emerged into the surface in the outer crater rim slope area. The sapping channel erosion is seen in abrupt channel origin from the canyon heads and their close relationship to the fault surfaces and directions. The main flow channel, together with the sapping valleys, is deeply carved into the surface with steep sidewalls. Within the depression, the main channel is straight as originally controlled by a tectonic fault zone. These characteristics may be similar to a valley eroded into permeable and fractured breccia regolith surface. A delta accumulation is visible in one of the craters the channel penetrated into.
This impact crater also served as a temporary lake as seen from the delta and from the fact that the flow channel neck out of the crater is actually higher than the crater floor itself. Finally the channel led water into the Icaria Planum forming there a distinct alluvial fan well visible in the Mars Express HRSC color data and its classification result.

Candidates for Organisms on Mars on the Basis of DDS, CBC, Desert Varnish and Cryoconites

Szathmáry, E.; Horváth, A.; Gánti, T.; Bérczi, S.; Pócs, T.; Gesztesi, A.; Kereszturi, Á.; Sik, A.

There are two groups of indications of Martian life: (1) Martian meteorites which earlier have shown signs of lithified microfossils and (2) dark dune spots (DDSs) as defrosting structures on MGS images of the Northern and Southern Polar Regions of Mars [1, 2].

The Collegium Budapest team proposed a biological interpretation for the DDSs [3]. One motivation for such a proposal has been that we are not aware of any rival mechanism that could explain the full set of observations. Spots start their annual growth process late winter as grey patches, which later develop black inner core, surrounded by a still expanding grey ring. By early summer all the frost is gone from the dunes but some grey remnant of them is clearly identifiable on the surface till the end of summer, when frost precipitates again. Spots are nearly circular on nearly flat surfaces and are elongated downwards on slopes. Some flows, presumably due to water seepage originate from the latter. We can interpret this set of data as indicative of the lifecycle of hypothetical Martian Surface Organisms (MSOs), the most important of which must be photosynthetic. MSOs would create their own living conditions by melting the surrounding water ice, which is thought by us to lie below layers of carbon dioxide ice and clathrate.

Next we looked for plausible earthly analogies of the MSOs. Terrestrial bacterial ecosystems found also within Antarctic ice are a good example. However, these are members of a wider group of candidates, such as terrestrial crypto-biotic crusts (CBCs) which cover many exposed surfaces on the Earth. We think that analogues to CBCs may live in the upper layers of the dark soil of Martian Polar regions [4].

Other candidates were also suggested by our Collegium Budapest ESA Team. One was the bright desert varnish cover on some terrestrial desert rock samples [5]. They may be analogues of an old fossilized CBC cover on the Martian surface. The third candidate is the bacterial community of the cryoconite phenomenon well known on terrestrial glacier and arctic snow-covered surfaces.

Based on our work we propose an observational strategy for Mars Express in order to collect wider photographic coverage of south and north polar dark dune regions during the late winter and spring period.

[1] Horváth A., Gánti T., Gesztesi A., Bérczi Sz., Szathmáry E. (2001) Probable evidences of recent biological activity on Mars: appearance and growing of dark dune spots in the south polar region. Lunar Planet. Sci. XXXII, #1543, Houston.

[2] Horváth, A., Pócs, T., Gánti, T., Bérczi, Sz., Szathmáry, E. (2004) On the Possibility of a Crypto-Biotic-Crust on Mars Based on Northern and Southern Ringed Polar Dune Spots. Lunar Planet. Sci. XXXV, #1914, Houston.

[3] Gánti, T., A. Horváth, Sz. Bérczi, A. Gesztesi, E. Szathmáry (2003) DARK DUNE SPOTS: POSSIBLE BIOMARKERS ON MARS? Origins of Life and Evolution of the Biosphere 33: pp. 515-557, Kluwer Academic Publishers, Netherlands.

[4] Pócs, T., Horváth, A., Gánti, T., Bérczi, Sz., Szathmáry, E. (2004) Possible Crypto-Biotic-Crust on Mars? Proc, of the III. European Workshop on Exo-Astrobiology. Mars: The search for Life, Spain, 18-20 November 2003. ESA SP-545, March 2004, pp.265-266.

[5] Horváth, A., Gánti, T., Pócs, T., Bérczi, Sz., Schweitzer, F. Szathmáry, E. (2004) Terrestrial analogues for possible Martian surface life forms: CBC, desert varnish, cryoconites, 35th COSPAR Scientific Assembly, F3.5/B0.11-0009-04 Scient. Commiss. B: "In-situ Search for Traces of Life on Mars", 18–25 July 2004, Paris, Advances in Space Research (assigned, manuscript number: JASR-D-04-00766).

The NASA Mars Exploration Programme

McCuistion, D.

The presentation on the NASA Mars Exploration Program will cover three broad topic areas. The first item will be to cover the current status of the NASA Mars Exploration Program by identifying the missions planned for the remainder of this decade, as well as the plans for missions to Mars next decade. This will lead into the second topic which is to discuss how NASA is beginning to think about the future exploration of Mars by humans. This will include examining how the current slate of scientific robotic missions and the new line of dedicated human precursor robotic missions will provide key information in the near-term, in order to meet the exploration community's broader long-term goals. Lastly, the presentation will describe how all of the NASA Mars activities are coming together in a new, on-going roadmapping activity to define the future of Mars Exploration.

NASA Mars Reconnaissance Orbiter (MRO) 2005 Mission

Saunders, R.S.; Zurek, R.W,

The MRO is preparing for launch in August 2005 on an Atlas V-401 launch vehicle. Instruments have been integrated onto the spacecraft, and the orbiter is undergoing environmental testing at the Lockheed Martin facility in Denver, CO. Science observations will commence in November 2006, following orbit insertion and aerobraking into a near-polar 265 x 320 km orbit with periapsis over the Martian south pole. From that altitude the MRO payload will achieve the following swath widths and ground sample (pixel) distances:

HiRISE: High Resolution Imaging Science Experiment
6 km, 0.3-m GSD, broadband visible
1.2 km, 0.6-m GSD, blue-green & nir channels
CTX: Context Imager
30 km swath, 6-m GSD, broadband visible
CRISM: Compact Reconnaissance Imaging Spectrometer for Mars
targeted: 11 km, 20-m GSD, ~10-nm over 0.4 – 4.05 microns
survey: 11 km, 150-200 m GSD in ~60 channels
MARCI: Mars Color Imager
Wide Angle Camera , 7 channels
MCS: Mars Climate Sounder (IR Atmospheric Profiler)
Limb sounder (6 km vertical)
SHARAD: Shallow Radar Profiler (20 MHz central frequency)
Profile to ~0.5 km depth, 15 m resolution in free space

The MRO mission will continue the "Follow the Water" theme of NASA's Mars Exploration Program by conducting new and higher resolution remote sensing investigations of the surface, subsurface, and atmosphere of Mars. These investigations will advance our understanding of the present and past climates of Mars, including implications for the search for life. MRO will conduct a campaign of global, regional and targeted observations for just over one Mars year, followed by a relay phase lasting until end of mission in December 2010. The science objectives are:

* Characterize Mars' seasonal cycles of water, dust & carbon dioxide.
* Characterize global atmospheric structure, transport and surface changes.
* Search sites for evidence of aqueous and/or hydrothermal activity.
* Characterize stratigraphy, geology, and composition of surface features.
* Characterize the Martian ice caps and the polar layered terrains.
* Profile the upper crust while probing for subsurface water and ground ice.
* Characterize the gravity field and upper atmosphere in greater detail.

The last objective is achieved by analysis of spacecraft tracking data during the primary science phase and of spacecraft accelerometer data during aerobraking. A prime objective of MRO is to identify areas of high scientific interest for future missions and to characterize surface hazards at the highest priority landing sites, such as the high-latitude site for the Phoenix Mars Scout. MRO also carries an optical navigation camera and a Ka-Band telecom system to demonstrate capabilities for future Mars missions. The MRO mission is managed by NASA's Jet Propulsion Laboratory in Pasadena, CA, for the NASA Science Mission Directorate, Washington, DC.

Mars Phoenix Mission Landing Site Characterization Studies

Arvidson, R.; Deal, K.; Seelos, F.; Bibring, J-P.; Boynton, W.; Golombek, M.; Hays, L; Marlow, J.; Smith, P.; Tamppari, L.; Poulet, F.; Mellon, M.

The Phoenix Lander will touch down on the northern plains of Mars in the summer of 2008 to characterize surface and near subsurface materials hypothesized to be enriched in water ice. The landing site will be between the latitudes of 65 and 72 degrees north and below -3500 m elevation to meet entry constraints. In addition, the site will be located where Mars Odyssey Gamma Ray Spectrometer (GRS) data and modeling suggest a relatively thin (less than 20 g/cm^2) soil cover over ice. The site should also have slopes at the 10 to 1000 meter length-scale consistent with favorable radar return during Entry, Decent, and Landing (EDL), modest slopes at the lander-scale to avoid adverse spacecraft tilts, and rock abundances comparable to or less that those found at the Viking Lander 2 site in Utopia Planitia. Further, the site should show geomorphic evidence of periglacial activity (e.g. patterned ground). Four broad regions (A: 250 to 270E, B: 120 to 140E, C: 65 to 85E, D: 230 to 250E) and subregions within these boxes have been identified to focus coverage of Mars Orbital Camera (MOC), Thermal Emission Imaging System (THEMIS), together with Mars Express HRSC and OMEGA instruments. Geomorphic maps and quantitative analyses of landforms and hazards will be presented for these regions, including slope distributions, rock abundances, and mineralogy based on data acquired during the current northern summer season. Particular emphasis will be placed on analyses of OMEGA data acquired during the northern summer season.

Poster Session 1
Martian Interior and Subsurface, Martian Geology and Mineralogy

The Martian Interior and Subsurface

The Martian Geology and Mineralogy

Isostatic Compensation Models of the Martian Lithosphere

Fels, M.; Pätzold, M.

Since Mars Global Surveyor Mission (MGS) global data sets of the Martian topography (MOLA, MOC) and gravity field are available in a very high resolution. By comparing these datasets 3D geophysical modelling of the internal structure, e.g. state and evolution of the Martian crust (lithosphere) and degree if isostatic compensation, is possible. For seven different Martian target regions the regional crust-mantle boundary was modelled by using as well Airy compensation models as elastic bending models (Vening-Meinesz). Based on these models, gravity anomalies were estimated and compared with gravity anomalies measured by MGS. This technique allows to constrict the possible range of Martian physical parameters for the respective area such as its elastic rigidity, the mechanical and elastic lithopheric thickness and the degree of isostatic compensation . For the Hellas impact crater for example a nearly 100% compensated crust is resulting, whereas the analyzed volcanic regions (e.g. Elysium, Alba Patera) show tendencies towards an rather uncompensated isostatic status.
These studies are going to be extended by using recent Mars Express Radio-Science and Image Data.

Study of Subsurface Structure of Water-Rich Regions on Mars by Data from HEND and GRS Instruments Onboard Mars Oddyssey

Kozyrev, A. Mitrofanov, I. Litvak, M.; Sanin, A.; Tretyakov, V.; Boynton, W.

Mars has a thin atmosphere and very small magnetic field. Therefore, cosmic rays freely propagate through its atmosphere and interact with the surface. Nuclei of the subsurface planetary layer with the thickness of 1-3 m produce a large number of secondary neutrons and gamma-rays. Two types of nuclear interactions take place between outgoing neutrons and nuclei: inelastic scattering, when neutrons are fast, and capture reactions, when neutrons have epithermal or thermal energies. The nucleus of each chemical element produces a unique set of gamma-ray lines, and the method of gamma-spectroscopy allows identifying the presence and relative quantity of chemical elements in the Martian subsurface.

Observation of Mars neutron albedo by HEND onboard 2001 Mars Odyssey is used for determination amount of hydrogen, or water (if we suppose that all hydrogen atoms are included to compound with oxygen forming molecule of water). The gamma-ray spectrometer (GRS) with a detector of high purity germanium is used for measuring the spectrum of nuclear gamma lines with very high spectral resolution. Intensities of induced gamma ray lines depend not only on corresponding nuclei, but also on the spectral density of flux of outgoing secondary neutrons. Thus, the knowledge of neutron albedo of Mars is necessary for determination of the abundance of primary chemical elements by gamma spectroscopy.

The comprehensive procedure of data analysis will be presented for modeling of subsurface structure for water-rich regions of Mars, which allows to compare numerical calculations of outgoing fluxes of neutrons and photons of major gamma-ray lines with observed data from HEND and GRS, respectively. The ratio between water ice and soil will be estimated by this procedure for Northern and Southern permafrost regions. The layering structure of shallow subsurface will be compared for these regions as well. Stratification of water and soil will also be studied by this procedure for water-rich equatorial regions in the Arrabia Terra and in the Memnonia.

Improvement of the Martian Gravity Field with MEX

Rosenblatt, P.; Beuthe, M.; Karatekin, O.; Paetzold, M.; Dehant, V.; Duron, J.; Marty, J-C.; Balmino, G.; Barriot, J-P.

The Mars Radio-Science (MaRS) experiment provides Doppler shifts measurements which are used to model the motion of MEX around Mars. These data are used to improve the knowledge of both local and global gravity fields. First, the lower altitude of the pericenter of MEX leads to an increase of the resolution of local gravity anomalies with respect to previous missions. Second, tracking data of the spacecraft over the whole orbit can improve the previous estimates of seasonal variations of the global gravity field.

The Evolution of Planetary Geodynamics Modulated by Water

van Thienen, P.; Lognonne, P.

The important weakening effect of water on the rheology of mantle rocks has been known for some time now, and studied in more detail more recently. The indirect effects on geodynamics on a planetary scale, however, have not been quantified yet, although qualitatively, they have been invoked to explain differences between Earth and Venus.
We present preliminary results from numerical modeling experiments in which the effects of redistribution of water in planetary mantles and mantle-hydrosphere interaction on the geodynamics through the coupling between rheology and water content are studied, in order to explain the different geodynamical evolutions of Mars, Venus, and Earth.

Coordinated Mars Express OMEGA and Mars Exploration Rover Observations

Arvidson, R.; Poulet, F.; Bibring, J-P.e; Wolff, M.; Squyres, S.; Bell, J.; The Athena Science Team; The OMEGA Team

The Spirit Rover touched down on the floor of Gusev Crater and the Opportunity Rover touched down on Meridiani Planum in January, 2004. Equipped with the Athena Science Payload, these two rovers have been acquiring high fidelity multispectral (0.4 to 1.0 micrometers) images, emission spectra (5 to 29 micrometers), and in-situ close-up imaging, APXS, and Moessbauer measurements on a variety of surfaces. As part of a coordinated set of experi-ments, the Mars Express Orbiter, with the OMEGA imaging spectrometer (0.35 to 5.08 micrometers) observed the sites and surrounding areas while the rover imaging systems and emission spectrometers were acquiring atmospheric and surface measurements. Near-simultaneous measurements were acquired during several passes. Cross-instrument analyses by the OMEGA and Athena Science Teams allowed detailed verification and modeling of spectral signa-tures for the surface and orbital observations. Results of the joint experiments will be presented, focusing on re-trieval of OMEGA-based surface reflectance spectra, and evidence for the role of water in forming landforms and materials.

Fusion of HRSC and MOLA Data for High Quality Mars DTM Computation

Attwenger, M.; Dorninger, P.; Scholten, F.; Neukum, G.

Digital terrain models (DTMs) derived from High Resolution Stereo Camera (HRSC) images by area-based matching exhibit some deficiencies. The method's dependency on albedo features of the surface results in noisy or even pointless regions. Furthermore, point matching methods are not able to directly reconstruct linear structural features such as sharp terrain edges or crater rims. Therefore, the resulting surface models may show unnaturally rough areas caused by measurement noise, may have more or less large gaps where image features are not detectable, and terrain discontinuities appear smoothed.

Our approach overcomes these problems and improves the quality and subsequently the interpretability of the final DTMs. The main ideas are aimed at eliminating the influence of the measurement noise by using point classification, bridging pointless areas with already available topographic information (e.g. MOLA, Mars Orbiter Laser Altimeter), and improving the modeling of linear structures with the help of an adequate structure line detection algorithm.

The classification method is applied iteratively starting from an initial surface model. First, a MOLA DTM was used as initial value. But, it turned out that a coarse DTM derived from the original HRSC point cloud can be used as well. Therefore, regions with sufficient HRSC point distribution are derived from these points only, whereas pointless areas are bridged by MOLA data.

The method has been tested in different areas. The mean measurement noise can be reduced by a factor of two from about ±43 m to ±24 m. It could be shown that features not discernable in the original point cloud stand out clearly in the DTM derived from the classified points. The presented approach is expected to provide the basis for improving the quality of subsequent products, such as orthoimages, maps, and results of specific investigations.

The geology of Western Olympus Mons as deduced from the analysis of the Mars Express HRSC camera images. A. Basilevsky[1,2], G. Neukum[2], B. Ivanov[2,3], S. Werner[2], S. van Gasselt[2], J. Head[4], R. Jaumann[5], H. Hoffmann[5], E. Hauber[5], and the HRSC Co-Investigator Team. *[1]Vernadsky Institute, RAS, Moscow, Russia atbas@geokhi.ru; [2]Institut fuer Geologische Wissenschaften, Freie Universitaet Berlin, Berlin, Germany; [3]Institute of Dynamics of Geospheres, RAS, 119334 Moscow, Russia. [4]Dept. Geol. Sci., Brown University, Providence, R.I. USA; [5]DLR-Institut fuer Planetenforschung, Berlin, Germany.*

The High Resolution Stereo Camera (HRSC) images taken at orbit 143 show a high-resolution view of the western Olympus Mons. Numerous lava flows, some as young as 2-3 m.y. [1], have been observed mostly at the southern and central parts of the studied segment of the volcano (Figure 1). At the edge of the edifice slope close to the scarp, several mesas and one ridge composed of layered deposits are observed suggesting sedimentation of dust (maybe ash) and ice. The presence of ice is deduced from the observation of deep rimless depression within one of the mesas and from the specific interaction of the mesa material with lava flows. Within the studied Western Olympus slope, three morphologic types of the slope are distinguished: Type 1 is the most steep and dominated by ravines in its upper part and by taluses beneath; Type 2 is intermediate in steepness and dominated by the down-slope trending linear depressions, part of which have channel-like morphology; and Type 3, the most gentle, is covered by lava flows, continuing from the summit plateau down to the lowland plains. In several parts of the Type 2 slope, chaos-like depressions, channels and chains of rimless craters are observed suggesting the melting of ground ice, perhaps due to lava invasion, and the resulted surface collapse and water run-off. At the foot of the scarp, and further to the lowlands, lobate flows, morphologically similar to terrestrial rock glacier deposits, are observed. Some of them are only 4 m.y. old [1], implying recent episodes of glaciation probably controlled by changes of the planet´s orbital parameters [2]. Morphologic evidence of older glacial deposits at high altitude (+7.5 km) above the scarp was also found. The suggested presence of the ice-bearing deposits in the Olympus Mons construct could be a cause of the large-scale landslides forming the detachment scarp along the Olympus Mons perimeter and the aureole deposits around.

References: [1] Neukum et al., Nature, 2005 (in press); [2] Lascar et al., Icarus, 170, 343-344, 2004.

Acknowledgement: This work was supported by the German Space Agency (DLR) and the German Science Foundation (DFG).

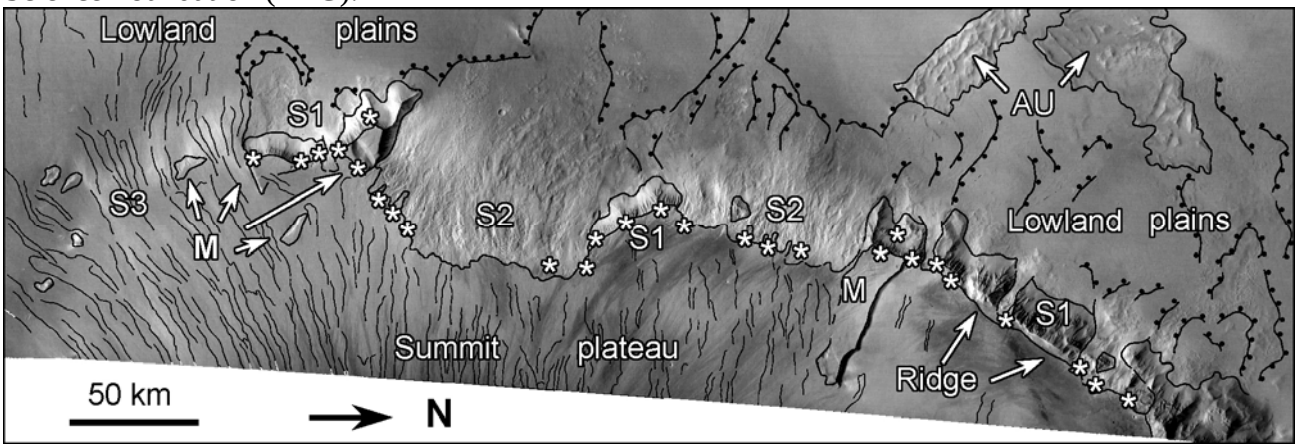

Figure 1. The HRSC synoptic view of the Western Olympus Mons. Legend: S1, S2, S3 designate slopes of Type 1, 2 and 3 correspondingly; M – mesas, stars ✿ designate outcrops of the layered deposits; thin black lines show boundaries of prominent lava flows; thicker lines with dots designate glacier-type flows, AU – aureole deposits.

Stability of Subsurface Ice on Mars – a Local and Global Perspective

Boettger, H. M.; Benkhoff, J.; Forget, F.; Lewis, S. R.; Read, P. L.; Foing, B.; Helbert, J.

In the current Martian climate water ice is not stable close to the surface at low and mid latitudes [1,2,3,4]. This is, however, assuming that equilibrium between the subsurface water content and temperature has been reached. The timescales for this process, certainly at depths of a few metres, can be extremely large and is dependant on soil properties (porosity, composition, etc.). When comparing this to the changes in the Martian obliquity, which has varied between 15° and 45° within the past 10Ma alone [5,6], with a pseudo-timescale of the order 100,000 years it is unlikely that any subsurface water ice present in low-mid latitudes at the depth of a few meters ever reaches equilibrium. There is also some geological and model evidence emerging for the current presence of ice very close to the surface in low latitudes [7,8,9]. It is therefore of interest, for both science and future missions, to assess how subsurface ice stability varies with changes in Martian obliquity, but also how long and at what depth ice deposits covered by dust deposits can persist under present conditions.

Here we use the LMD Mars General Circulation Model (GCM) [10] as well as the Berlin Mars near Surface Thermal model (BMST) model developed at DLR [11], to assess the stability and longevity of subsurface water at different obliquities as well as locally under present climate conditions.

References:

1. Clifford, S.M. and D. Hillel, J. Geophys. Res. 88, 2456-2474, 1983.
2. Mellon, M.T. and B.M. Jakosky, J. Geophys. Res. 98, 3345-3364 1993.
3. Mellon, M.T. and B.M. Jakosky, J. Geophys. Res. 100, 11781-11799, 1995.
4. Mellon et al. , Icarus 169, 324-340, 2004.
5. Laskar, J. and P. Robutel, Nature 361, 608-612 1993.
6. Laskar J. et al., Icarus 170, 343-364, 2004.
7. Neukum G. et al., this issue.
8. Helbert J. and J. Benkhoff, 6th International Conference on Mars, #3019, 2003.
9. Helbert, J. et al., this issue.
10. Forget et al. , J. Geophyis. Res. 104, 24155-24175, 1999.
11. Helbert and Benkhoff, J. Geophys. Res. 108, 28-1, 2003.

Laboratory Spectra of Hydrated Sulfates: Implications for OMEGA Detection on Mars Surface

Bonello, G.; Bibring, J-P.; Berthet, P.; Gendrin, A.; d'Hendecourt, L.

We have reproduce laboratory reflectance spectra on samples of sulfate powders in different hydratation states. For this, we have used thermogravimetric analyses of MgSO4.7H2O for different temperature exploration curves in dry air conditions. Both temperature and time are playing a role in the dehydratation process. The spectra recorded show a clear evolution of the hydrated features from hydrated to anhydre phases including mixture of different phases. Then, we discuss the implications of this labotary results in the interpretation of the OMEGA spectra for sulfate indentification on the surface of Mars.

A 2 Square Metre True-3D Image Map of Chaotic Terrain, Lower Vallis Marineris, Mars

Buchroithner, M.; Habermann, K.; Gruendemann, T.

Following the conceptual idea "from 3D camera to 3D view", the production of a large-format true-3D image map for the glasses-free stereo-viewing of a characteristic part of the Martian surface is described. The image data have been acquired by the DLR High Resolution Stereo Camera (HRSC) as a part of the Mars Express Mission of ESA. This multi-line scanner delivers digital multispec-tral scanner data of highest quality in a fore, aft and nadir mode, thus offering a perfect data set for true-3D visualization.

For the purpose of representation and education a map of a high-reliefed Martian terrain was produced. The depicted chaotic terrain is located at the Ophir Chasma in the lower course of the Vallis Marineris, covered by the HRSC orbit 18. The map size of 2 metres West-East and 1 metre North-South offers the possibility of synchronous true-3D viewing for many a whole group of viewers at viewing range from 1 to 6 meters. A true-colour image map in true-3D appears to cover both the requirements of the Mars research community and of the public best. In order to be able to view the map without viewing aids such as polarisation glasses the decision was made to generate it on the basis of lenticular foils.

The present paper describes the workflow from the georeferenced image data set and the DTM to a true-3D visualization, especially the challenges of large-format maps and multi-user capability. The principle of lenticular foils is explained. Micro-lenses on a trans-parent plastic foil allow the map user to view the integral of two or more interlaced strips of stereo-mates through this foil with his or her left and right eye respectively. The 3D modelling as well as the calculation of both the strip width and the interlacing is done by means of commercially available software.

For the large-format map a lenticular foil with appr. 20 lenses per inch and 12 stereo-mates were used, the whole map consists of two contiguously attached parts, because the commercially lenticular foils are only available with a maximum width of one metre.

Juventae Chasma: a Case Study of the Association of Light-toned Layered Deposits, Chaos, and Outflow Channels

Catling, D.; Wood, S.; Leovy, C.; Montgomery, D.; Greenberg, H.; Glein, C.; Moore, J.

Interior layered deposits (ILDs) and their association with chaotic terrain and outflow channels provide critical clues for understanding the evolution of Mars. Juventae Chasma is a place with all the aforementioned geomorphic units. We examine Juventae Chasma using a combination of data from Mars Global Surveyor's Mars Orbiter Camera (MOC), Mars Orbiter Laser Altimeter (MOLA), and Thermal Emission Spectrometer (TES), as well as Mars Odyssey's Thermal Emission Imaging System (THEMIS). These data allow us to map Juventae Chasma into geomorphic units of (i) chasm wall rock (ii) heavily cratered hummocky terrain (iii) a mobile and largely crater-free sand sheet on the chasm floor (iv) light-toned interior layered deposit (ILD) material, and (v) chaotic terrain. The ILDs are composed of ancient sedimentary rock that is undergoing exhumation and erosion in the present epoch. Small outliers in MOC narrow angle images show that the ILD material is much more extensive than previously reported. MOC and THEMIS images indicate the erosional styles of the ILD surfaces; these are largely crater free and sculpted by the wind. In several MOC images, ILD material underlies mounds of heavily crated chaotic terrain. We suggest that ILD material is associated with the formation of chaos. Using THEMIS infrared data and MOLA slopes, we derive maps of the thermal inertia, which show ILD thermal inertias up to about 800 J m-2 K-1 s-1/2. These maps place thermophysical constraints on the possible nature of the ILDs and associated geology. The new data allow us to reassess possibilities for the origin of the Juventae ILDs, at least one of which is reported by the OMEGA team to be sulfate-rich. The data are consistent with formation either from an ancient body of water or possibly from airfall deposition.

Martian Surface Texture Study by a Filtering Approach Using Mars Express HRSC Data

Cord, A.; Martin, P.; Foing, B.; Jaumann, R.; Hauber, E.; Hoffmann, H.; Neukum, G.

Texture content analysis in digital image data has received much attention during the past decades in the context of image classification and segmentation [1]. Existing tools developed for this purpose can be adapted to the description of the Martian surface in order to provide a characterisation of the texture at a few tens of meters scale.
For this study, we use one HRSC nadir image with a resolution of 12 m/pixel, from which we extract numerous smaller images of unvarying textures. These images containing a variety of different textures are then subject to a filtering approach [2]: First, textured images are submitted to a set of linear transforms, using filter banks. For each filter, an energy measurement is provided, through a non-linear process, basically rectifying and smoothing the filter response. Some statistical parameters (means, quartiles, standard deviation) are then extracted giving a characterisation of the texture in each image. Finally, a non-supervised classification allows the identification of properties of each group of textured images.
This provides us with a powerful method for the description of the surface texture and a link to the geological and geomorphologic properties of the considered area. It may lead to a systematic analysis and classification of the Martian surface texture.

References: [1] Reed T. R. and du Buf J. M. H. (1993), CVGIP: Image Understanding 57, 359-372, [2]. Randen T. and Husoy J. H. (1999), IEEE Transactions on Pattern Analysis and Machine Intelligence 21 (4), 291-310

Photometric Study of the Martian Surface Using Mars Express HRSC Data: the Gusev Crater Region

Cord, A.; Martin, P.; Pinet, P.; Daydou, Y.; Jehl, A.; Jaumann, R.; Hauber, E.; Hoffmann, H.; Neukum, G.; Foing, B.; HRSC, Co-Investigators tea

The semi-empirical model developed by Hapke [1] is widely used to analyze reflectance data from planetary surfaces (e.g. [2], [3], [4]). It requires the knowledge of six parameters to calculate the bidirectional reflectance. Its application relies on some physical quantities characterizing the optical properties of the materials under examination: the phase function, the opposition effect, and the roughness. The multi-angular data acquired by the HRSC camera onboard Mars Express can be used to determine the photometric properties of the Martian surface.

This study presents a method for the determination of the global set of parameters required by Hapke's model, relying on powerful inversion algorithms [5,6]. As a demonstration, it is applied to the Martian surface in the Gusev crater region. A set of 10 angular conditions provided by two overlapping orbits (# 24, 72) covered by HRSC are used.

Following the approach and results presented in [7], this work focuses on the link between the photometric parameters and the physical properties of the surface in context with the unique "ground truth" from the Spirit rover. This photometric description of the surface can be used to appropriately calibrate the HRSC colour bands thereby allowing for colour and multispectral analysis of the mineralogical properties of the area (see linked talk [8]).

References: [1] Hapke B. W. (1993), Cam. Univ. Press, [2]. Johnson P. E (1983), JGR, 88, 3557-61, [3] Helfenstein P. and Veverka J. (1987), Icarus, 72, 342-357, [4] Cheng A. F. and Domingue D. L. (2000), JGR, 105, E4, 9477-9482, [5] Cord et al. , (2003), Icarus, 165, 414 – 427, [6] Nash, S. G. (1984), SIAM J. Numerical Analysis, 21, 770-778, [7] Pinet et al. (2004), Ischia Mars Intern. Conf., abst., [8] Martin P. et al. this issue.

Analysis of Alluvial Fans and Deltas in Xanthe Terra using HRSC Data

Di Achille, G.; Ori, G.G.; Marinangeli, L.; Gwinner, K.; Scholten, Frank; Reiss, Dennis; Jaumann, R.; Hauber, E.; Neukum, Gherard; HRSC, Co-Investigator Team

The accuracy of HRSC data allows, for the first time, a detailed morphometric analysis of small sedimentary features such as alluvial fans and fan deltas. We will present and discuss some examples of fan-like features found in Xanthe Terra (Fig.1). Using HRSC data (H0894, H0905 and H0927 orbits) and other datasets (MOC, THEMIS), we have performed a geological mapping of the area and of the relative hydrographic system in order to reconstruct the different phases of activity of the fan features. The study area shows numerous sapping channels and many fans are located at the mouth of these valleys (see Hauber et al., this conference). Sabrina and Tyras Vallis show two different base levels and terraced walls: Tyras Vallis flows toward an unnamed complex crater (close-up below) and forms one of the largest fan in the area. This fan covers an area of about 83 km2, with ~12 km in radius and ~750 m in height. The rim of the crater is incised by a dense and centripetal drainage system that likely fed a lacustrine basin. The detailed topography derived by HRSC allows the recognition of small-scale scarps along the longitudinal profiles of the Tyras fan, suggesting different phases of deposition and erosion during its development. The complex evolution of this fan with terrace and fan-head incision suggests both alluvial and deltaic activities. These observations may fit with a drop in the water level of the basin due to the decrease of the water discharges from the feeder channels. The influence of climatic fluctuations on the sapping phenomenon may have produced such as pulsating discharges of water and sediments, affecting the transport capacity of the systems, and thus, the erosional/depositional ratio. The comparison of the alluvial fans and deltas in the study area will help in understanding the fluctuation of the water discharge and the evolution of the hydrological system trough time.

Hydrological Analysis of the Mars Topography

Dorninger, P.; Attwenger, M.

Ever since the surface of Mars is investigated in detail, scientists have been discussing if liquid surface water was involved in the surface forming process in former times. Many scientific investigations aim at interpreting albedo features from high-resolution image data (e.g. MOC, HRSC). The following approach is based on geometric analysis of the Mars topography.

The raster-based analysis methods used are implemented as systolic processes. The conditions of the cells in a rectangular grid array, i.e. a digital terrain model (DTM) representing the topography, are derived synchronously by taking only their neighbors into consideration. The visualization of the results is prepared by means of special filtering operations.

Especially hydrological analysis seems to have a high potential to support the derivation of models which can be applied to reconstruct the behavior of possible former surface water on Mars in a plausible manner. Results of the analysis of three selected regions on Mars, which are very likely to have been formed by surface water, are discussed in detail:

- simulated outflow behavior in Ma'adim Vallis and Gusev Crater;
- outflow channel detection in the Elysium Region;
- hydrological mapping of the Tharsis Highlands and Valles Marineris.

For further scientific investigation and interpretation it might be helpful to visualize the results of the hydrological analysis. Thus, several methods for 3D visualization of DTMs and corresponding raster image overlays are presented, as well. E.g. a hydrological map comprising the rivers and lakes derived from the topographical model is representing a visualization of surface-water behavior on an impermeable surface during permanent, homogeneous rainfall.

Most results have been derived from MOLA data. Currently, these results are verified using HRSC images. It is also planned to apply the same methods to DTMs derived from HRSC data by area-based matching methods.

Mars Express HRSC Context for MER Spirit in Gusev Crate

Foing, B.; Zegers, T.; van Kan, M.; Pischel, R.; Martin, P.; Cord, A.; Boettger, H.; Hauber, E.; Hoffmann, H.; Pinet, P.; Jaumann, R.; Greeley, R.; Jehl, A.; Werner, S.; Neukum, G.; HRSC Co-I Team, .

We report on the analysis of data on Gusev crater and surroundings, obtained with the Mars Express HRSC camera, Themis IR and visual images, combined with narrow angle MOC images. We mapped the wider region of the Gusev crater (172° E to 179° E by 10° S to 18° S), focussing on the geological units and their geometrical relationships. HRSC data from orbits 24, 72, 283, 335, 637 and 648 were used, covering the central and eastern part of the Gusev crater. The

HRSC nadir channel (panchromatic), with 12 m/pixel resolution fills the resolution gap between the Themis IR 100 m/pixel and Themis visual at about 20 m/pixel on the one hand and MOC images with 2 m resolution on the other hand. This makes it possible to study geological units and structures in detail, and within the wider context. Six different units were mapped within the Gusev Crater. The youngest of these units is the picritic (high-Mg-basalt unit) in which Spirit landed. In addition to the image data, the stereo data from HRSC were used to study the three-dimensional geometry of units and structures. To this end a number of geological cross sections were constructed, based on HRSC digital elevation models. The cross-section are used to establish the relative age relationshipin Gusev Crater. The geological mapping and cross sections make it possible to more accurately define the geological evolution of the Gusev crater, in context with the unique "ground truth" from Spirit rover.

High Resolution Simulations of Martian Tropical Glaciers

Forget, F.; Montmessin, F.; Levrard, B.; Haberle, R. M.

Numerous geological features suggest the presence of ice flows on the surface of Mars. In particular, the HRSC camera has recently obtained very high quality observations of dropped moraines and other characteristics that tend to confirm the presence of glaciers on the flanks of the Tharsis volcanoes, as previously suggested by Lucchita(1981) and Head and Marchant (2003) of glacier on the flanks of the Tharsis volcanoes.
The presence of ice in such location is now better understood in the light of climate simulations performed with Global Climate Model similar to the one used to model in details the current martian general circulation and water cycle, but with other orbital parameters and obliquity as expected a few millions years ago. In particular, the LMD GCM has predicted that at obliquities larger than 40 degrees, the north polar water ice could be moblized southward and deposited near the
equator, especially on the flanks of the large Tharsis Volcanoes and Olympus Mons (Levrard et al. 2004). Ice tend to accumulate in such locations because of enhanced precipitation due to adiabatic cooling in topography induced updraft. So far, the comparison between observations and model has been limited by the horizontal resolution of the model used for these studies. Here, we shall present further simulations performed
with a version of the GCMs that include a "zoom" which allows to simulate the atmospheric circulation and simulation in the Tharsis area with resolution reaching a few tens of kilometers. Such a model is used to improve the comparison with the observations and better understand the exact processes at work.

- Lucchita, B. (1981), Icarus, 45, 264.

- Head, J.W. and Marchant, D.R. (2003) Geology 31, 641-644.

- Shean, D.E., Head, J.W., Fastook, J.L. and Marchant, D.R. (2004) Lunar Planet. Sci. XXXV Abst. 1428.

- Levrard, B., Forget, F., Montmessin, F. and Laskar, J. (2004)
Nature, 431, 1072-1075.

Attitude Determination of Geological Layers using HRSC Data and Orion Software

Fueten, F.

Previous work has demonstrated that MOLA and MOC data can be combined in Orion software to determine attitudes of chasma wall layering in the eastern portion of Va lles Marineris. The layers fairly consistently dip into the canyon, an orientation that may record the collapse that produced the early ancestral basins. Recent work using HRSC data appears to confirm those initial findings. Unfortunately, the application of Orion was limited to examining large features by the coarse resolution of the MOLA grid. Use of higher resolution HRSC imagery and DTMs allows for the examination of geological layering at a much finer resolution.

As an example of using HRSC data, we studied a semi-circular feature in western Candor Chasma, approximately 12km by 8km in extent, displaying good internal layering suitable for analysis with Orion. Similar, though smaller, whorl-shaped enigmatic features within Candor Chasma have been modelled as diapirs or are suggested to be due to permafrost. An understanding of the three-dimensional geometry of this feature can constrain the number of hypotheses regarding its origin.

While some layers can be traced around the entire feature, analysis with Orion suggests that layers in the NE and SW quadrants show good planarity. Curvature apparent in the imagery in these regions is produced by gully–shaped topography intersecting north-easterly dipping planes in the NE and SW quadrants. The dip of the plane in the NE quadrant is approximately 20°NE, while that in the SE quadrant is approximately 7°NE. However, the apparent curvature of the layers in the NW and SE quadrant of this feature cannot be explained in this fashion. Analysis indicates that no single rectiplanar feature can fit this outcrop trace. Rather, the layering itself is non-planar, adding to the topographic sectional effect. We infer this feature to be an asymmetrical open fold with a NW-SE trending fold axis and limb dips of approximately 20° and 7° to the NE. Further, the SW fold limb (dipping 7°NE) is unconformably overlain by a planar layer dipping approximately 6°SW.

The accurate determination of layer attitudes facilitates a true understanding of the three-dimensional geometry of the geology and places valuable constraints on the interpretation of features of Martian geology. While the origin of the fold and unconformity and their geological implications are debatable, possible models must account for this geometry. Use of Orion with HRSC data will constrain the interpretation of geological features on Mars.

Identification of Low Calcium Pyroxene Rich Areas by OMEGA, and Comparison with other Datasets

Gendrin, A.; Mustard, J.; Mangold, N.; Bibring, J-P.; Langevin, Y.; Gondet, B.; Poulet, F.; Platevoet, B.; and the OMEGA team

Areas very rich in Low Calcium Pyroxene (LCP) are identified by OMEGA inside the ancient terrains on Mars. To study these deposits, we use the Modified Gaussian Model, and we obtain the band depths of LCP and HCP (High Calcium Pyroxene). We then systematically search the dataset to identify locations with enhanced band depths of LCP. These areas show a variety of geological contexts, but are mostly associated with outcrops, especially on crater rims or central peaks. Some interesting deposits are also identified inside the walls of Valles Marineris.
We will discuss the spectral properties of these outcrops, and compare them with other datasets so as to track down a systematic relationship with altimetry or thermal inertia. We will also detail the general location of these outcrops over the Martian surface.

Geologic Evolution of the Harmakhis Vallis Region

Glamoclija, M.; Ori, G.G.; Marinangeli, L.; Komatsu, G.; Neukum, G.

Large areas of the eastern Hellas region display enhanced modification of the initial topography formed by the Hellas impact. Diverse geological factors caused a long and complex history of degradation and modification. These processes include fluvial activity, volcanism, tectonics and mass wasting processes. The presence of the outflow channel systems of Harmakhis, Niger, Dao, and Reull Valles along with smaller fluvial features provide important clues for past Martian environmental conditions.

This study focuses on the geological reconstruction of the Harmakhis Vallis region (lat. -35? to –42?S; lon. 91? to 98?E) where a complex interaction of different water-related environments can be identified. Harmakhis Valles is located adjacent to Tyrrhena Patera flank flows which has been thought to be the source of heat for the mobilization and release of subsurface volatiles and consequent valley formation.

Geological mapping has been performed on multiple co-registered datasets of Viking images, MOLA altimetry, MOC and THEMIS (VIS and IR) images, and HRSC data (H0038, H0528). The contribution of HRSC images and stereo-derived topography is of crucial importance in this area because it fills a resolution gap with the Viking dataset (generally at ~100m/pixel). The resolution of HRSC allowed the observation of features that were not described in previous geological mapping based on Viking data [1,2].

Water has been present on the surface during different stages of the geological history of the area. Partially buried channels have been recognized in the surrounding areas of the uppermost Harmakhis Vallis. Stratigraphic correlations of these channels with surrounding units show that they are the oldest channel systems in the Harmakhis study area. These old channels may have been connected into a larger system that was likely active during the early Hesperian. The plains between Niger and Harmakhis exhibit a series of landforms that are indicative of fluvial activity. Channels hundreds of km long appear to be generated from chaotic areas, suggesting that the water derived from the subsurface. This was likely triggered by local geothermal anomalies. Some of these channels appear to be older of the formation of the upper portion of the Harmakhis.

The stratigraphically younger geological units are likely related to a glacial environment. Kettle-like structures and creep textures have been found in several places. Numerous debris aprons shed from the slope of the surrounding Noachian mountains. The glacial activity in this area has been defined of Amazonian age [1, 2].

The variety of geological units recognized in the Harmakhis region depicts a complex interaction of different processes occurring mainly during the Hesperian-Amazonian transition, possibly influenced by variations and intensity of the volcanic activity.

[1] USGS map I-2557 [2] USGS map I-2694

Bidirectional Reflectance observed by Mars Express HRSC and first Assessment of its Deviation from the Lambert and Lommel-Seeliger Approximations

Gwinner, K.; Jaumann, R.; Inada, AA.; Hoekzema, N.; Hoffmann, H.; Neukum, G.; HRSC Co-Investigator, Team

The High Resolution Stereo Camera (HRSC) experiment onboard the European Mars Express mission provides unprecedented opportunities to analyze the scattering properties of the planet's surface and atmosphere. The multi-line pushbroom channels (one nadir and two pairs of forward/backward-looking channels at approximately +/- 13° and +/- 19°) as well as 4 multi-spectral channels. All of these can be operated simultaneously, providing multi-angle and multi-spectral observations acquired within a time interval of less than one minute for each specific site. For the first time, therefore, we can derive multi-angle scattering properties from Mars orbit without possible bias by large-scale atmospheric changes and variable surface features.

We approach the study of bi-directional scattering properties by quantifying the deviationof the observed multi-phase panchromatic radiance from the angular distribution of reflectance expected from the Lambert and Lommel-Seeliger approximations, applying to the compound surface-atmosphere-surface system. After photometric normalization, remaining intensity differences between multi-phase images are evaluated in terms of root mean square error (RMSE) of modeling. the interest for this study is two-fold: first, we want to guide and facilitate the detailed analysis of scattering properties applying more elaborate photometric models. Second, geoscientific surface mapping studies will rarely have comprehensive radiative transfer modeling at their disposal. Thus, these studies may benefit from an improved estimation of signal variations due to directional effects and thus of uncertainty.

Our data analysis uses map-projected, ortho-rectified imagery together with complementary geometry data. The utilization of ortho-rectified imagery insures precise spatial co-registration of the multi-phase and multi-spectral data. the complementary geometry data include local ellipsoid normals, sun positions and observation verctors (as used during ortho-rectification). Furthermore, the stereo capabilities of HRSC enable the derivation of Digital Terrain Models (DTM) at lateral resolution similar to the spatial resolution of the image data. This allows us to model incidence and emission angles according to a close approximation of the local topographic slope alternatively. We will present results for a number of examples from different orbits, including reflectance maps and their RMSE obtained by photometric normalization based on each of the two scattering laws. Implications for photometric normalization of HRSC and OMEGA imagery in the visible and near-infrared are discussed.

Interior Layered Deposits in Valles Marineris, Mars: Insights From 3D-Data Obtained by the High Resolution Stereo Camera (HRSC) on Mars Express

Hauber, E.[1], K. Gwinner[1], R. Stesky[2], F. Fueten[3], G. Michael[1], D. Reiss[1], H. Hoffmann[1], R. Jaumann[1], G. Neukum[4], T. Zegers[5], and the HRSC Co-Investigator Team

[1]Institute of Planetary Research, German Aerospace Center (DLR), Berlin, Germany
[2]Pangaea Scientific, Brockville, Ontario, Canada
[3]Department of Earth Sciences, Brock University, St. Catharines, Ontario, Canada
[4]Remote Sensing of the Earth and Planets, Freie Universitaet, Berlin, Germany
[5]ESTEC, ESA, Noordwijk, The Netherlands
Ernst.Hauber@dlr.de

The Interior Layered Deposits (ILD) in the Valles Marineris depressions on Mars may be of volcanic or sedimentary origin. Either way, their presence has profound implications for the formation of the Valles Marineris itself. The High Resolution Stereo Camera (HRSC) on board the Mars Express mission obtains high-resolution stereo and multipectral images, which are particularly well suited for the geomorphologic analysis of the ILD. One possible key to decide whether the layers are volcanic or sedimentary is their layering geometry, i.e., their strike and dip. At first order, sedimentary, water-lain deposits should have a horizontal layering. On the other hand, volcanic layers from pyroclastic eruptions, including subglacial eruptions, might be inclined, e.g., as a part of tuff cones or in subglacial volcanoes. The strike and dip of layers should then display a concentric pattern around the vent. Digital Elevation Models and orthoimages derived from HRSC data have been used to measure the strike and dip of several ILD in the troughs of Hebes, Ophir, Candor, Melas, and Juventae Chasmata. In some cases, the layers have dips of 10°-20°, dipping outward from the centers of the ILD. This pattern would be in agreement with a volcanic origin. At Juventae Chasma, the layering of one ILD at –4.5°S, 297.3°E is subhorizontal. This particular ILD is also distinguished from the other ILD covered by this study by its morphology, as revealed by HRSC, Themis, and MOC images, and by its mineralogy, as revealed by the imaging spectrometer Omega on Mars Express [*Bibring et al.*, COSPAR 2004]. Here, a sedimentary origin would be consistent with our measurements. An ILD in Coprates Chasma is particular, because its base is located high above the main canyon floor in a re-entrant of the chasma wall. It will be treated in a separate contribution (Michael et al., this conference).

The Berlin Mars near Surface Thermal Model (BMST) – a New Approach to Assess the Burial Depth of Ice on Mars

Helbert, J.; Benkhoff, J.

While Mars has been considered for a long time a dry place, this view has changed in recent years. This started mainly after the MOC imagery showed features like the gullies and morphological features which can be associated with glacial activity. Now the motion was discussed that at least small amounts of water or ice had been present in the recent past on Mars. Still, the common notion was that Mars today is a dry place. With the excellent dataset of the Gamma and Neutron spectrometer (GRS and HEND) on board of Mars Odyssey this view had to be corrected. The instrument detected water abundance of at least 8wt% in the equatorial regions of Mars and this water is found within the first 2m below the surface, the penetration depth of the instrument.

There are three main explanations for this observed amount of water which are not mutually exclusive. Some of the water measured is most likely adsorbed water. While it is still unclear how much water the Martian soil can adsorb, this mechanism can not explain the high abundances measured in some place. We might see highly hydrated minerals. Some of the suggested minerals are indeed capable of holding large quantities of water. The last and maybe most exciting possibility are near surface ice deposits. However if it is ice, the question is, how did it survive close to the surface under the hyper-arid conditions we encounter on present day Mars. And how much ice is there really on present day Mars?

Over the recent years we have developed the Berlin Mars near Surface Thermal model (BMST) to address this question (Helbert and Benkhoff, 2003). Most models used up to now assume a thermo-physical steady state for the Martian soil. Under such conditions ice could not be stable close to the surface in equatorial regions. However modelling shows that the obliquity of Mars changes dramatically over time (Lasker 2004). There are observational evidences showing at least two climatic cycles on Mars. There is a long term cycle in the order of 5-10 Mio. years as shown evidence of glaciation in equatorial regions (Hauber et al. 2004) and a medium term cycle in the order of 100-300ka as shown for example by the layering in the polar caps (Milkovich et al. 2004).

The BMST is focused on studying the stability of recently deposited ice. While most models used today for the near surface layer of Mars assume constant physical properties with depth, our model is based on a layered structure of the subsurface material, in which each layer can have different physical and thermo-physical properties. The main features of the BMST are a high lateral resolution down to the centimeter range, the realistic treatment of the thermal properties of ice-rock mixtures, a detailed treatment of gas flux within the surface and into the atmosphere and a variable temporal resolution which allows to study daily as well as annual variations. Using the model we can study the redistribution of volatiles with the subsurface over time. This allows to predict limits for the burial depth of ice assuming non-equilibrium conditions.

Simple estimate for Gusev infilling thickness.

B. A. Ivanov (1,2), S. Werner (2), G. Neukum (2)
(1) Institute for Dynamics of Geospheres RAS, Moscow, Russia (baivanov@idg.chph.ras.ru);
(2) Free University, Berlin, Germany (swerner@zedat.fu-berlin.de)

HRSC data are very useful for joint analysis of HRSC and MER (Spirit) data. The geologic history of Gusev crater is very complicated including, possibly, filling of the initial impact depression with lava flows and water-bearing sediments. To estimate the infilling thickness we use MOLA data to study craters with diameters similar to Gusev (~150 km) but located in different areas and with visibly different geologic history.

Most of craters of craters with diameters >150 km looks partially filled. However many of them have a distinct central feature (central peak or central peak ring) above the level of possible floor sedimentary infilling. Gusev has a flat visible floor. It means that Gusev infilling has larger thickness than in other large craters. For several studied Gusev-like craters (data for 2 of them are presented in Figs. 1 and 2) the visible rim-to-floor depth is about 2.5 to 3 km. For Gusev the same parameter is in the range 1 to 1.5 km. Hence we estimate that post-impact infilling of Gusev crater has the thickness not less than **1 to 1.5 km** (Fig. 2). This is an important constrain for any assumed geological history of Gusev and the area around.

We also discuss the depth-diameter relation comparing Mars with Mercury, Venus and the moon. Reconnaissance results of the numerical modeling of large Martian impact craters will be presented to analyze possible pristine structure of large impact craters imaged by HRSC.

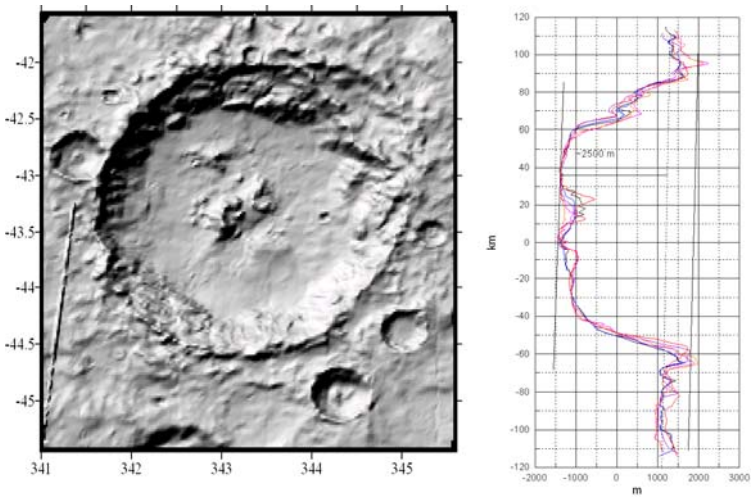

Fig. 1. MOLA-based shaded reliefe and central MOLA tracks for Crater-1 (43°S, 343°E). The rim-to-floor depth is ~2.5 km, the central feature (central peak ?) is about 2 km below the preimpact level.

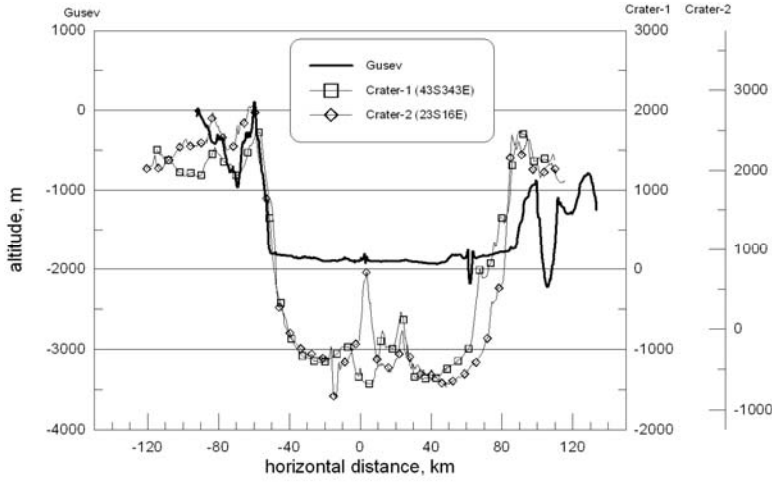

Fig. 2. Comparison of central MOLA profiles for Gusev crater and 2 other craters of comparable size. Crater-1 is presented in Fig. 1, coordinates for a similar Crater-2 are presented in the legend insert.

Water and Sediment Dynamics and Delta Formation in Ma'adim Vallis and Gusev Crater

Kleinhans, M.; Zegers, T.; Foing, B.; Jaumann, R.; Neukum, G.

The lower reach of the Ma'adim Vallis and the delta relics in Gusev Crater were studied with Mars Express HRSC data and Themis images. A chronology of active channels and terraces including the delta was based on height and slope. Flow discharge (assuming water) was reconstructed for measured channel slopes, channel widths and depths, and with a recent model for hydraulic roughness (Wilson et al. 2004). Sediment mobility and transport were computed based on the flow discharge with various models. Based on the sediment transport per unit time and the measured sediment volume of the delta and of the channel, time scales for the erosion of the channel and the formation of the delta were obtained.

The delta relics are superelevated with 200 m above the terraces in the New Plymouth crater at the downstream end of Ma'adim Vallis, and was formed earlier. The downstream slope of the delta mesas is 3:10, which is comparable to the maximum angle of repose at the downstream side of Gilbert-type deltas on Earth. A flow discharge in the order of 5e6 m3/s and a flow velocity of about 20 m/s were computed which agrees with earlier estimates (Cabrol et al. 1998, Irwin et al. in press). The flow was slightly supercritical (Froude>1), and Shields (sediment mobility) numbers are far above the upper stage plane bed criterion (\theta>>1) which is consistent with the lack of relic bedforms on the channel floor. These estimates are not sensitive to the assumed grain size of 0.01 m because there is a trade-off between hydraulic roughness (related to grain size) and sediment mobility (related to hydraulic roughness and inversely to grain size). Given earlier estimates of upstream lake overflow volumes, the flow discharge was maintained for about 400 days. Preliminary sediment transport predictions are in the order of 5 km3/400days including pore space. This implies a delta formation time in the order of 100 times longer than of the lake surplus drainage, which suggests persistent reloading of the lake. The volume concentrations of sediment are orders of magnitude smaller than assumed in literature so far which were based on older models (e.g. Komar 1979, Cabrol et al. 1998).

ACHERON FOSSAE, MARS: A MARTIAN RIFT OBSERVED BY THE HIGH RESOLUTION STEREO CAMERA (HRSC)

P. Kronberg (1), E. Hauber (2), K. Gwinner (2), B. Giese (2), P. Masson (3), T. Schäfer (1), G. Neukum (4), and the HRSC Co-Investigator Team
(1) Institute of Geology, TU Clausthal, Germany, (2) Institute of Planetary Research, German Aerospace Center (DLR), Berlin, Germany, (3) Lab. Orsayterre (CNRS FRE 2566), Univ. Paris-Sud, Orsay, France, (4) Institute of Geosciences, FU Berlin, Germany.
kronberg@geologie.tu-clausthal.de

Several large extensional tectonic structures on Mars have been described as possible analogues to terrestrial continental rifts. With few exceptions (e.g., Hauber and Kronberg, 2001), however, there was no detailed description of the rifts, partly because there was no accurate topographic information available. The HRSC on the Mars Express mission began to acquire high-resolution stereo colour images in January 2004. Orbits 37 and 143 in January and February 2004 covered large parts of the Acheron Fossae north of Olympus Mons, respectively. We constructed a Digital Elevation Model (DEM) and registered orthoimages in colour. Our preliminary analysis shows that several rift-like surface features can be identified at Acheron Fossae. We see some large horst and graben structures, the latter being filled with a relatively dark and smooth material. This material is smooth and seems to have been subject to viscous flow. In places, its distribution is obviously controlled by sun exposure, so it may be related to climatic processes. The extensional structures are situated on a topographical high. The graben shoulders are elevated, and this may be the result of rift flank uplift. At least one small, conical volcano can be distinguished. We measured fault offsets in the DEM, and obtain a minimum extension of 3.5 km across the Acheron Fossae system. The actual value is probably higher, since the graben filling obscures the actual vertical offset. Our preliminary conclusion is that the Acheron Fossae are indeed comparable to a terrestrial continental rift.

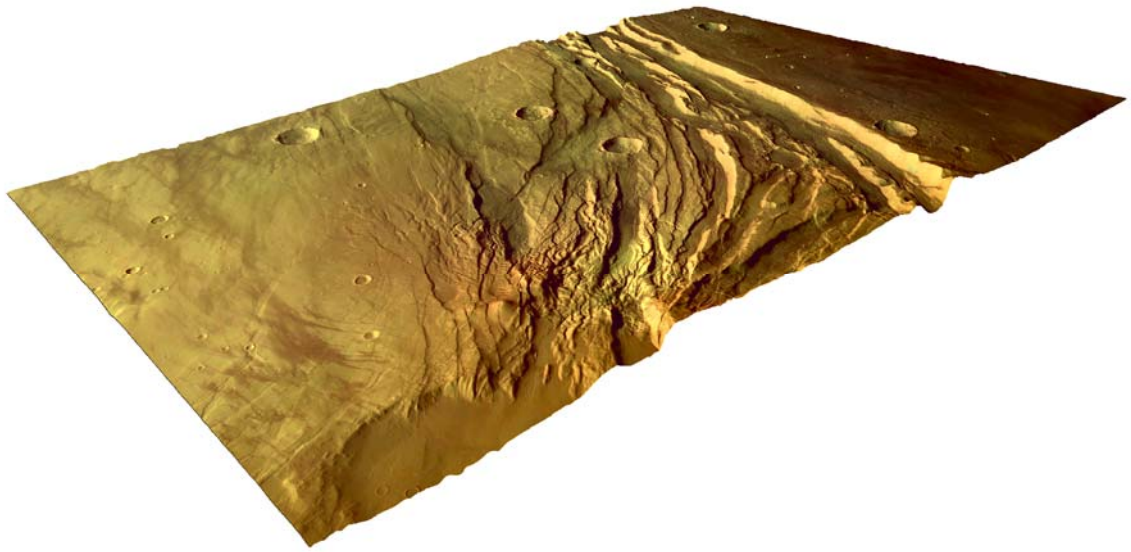

Perspective 3D-view from the southeast (North is toward the upper right) of orbit 37, showing the eastern part of the possible rift system. Note the prominent graben on the northern part of the scene, and the heavily fractured area in the foreground with a possible small volcanic cone in the center.

Multispectral Investigation of the Gusev Crater Region Using Mars Express HRSC Colour Data: Preliminary Results

Martin, P.; Cord, A.; Foing, B.; Zegers, T.; Van Kan, M.; Pinet, P.; Daydou, Y.; Hoffmann, H.; Hauber, E.; Jaumann, R.; Neukum, G.

Evaluation of the composition and distribution of planetary surface materials provides important information about surface processes and regional or local stratigraphy. The focus of this investigation is to use the potential of the HRSC multispectral colour data, combined with the available high spatial resolution, to characterize and constrain the compositional heterogeneity of Martian surface units.

HRSC data of the Gusev crater region are used as a first geologic study area to identify colour and compositional units, to assess the relationships with geological units and other information, and to provide further insight into the regional geologic, climatic history. Other collaborative investigations (Cord et al., Pinet et al., this issue) deal with the characterization of photometric and surface physical properties (e.g., surface roughness, texture) through multi-angular investigations in the same region.

Mosaics of calibrated HRSC frames of the Gusev area, produced for each of the five colour bands and co-registered to form the corresponding image cube, are used to derive various sets of data analysis products such as multispectral image composites. The latter enhance and isolate the colour and spectral differences related to surface composition and mineralogy. Support data sets for this work include multi-angular HRSC measurements, HRSC Digital Terrain Model, MGS/MOC and MOLA data sets, and Mars Odyssey/THEMIS data sets. The preliminary results derived from our investigations will be presented.

Chaotic Terrain Development and the Origin of Layered Deposits – Re-Investigation Combining up to Date HRSC Data and Other Available Datasets

Masson, P.; Lanz, Julia; Peulvast, J-P.; Ansan, V.; Neukum, G.

We are re-investigating the Martian outflow channels, i.e. their source regions in particular, using new HRSC data in combination with other datasets (MOC, Themis) currently focussing on Aram Chaos, Juventae Chasma and Aureum Chaos. All three regions have good HRSC coverage and are of particular interest as they exhibit large units of layered deposits of the kind identified in numerous equatorial regions on Mars. It has been proposed that they are evaporites formed in former standing bodies of water on Mars, eolian deposits or volcanic pyroclastic deposits.
Based on our observations drawn from the combination of all available datasets we interpret these deposits at least in Aram Chaos to be in fact eolian deposits that have been altered by hydrothermal processes in connection with the development of the chaos terrain. We find no clear indication whatsoever for the existence of a large standing body of water in Aram Chaos. Furthermore, the improved morphologic insight in the region gained from the very valuable HRSC context information and stereo data supports the proposed eolian origin of the deposits and shows features of possible hydrothermal or even volcanic origin. As to what extent our observation can be applied to other layered deposits or chaos regions needs yet to be investigated.

HRSC Observations of Valley Networks and Inverted Channels in the Valles Marineris Region

Masson, P.; Mangold, Nicolas; Ansan, V.; Lanz, Julia; Quantin, C.; Neukum, G.

Shallow valleys with a dendritic pattern are observed on the plateau West of Echus Chasma. They extend over 200 km along the plateau border with drainage densities reaching 1.3 km-1. Juventae plateau also displays lineations connecting together. A detailed observation shows that they likely consist of inverted channels, i.e. channels formed by fluvial processes and then exhumed by differential erosion of the surficial layer. These lineations are indeed different from any tectonic or volcanic features such as wrinkle ridges. Both features on Echus or Juventae region are too pristine to be visible on HRSC DTM. The plateau in the Valles Marineris consists of a thick accumulation of volcanic material dated of the Hesperian epoch. Fluvial features cutting these Hesperian layers are thus unexpectedly young relative to the fluvial history of Mars.

Emissivity Spectra of Planetary Analog Materials: a Key for the Interpretation of Remote Sensing Measurements

Maturilli, A.; Witzke, A.; Moroz, L.; Helbert, J.; Arnold, G.; Wagner, C.

Reflection and emission spectra of planetary surfaces contain extensive information on the surface properties and in particular on mineralogical composition. The compositional information is provided by diagnostic mineral absorption features a ected by their composition and structure.

To interpret features of planetary spectra in a right way, it is essential to study the spectral behaviour of terrestrial analog materials using laboratory measurements. We present here a device that enables us to measure emissivity spectra of analog materials in the mid-infrared wavelength region.

We have collected spectra of various rock-forming minerals relevant for surfaces of terrestrial planets. To study the important influence of grain size on the spectra, dierent grain size fractions of the materials have been prepared ranging from coarse to very fine grains. In addition, spectra of mineral mixtures have been measured to investigate the opportunity to apply a linear deconvolution method using the end-member minerals.

Interior Layered Deposit in Coprates Chasma north wall: results from Mars Express High Resolution Stereo Camera (HRSC) derived topography

Michael, G.[1], E. Hauber[1], K. Gwinner[1], R. Stesky[2], F. Fueten[3], D. Reiss[1], H. Hoffmann[1], R. Jaumann[1], G. Neukum[4], T. Zegers[5], and the HRSC Co-Investigator Team
[1]Institute of Planetary Research, German Aerospace Center (DLR), Berlin, Germany
[2]Pangaea Scientific, Brockville, Ontario, Canada
[3]Department of Earth Sciences, Brock University, St. Catharines, Ontario, Canada
[4]Remote Sensing of the Earth and Planets, Freie Universitaet, Berlin, Germany
[5]ESTEC, ESA, Noordwijk, The Netherlands

The interior layered deposit (ILD) in the north wall of Coprates Chasma differs from those we have examined in Hebes, Ophir, Candor, Melas, and Juventae Chasmata (Hauber et al., *EOS Trans. AGU, 85*(47), Fall Meet. Suppl., Abstract V33C-1471, 2004; and this conference) in that its base apparently occurs some 2300m above the main chasma floor. Situated in a re-entrant of the main chasma wall, it has two main sections, the maximum lateral extent of the larger deposit (A) being about 15 km. As for several of the other ILDs, its layering appears not horizontal, but dipping outwards from the centre. If this deposit were of volcanic origin, which would be consistent with the present layer geometry, its formation might be expected to be associated with the increased degradation of the chasma wall in the region. If it were a remnant of a much larger sedimentary deposit, we need to understand what caused the deformation of the layers from their original horizontal orientation. The scale of curvature of the layering corresponds to the present deposit size, suggesting that it would be the remnant, and not the original deposit which was deformed. Using a digital terrain model derived from HRSC stereo together with projected nadir and colour channels and manually coregistered MOC images, we investigate the structure of the layering, the present erosional features, the contact with the degrading chasma wall, and the relationship between the alcove and deposit. G. Michael acknowledges the financial support provided through the European Community's Human Potential Programme under contract RTN2-2001-00414, MAGE.

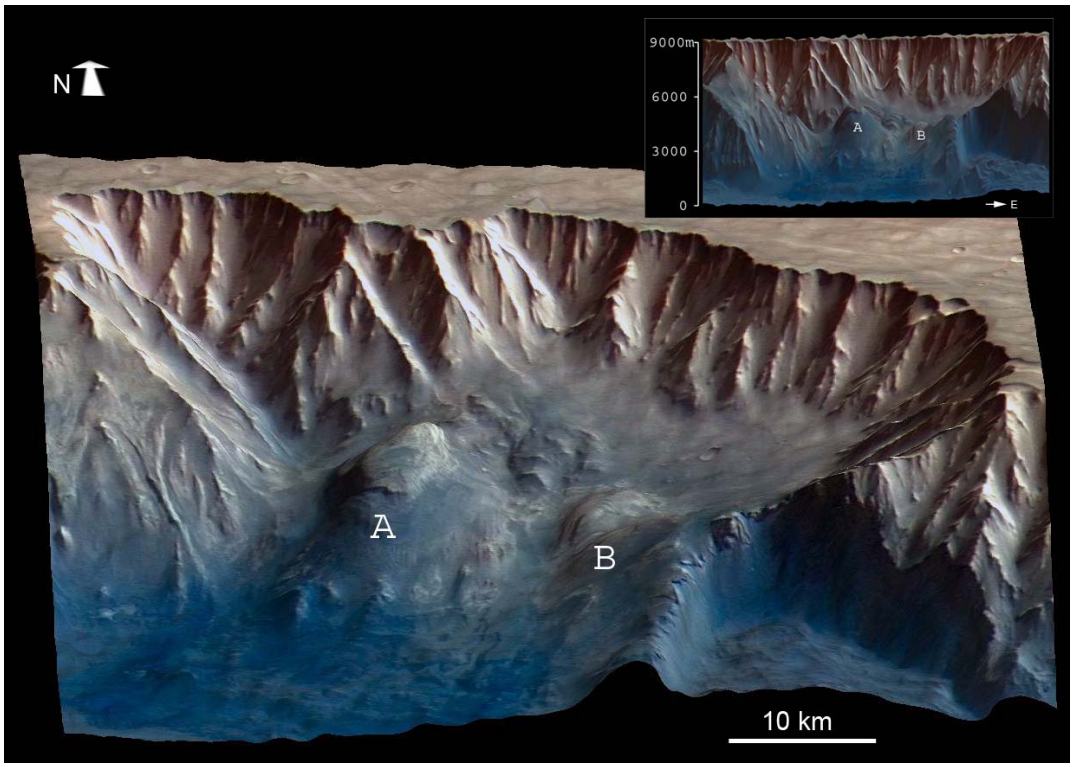

Perspective view of the Coprates wall ILD. The two sections (A, B) also shown in front view with vertical scale (inset)

Extent and Further Characteristics of Former Glaciated Terrain Owing to a Retreating Frozen Lava-Covered Water Lake in Elysium Planitia, Mars

Nussbaumer, J.

Ice sheets from a retreating and sublimating frozen lake changed the planet's surface in southeastern Elysium Planitia, Mars, significantly, leaving different characteristic morphologies, well known from similar glacial terrestrial environments. An interesting aspect in this region is the relatively young age of the deposits, derived from the small amount of impact craters.

The presence of rootless cones indicating shallow subsurface ice in recent times close to the Mars equator [1] suggests that lava partly covered a frozen lake, which was filled with water, originating from the Athabasca Valles outflow channel. The partial burial of the frozen ice by lava may have conserved water reservoirs, which were freezing to a significant depth, until an equilibrium of salinity, pressure and temperature was reached. The existence of submarine fans on Mars elsewhere on the planet in equatorial regions (e.g. Themis VIS V10074013) shows that liquid water under an overlying ice cover could have existed in southern Elysium, too, and could exist to the present day. Meteorite impacts into this overpressured aquifer may have led to either outbursts of still liquid water or the deposition of dust and ice subsequent to an impact. This mechanism was likely responsible for the formation of an overlying deposit, the Medusae Fossae Formation, which shows signs of sublimating ice at different places. For example, circular rings at the margin of this formation (MOC e1701551) are abandoned ice, which was left over after the sublimation and retreat of the Medusae Fossae Formation. Similar features have been observed in the wadden sea in a smaller scale on earth in winter. Here, snowpacks were buried with sand owing to tidal action. After the melting of an inner snow core, the small hillock collapses, leaving behind an outer ring structure. Channels, which are running out of such pingolike hills (MOC E1201250) additionally suggest the melting of a water ice core.

The northward actively retreating ice border, part of the sublimating frozen lake, left sander plains, dead-ice holes, flutes and moraines (Themis IR I01842008). The imprints of grounded ice blocks in smooth terrain suggest the former existence of a proglacial lake south of the ice margin. Soft material from the smooth and wet subsurface underneath the ice was pressed into crevasses (possibly from meteorite impacts) of the surrounding ice. The subsequent sublimation of the ice left behind wall-like structures in a staircase pattern (Themis IR I09394006), a mechanism well known from areas in Iceland. Martian channels, which run extremely parallel to each other (MOC E1301135), resemble terrestrial tunnel channels, since these kind of channels are often oriented in the same parallel manner.

Reference:

[1] Lanagan, P. D.; et al. 2001, Geophysical Research Letters, Volume 28, Issue 12, p. 2365-2368.

High-resolution Morphological Analysis of the Central Part of Ares Vallis using HRSC, MOC and THEMIS Data

Pacifici, A.; Ori, G.G.; Neukum, G.

Ares Vallis is one of the biggest outflow channels of Mars and the easternmost outflow channel entering in Chryse Planitia. It is was inferred to have been formed by cataclysmic floods of water conveyed from sources areas, which are marked by chaotic terrain named Hydaspis Chaos, Aram Chaos and Iani chaos. Different hypothesis propose a glacial origin, or, more likely, a combination of glacial and fluvial processes. The TES data of Ares Vallis show a relatively high thermal inertia surface not observed in the surrounding outflow channels.
This study is focused on the detailed morphological analysis of the floor area at the central portion of Ares Vallis and the neighbouring region using HRSC, MOC and THEMIS images.
The observed morphological units are mapped using visible data and infra-red data. This allows the discrimination of a qualitative association between morphological units and theirs thermal properties, such as thermal inertia. Visible data observation lead to the identification of three major morphological units: rock unit, dunes unit and pitted-surfaces unit. Each kind of units shows also a proper different thermal inertia degree.
Several of the morphologies characterising pitted-surface unit such as pits, pits whit entering channel, and polygonal terrains are possibly correlated to periglacial environment or permafrost rich soil. They display the highest degree of thermal inertia with respect to near rock and dunes units. Furthermore, some decametre-scale and pristine channels are associated to pitted-surfaces unit.
In our hypothesis, association of periglacial structures, or ice rich soil, and channels to high thermal inertia bodies, could suggest the presence of buried ice, likely remnant of glacial period of Ares Vallis.

Derivation of Mars Regional Photometric Surface Properties from Omega Spot Pointing Observations

Pinet, P.; Daydou, Y.; Cord, A.; Chevrel, S.; Bibring, J-P.; Poulet, F.; Erard, S.; Melchiorri, R.; Arvidson, R.

During Orbit 604 the Mars Express spacecraft was rotated to allow the OMEGA instrument to obtain data of contiguous regions at varying emission angles to derive an Emission Phase Function (EPF). We have explored the possibility of deriving surface photometric properties from the EPF observations. The objective is to determine and map soil/bedrock physical properties and to relate them to the spectroscopic and thermal observations produced by OMEGA, TES and THEMIS instruments, and from in situ data.

For this purpose, an inverse method optimizing the determination of the global set of Hapke parameters, developed and tested on experimental data produced with a laboratory wide-field multispectral imaging facility [Cord et al., 2003], has been utilized to reduce the OMEGA EPF data. First results characterizing the photometric behavior of the martian surface/atmosphere system through its optical scattering properties are produced. For the surveyed area (Medusae fossae, south of Amazonis / Cerberus), with intermediate albedo, topographic roughness and thermal inertia (70-90 S.I.) terrain properties, the regional photometric properties derived from VNIR (0.35 to 1.07 micrometers) and IRC (0.9 to 2.6 micrometers) OMEGA detectors are quite consistent with in situ Viking and Mars Pathfinder soils / rocks photometric observation (bright soils / gray rocks) [Arvidson et al., 1989; Guinness et al., 1997; Johnson et al., 1999],. These results have implications for the OMEGA spectroscopic interpretation (e.g., spectra for granular mixtures) (to be linked with MER) and for the preparation of MRO/CRISM observations.

Iron-reach Silicate as Water Marker: Olivine in OMEGA Spectra

Politi, R.; Fonti, S.; Altieri, F.; Bellucci, G.; Bibring, J-P.; Blanco, A.; Verrienti, CC.

The presence of liquid water on Mars in the past is one of the main issues concerning the Red Planet. Geological suggestions about the ancient presence of liquid water are given by the network valleys and the presence of rubble cones in some craters. From the spectroscopic point of view the presence of liquid water on the surface of Mars can be checked through the detection of carbonate and sulfate deposits. In this work we present an alternative method involving the alteration of iron reach silicates. The presence of olivine deposits in some Martian locations, like Nili Fossae, suggests that this mineral could be a good candidate for this test. We focalize our attention on two features at 0.45 and 0.65 micron induced by the aqueous alteration of Fe2+ in Fe3+. We shall discuss our method and present the preliminary results of its application to the spectra recorded by OMEGA.

Possible Origins of Light-toned Materials in Margaritifer Sinus

Popa, I.C.; Ori, G.G.; Komatsu, G.; Neukum, G.

Data from Mars Express instruments indicate that light toned deposits located in regions of Oxia Palus and Terra Meridiani correspond to diverse mineralogy, but all of them appear to be related to water deposition.

The examination of visible image data (HRSC, THEMIS VIS and MOC) shows that light-toned dust-covered layered materials expand in Margaritifer Terra, and covers most of the central part of Aureum Chaos (northwestern part of Margaritifer Terra), western part of Iani Chaos, Margaritifer Chaos and central part of Aram Chaos. These structures seem to be deposited at the bottom of large bodies of stagnant water, which resided there long enough for them to form under evaporitic conditions. Detailed geologic, mineralogical, and morphometric mapping of the Aureum, Iani and Margaritifer Chaos systems permits evaluation of possible mechanisms for chaos formation and pre- or/and post-chaos evolution. Geomorphic and multispectral thematic mapping was made using visible and IR datasets: MOC, THEMIS VIS and IR (nighttime and daytime) and HRSC images and stereo-derived digital terrain models of the area situated from latitude: 0-8? S and longitude: 15-30? E.

Deconvolution of OMEGA Spectra: a First Quantitative Analysis of the Maficcomposition

Poulet, F.; Arvidson, R.; Mangold, N.; Platevoet, B.; Bardintzeff, J.-M.; Mustard, J.; Gendrin, A.; Bibring, J.-P.; Langevin, Y.

OMEGA provided detailed mineralogical composition of the basaltic spectraltype of the surface of Mars. Using the modelling method described in Poulet and Erard (2004), we will present non-linear deconvolution of the atmospherically corrected spectra of some selected martian regions showing strong mafic features. Quantitative estimates of the abundance and grain size of the minerals used in the mixture (typically high- and low-calcium pyroxene, olivine, plagioclase, oxide) will be derived.

Surface Type II: a New Assessment from OMEGA

Poulet, F.; Mangold, N.; Gendrin, A.; Mustard, J.; Arvidson, R.; Bibring, J.-P.; Langevin, Y.

ES spectra have been interpreted to represent two general spectral classes: the basaltic type TES I (confirmed by OMEGA, Mustard et al. 2005),and the andesitic type TES II (Bandfield et al. 2000). Several alternative hypothesis have been presented to explain the apparent andesistic character of the Acidalia-type spectrum: weathering of basalt to produce clay minerals (Wyatt and McSween 2002), silica coating basalt (Kraft et al. 2003), oxidation and recrystallisation of a SNC-type basalt (Minitti et al. 2002), palagonization of basalt (Morris et al. 2003). OMEGA observations show that the northern dark regions present unique spectral characteristic: strong blue slope with no hydration with no clear evidence of hydration band at 1.9 µm. Very weak mafic signature may be present in some locations. In the light of the NIR spectral characteristics, the previously proposed compositions will be discussed.

Erosion-Deposition History of the Eastern Hellas Region

Raitala, J.; Ivanov, M.; Korteniemi, J. ; Kostama, V-P..; Lahtela, H.; Aittola, M.; Neukum, G.

The Hellas Basin impact structure, an old, ~2000 km wide and ~9 km deep circular depression, is located on the southern Martian hemisphere where it is surrounded by ancient highlands. There are numerous volcanic, fluvial, and glacial features within and around the basin. The HRSC instrument has provided us with new insights to the depositional evolution of the Hellas impact basin and its surroundings. When studying the new HRSC data sets we find that the region has undergone a broad spectrum of erosional and depositional events.

Hesperia Planum, a high-standing volcanic plateau of Hesperian age (1300x1700 km, area ~1.5 106 km2), forms part of the NE section of the Hellas Basin rim. The Hesperia Planum region and surrounding uplands host a rich array of volcanic and fluvial landforms suggesting that the interaction of volcanic and fluvial processes is the main theme of both the evolution of Hesperia Planum and the history of deposition in the Hellas Basin.

The distributed (lava plains) and centralized (paterae) volcanism in Hesperia Planum probably played the major role in mobilization and release of the volatiles around and in the Hesperia Planum basin. The volcanism of Hesperia Planitia had resulted in the formation of up to 500 m thick lava layer. A large amount of lavas appeared to flow to Hellas Basin floor. It is likely that the volcanic activity had induced the main episode of erosion in Hesperia Planum and it is also possibly that later magmatism triggered formation of the channels.

The evidence for volatile transport, erosion, and sedimentation is presented in the southern part of Hesperia Planum where Morpheos basin had served as a transient reservoir for the volatiles (water) that flowed out from beneath the Hesperia Planum lava plains. Possible catastrophic discharge of Morpheos basin had carved the distinct channel of Reull Valles. The continued, and evidently more localized, magmatism later triggered the formation of Dao, Niger and Harmakhis channels by releasing water from the sub-surface volatile reservoirs.

The eastern Hellas rim region has also numerous smaller paleolakes - mostly situated in craters - and lake chains. This accentuates the importance of repeated water releases in the development of the area as well as indicates that it, anyway, deminished along the time. Some amount of water was also trapped inside certain impact craters in the region as seen from the features indicative for indicating evaporation/sublimation of buried volatile rich sediments.

The glacial-type depris aprons and glacier-like flows characterize additional late aspects of the evolutionary history of the region and the trend of diminishing both amount and activity of water in the time and space in Martian history. These more restricted viscous flows may not have been related to volcanic activity and they represent flows from the largely depleted initial reservoir of volatiles within the Hesperia Planum and eastern Hellas rim area.

Conclusion: The hydrologic history of Hesperia Planum was alternating with volcanism and apparently began with the accumulation of volatiles around and in the Hesperia Planum basin and with the formation of a large reservoir of volatiles in late Noachian. Since then the reservoir was emptied in different modes that reflect diminishing amount of stored volatiles. 1) The massive areal erosion that smoothed out the surface within the Hesperia Planum area and erased the Noachian crater record there before emplacement of volcanic plains may also have been connected to the first erosion phase in the eastern Hellas rim area. 2) Filling the Morpheos basin from the reservoir below the lava plains resulted in the subsequent formation of Reull Vallis. 3) Concentrated major outflows carved Dao, Niger, and Harmakhis Valles while there were also more restricted flow activities as seen from several crater lakes, lake chains and adjoining smaller channels. 4) More present dispersed viscous, or glacial-like, flows are presented by debris aprons and in-crater glaciers. Sublimation of water from volatile-rich layers inside impact craters is seen from certain pitted crater floor units. The multi-spectral Mars Express HRSC data provide excellent imagery to study the volcanic and volatile-related evolution of Hesperia Planum and the rim history and depositioal units of the Hellas Basin, Mars.

Influence of the Thermal Properties of a Regolith Cover on the Depth of the Melting Point of Water and the Sublimation Rate of Ice

Schumacher, S.; Breuer, D.; Spohn, T.

The thermal state of the immediate subsurface is mainly defined by the thermal properties of the regolith, which covers extensive areas of Mars. Although the exact vertical extend of the regolith, its porosity and therefore thermal conductivity are unknown, it is possible to deduce maximum values by using analogues to lunar material. Given a lunar regolith thickness of about 22 km, gravitational considerations lead to a maximum Martian regolith cover of approximately 10 km. At this depth the temperature will likely be above the melting temperature even if conservative values for surface temperature and thermal conductivity are assumed. The thermal conductivity of the regolith still poses a problem as only the upper and lower bounds are fairly well known. The upper limit is given by the thermal conductivity of solid crustal material which is in the range of about 2 W/(mK). The lower limit can be inferred from measurements of thermal interia which yields values of 0.001 to 0.05 W/(mK) for very fine grained unconsolidated regolith. Asumming an increase of the thermal conductivity with depth due to increased pressure and reduced porosity, it is possible to extrapolate reasonable models for the thermal conductivity.

Based on these models the depth of the melting point of water can be calculated depending on surface temperatures and heat flow from below. Both parameters have changed considerably in certain areas (e.g. Olympus Mons) in the recent past due to changes in obliquity and volcanic activity. It is therefore necessary to understand the effect of these variations on the temperatures within the regolith to assess the stability of ground ice especially in low latitude regions. As new results of the HRSC indicate the occurrence of glaciers at equatorial latitudes on the flanks of volcanoes, the sublimation rate and long-term stability of these near-surface ice layers is analysed considering different burial depths, changes in the thermal properties of the regolith as well as variations in obliquity during the last 10 Ma.

Volcanic History of Hadriaca Patera Constrained by HRSC Data

Williams, D.; Greeley, R.; Zuschneid, W.; Werner, S.; Neukum, G.; Raitala, J.

Hadriaca Patera is one of several "highland paterae", or low-relief, areally extensive central vent volcanoes located on the Hellas basin rim in Mars southern cratered highlands. Hadriaca exhibits a central caldera and deeply incised slopes containing radial channels and ridges, which are thought to be associated with fluvial erosion of very friable layered materials, most likely explosively-emplaced pyroclastic deposits. Crown and Greeley (1993) mapped the geologic units around Hadriaca using Viking imagery to investigate the styles of geologic activity in this area.

Recently, the High Resolution Stereo Camera (HRSC) on Mars Express imaged Hadriaca Patera in color and stereo on orbits 528 (19 June 2004) and 550 (25 June 2004), at nadir resolutions of 25 and 50 m/pixel respectively. Two Super Resolution Camera (SRC) mosaics at 10 m/pixel were also obtained of the caldera rim. These higher resolution HRSC and SRC images will enable the reassessment of the mapping of Crown and Greeley (1993) through identification of the geologic processes that have shaped the volcano, and through estimates of ages for specific map units obtained by crater counts. For example, Crown and Greeley (1993) mapped the Hadriaca caldera as a single geologic unit, Hesperian caldera floor material. In the HRSC images we have been able to delineate four subunits in the caldera, with ages ranging from 1.1 to 3.5 Ga, suggesting volcanic resurfacing was continuous on the caldera floor through much of early Martian history. Further study and analysis is in progress, which will provide a better understanding of volcanic processes in this region of Mars.

Estimation of the Detectibility of Anhydrous and Hydrous Sulfates in Martian Soil From Laboratory Reflectance Spectra

Witzke, A.; Arnold, G.

Measurements of the elemental composition of Martian soil at Viking 1, Viking 2 and Pathfinder landing sites show a significant amount of the element sulfur in the soil. These measurements have recently been verified by the APXS instruments installed on the two NASA Mars Exploration Rovers. The environmental conditions on Mars lead to the assumption that most of the sulfur is bound in sulfate minerals. However, spectral remote sensing data for the Martian surface did not show clear evidence for significant amount of sulfates in Martian soils. To estimate the general detectibility of sulfates by remote sensing spectra provided by the PFS and OMEGA instruments on Mars Express, we acquired laboratory reflectance spectra of various fine-grained sulfates mixed with a palagonite powder that is a reasonably good spectral analog for Martian soils. Our reflectance spectra cover the spectral range from 1.4 to 17 µm. By varying the amount of the admixed sulfate mineral we were able to estimate detection limits of sulfate absorption features. Results of the Gamma Ray Spectrometer onboard Mars Odyssey spacecraft suggest significant amount of hydrated minerals on the surface. Therefore we studied hydrous sulfates as well as anhydrous sulfates to investigate if they show different detectability. The spectra presented here include mixtures of palagonite with anhydrite, gypsum, anhydrous magnesium sulfate, kieserite and epsomite.

Is Mars Hiding some Ice in Terra Arabia?

Helbert, J.; Formisano, V.; Benkhoff, J.; thePFS-Team

The SWC channel of the PFS instrument on MarsExpress has detected an enhancement in the atmospheric water vapour content close to the surface over Terra Arabia (Formisano et al. 2003). Interestingly this is one of the equatorial areas in which GRS on Mars Odyssey reports an increased water content in the soil (Boynton et al. 2003). The HEND instrument of the GRS instrument suite reports a water abundance of 12 wt% below an at least 19cm thick layer of dry soil (Mitrofanov et al. 2003).

There are three main explanations for this observed amount of water which are not mutually exclusive. Some of the water measured is most likely adsorbed water. While it is still unclear how much water the Martian soil can adsorb, this mechanism can not explain the high abundances measured in this area. We might see highly hydrated minerals. Some of the suggested minerals are indeed capable of holding large quantities of water. The question in this case is how easy these minerals would desorb water to explain the enhancement of water vapour seen in the atmosphere. The last and maybe most exciting possibility are near surface ice deposits. However if it is ice, the question is, how did it survive close to the surface in the equatorial region. And how can we explain in such a scenario the enhanced water vapour content in the atmosphere.

To investigate the possibility of near surface ice deposits in Terra Arabia we have performed a detailed study of the area using the Berlin Mars near Surface Thermal model (Helbert and Benkhoff 2003 and poster this conference). This model allows to study in detail the distribution and movement of volatiles within the subsurface over time. For the study classified several areas in Terra Arabia with very distinct thermophysical properties.

We will show a scenario in which ice placed in Terra Arabia during a recent ice age in Mars is indeed stable within 1m below the surface over several 10ka. GCM calculations as done for example by Haberle et al. (2004) show, that during phases of higher obliquity larger amounts of high can be deposited in this area. The ice deposit is protected until present time by a lag deposit consisting of a layer of very fine, bright dust with a very low thermal conductivity. We find this dust layer in one of the area which geographical coincides with the areas showing the highest content of water in the soil in GRS measurements.

While such a long time stable ice deposit would explain the GRS observations, it contradicts the observations by PFS. However we have identified adjacent areas in which ice might have migrated downward after deposition on or close to the surface. This downward migration can lead to the formation of an ice lens with the first few meters below the surface. The modelling shows that a destruction of this ice lens by sublimation can lead to a significant increase of water vapour being released in the atmosphere. This might by observed by PFS right now.

Age Measurements and Stratigraphic Relationships in the Hadriaca Patera, Dao and Niger Valles Regions

Zuschneid, W.; Neukum, G.; Werner, S.C.; Greeley, R.; Williams, D.; HRSC co-I, Team

New image data, acquired in orbit 528 by the High Resolution Stereo Camera on the ESA Mars Express mission, cover the outflow channel system of Dao and Niger Valles as well as the highland volcano Hadriaca Patera. On the basis of these high resolution data, age measurements have been made that provide new insights into the evolution of the volcano and the outflow channels[1-3]. The measurements show that the formation of the oldest surfaces of Hadriaca Patera took place at about 3.8 Ga and precedes the emplacement of the surrounding volcanic plains at 3.5 Ga. Contemporaneous with the formation of the plains, the volcano built up most of the preserved flank units, which have an age similar to the interior of the caldera. Resurfacing of the flanks occurred at 2 Ga, possibly caused by the formation of the radial drainage system. In the central region of the caldera, resurfacing occurred at 2.5 Ga, while in the northeastern and southwestern regions, it occurred at about 1.6 Ga to 1.1 Ga. These subsequent resurfacing processes were also active in the shallow depression between the caldera and the system of fractured plains east of Hadriaca Patera. This late-stage activity has been attributed to a shift from explosive to effusive activity [2]. The youngest observed units are the smooth deposits on the floor of Dao Vallis with an age of 0.3 to 0.5 Ga. These new measurements, in combination with stratigraphic analysis, provide constraints on the evolution of the Dao and Niger Vallis outflow system and its proposed genetic connection to ground ice melting by intrusive volcanism [5]. References: [1] Crown, D.A. and Greeley, R. (1993) JGR 98, 3431-3451; [2] Hartmann, W.K. and Neukum, G.(2000) Space Sci. Rev. 96, 185-194; [3] Ivanov, B.A. (2001) Space Sci. Rev. 96, 87-104; [4] Gregg, T.K.P., et al. (2002), LPSC 2002, 1560; [5] Squyres, S.W. et al. (1987) Icarus 70, 385-408

Poster Session 2
Surface Chemistry , Martian Polar Regions, Atmosphere and Climat

Surface Chemistry from Orbit and In-situ

The Martian Polar Regions

The Martian Atmosphere and Climate

Martian Soil and Atmosphere as Seen through Their Gamma-Ray Continuum

Gasnault, O.; d'Uston, CC.; Maurice, S.; Reedy, R.; Boynton, W.; Brückner, J.; GRS Team

Since 2002, the Gamma-Ray sensor Head (GSH) onboard Mars Odyssey has been measuring the high-energy photons emitted by the Martian surface through its atmosphere [Boynton et al., 2004]. These photons are produced by the nuclear reactions of the cosmic rays with the planetary surface bulk elements. The measured signal is therefore the result of the cosmic rays going through the atmosphere, the reactions in the surface, and the photon transport from some depth under the surface to the spacecraft above the atmosphere.

A gamma-ray spectrum is made of narrow lines sitting above a large continuum. The lines are representative of specific chemical elements and are used to build composition maps [Brückner et al., and Boynton et al., this conference]. The continuum component mainly results from the Compton scattering and the Bremsstrahlung electrons in the soil and in the atmosphere. Numerical simulations reveal that the continuum from the planet dominates the spectrum below 2 MeV, while above 8 MeV the direct interactions of the cosmic rays with the germanium detector take over. On the Moon, the gamma-ray continuum has been used to map the main chemical terranes [Bielefeld et al., 1976; Gasnault, 2004].

Here we choose to use the low-energy continuum in the range 200 keV to 300 keV, to derive some information on the Martian atmosphere. Seasonal variations are clearly seen in the observations. They are related to the variation of the atmospheric transmission linked to the variations of the atmospheric column density. Not only do they reveal the seasonal breathing of the atmosphere, but they also show that the variations have not exactly the same time profile from place to place; this is shown when comparing the southern highlands with northern lowlands,the volcano areas or the Hellas basin area. In the specific case of the lower latitude measurements, part of the variation may be due to the partial covering of the surface by a layer of CO2 ice during southern winter. The aim of future work will be to analyse systematically these differences to put some constraints on the atmospheric movements during the Martian year. The measurements show also a continuous increase of the counting rate that could be associated with the long trend variation of the cosmic ray flux, as well as temporary effects of the solar particle events.

Bielefeld, M.J., R.C. Reedy, A.E. Metzger, J.I. Trombka, and J.R. Arnold (1976), "Surface Chemistry of Selected Lunar Regions", in: Proceedings of the 7th Lunar Science Conference, vol. 3, pp. 2661-2676, Pergamon Press

Boynton, W.V., et al. (2004) "The Mars Odyssey Gamma-ray Spectrometer Instrument Suite", Space Sci. Rev. 110, 37-83.

Gasnault, O. "Lunar Mapping from Low-Energy Gamma-Ray Continuum", International Conference on Exploration and Utilization of the Moon, Udaipur, Nov. 22-26, 2004

Chemical Diversity of the Gusev and Meridiani MER Landing Sites

Gellert, R.; Brückner, J.; Dreibus, G.; Rieder, Ruda.; Zipfel, J.; Lugmair, G.; Wänke, H.; Clark, B.; Yen, A.; Squyres, S.

Each of the two Mars rovers of the NASA MER mission carries an Alpha Particle X-Ray Spectrometer (APXS) to determine the elemental composition of rocks and soils at Gusev crater and Meridiani Planum. Chemical compositions distinguish between basaltic rocks, evaporite-rich rocks, basaltic soils, hematite-rich soils, and sulphur-rich subsurface layers. Although top surface soils of Gusev and Meridiani are compositionally similar to those at previous landing sites, differences in iron and some minor element concentrations suggest the addition of local components. Abraded rock surfaces at Gusev plains resemble volcanic rocks of primitive basaltic composition with low intrinsic potassium contents. Rock coatings and high abundance of bromine in rock interiors may be indicative of surface alteration formed during a past period of aqueous activity in Gusev crater. Rocky outcrops at Meridiani are rich in sulphur and variably enriched in bromine relative to chlorine. The interaction with water in the past is clearly indicated by the chemical features in rocks at this site. Orbital investigations of Martian surfaces have to take into consideration the chemical diversity on a small scale.

Water Alteration and Biogenic Activity on Mars

Gibson, E.K.; McKay, D.S.; Thomas-Keprta, K.; Clemett, S.; Wentworth, S.; Socki, R.

The Mars Express Mission, Mars Exploration Rovers and surface samples from Mars (i.e. the Martian meteorites) offer a unique opportunity to investigate the history of water and possible biogenic activity on Mars. While we anticipate sample return within the next 15 years or so using robotic missions, we currently have more than 81 kgs of Mars in the form of the ~33 Martian meteorites. To this end, we have continued to integrate the biogeochemical analysis of Martian meteorites along with information returned from measurements obtained from orbit or on the surface of Mars.

Weathering studies: Martian meteorites (at a submicrometer scale) contain traces of secondary phases formed by aqueous alteration processes. In some cases, these secondary materials have been proven to have formed on Mars. While the conditions of formation of these precipitated minerals on Mars is still not well understood, most researchers agree that many of the phases wwere formed at relatively low temperatures in an aqueous environment. The MER Rovers have returned clear evidence for aqueous alterations and enrichments in chlorine, bromine and sulfur contents on weathered surfaces of surface materials. It has been shown that the Cl/Br ratios obtained from selected samples examined by the MER are essentially identical to ratios found within Martian meteorites. Recent results show indigenous Fe-sulfate present in alteration products from Martian meteorite EET79001: this is the first report of Fe-sulfate in a Martian meteorite. Its presence allows us to begin to outline the sulfur-cycle in Martian surface processes and it documents a potential major source of energy for microbial metabolism. Martian meteorites have already demonstrated that water has been actively present near the Martian surface, and has profound implications for the possibility of life.

Magnetite studies: One of the strongest lines of evidence that microbial life existed on ancient Mars is the presence of tens-of-nanometer sized magnetite crystals in carbonate globules and their associated rims. Approximately one quarter of the ALH84001 magnetites have morphological and chemical similarities to magnetites produced by magnetotactic bacteria strain MV-1, which occur in aquatic habitats on Earth. This similarity has been confirmed using electron tomography. Moreover, these types of magnetite are not known or expected to be produced by abiotic means anywhere in nature.

Laboratory synthesis of these magnetites is difficult or impossible. More than five years of inorganic laboratory work has failed to produce even a single magnetite grain having the combination of size, morphology, and chemistry,characteristic of the truncated hexaoctahedral magnetite produced by bacteria strain MV-1. Yet all evidence shows that this form of magnetite occurs in ALH84001 as an indigenous Martian product. In addition, initial SXRF analysis of trace elements in magnetite control samples shows that those biogenic crystals produced intracellularly are chemically pure. We have extended this work to include the trace chemical analysis of magnetites extracted from the ALH84001 carbonate globules.

In situ analysis of organic compounds: All analyzed Martian meteorites contain detectable organic compounds. However, each Martian meteorite also contains some terrestrial organic compounds or contaminants. The challenge is to sort out the terrestrial organics from the Martian organics. Our strategy has been to compare and contrast the organic composition of Martian meteorites with abiotic organic matter formed in the early prebiotic solar system. A laser desorption laboratory has recently been established that utilizes a novel technique that will analyze in situ organic constituents in meteorites and control samples. The recent putative presence of methane in the Martian atmosphere provides supporting evidence of possible Martian biogenic activity. The possibility of enhanced methane abundances in basins which may contain greater abundances of water offers intriguing possibilities for associations with possible biogenic activity. We know on Earth where there is water there is likely to be life.

Lab Simulation of the UV-Radiation at the Martian Surface: Performance and Experiments

Kolb, C.; Hohenau, W.; Lammer, H.; Kargl, G.; Cockell, C. S.; Patel, M.R.; Bercés, A.; Abart, R.; Rettberg, P.

UV radiation can cause specific damage and modifications in the DNA of living systems and it is involved in the formation of catalytically produced oxidants such as superoxide ions and peroxides. Lab simulations are necessary to investigate and understand the effects of organic matter destruction at the Martian surface. We designed a radiation apparatus which simulates the solar spectrum at the Martian surface between 200 and 400 nm. The system consists of an UV-enhanced xenon arc lamp and special exchangeable filter-sets and mirrors for simulating the effects of the Martian atmospheric column and dust loading. We present data on system performance and results of initial experiments. The simulator is integrated into the Austrian Mars simulation facility. The design was focused on portability, thus the Mars-UV simulator represents a device for Mars simulation facilities with emphasis on other Mars research topics, too.

The Chemical Variability at the Surface of Mars: Statistical Analysis on Lander Data

Kolb, C.; Abart, R.; Lammer, H.; Martín-Fernández, J.; Antona.; Pawlowsky-Glahn, V.; Thió Fernández De Henestrosa, S.

The chemical composition of sediments and rocks, as well as their distribution at the Martian surface, represent a long term archive of processes, which have formed the planetary surface. Several sources are envisaged, which may have delivered the matter processed in soils. The materials may originate from basalts, andesites, evaporites and meteoritic matter. Important information on these source materials and on their weathering products is stored in the chemistry and the mineralogy of the soils. In order to extract this information, data reduction is necessary. We applied factor analysis in the simplex vector space under consideration of closure effects on data. The results give evidence for multi-component mixing as well as weathering processes and are visualized by means of biplot techniques and ternary diagrams. The treatment in the simplex vector space allows to quantify weathering effects.

Solid State Oxidation of Fe(II) in an Environment Similar to the Martian Surface

Nornberg, P.; Ricardou, G.; Merrison, J.P.; Gunnlaugsson, H.P.; Jensen, S.K.

Recent explorations of the Martian surface indicate an abundance of reddish Fe(III) species in a thin surface layer whereas darker Fe(II) species dominate below. In order to demonstrate that the oxidation of Fe(II) can proceed readily in the absence of water we have investigated two Fe(II) compounds, anhydrous $FeCl_2$ and ferrocene, $Fe(C_5H_5)_2$, embedded in a pumice matrix. Both systems are exposed to UV radiation of wavelengths similar to those found on the Martian surface. After the radiation the oxidation state of Fe is analyzed with Mössbauer spectroscopy, which shows a clear oxidation of Fe(II) to Fe(III).

Spatial Variability of the Martian Polar Caps: PFS/MEX Preliminary Results

Giuranna, M.; Hansen, G.B.; Formisano, V.; Grassi, D.; Ignatiev, N.; Maturilli, A.; Zasova, L.; Khatuntsev, I.

When in orbit around Mars, PFS has observed several times both the North (LS >= 20°) and the South residual (LS ~ 340°) Martian polar caps in illuminated conditions. The PFS spectral resolution (1.3 cm-1) and spectral range (1.2 ÷ 45 mm) allow identification of unambiguous polar ices features. Different kinds of spectra were observed, with varying CO2 frost cover, water ice abundance and dust contamination.

Seasonal Evolution of the Northern Martian Polar Cap: Comparisons Between MEX/OMEGA, TES (MGS) Observations and LMD GCM Predictions

Levrard, B.; Forget, F.; Schmitt, B.; Doute, S.; Titus, T.N; Bibring, J-P.; Langevin, Y.; Poulet, F.; Montmessin, F.

MEX/OMEGA infrared and visible spectrometer onboard Mars Express allows a detailed, improved and quantitative study of martian polar ices. The seasonal evolution of the martian northern permanent cap as well as associated physical processes is a clue to understand its interaction within the water cycle and its long term evolution.

Previous works have shown the great seasonal variability of the cap including local changes in albedo, return of water ice in spring, accumulation of bright deposits at the cap center, correlation between polar cap surface and water vapor...

(Bass and Paige, Icarus, 2000).

Here, we will report comparisons between the TES spectrometer observations (Kieffer and Titus, Icarus, 2001) and recent MEX/OMEGA observations. Detailed comparisons with the predictions of the 3D-LMD GCM climate model will be also made to improve the meteorological and physical understanding of these processes.

Distribution of CO_2 Deposit Density within Martian Seasonal Caps from HEND/Mars Odyssey and MOLA/MGS Data

Litvak, M.

In this study we have performed comparative analysis between neutron spectroscopy data from High Energy Neutron Detector (HEND) onboard Mars Odyssey Mission and direct measurements of CO2 snow depth obtained by Mars Orbiter Laser Altimeter (MOLA) onboard MGS to extract information about volume density of CO2 deposition at different places within Martian seasonal caps.

It is important to measure volume density because it represents the physical conditions of condensation process, which are different at north and south, and at lower and higher latitudes. The founded constraints on volume density of seasonally exchanged material should be considered in models of the Martian climate system and volatile cycles.

The neutron and gamma measurements are sensitive to the column density (g/cm2) and cannot provide full information about linear thickness (cm) and volume density (g/cm3) of the CO2 deposition. Taking into account that density of the CO2 deposit column density = linear thickness x volume density we may estimate the volume density of CO2 frost with higher accuracy than in previous attempts based on analysis of variations of gravity field of Mars. We also may get more detailed information about distribution of deposit density within Martian seasonal caps in comparison with results of similar analysis presented in recent papers.

In our approach we have selected for analysis a data gathered in latitude zone (70o-85o) within Martian seasonal caps where HEND and MOLA measurements have comparable relative accuracy. Here we present results for two northern/southern latitude belts: 70N-80N/70S-80S and 75N-85N/70S-80S. It was found that volume density of CO2 deposition is approximately the same at southern and northern seasonal caps: ~0.9±0.2 g/cm3 for 75N-85N/75S-85S and ~1.1±0.2 g/cm3 for 70N-80N/70S-80S.

Comparison of UV Albedo of CO_2 and H_2O Ices t North and South Poles Perennial Caps

Perrier, S.; Bertaux, J-L.; Schmitt, B.; Reberac, A.; Dimarellis, E.; Korablev, O.

Perennial polar caps appear very bright in visible light images (Viking, MOC, HRSC). This is also true in the UV range from 200 to 300 nm as seen by SPICAM UV spectrometer, where the albedo is found larger by a factor 3 to 4 higher than surrounding areas outside the caps, both on south and north polar caps. On the south polar cap, which was visited first by Mars Express in January 2004, the UV albedo was found to decrease strongly with wavelength from 300 to 200 nm in the bright regions. Since H2O is not suspected to have such a strong slope in that range, this spectral albedo variation seems to be typical either of CO2 ice or of dust mixed in the ice. A comparison with the north polar cap data, which contain only H2O ice, will be useful to better understand the different spectral signatures of the two types of ices in the UV. Also, it appears that in the visible, the albedo of the south polar cap is distinctly lower in peripheral regions of the perennial cap, interpreted as being the sign of dominating dusty H2O ice. A comparison between visible albedo and UV albedo will be presented on both poles.

Exploration of Martian Residual Polar Caps Based on HEND/Mars Odyssey Data

Sanin, A.; Mitrofanov, I. Litvak, M.; Kozyrev, A. Tretyakov, V.; Boynton, W.

In this study we have used advantages of Mars Odyssey near polar orbit to get detailed information about average composition of Mars residual polar caps based on neutron spectroscopy data from High Energy Neutron Detector installed onboard Mars Odyssey spacecraft. We performed comparison between average composition of residual caps with the subsurface material of northern and southern permafrost nearpolar regions. One of our primary goals was also to provide a direct comparison of CO2 and water ice composition of North and South residual polar caps (within 50 cm depth) during different Martian seasons.

Understanding the Physical Evolution and Chemical Differentiation of the Northern Seasonal Condensates on Mars from the Analysis and Modelling of OMEGA Spectra

Schmitt, B.; Douté, Sylvain; Forget, François; Langevin, Y.; OMEGA Team

The determination of the physical state of the ices composing the seasonal condensations is of prime importance for the understanding of the microphysics of the sublimation/condensation/deposition processes of volatiles. It is also a prerequisite for an accurate mapping of the abundance of the ices and of their physical characteristics by spectral inversion of the OMEGA observations.

Several tens of observations of the northern seasonal condensates at different longitudes and times have been recorded by the OMEGA imaging spectrometer during northern spring.

Statistical analyses (PCA) performed on the observations clearly shows a continuum evolution of the seasonal ice deposits from CO2- rich ice to dusty water ice then to bare hydrated soil when going to lower latitudes. The initial sublimation of CO2 ice leads to the progressive enrichment in water ice and dust of the CO2-rich seasonal deposits. Then a segregation of dusty water ice occurs to finally form a CO2-free ice layer. Finally the progressive sublimation of water ice of the top surface layers lead to an ice-free soil in the optical layer of dust.

Spectra extracted at the different stages of the ice sublimation sequence have been modelled using our radiative transfer code in layered media (Douté and Schmitt 1998) in order to determine the coexistence modes of CO2 ice, H2O ice and dust and their evolution with latitude. Their relative abundances as well as their grain size are also determined. In addition we try to constrain the temperature of the H2O ice in the area where it is freely exposed at the surface by using a set of temperature dependent laboratory experiments on H2O ice performed at LPG (Grundy and Schmitt 1998).

A sketch of the sublimation sequence can be drawn using longitude profiles of the condensate structure and composition at different times (Ls). From these results we discuss the sublimation processes of volatiles and the segregation of water ice and dust during spring.

Structure of theMartian Atmosphere in the Northern Polar Region and Distribution of the O_2 Emission and O_3 Column Density at Late Winter OMEGA and PFS Experiments

Zasova, L.; Altieri, F.; Bellucci, G.; Bibring, J.P.; Formisano, V.; Ignatiev, Nikolay I.

We present some results of PFS and OMEGA measurements, obtained at unique orbit 68, which passed over N pole of Mars at late winter season. Temperature profiles, obtained from the PFS data show that condensation of the CO2 in atmosphere may occur at latitudes exceeding 70°N in the altitude range below 20 km, where the temperature inversion is observed. The boundary of the CO2 cap, where the CO2 is observed as condensate on the surface, is around 62N. The OMEGA image of the polar region in the O2 1.27μm emission band, reveals the wave-like structures in the latitude range from around 70 ° up to the terminator (80°). The crests of these waves are parallel to terminator, and their wavelength changes from several tens of km up to 100 – 150 km near terminator. Similar wave-like pattern is found in the map of the 1.43 μm CO2 ice absorption feature and the 1.52 μm H2O ice. Such structures may be caused by gravity waves, modeled by Tobie et.al. Icarus,164, p.33, for winter polar night condition. Apparent column density of the O3 is obtained from the O2 emission band at 1.27 μm (Fig.1). Its maximal value is found at 62-65°N. In the polar hood at latitudes less than 600 the O3 abundance decreases to South and at φ = 500 it becomes too low to be detected by OMEGA .

Fig. 1. Ozone distribution in the Northern Polar region at late winter, orbit68-5.

Undulatory Patterns in the Martian Atmosphere as Seen by theOMEGA Instrument

Altieri, F.; Bellucci, G.; Zasova, L. V.; Melchiorri, R.; Drossart, P.; Bibring, J-P.; Blecka, M.I.

We report on the observation of regular patterns, usually wave-shaped, in Martian atmosphere. These patterns occur close to the terminator, when the incidence angle is close to 90°. They are recorded in the 1 – 2.5 micron spectral range of the OMEGA imaging spectrometer. The amplitude of these waves is about 5 – 10% and they involve CO2 and H2O clouds and O2 emission too. The cause of this phenomenon is presently unknown. Gravity waves may play a role explaining this effect. This hypothesis is supported by a similar modulation in the slope of the continuum : variation of temperature influences a process of condensation-evaporation resulting in a change of particle size.

Detection of a New Population of Small Particles in the Atmosphere of Mars from UV Occultation Measurements with SPICAM

Bertaux, J-L.; Quemerais, E.; Rannou, P.; Perrier, S.; Korablev, O.; Fedorova, A.; Fussen, D.

The extinction spectrum of aerosol particles is measured from stellar occultations above 10-20 km. In the UV range (200-300 nm) this optical thickness extinction text varies with wavelength. It can be approximated by a power law of the wavelength:

text=N sext= K l-a

The power law exponent is found to vary over a wide range: -0.2 >a>-1.5, with altitude and location. A comparison with power law derived from Mie's theory indicates that the size of observed particles is determined to be in the range Reff= 0.05-0.2 µm effective radius. This differs considerably from dust parameters derived from IR measurements, or visible measurements of sun and solar halo from landers, finding a radius of 1.8 µm. It means that, in addition to low altitude dust particles (which dominates the radiation field seen from ground), there exist a new population of small particles which dominate at high altitudes. They may serve as condensation nuclei (both for CO2 and H2O ices) everywhere. This newly found particle population is a likely left-over from overall atmospheric dust upwelling: diurnal, or dust storms? This population of small particles constitutes a new and essential component of Mars dust cycle (and also H2O cycle), important for temperature/density profiles and cloud formation.

Measurements of the Martian Dust by Planetary Fourier Spectrometer Aboard the Mars Express

Blecka, M.I.; Formisano, V.; Jurewicz, A.; Zasowa, L.; Orleanski, P.; Rataj, M.; Michalska, M.; Nowosielski, W.; Andrzejewska, N.; Maturilli, A.

The presented work is directly connected with measurements by the Planetary Fourier Spectrometer (PFS) during the present mission to Mars - "Mars Express".
Several dusty spectra from various regions of Mars were selected from PFS measurements. The measured spectra were compared with simulations in which we used the parameters calculated also from PFS measurements. The measured data were analyzed by taking into account the features of minerals known from modelling, literature and existing databases. Preliminary conclusions about density and mineralogical composition of dust are shown.

Studying the Past Climate of the Gusev Crater Region with the European Mars General Circulation Model

Bottger, H.

The Gusev Crater has experienced a complex geological history [E.g. 1,2,3]. Centred at 175.5°E and 14.5°S it straddles the Dichotomy boundary of Mars. To the north is the Apollinaris volcano, to the north-east lies part of the Medusea Fossea Formation and from the south Ma'adim Vallis fluvial channel enters the Gusev Crater. The Ma'adim Vallis is presumed to have deposited large volumes of sediment on the crater floor during fluvial activity which began early on in Martian history but may have continued for 1-2 Ga [4,5], with its potential source a large impact crater to the south acting as an effective drainage basin [5]. There is further evidence for the actions of ground water in the Gusev Crater region in the form of sapping channels and mass wasting, as well as potential glacial activity. In fact the Odyssey Gamma Ray Spectrometer finds the Gusev Crater region to have increased hydrogen content indicating the possibility of near surface water ice [6]. The region also displays some significant changes in elevation over relatively small distances, which could result in preferential deposition of water ice and dust at different obliquities.

In this study we examine the past climate of the Gusev Crater region. We use the European Mars General Circulation Model [7] to look at the effects on the water history in this region with variations in obliquity, eccentricity and argument for perihelion. The effects of localised and regional changes in elevation are also considered.

References:

1. Kuzmin, R.O. et al., U.S. Geological Survey, i-2666, 2000.
2. Milam, K.A. et al., J. Geophyis. Res. 108, DOI: 10.1029/2002JE002023, 2003.
3. Zegers, T. et al, this issue.
4. Cabrol, N.A. et al., Icarus 133, 98-108, 1998.
5. Irwin, R.P. et al., Science 296, 2209-2212, 2002.
6. Boynton, W.V. et al., Science 297, 81-85, 2002.
7. Forget, F. et al., J. Geophys. Res.104, 24155-24175, 1999.

DIURNAL VARIABILITY IN MARTIAN ATMOSPHERIC WATER VAPOUR: GCM SIMULATIONS OF NEAR SURFACE WATER ICE. H. M. Boettger[1] , B.H. Foing[1], P.L. Read[2] and S. R. Lewis[2], [1]ESTEC, ESA, Noordwijk, Netherlands, hboettger@rssd.esa.int, [2]AOPP, Oxford University, Oxford, UK.

Introduction: In this study we attempt to test the hypothesis that the observed diurnal variability in column water vapour abundances is driven by the supply of water vapour from subsurface water sources which are out of equilibrium with the current Martian climate

Background: The seasonal variations in column water vapour abundance in the atmosphere of Mars are now relatively well know. The combination of Mars Atmospheric Water Detector (MAWD) Viking data and Thermal Emission Spectrometer (TES) Mars Global Surveyor data has supplied more than 4 years of observations and more is currently being gathered [1],[2]. The TES data in particular has enabled significant advances in the modeling of the Martian water cycle with models now capable of replicating the seasonal variations of water vapour and water ice with reasonable accuracy [3],[4],[5]. Unfortunately there is a lack of observations covering details of vertical distribution of water vapour and the diurnal variations in column water vapour abundance. The data which does exist is often puzzling suggesting diurnal variations in column water vapour abundances of up to a factor of 2 or 3 e.g. [6],[7].

This diurnal variability in column water vapour has been suggested to be due to exchange with the regolith forced by diurnal changes in temperature [8]. Simulations have been conducted using a regolith model based on that by [9] which suggests that in equilibrium a 1D atmospheric column loaded with 12 prmicrons of water vapour will only exchange around 10% of its total column abundance [4]. This is well below the values suggested by the observations. It is also difficult to reconcile this discrepancy between the model and observations, given that for exchange between atmosphere and regolith to take place the water needs to be confined close to the surface. Certainly in equatorial and tropical regions the General Circulation Models (GCM) suggest that this is not the case. It is, therefore, easy to conclude that maybe the errors in the observations are sufficiently large to account for the differences between observations and models.

However, we would like to examine an alternative approach. It may be possible that this diurnal signature is caused by a near surface water source which is supplying the atmosphere with water vapour on a daily basis. In equatorial regions this water source would of course be out of equilibrium with the current climatic conditions on Mars and would hence need to be a remnant from a previous epoch. This idea is further backed up by the Gamma Ray Spectrometer on board Odyssey [10], which has found localized regions away from the high latitudes which are enriched in Hydrogen. Here, we will examine the potential for buried subsurface ice to act as a source for the observed diurnal variability in atmospheric column water vapour abundance.

Model: This study uses the Oxford Mars GCM as described in [11]. In addition the model includes a suite of parameterizations to model the water cycle, which include a condensation sublimation scheme, a bulk cloud scheme and a 10 layer regolith model [4]. The regolith model is based on that of [9] and models the movement of water in the subsurface in the vapour, adsorbed and ice phases and further allows for the exchange of vapour between the upper subsurface layer and the lowest atmospheric layer.

Method: It has already been shown that in equilibrium a diurnal exchange between the regolith and atmosphere will only account for around 10% of the total column water abundance. We will, therefore, focus our attention on the behaviour of subsurface water away from equilibrium. There are two stages to our investigation. 1. In 1D how much water at what depth is required in order to supply the atmosphere with the observed daily variability. This allows us to establish whether this is a realistic hypothesis within the constraints of the GRS observations as well as the constraints set upon the longevity of an ice source at depth away from the high latitudes. 2. How is the water vapour, once released, removed from the column in order to adhere with the observations. Because water is released from a source during the course of only one sol, the water is confined lower in the atmosphere and hence a stronger diurnal exchange then was observed in the equilibrium case can be expected. However, advection will also play an important role. In 1D the role of advection cannot be suitably studied and hence 3D studies will be conducted to examine the role of advection.

Conclusions: Our study will allow us to test the hypothesis that the observed diurnal variability in column water vapour abundances is driven by the supply of water vapour from subsurface water sources which are out of equilibrium with the current Martian climate, constrained by GRS observations

References: [1] Farmer C. B. et al. (1977) *JGR, 82,* 4225–4248. [2] Smith M. D. (2004) *Icarus, 167, 148-165*. [3] Montmessin F. et al. (2004) *JGR,* 109, E10004. [4] Boettger H. M. (2004) *Icarus,* Submitted. [5] Richardson M. I. et al. (2002) *JGR, 107,* 5064. [6] Titov D. V. et al. (1997) *Ann. Geophys, 15 (Suppl. III),* C774. [7] Formisano V. et al. (2001) *Plan. and Space Sci., 49,* 1331–1346. [8] Titov D. V. (1977) *Adv. Space Res., 29,* 183–191. [9] Zent A. P. et al. (1993) *JGR, 98,* 3319–3337. [10] Boynton W. V. et al. (2002) *Science, 297,* 81–85. [11] Forget F. et al. (1999) *JGR, 104,* 24155–24175.

Observations of CO in the Martian Atmosphere with Omega/Mars Express

Encrenaz, T.; Drossart, P.; Fouchet, T.; Melchiorri, R.; Lellouch, E.; Combes, M.; Bibring, J-P.; Titov, D.; Ignatiev, N.

Spectra of Mars recorded with the OMEGA/Mars Express experiment have been used to study the CO mixing ratio over the planet. We have used simultaneously the CO(1-0) band at 4.7 microns and the CO (2-0) band at 2.35 microns. In particular, we have searched for possible variations of the CO mixing ratio over Olympus Mons. The sensitivity of the method appears to be limited by the possible presence of mineralogic features in the vicinity o the two CO bands. Results will be presented and implications will be discussed.

Structure of the Martian Wake

Fedorov, A.; Sauvaud, J-A.; Budnik, E.; Barabash, S. Lundin, R.; Acuna, M.; ASPERA Team

PHOBOS observations and the last Mars-Express measurements of martian space environment with mass-analyzer IMA (ASPERA-3) show that the wake of the planet consists of two different ion regimes. In the first regime ions of planetary origin form the layer adjacent to the the magnetic pile-up boundary. These ions are accelerated mostly by pick-up mechanism and demonstrate gradually decreasing of their energy from the pile-up boundary down to the tail. The second plasma regime is observed in the planetary shadow. This regime is usually called "plasma sheet" and manifests itself by heavy ions accelerated up to the energy equal to the energy of solar wind protons. Study of two plasma regimes in the frame referred to interplanetary magnetic field (IMF)(obtained by MGS data) shows their strong spatial anisotropy. The monoenergetic plasma in the plasma sheet is observed only in the narrow angular sector around the positive direction of the interplanetary electric field.

Measurement of Water Vapor at 1.38 Micron in the Mars Atmosphere with the SPICAM AOTF Near-IR Spectrometer

Fedorova, A.; Korablev, O. ; Rodin, A.; Bertaux, J-L.; Perrier, S.

Among other goals, SPICAM IR experiment of Mars-Express mission carries out monitoring of H2O in the 1.37-micron spectral band. AOTF spectrometer of SPICAM is operating in the spectral range 1-1.7 micron with spectral resolution around 1700 in water vapor band. Results of water vapor retrievals including the spatial and seasonal distributions are presented. The comparison of retrieval results with general circulation models is done for various seasons and locations.

A New Mars Climate Database in Support of Mars Express Science

Forget, F.; Dassas, K.; Angelats i Coll, M.; Wanherdrick, Y.;
Hourdin, F.; Lebonnois, S. ; Lewis, S.; Montabone, L.; Read, P.

We report the release of a new, improved version of the Mars Climate database (version 4.0). For several years, a database of statistics which describe the climate and surface environment of Mars has been constructed by several European teams from LMD (France), AOPP (UK) in collaboration with IAA (Spain) and with the support of ESA and CNES. The database may be used as a tool for mission planning as well as to provide some enviromental data to analyse spacecraft data such as the Mars Express observations. A full version of the Mars Climate Database is available for distribution on a DVDrom. Alternatively, access to the database is also possible through an interactive WWW interface: http://www-mars.lmd.jussieu.fr/.

The database is based on numerical simulations performed with state-of-the-art General Circulation Models (GCM). The models have been developped and validated to reproduce the main features of the meteorology of Mars as observed by spacecraft missions. These models and the derived climate database are constantly improved. In particular, our General Ciculation model now includes all the key processes controlling the thermal structure and temperature in the thermosphere (EUV heating, molecular conduction, etc...) with the atmospheric composition obtained taking into account molecular diffusion, photochemistry and 3D transport of 15 species. The atmospheric composition, dynamics, density and structure up to 250 km is now available in the database for various solar conditions and atmospheric dust conditions. The model also includes a realistic water cycle, and the 3D distribution of water vapor and water ice is now available in the database. To represent the variability of the dust loading in the atmosphere, we provide results from several simulations with various dust "scenarios". In particular, detailed scenario based on data assimilation of the MGS TES observations has been built, allowing us to provide a database representing the atmosphere as it was seen by Mars Global Surveyor (outside the 2001 great dust storm period). Last, we have developed a specific tool to compute as accurately as possible the surface pressure anywhere on Mars. This tool combine our best knowledge of the pressure at one reference point (Viking Lander 1) with a high resolution topography map from MOLA and dynamical pressure variations as simulated by the GCM.

Vertical Profile of the Upper Atmosphere Temperature and Density retrieved from SPICAM Stellar Occultations. Data Analysis and Comparison with General Circulation Model Predictions

Forget, F.; Lebonnois, S.; Quemerais, E.; Bertaux, J. L.; Angelats i Coll, M.; Gonzalez Galindo, F.; Lopez Valverde, M. A.

The observation of numerous stars rising or setting through the Martian atmosphere as seen by the SPICAM UV spectrometer aboard Mars Express allows to retrieve the atmospheric density and temperature from below 40 km to above 120 km (see companion abstract by Quemerais et al.).
This part of the atmosphere was previously almost unknown since almost no measurements were available (a few entry profiles). Moreover, General Circulation Model simulations have shown that this part of the atmosphere should present a very active and interesting dynamic, but that simulation prediction are extremely model dependent.

In this talk, we shall present for the first time the results of inversion
of several tens of profiles obtained around northern spring and summer. These profiles will be interpreted with the help of the LMD general circulation model which has recently been extended up into the thermosphere and is thus ideally suited for this analysis.

~

2- Atmospheric Oxygen Emission at Mars Studied with PFS Data

Formisano, V.

In a few recent orbits PFS has been able to detect the Oxygen emission resulting from the ozone photodissociation. With the resolving power of PFS more than 5000 at 1.27 microns , where the emission is) we are able to study the actual spectrum of the emission. Dividing the measured average spectrum by the assembled solar spectrum , we identify a number of lines , the main one being at 7883 cm-1. For wavenumbers larger than this value the lines are more intense than the lines observed for wavenumbers lower than this value. Imbedded in the emission lines there are 2-3 absorption lines whose identification is being studied. A synthetic spectrum simulating the observations has been computed and will be illustrated.

PFS Limb Measurements

Formisano, V.

Figure 1 – CO and CO2 limb emission . Spectrum 165 is just above the horizon spectrum 174 is 120 Km above the surface.

We report about PFS limb measurements observations. Non LTE emission of CO2 and CO was observed on orbit 44 and on orbit 72 both inbound and outbound. The CO2 isotopic band of C13 was observed emitting. CO2 is observed emitting not only in the 2330 cm-1 band but also in the 2030 – 2080 cm-1 band. Differences between the 3 observations will be discussed.

First Analysis of the Circulation of the Martian Atmosphere from PFS Data

Fiorenza, C.; Khatuntsev, I. Ignatiev, N.; Grassi, D.; Formisano, V.; Visconti, G.; Maturilli, A.; Giuranna, M.

The Planetary Fourier Spectrometer (PFS) on board the Mars Express mission provides atmospheric column dust opacities and vertical temperature profiles. The satisfactory temporal and spatial coverage of these data allows the computation of circulation in the Martian atmosphere. In this paper we focus on zonal-mean zonal winds and meridional circulation.

Zonal-mean zonal winds are calculated by assuming gradient wind balance and zero surface zonal wind [Fiorenza and Khatunsev, 2004].

The net effect of the zonal-mean meridional circulation can be approximated by the diabatic ciculation, which is defined from the atmospheric thermal structure and net radiative heating rates. The radiative transfer model developed by N. Ignatiev (2004) is used to compute solar heating and thermal cooling rates from the retrieved PFS temperature and dust distributions.

In this work we present the first results about zonal wind and meridional circulation during the end of the Northern winter and the early Northern summer.

Extension of a Martian GCM to the Thermosphere

González-Galindo, F.; Angelats I Coll, M.; Forget, F.; López-Valverde, M.Á.

The Laboratoire de Météorologie Dynamique (LMD-CNRS, Paris) and the Instituto de Astrofísica de Andalucía (IAA-CSIC, Granada) have been working together in an extension of the LMD Martian General Circulation Model (LMD-GCM) to cover the Martian thermosphere. A number of schemes have been developed for that purpose and the current upper boundary is located at about 240 km above the planet's surface. This makes this GCM the first one able to fully simulate the Martian atmosphere from the ground to the thermosphere. As a result, we are starting to study in a more self-consistent way than what was done so far the different couplings, interactions and feedbacks between different processes operating at different altitudes. The model still requires active validation analysis, but some useful research is already possible. In particular, we studied the impact of the gravity wave parameterization over the thermospheric temperature and winds (Angelats i Coll, 2004), obtaining a deceleration of the zonal winds due to the interaction with gravity waves.

Among the applications of the new model is the analysis and validation of satellite data, like those from Mars Express. In particular, this GCM can be very beneficial to analyse data from high altitude observing instruments like OMEGA and SPICAM. For example, the limb infrared emissions from OMEGA and the temperature and constituents profiles from SPICAM require specific forward model calculations. This GCM could be used to simulate appropriate atmospheric conditions as input/a priori for those radiative models. Also the present GCM could be used to correlate independent measurements from different instruments, both analysing their consistency and examining what their combined simulation tells us about the upper atmosphere of Mars.

We will present some of the thermospheric fields we are currently obtaining, and will propose a number of validation exercises using Mars Express data.

Comparison of Atmospheric Temperature Fields Measured by PFS with SPICAM Temperature Profiles from Star Occultations

Grassi, D.; Quemerais, E.; Bertaux, J-L.; Formisano, V.; Lebonnois, S.; Forget, F.

The purpose of the present work is to compare the temperature vertical profiles retrieved by PFS and by SPICAM in the atmosphere of Mars in similar conditions. We have identified a number of coincidences, for which we will present the temperatures and density profiles. The purpose of the comparison is to cross-validate the two techniques, which are totally different. Discrepancies may point to short-comings of one method or the other.

The PFS air temperature fields are retrieved in the indicative range 3-45 km above the surface by means of numerical inversion of the radiance observed in the CO2 15µm band, performed on single-spectrum basis. Namely, measurements considered in this study were acquired observing the surface of the planet and the overlying atmosphere. The thermal emission of the carbon dioxide, driven by the gas temperature, sums to the thermal emission of the surface, attenuated by the extinction of the CO2. Resulting profiles have a vertical resolution in the order of some kilometers, intimately limited by the nature of radiative transfer.

The SPICAM vertical profiles are obtained by stellar occultations. The atmospheric transmission is measured as a function of wavelength in the range 110-310 nm, and altitude in the range 140-30 km (the lower limit is due to star signal extinction by the dust, and may vary somewhat from one profile to the next). There is one measurement at each second. From each transmission spectrum, the CO2 slant density is extracted (density integrated along the line of sight). Then a vertical inversion is performed to yield the vertical density of CO2. then, assuming a hydrostatic equilibrium, the profile is integrated from top to bottom to yield the pressure at each altitude, and the temperature form the perfect gas law.

The vertical profiles of PFS and SPICAM are overlapping in the region 30-45 km. Each data set, from SPICAM and PFS, will also be compared to the GCM climate model LMD-AOPP-IAA, developed with the support of ESA and CNES. The use of the model will also allow to compensate (at least partially) for not exact coincidences.

Optical Depth Retrievals from HRSC Stereo Images of Apollinaris Patera, of Lowlands During a Dust Storm, and Around Vallis Marineris

Hoekzema, N.; Inada, AA.; Markiewicz, Wojtek; Keller, H.U.; Gwinner, K.; Hoffmann, H.; Neukum, G.

The stereo images taken by the High Resolution Stereo Camera (HRSC) onboard the Mars Express orbiter offer a unique and powerful way to study the Martian atmosphere. Here we present optical depths that were retrieved with the so-called 'stereo method', i.e., by analyzing contrast differences between images from the stereo and nadir channels of HRSC. The stereo-method appears to work well and has been validated by comparing its results for Gusev crater with ground truth data available from the Spirit rover in Gusev. Application to mountainous regions can however produce large errors and variations in the results of the stereo-method. One reason is that the dust content of the atmosphere varies with pressure and altitude. Another is that a field that contains both low and high optical depths may show a contrast distribution that confuses the stereo-method. Therefore, very careful consideration of the surface topography is important. We use HRSC stereo images taken on January 16.04 during MEX's orbit 24, and the Digital Terrain Model (DTM) derived from these, to study how surface topography and altitude influence stereo-method retrievals on the slopes of Appolinaris Patera. Next, we study optical depths in a dust storm covering the lowlands to the North of the volcano. We also use images taken during orbit 438 on May 25.04 for similar analysis of regions in and around Vallis Marineris.

The Influence of Irregularly Shaped Dust Particles on Reflectivities and Polarisation of the Martian Atmosphere

Laan, E.; Stam, D.; Volten, H.

The intensity and polarization of sunlight that is scattered by dust particles in planetary atmospheres depends on the composition, size and shape of the dust particles. When analyzing measurements of reflected sunlight, dust particles are usually assumed to be spherical, although it is well-known that natural dust particles, such as the dust particles found on Mars, have irregular shapes. Spherical dust particles scatter light according to Mie-theory. To take into account the scattering of light by irregularly shaped dust particles, we embedded measured scattering properties of Mars-type dust particles in a radiative transfer code. This code employs the doubling-adding scheme to simulate the radiation in a layered model of the Martian atmosphere and includes both multiple scattering and polarisation. We will show the differences between simulated reflectivities with and without taking into account the natural irregularity of dust particles,for wavelength ranges employed by several instruments on-board the Mars Express.

Mars Ozone Profiles Retrieved from SPICAM Stellar Occultations, and Interpretation Using the LMD Mars Climate Model

Lebonnois, S.; Lefevre, F.; Quemerais, E.; Perrier, S.; Bertaux, J-L. ; Forget, F.

Stellar occultations data obtained from SPICAM have been analyzed, and ozone vertical profiles retrieved for different latitudes, longitudes, local time and seasons, in the range 20-30 to 60-70 km. An ozone layer is observed on some profiles in this altitude region, but this ozone layer is also absent on many profiles. Using the LMD Mars Climate Model, which includes the computation of the atmospheric composition, this ozone layer has also been predicted at night, for given seasons (Lefèvre et al, JGR 109, 2004). We will compare model and observations, and analyze agreements and discrepancies as a function of season, local time, and location. Some possible interpretations will then be discussed.

Study of the Martian Atmosphere by the Radio Science Experiment Mars During the first Occultation Season of Mars Express

Pätzold, M.; Häusler, B.; Tyler, G. Leonard; A., Sami W.; Carone, L.; Griebel, H.; Hinson, D.P.; Schaa, R.; Selle, J.; Simpson, R. A.; Stanzel, C.; Tellmann, S.; Twicken, J. D.

The prime objective of the radio science experiment MaRS on Mars Express is the sounding of the Martian atmosphere and ionosphere during the Earth occultation seasons in order to derive vertical density, pressure and temperature profiles in the altitude range from the surface to about 50 km and to derive vertical ionospheric electron density profiles from 80 km to over 400 km as a function of latitude, longitude, local time and planetary season. More than 100 vertical profiles of density, pressure and temperature of the neutral atmosphere have been obtained during the first Earth occultation season from April to mid August 2004 located in regions ranging from the northern mid-latitudes to low southern latitudes during northern spring time. More are expected from the second occultation season starting in early December. Quite a number of coordinated observations with SPICAM have been planned and performed during both seasons in order to derive a combined density and temperature profile ranging from the surface to about 150 km altitude.
Results and example profiles will be presented, also in comparison with a GCM model from LMD.

Simultaneous Ozone and Water Vapour SPICAM Nadir Measurements: Revisiting the Mars Anti-Correlation Paradigm

Perrier, S.; Lefèvre, F.; Bertaux, J.L.; Lebonnois, S.; Fedorova, A.; Quemerais, E.; Korablev, O.

Early measurements of ozone by Mariner 9 in 1969 found that ozone was present mostly during the winter season, showing a correlation between ozone and low atmospheric temperatures. This was explained by the catalytic destruction of O3 by HOx molecules, which are produced as a result of H2O photo-dissociation. Since H2O abundance is controlled by temperature, an anti-correlation between ozone column and water vapour was inferred to be established by Mariner 9 observations. Recent calculations with a 3D GCM model including photochemistry (F. Lefèvre et al., 2004) showed that near the equator, for the same integrated vertical quantity of H2O, the vertical column of ozone changes, as a function of the height of the hygropause: a high hygropause implies more ozone destruction in the upper ozone layer. Therefore, a perfect anti-correlation is not expected in these conditions. In the nadir geometry on the day side, SPICAM/MEX is measuring simultaneously the integrated vertical quantity of H2O at 1.38 µm, and ozone in the UV near 250 nm. We will present an analysis of the observed correlation/anti- correlation of these two species, in order to test the revisited paradigm.

Lee Wave Clouds in the HRSC Images: Wind Velocity Measurements

Portyankina, G.; Markiewicz, W.; Inada, A.; Neukum, G.; HRSC Co-Investigator Team

Lee wave clouds are well-known to form in Earth's atmosphere. These usually large scale and dense clouds often form in mountain regions and hover over the tops of the mountains. They prevail for long periods of time and move around very little in spite of very strong winds. Lee wave clouds form by vertical deflection of wind above a topographic obstacle. Air undergoes a wave-like oscillation in the lee of the obstacle. In the crest of the wave air rises up to the cooler region where condensation occurs due to the adiabatic cooling. In such a way a regular train of elongated clouds forms. This train of clouds is aligned orthogonal to the prevailing wind if the obstacle is a mountain range.

In the Martian atmosphere lee wave clouds were observed for the first time by Mariner 9. They were subsequently regularly detected by Viking Orbiter and Mars Global Surveyor [Wood et al., 2003]. The High Resolution Stereo Camera (HRSC) onboard Mars Express has atmospheric observations as one of the priorities of its scientific program. From the beginning of the mission it has detected quite a number of clouds in the Martian atmosphere. Several of them are lee wave clouds in the middle latitudes and in the polar regions. These polar lee wave clouds appear superimposed on the haze and streak clouds. The wavelength, height and propagation characteristics of lee waves are mostly determined by the velocity of driving wind and the obstacle dimensions. Other critical parameters include atmospheric temperature and moisture in the flow. We used images of lee wave clouds to infer the velocity of the driving wind. HRSC image taken during orbit 68 shows a lee cloud already smeared by the motion of the atmosphere. Unfortunately, the mountain over which this lee wave was formed is outside of the image frame. The lee wave structure is distinct enough however, to measure its wavelength. Preliminary result for the wind speed inferred from this image is 25.2 m/s that is in agreement with measurements of Martian wind speed from Hubble Space Telescope [Mischna et al., 1998] and estimates from dust devil motion [C. Stauzer, personal communication].

Mischna, Michael A., Bell, James F., James, Philip B., Crisp, David, Synoptic measurements of Martian winds using the Hubble Space Telescope Geophysical Research Letters, Volume 25, Issue 5, p. 611-614, 1998

Wood, S. E., Catling, D. C., Rafkin, S. C. R., Ginder, E. A., Peacock, C. G., MGS Observations and Modeling of Martian Lee Wave Clouds, Sixth International Conference on Mars, July 20-25 2003, Pasadena, California, abstract no.3283, 2003

Studies of HEND/Odyssey Neutron Data From Mars in Correspondence with the Recent Results from PFS Instrument of Mars Express

Sanin, A.; Mitrofanov, I. Litvak, M.; Kozyrev, Alesander; Boynton, W.; Tret'yakov, V.

Recent data from PFS instrument on Mars Express has shown the enhancement of water vapor over some regions on Mars with low and middle latitudes. These results are studied in the correspondence with neutron data from High Energy Neutron Detector onboard NASA Mars Odyssey. The HEND data for epithermal neutrons allows to detect the presence of water in the shallow subsurface, which may be the source of water vapor in the atmosphere. The HEND data for neutrons at MeV energy range is more sensitive for the presence of water at the very top surface and in the atmosphere, so the data for these particles could be complementary to the PFS data.

The previously available data of HEND mapping were based on the longest possible exposure period of each surface area for getting the highest statistics. To make more accurate comparison with PFS data for individual orbits, HEND data will be selected for the similar time period with the same conditions on the surface and in the atmosphere. Possible coincidence will be discussed between the water-rich Arabia area, as seen in the epithermal neutrons, with the high water vapor area at about the same place, as seen by PFS. Another cases of comparison between HEND and PFS will be also presented, which either do not show any consistency of data from two experiments, or even display some disagreement between them. Possible reasons for that will be also discussed.

Remote Sensing of the Surface Atmospheric Pressure with Omega

Vinatier, S.; Forget, F.; Melchiorri, R.; Drossart, P.; Bezard, B.; Fouchet, T.

In order to map the variation of the surface pressure on Mars, we propose a method using the data taken by the instrument OMEGA. It focuses on the analysis of the 2-micron CO2 band which is quite sensitive to the variation of the CO2 column opacity, as well as to other parameters (e.g. atmospheric temperature) which are sufficiently known to allow an estimation of the surface pressure in each pixel. To reach this goal, a first challenge is to develop a radiative model / inversion tool sufficiently accurate but fast enough to process the thousands of spectra obtained in an OMEGA image. For this purpose, a line by line radiative transfer model has been used to model this band with great accuracy between 1.8 and 2.2 microns. Using this model, it is then possible to create a look up table of this band with a sample of parameter values caracterising of Mars atmosphere. Fixing these parameters from the observations, the surface pressure can be deduced by minimising the distance between the observed spectra from OMEGA and synthetic ones corresponding to the same parameters (other than pressure) carefully interpolated from the look up table.

With such a tool it is possible to produce maps of the surface pressure with an accuracy sufficient to detect meteorological variations. In particular, using the accurate topography provided by the MOLA altimeter, we should be able to distinguish the meteorological components of the pressure variations from the topographical components. This will allow the detection of local wave-like structure and possibly large-scale variations.

Water Ice Clouds From the LWC PFS Data

Zasova, L.; Formisano, V.; Ignatiev, N.; Grassi, D.; Giuranna, M.; Khatuntsev, I.

We use the long wavelength channel of PFS (300-1500 cm-1) for the water ice clouds identifications. Temperature profiles and aerosol opacity are obtained in a self consistent way from the same spectrum. The most pronounced water ice absorption band is at 825 cm-1. Position of its maximum and its shape depends on particle size. Absorption is strongly asymmetrical in the wings of the 15 μm CO2 for the particles of 1 μm band and practically symmetrical for the particles of 4 μm. This difference allows to estimate the effective particle size from thermal IR observations. Measurements carried out at Mars Express started at late southern summer. They allowed to identify the water ice clouds above Ascraeus and Olympus Mons and in Tharsis region around Ascraeus Mons. At the same time for other orbit passing through Hellas, the aerosol was presented by dust only, well mixed in the atmosphere. The Northern polar hood has a boundary at lowest latitude around 45° - 48° N. Processes of seasonal evolution of the equatorial clouds, a decay of the northern polar hood, and appearances of the southern polar hood and clouds above volcanoes and in Valles Marineris will be discussed.

Poster Session 3
Space Environment of Mars, Martian Moons, Methods, Instruments & Future Missions

The Space Environment of Mars

The Martian Moons

Methods, Instruments, Missions and Archiving

Influence of the Magnetic Barrier on Kelvin-Helmholtz Instability Driven by the Solar Wind Flow around Mars

Amerstorfer, U.; Erkaev, N.; Biernat, H.; Lammer, H.

Similar to Venus, the solar wind flow around the Martian ionosphere forms the magnetic barrier in the vicinity of the ionopause where the magnetic pressure is dominating over the plasma pressure. In the magnetic barrier, the magnetic tension accelerates plasma in the direction perpendicular to the ambient magnetic field away from the stagnation line. This stagnation line, including the stagnation point, is coplanar to the plane of the solar wind velocity and the interplanetary magnetic field. The regions of fast plasma flow along the ionopause in the direction perpendicular to the magnetic field lines are the most unstable with respect to the Kelvin-Helmholtz instability which is studied on the base of stationary one fluid magnetohydrodynamic flow model. Mass loading is included in this model as a stationary source of heavy cold ions. The distribution of the instability growth rate along the ionopause is found for typical solar wind parameters. The region at the ionopause is especially analyzed, where the instability can evolve into a nonlinear stage. The effects of a finite Larmour radius are taken into account, which bring about an asymmetry of the unstable region. The position of the unstable region is closely related to the direction of the interplanetary magnetic field (IMF). The perpendicular component of the IMF with respect to the solar wind velocity is most important for the instability region. The rotation of this component with respect to the solar wind velocity leads to a corresponding rotation of the flow pattern with unstable region.

Filamentary Structure of Neutral Atoms at Mars - Aspera Observations

Fraenz, M.; Aspera Team, MEX; Dubinin, E.; Woch, J.

The NPD sensor on the Mars Express Aspera experiment measures energetic neutral atoms (ENAs) with energies between 0.1 and 10 keV. It has an angular resolution of 5x30deg and can separate hydrogen and oxygen ENAs. In the Martian magnetosheath and upstream of Mars the sensor observed a filamentary structure of the ENA flow with a typical filament angular size of 5deg.
At these times the sensor was pointing towards Mars. We discuss instrumental influences on the measurements and compare the observations with similar structures observed in cometary outflow and give some possible interpretations.

Electron Oscillations in the Martian Sheath

Winningham, J. D., R. A. Frahm, J. R. Sharber,
(Southwest Research Institute, San Antonio, Texas 78228, USA)

A. J. Coates, D. R. Linder, Y. Soobiah,
(Mullard Space Science Laboratory, University College London, United Kingdom)

Esa Kallio,
(Finnish Meteorological Institute, Box 503 FIN-00101 Helsinki, Finland)

J. R. Espley,
(Department of Physics and Astronomy, Rice University, Houston, Texas 77005, USA)

S. Barabash, R. Lundin, and the ASPERA-3 Team
(Swedish Institute of Space Physics, Kiruna Division, Kiruna, Sweden)

The Analyzer of Space Plasmas and Energetic Atoms (ASPERA-3) experiment flown on the Mars Express (MEx) spacecraft includes the Electron Spectrometer (ELS) instrument as part of its complement. The ELS instrument measures the differential electron flux spectrum in a 127 logarithmic energy sweep within a time period of 4 sec. The orbital path of MEx traverses the Martian sheath where ELS frequently measures periodic electron oscillations (see Figure). These oscillations are seen as periodic variations of up to an order of magnitude (peak to valley) in energy flux with the largest amplitudes occurring in the tens of eV to ~100 eV range. Observed oscillations can have periods from minutes to the instrument sweep resolution of four seconds. For the oscillations shown in the Figure, the frequency of the integrated electron energy flux is about 0.02 Hz. Depending on the local magnetic field, this could be close to the typical O+ gyrofrequency found using the Magnetometer data from Mars Global Surveyor. Examples of electron waves in the Martian sheath will be presented. Due to the motion of the spacecraft, it is unclear if the wave structures observed are a permanent standing wave feature within the sheath or if waves are propagating past the spacecraft.

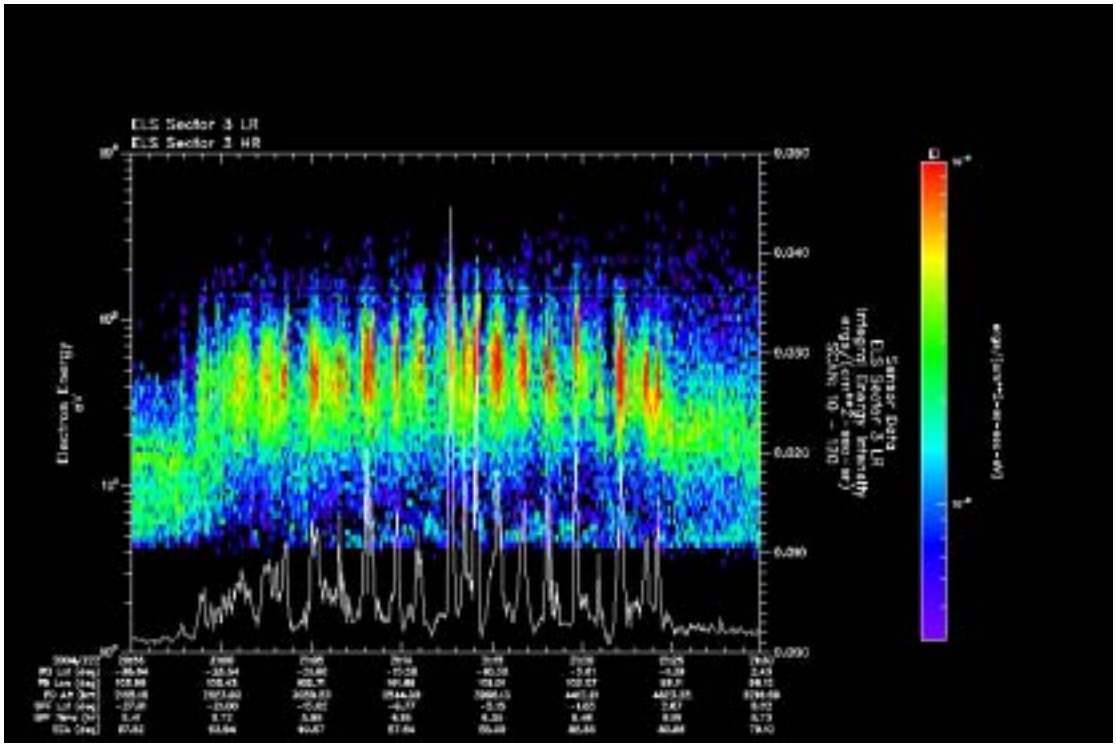
ELS Sector 3 LR
ELS Sector 3 HR
Electron Energy
eV
ELS Sensor Data
ELS Sensor 3 LR
Integral Energy Intensity
erg/(cm²-sec-sr)
SCAN: 10 - 130
Spin-Seconds

ASPERA-3: First Results of Neutral Particle Measurements

Galli, A.; Wurz, P.; Lundin, R.; Barabash, S.; Grigoriev, A. Fedorov, A.

The ASPERA-3 experiment on Mars Express consists of four sensors that measure in situ fluxes of ions, electrons and energetic neutral particles. We will present first results of the energy spectrum reconstruction of particle fluxes measured by the Neutral Particle Detector. We focus the analysis on measurements where hydrogen fluxes are recorded while the NPD field of view is directed away from Mars. Since there is no apparent planetary origin these unexplained neutral beams might carry information about the outer heliosphere, possibly allowing a look at the boundaries of the solar system.

Analysis of the Martian Ionosphere and Thermosphere Environment

Kazeminejad, S.; Lammer, H.; Kirchengast, G.; Lichtenegger, H.

The heating of the thermospheres and the formation of the ionospheres of terrestrial planets like Venus, Earth and Mars are mainly controlled by the solar XUV radiation (0.1 - 100 nm). The current estimates of the Martian exosphere temperature (in the order of about 300-350 K) are based on hydrogen Lyman-alpha measurements. There is much evidence however, that these exospheric temperature estimates are to high. The reason for that comes mainly from to the fact that hot neutral hydrogen particles may have contaminated the used data. Our study will compare the ionospheric data obtained by the European Mars Express spacecraft currently in orbit around Mars with previous ionospheric data obtained by observations of US and Russian spacecraft. As the various data sets were obtained during different solar activity periods, it is planned to study the behaviour of the dependence between the neutral temperature in the thermosphere obtained from a Chapman ionospheric profile near the ionospheric peak, and the solar 10.7 cm radio flux (F10.7). Further, ionospheric data obtained at higher latitudes will be used as input in studies regarding solar wind plasma interactions, which cause ionospheric clouds and viscous momentum transfer effects related to the loss of water from Mars. The results will then be compared to known observations (measurements of ionospheric profiles, F10.7 flux, and neutral gas temperatures at the exobase level) on Venus.

This study will provide important results in the field of comparative planetology as it will help to obtain a good estimate of the Martian exobase temperature which has so far (in contrast to Venus) not been directly measured. This study will furthermore contribute significantly to the overall analysis and understanding of the Mars Express mission data taking into account that the Japanese Nozomi spacecraft (equipped with a mass spectrometer allowing to infer the Martian exosphere temperature) failed.

This study is performed in the framework of the Mars Express participation of the Institute for Geophysics Astronomy and Meteorology (IGAM) of the Karl-Franzens University Graz/Austria and the Space Research Institute (IWF) of the Austrian Academy of Sciences.

Numerical Interpretation of High-Altitude Photoelectrons Observed by ASPERA-3

Liemohn, M.; Kozyra, J.; Ma, Yingjuan; Nagy, A.; Frahm, R.; Winningham, D.; Brain, D.; Mitchell, D.; Luhmann, J.; Lundin, R.; Barabash, S.

The Electron Spectrometer (ELS) instrument of the ASPERA-3 package on the Mars Express satellite has observed photoelectron energy spectra at altitudes of up to 5000 km. The characteristic photoelectron shape of the spectrum is sometimes seen at these altitudes in the evening sector at near-equatorial latitudes. The hypothesis that these electrons are traveling along magnetic field lines draped across the dayside of Mars is explored with the use of two numerical models. The first is a global, multi-species MHD code that produces a 3-d representation of the magnetic field and bulk plasma values around Mars. It is used here to examine the possibility of magnetic connectivity between the high-altitude flanks and the subsolar ionosphere. The second model is a kinetic electron transport model that calculates the electron velocity space distribution along a non-uniform magnetic field line. It is used here to simulate the high-altitude ELS measurements. Data-model comparisons are also made against Mars Global Surveyor electron reflectometer data near the subsolar location. A discussion of the ability of our hypothesis (as well as these numerical models) to explain the observations is presented.

Feasibility Study for a Precise Mass Determination of the Moon Phobos by the Radio Science Experiment Mars on Mars Express

Andert, T.P.; Pätzold, M.

Mars Express will perform a number of close flybys (< 400 km) at the moon Phobos. Gravity attraction by the moon onto the spacecraft will change the orbit slightly and therefore will lead to an additional Doppler frequency shift of the radio carrier signals exchanged between the spacecraft and the ground station. This frequency shift depends on flyby distance, flyby velocity and finally on the mass of the moon.
Based on a Phobos topography model by Duxbury (1991) the moon's gravity field was modeled assuming constant body density. Numerical values of the low degree and order gravity coefficients C_{20} und C_{22} have been estimated. Using this gravity model for Phobos and taking further perturbing forces into account, several flybys which will occur in 2005 have been simulated to study the effect on the motion of the spacecraft and to assess the feasibility to extract the gravity field of Phobos.

High-Resolution Mapping of Phobos by the HRSC on Mars-Express

B. Giese[1], K. Gwinner[1], J. Oberst[1], G. Neukum[2]
and the HRSC Co-Investigator Team

[1] Institute of Planetary Research, German Aerospace Center (DLR), Berlin Germany
[2] Remote Sensing of the Earth and Planets, Freie Universität Berlin, Germany
bernd.giese@dlr.de

In August 2004, Mars Express had an exceptionally close encounter (150 km) with the small Martian satellite Phobos (radii: 13x11x9 km). During this flyby, the High-Resolution Stereo Camera (HRSC) on board obtained stereo images showing details down to 6 m resolution.

Using methods of stereogrammetry we derived a Radius Model (RM) of Phobos covering approx. 30% of the satellite's surface. The RM has a horizontal resolution of ~ 100 m and a vertical accuracy of better than 10 m. The model is limited in coverage, but higher in resolution than the global shape model from the Viking era (Fig.1). Once data from more flybys become available, we hope to obtain full global coverage at high-resolution.

The HRSC is equipped with four color and two photometry channels in addition to the stereo channels. We used the RM to rectify the HRSC-color images (R, G, B) and generated a reflectance map which shows the color contrast of Phobos at 40m resolution. We also used the RM to study photometric effects in the images for different photometric models and parameters.

The RM allows us to perform morphological studies of surface features at scales < 1km; however, the spectacular grooves on Phobos (Fig.1, left) are at the limit of model resolution.

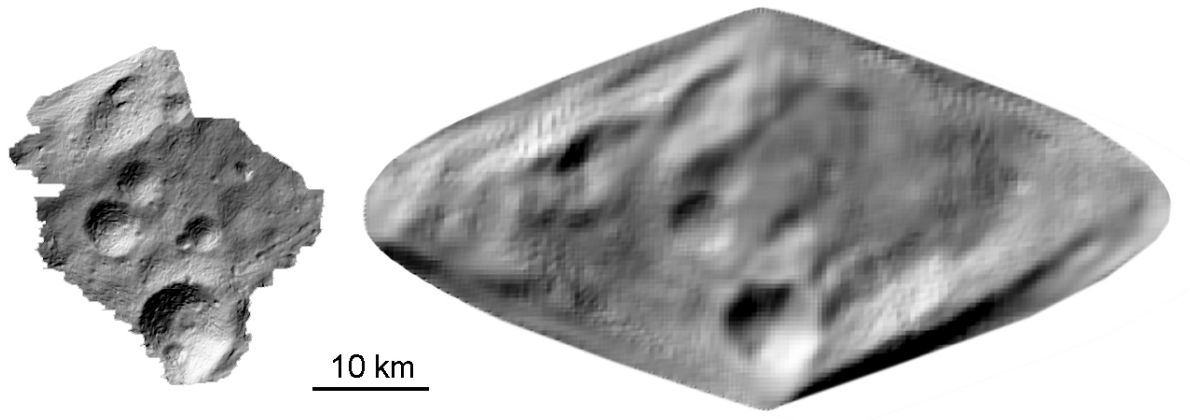

Fig.1: Shaded relief of radius models. (Left) based on HRSC-stereo images, (Right) from Viking images (P. C. Thomas, 1993).

Mars Express and Phobos Mass: a Challenge for Celestial Mechanics

Lainey, V.

Despite many estimations found in the past, Phobos mass is still largely unknown. Strong correlations in the reduction techniques and some obvious systematic errors in the former results do not allow strong certitude on the Phobos internal structure (porosity, internal stress, etc.).
We plan to use the opportunity of the close encounters between Mars Express and Phobos to deliver the most realistic value of Phobos mass. To achieve this goal, new high accurate ephemeris of Phobos is under development. In addition the observational data will be treated by two softwares exclusively specialized in respectively Mars Express orbital motion determination and the fit of Phobos mass.

Reflectance Spectra of Possible Phobos Analogue Materials as a Support for Interpretation of Mars Express Data

Moroz, L.; Hiroi, T.; Shingareva, T.; Basilevsky, A.; Fisenko, A.; Semjonova, L.; Pieters, C.

Origin and mineralogical composition of Phobos and Deimos remain a mystery. Although telescopic observations provided some clues, up to now the only spatially resolved spectral data were obtained by Phobos 2 spacecraft in 1989. Serious calibration problems precluded unambiguous interpretation of those data in terms of mineralogy and composition. Mars Express mission has delivered Phobos images of unprecedentedly high spatial resolution (HRSC camera) and optical spectra in a wide spectral range from visual to thermal infrared (OMEGA and PFS spectrometers). A spectral library of relevant analogue materials is essential to interpret the spectral/colour data in terms of mineralogy. Here we present laboratory reflectance spectra of several materials which extend available spectral data for possible Phobos analogues and may help to extract compositional information from the spectra provided by the instruments onboard Mars Expess spacecraft. Optical properties of Phobos regolith may be significantly modified by micrometeoritic bombardment. We present reflectance spectra of a CM2 carbonaceous chondrite Mighei and artificial mineral mixtures irradiated with a microsecond pulsed laser to simulate optical effects of micrometeoritic bombardment. We show that such a processing causes dehydration, modifies spectral shape in the visible and near-infared, and enhances spectral signatures of olivine in the thermal infrared. In addition, we present reflectance spectra of various size fractions of the complex Kaidun microbreccia meteorite. Phobos has been suggested as a possible parent body of this unique meteorite (Zolensky and Ivanov 2003, Chem. Erde 63, 185-246).

Thermal Infrared Observations of Phobos

Palomba, E.; D'amore, M.; Esposito, F.; Colangeli, L.; Maturilli, A.; Formisano, V.; the PFS International Team

The mineral composition of the Phobos surface is a matter of controversy. Phobos has an unexpectedly low density of about 2 g cm-3 and this would imply an high porosity. Thanks to this peculiar bulk characteristic and to the very low albedo it was often related to the carbonaceous meteorites. However, recent studies have found that the satellite surface exhibits a significant red slope in the visual near infrared (VisNIR), which is inconsistent with a carbonaceous chondrite composition. Moreover, the infrared spectrometer on board the PHOBOS 2 mission (ISM), found that the Phobos spectra are distinct from the spectra of C and D class asteroids, with which Phobos has commonly been compared but is most closely matched with T-type asteroid spectra, a highly space-weathered mafic mineral assemblages.

The properties of the Phobos surface inferred by the VisNIR observations are in contrast with the bulk characteristics: porosities of about 50% are required to explain the density values for the mafic and volatile-poor material. More reasonable porosities, of the order of 10-30 %, are expected with the presence of volatile-rich materials on the satellite, even if no absorption due to H2O around 3 µm was observed, indicating a nearly anhydrous surface composition.

Analysis of the Thermal Infrared (TIR) spectral region is of particular interest because in this region are more evident the mafic signatures of the planetary materials, but very few are the existing observations of Phobos in this spectral region. An interesting opportunity comes from the observations of the Martian Moon that were performed by the Mars Express (MEX) mission in the routine phase of its science operations in some orbits. In this work we show the preliminary analysis of TIR data acquired by the Planetary Fourier Spectrometer onboard the MEX which are actually in the calibration phase. In comparison we show the Phobos spectra measured by the Thermal Emission Spectrometer (TES), which seem to favour the mafic versus the organic signatures, as suggested by the VisNIR measurements.

MIMS – the Mars Image Mining System

Alves, E.I. Vaz, D.; Pina, P.; Barata, T.

The amount of scientific data on Mars is no longer manageable by conventional procedures. The image databases have been growing exponentially in size from the 22 Mariner 4 TV pictures to the presently more than 175,000 Mars Global Surveyor (MGS) Mars Orbital Camera (MOC) images and is certain to grow still with the steady release of Mars Express High Resolution Stereo Camera (HRSC) images.

In the context of project MAGIC [1] an attempt is in progress to identify ongoing processes on the surface of Mars by comparing images of the same areas that were captured by different missions.

As a first attempt, we compared MOC-NA and 2001 Mars Odyssey (MO) THEMIS (Thermal Infrared Imaging System) images. To that purpose, we have developed a very simple data (image) mining software that selects, from both images' databases, those pairs whose centres are nearer than a specified distance (typically 0.1 degrees), within a operator-chosen latitude-longitude window (which can span the entire planet). Queries can also include text key-words that may be present on one of the databases.

One of the overlapping pairs that were found was that of images MOC 2-240, captured on July 12, 1999 and THEMIS V01138003, captured on March 18, 2002. Visual comparison of this pair of images seemed to evidence the presence of a putative new gully, on the northern bank of Nirgal Vallis, among previously existing ones (29.7º S; 321.4º E). This new gully, less than three years old, would indicate that fluid release is occurring on Mars in the present. However, the poor resolution of THEMIS images (18 m/pixel) still leaves much room for doubt.

This indetermination can only be resolved with the help of HRSC images of the same location. In fact, the image mining system that we have developed is especially suited to allow the comparison of MOC and HRSC images, which are of similar resolutions. Such comparison will certainly be a useful tool for revealing ongoing geodynamic processes on Mars.

References

[1] - Roos-Serote et al. (2005) – MAGIC, the Portuguese participation in Mars Express. (This conference).
[2] – Alves, E. I., et al. (2003) – Identification of present fluid seepage in Nirgal Vallis, by comparing Mars Global Surveyor and Mars Odyssey images. Geophys. Res. Abs. 5 (CD-ROM).

OMEGA: a Statistical Method for Spatial Contrast Improvement

Bellucci, G.; Altieri, F.; Bibring, J-P.

The OMEGA imaging spectrometer on board Mars Express is composed of two separate spectrometers, covering respectively the 0.36 – 1.05 ìm and 0.89 – 5.2 ìm wavelength range. The theoretical angular resolution of both spectrometers is 1.2 mrad along/across track. However, due to a residual optical aberration induced by thermal gradients, the actual angular resolution of the visual spectrometer is, respectively, 1.3 along and 3.5 mrad track. In this paper we present a method, which makes use of statistical techniques as PCA and MNF, which can be used to reduce the aberration effect. The method can be applied to similar imaging spectrometers composed by two separate channels.

Surface Features Extraction from Mars Express Planetary Fourier Spectrometer (PFS) Spectra: Application of Factor Analysis Technique on Remote Sensing Infrared Data

D'Amore, M.; Palomba, E.; Colangeli, L.; Esposito, F.; Maturilli, A.; Formisano, V.

Martian surface is commonly formed by a processed rock particulate composed with grains of various sizes called soil. A fundamental goal in planetary science is the determination of soils composition in order to reconstruct the evolutionary history of planetary surfaces at local and global scale.

Today researches are based on the analysis of remote sensing data coming from spacecraft carrying instruments suite able to collect radiation coming from the planet in a wide spectral range. The most useful spectral interval to investigate the composition of soils and atmosphere is the infrared band (broadly 1-50 ?m) because primary spectral signatures of these objects fall in this spectral range (stretching and roto-vibrational band of Si-O, O-H-O, C-O and other).

The Planetary Fourier Spectrometer, onboard the Mars Express mission, collects radiation in the 1-45 ?m range with the very high spectral resolution of 1 cm-1. Data acquired by this instrument offer the unique chance to extract, whit high accuracy, minor mineral components of surface and atmosphere.

Surface analysis from remote data of Mars needs a first step to separate the contribution of the atmospheric components. These show strong signatures in the spectra, such as the absorption bands of carbon dioxide and of atmospheric aerosols. This work is accomplished by the Factor Analysis (FA) technique that, as shown in previous works, is able to extract the independent variable components and recover the spectral end-members present in a dataset.

Previous works showed also that Martian emittance spectra could be modelled using linear combination of two atmospheric spectral shapes (water ice and dust) when observations are taken in a region of high atmospheric opacity. When this model does not give an accurate fit to the data, it usually needs only an additional component to accurately reproduce the observation, i.e. it need the surface spectrum to reproduce the observation. Hence, knowing the shape of the atmospheric components, we are able to made up a model of the observation and, if there is a significant residual between the observed spectrum and their fit, we can extract the contribution due only to the soils.

To accomplish the extraction procedure we need to determine the shape of the atmospheric components involved. They are deducted via FA technique from a large PFS data subset. The subset is chosen in order to cover a wide range of observational scenarios, i.e. with as more different as possible dust and water ice atmospheric opacities. The FA allow us to extracting the independent variable components in the dataset, i.e. the spectral shape of the atmospheric components.

So we obtain only the shape of the atmospheric dust suspension and water ice cloud, because we neglect the high carbon dioxide opacity region near 15 um because it is so strong that cover all the signature coming from the ground.

This spectral shape, joined with a library of mineral spectra, is used to deconvolve in a linear manner the observation and estimate the relative abundance of the atmospheric components and the beneath soil mineral composition.

Instrument Independent Definition of theGeometrical and Positional Information for the Mars Express Mission

Diaz Del Rio, J.; Zender, J.; Heather, D.

The expected data volume of the Mars Express long-term archive is in the range of several terabytes and the newest database technology has to be used to guarantee flexible access and retrieval of the data. ESA has designed and implemented a set of online services to help the scientific community to retrieve the Mars Express scientific data, as part of the Planetary Science Archive (PSA). PSA allows multi-instrument searches within the Mars Express Mission archive.

The diversity in instrument characteristics, data structure definition and derived data quantities requires the provision of a predefined, uniform set of parameters for each observation. Within the PSA, an important set of geometrical and positional parameters have been identified as being of interest for a general database-wide query. We categorized these parameters into instrument dependent, spacecraft dependent, solar related and general information. These parameters are computed for all Mars Express instruments.

A Geometry Library, called GeoLib, was implemented as part of the support given to the Mars Express teams. GeoLib computes the instrument related information using instrument-independent algorithms.

This paper describes the most relevant algorithms implemented in the Geometry Library, gives some results and shall be used as an outlook for future missions.

Experiences with Shape-from-Shading for the Refinement of Spatial Data for Mars Cartography from MARS EXPRESS HRSC Imagery

Dorrer, E.; Mayer, H.; Ostrovskiy, A.; Renter, J.; Reznik, S.; Neukum, G.

The paper is an account of investigations into the use of shape-from-shading (SFS) as a method for the improvement of spatial data obtained from photogrammetric processing of HRSC imagery on ESA's Mars Express Mission. Acronym for 'High Resolution Stereo Scanner Camera', HRSC is one of seven scientific instruments onboard the Mars Express Orbiter for the purpose of gathering data for geological, mineralogical, atmospheric, gravitational, and cartographic studies. Guided by G. Neukum as Principal Investigator, the Mars Express HRSC Co-Investigator Science Team consists of five working groups of which the Photogrammetry Cartography Working Group (PCWG) is solely dedicated to the derivation of spatial data and generation of digital image maps of the Martian surface. Within PCWG our subgroup is primarily concerned with optimization and homogenization of map relief shading, prerequisite of which is a refined elevation model (DEM) compatible with the imagery.

The paper first deals with the description of a process denoted De-Re-Shading for the purpose of modifying illumination induced shades in the image scenes. Kernel is a global SFS-method known from the computer vision community where it has mostly been investigated concerning mathematical and numerical objectives. Depending on numerous, partly merely estimable geometrical and physical factors such as surface reflectance, shadows, light source distribution, image resolution, accuracy of initial elevation map, etc., SFS applied to real-world imagery constitutes a highly non-trivial, generally ill-posed problem. By exploiting a priori knowledge on the stochastic model of the initial elevation map, SFS enables a distinct refinement of the photogrammetric DEM generated previously by matching alone. This then is the basis for subsequent modifications of image shades towards rigorous homogenization and optimization of relief shading in the computed ortho-image maps.

Then SFS is described from a methodical point of view. This concerns the definition as a problem of Variational Calculus with one constraint solved through direct discretization of the minimization functional by the Method of Conjugate Gradients as efficient algorithm. Performance deficiencies due mainly to the large number of elevations as unknowns can only be reduced by rigorous program optimization. Limitations to the method originate from space-variant surface albedo, severe atmospheric disturbances, and the only estimable reflectance function (BRDF). Both the advantages and disadvantages of the DRS-method are discussed by a variety of processed scenes of different topography. The results clearly indicate the method's refinement capability for spatial data.

Automatic Recognition of Crater-Like Structures in Satellite Images of Earth and Mars

Earl, J.; Chicarro, A.; Koeberl, C.; Marchetti, P-G.; Milnes, M.

Impact cratering is recognized to be a dominating (if not the most important) surface-modifying process in our planetary system. During the last few decades, planetary scientists have demonstrated that our moon, Mercury, Venus, Mars, the asteroids, and the moons of the giant planets are all covered (some surfaces to saturation) with meteorite impact craters. Detecting impact craters on Earth is much more difficult. Part of the problem regarding recognition of the remnants of impact events is the fact that terrestrial processes (weathering, plate tectonics, etc.) either cover or erase the surface expression of impact structures on Earth. Many impact structures are covered by younger (i.e., post-impact) sediments and are not visible on the surface. Others were mostly destroyed by erosion. Recent advances in Earth Observation, i.e., the availability of synthetic aperture radar and multispectral images covering most of the Earth, has the potential to aid the search for terrestrial impact craters through use of image processing for the identification of crater features, their detection, and possible recognition. Whereas it is not possible to unambiguously confirm that a crater-like feature on Earth has indeed formed by hypervelocity impact just by using remote sensing alone, such data can identify potential candidates for further studies. Information that can be derived from remote sensing products refers mainly to crater morphology, which, using relevant criteria, can aid in the identification of potential impact craters.

On Earth we know two distinctly different morphological forms: simple craters (small bowl-shaped craters) with diameters of up to £2 to 4 km, and complex craters, which are larger and have diameters of >=2 to 4 km (the exact change-over diameter between simple and complex crater depends on the composition of the target). On Mars, the change-over diameter from simple to complex craters is about 10 km. Complex craters are characterized by a peak or peak ring that consists of rocks that are uplifted from greater depth and would not normally be exposed on the surface. The stratigraphic uplift amounts to about 0.1 of the crater diameter. Fresh simple craters have an apparent depth (measured from the crater rim to present-day crater floor) that is about one third of the crater diameter, whereas that value for complex craters is closer to one sixth. In reality, most craters are shallower because of erosion and/or infilling (e.g., by crater lakes). On Earth basically all small craters are relatively young, because erosional processes obliterate small (0.5–10 km diameter) craters after a few million years, causing a severe deficit of such small craters. In this context, we address the issue of recognition and detection of impact craters on the Earth by applying processing techniques to Earth Observation products, complemented by digital elevation data, to automatically highlight potential targets for future exploration. The relevant algorithms and techniques have been validated by using images of the surface of Mars. A prototype impact crater detection system has been developed, which has been successfully used to identify a number of known terrestrial craters, and has the potential to search other areas of the Earth for previously undiscovered candidate sites.The prototype system comprises two parts:

i) An interactive standalone tool, for the development and refinement of crater detection and filtering algorithms, which is designed for use with relatively small satellite image scenes.

ii) A more comprehensive batch-processing tool, for the offline processing of large areas of data.

The results may be output in various formats for rapid assimilation and assessment of the identified crater candidates. The core stages of processing involved in the detection of crater candidate sites are:

<sum> Import from a range of different data sources, including satellite data.

<sum> Pre-processing of the input data.

<sum> Automatic detection of circular features.

<sum> Filtering of features based on crater-like characteristics.

This generally results in a small number of likely candidates, which then need to be expertly assessed, in order to determine whether or not further analysis is required.

An accompanying demonstration system will show the application of the prototype to a range of sites on the Earth and on Mars.

Component Separation of OMEGA Spectra Using ICA : Denoising and Spectra Identification

Forni, O.; Bibring, J-P.; Erard, S.; Fouchet, T.; Langevin, Y.; Poulet, F.; Omega Science Team

The OMEGA hyperspectral imager (0.35 to 5.1 micrometers) with its 352 spectral channel allows to use efficient separation techniques only based on the statistical properties of the data. These techniques have no a-priori knowledge of the mineralogical and/or atmospherical content of the spectra. We will present results obtained by the Independent Component Analysis (ICA) technique, based on the maximisation of the non-Gaussian properties of the signal. We will show that this technique is efficient for denoising purposes as well as for identifying regions that shares the same spectral properties.

Conversion Electron Mössbauer Spectroscopy on Mars?

Gunnlaugsson, H.P.; Butz-Jörgensen, C.; Klingelhöfer, G.; Kuvvetli, I.; Madsen, M.B.; Merrision, J.; Nørnberg, P.; Weyer, G.

Given the spectacular success of backscattering Mössbauer spectroscopy (b-MS) on the Mars Exploration Rovers, the inclusion of the method in future robotic missions to Mars seems evident. The addition of a Conversion Electron Mössbauer Spectroscopy (CEMS) facility will be possible in an extremely simple way. This is due to the fact that both techniques to a large extent make use of the same hardware, and that the Martian atmosphere can be used as an electron counting gas. b-MS spectra and CEMS spectra will be obtained simultaneously.

The main difference in the two techniques is the depth selectivity. By means of CEMS information from approximately the top 0.2 µm of material is obtained, while information from the top 100-200 µm is obtained by means of b-MS. Comparison of spectra obtained by each method can provide depth-selective information on the dust/soil, soil transport, oxidation processes or weathering of rocks and the role of water in these processes. In this contribution, we shall give examples of what can be learned about the geological history of a given sample by the use of CEMS together with b-MS.

The CEMS experiment further gives new opportunities for very sensitive dust detection, and can be supplemented by methods that gather distinct sub-populations of dust particles in terms of different properties. We demonstrate how CEMS can increase the usefulness of a b-MS spectrometer, allowing for measurements on samples that are not accessible by usual b-MS and give examples of experiments that can be done on Mars when having access to both techniques.

Results from our laboratory studies using a Martian atmosphere will be shown, together with results that show that the technique can contribute significantly to the understanding of geological systems and our current ideas on how to construct a CEMS detector and how to operate it on Mars.

Distribution of Mars Express Science Data via the Planetary Science Archive

Heather, D.; Zender, J.; Arviset, C.

The Planetary Science Archive (PSA) is an online archive facility supporting all of ESA's planetary missions. Scientific and ancillary data from the Mars Express (MEX) mission will be distributed via the PSA, which is open to the worldwide scientific community, and should be the first port of call for all scientists looking for MEX data.

In the long run, the PSA will also be the repository for all of ESA's planetary missions such as Huygens, Smart-1, Rosetta and Venus Express.

This presentation gives a demonstration of the use and functionality of the PSA to show how data products and data sets should be queried, requested and retrieved from the archive.

An overview of the data flow from the spacecraft to the scientific community is also provided. The data release policy and the envisaged schedule of the expected data releases are given, and the archive process is detailed including the definition of data types and products, database ingestion and reviews for all instruments on-board of Mars Express.

Exploring Mars by a European Small Mars Mission

Hoffmann, H.; Bischof, B.; Frisk, U.; Harri, A-M.; Makkonen, P.; Van Scheele, F.; Siili, T.; Walther, S.

Three independent small Mars Mission concepts had been developed in Finland, Sweden and Germany. The high degree of commonality resulted in a unified small mission concept for a combined orbiter and lander mission which will carry an overall payload mass of up to 45 kg including the lander to Mars. The baseline scenario is a launch in 2009. Two different alternatives have been analyzed with a launch by Ariane ASAP 5 and a direct injection into Mars transfer orbit by a small dedicated launcher (Rockot). A trade-off between the different scenarios favors the direct launch which reduces the overall mission duration and complexity and would provide more volume. The estimated total cost of the mission including the payload is below 100 M€.

The key objective of the mission is to perform simultaneous measurements from the orbit and on ground of the Martian atmosphere, the magnetic field, and the radiation environment. The orbiter payload with an overall mass up to 25 kg consists of a very high-resolution and wide-angle camera instrument, a microwave sounder, a plasma package including a magnetometer, and a dosimeter. The telecommunication system is equipped with an ultra-stable oscillator for radio science investigations. The orbiter experiments thus combine new atmospheric science, detailed geophysical and surface observations, and measurements of the space environment around Mars, something that will not be provided by any other present or planned mission.

A small landing device is foreseen to carry payloads down to the Martian ground for in-situ measurements of the Martian environment and its lower atmosphere. The baseline payload package consists of sensors to measure the magnetic field, charged particles and UV radiation, and thermal radiation. A suite of atmospheric sensors shall measure pressure, temperature, humidity, wind and atmospheric optical depth. A small panoramic camera will image the surrounding landing site. Due to the simple needs of the payloads and the absence of high power consuming devices, a relatively long lifetime of the small Mars station is envisaged, to get daily measurements for at least one Martian year. The landing device weighs about 20 kg overall including the entry, descent and landing systems and would serve as a technical demonstrator for several phases in landing. The mass of the surface module is about 5 kg. Once developed, this light-weight lander could be used whenever a Mars probe allows an additional mass of 20 kg. Thus, a network of small atmospheric and environmental surface stations on Mars could eventually be established.

Automatic crater detection and 3D reconstruction for Mars geochronology

Kim, J.-R., Muller, J.-P., Morley, J.G., van Gasselt, S., Neukum, G. and the HRSC Col team

Crater counting and shape detection of topographic features on planetary surfaces are crucial to dating the age of a surface and other geological studies. An automated crater detection algorithm has been developed (Kim et al., 2004) which exploits both image and 3D data. A quantitative assessment of the detection results using pre-existing crater sets and manually measured data showed a detection accuracy of around 85% on MOC WA and 70% on HRSC respectively. Some large-scale tests of this algorithm were as applied to crater map generation using MOC WA. The automated method was also applied to generate crater Size-Frequency Ditsributions (SFDs) using HRSC and these were compared against manually derived SFDs (Neukum et al., 2004)

One of the most exciting potential applications of our algorithm is the derivation of highly detailed crater 3D morphologies from an automated stereo analysis of HRSC image pairs using automatically detected crater centres and locations. A new image matcher based on the Gruen-Otto-Chau algorithm (Day et al., 1992, Cook et al., 1999) and Okutomi and Kanade (1994)'s adaptive window and our own annular point matching method (Kim, 2005) was developed and tested. This showed a good performance with crater rims with radius, R > 0.5 km (40 pixels in 12.5m resolution HRSC image) which are clearly detected in the re-constructed stereo DEM. Smaller craters with a radius down to 0.25km (20 pixels) can be detected in the DEM and their depths, rim heights and other geomorphometrics can be estimated. We recently implemented a semi-automated 3D crater reconstruction routine which still requires manual adjustments to get the best possible 3D reconstruction.

The next steps in our research will be to update the crater detection reliability and extend the limits on 3D reconstruction to the sub km scale in order to develop a fully automated process with the potential to produce a planet-wide 3D crater database.

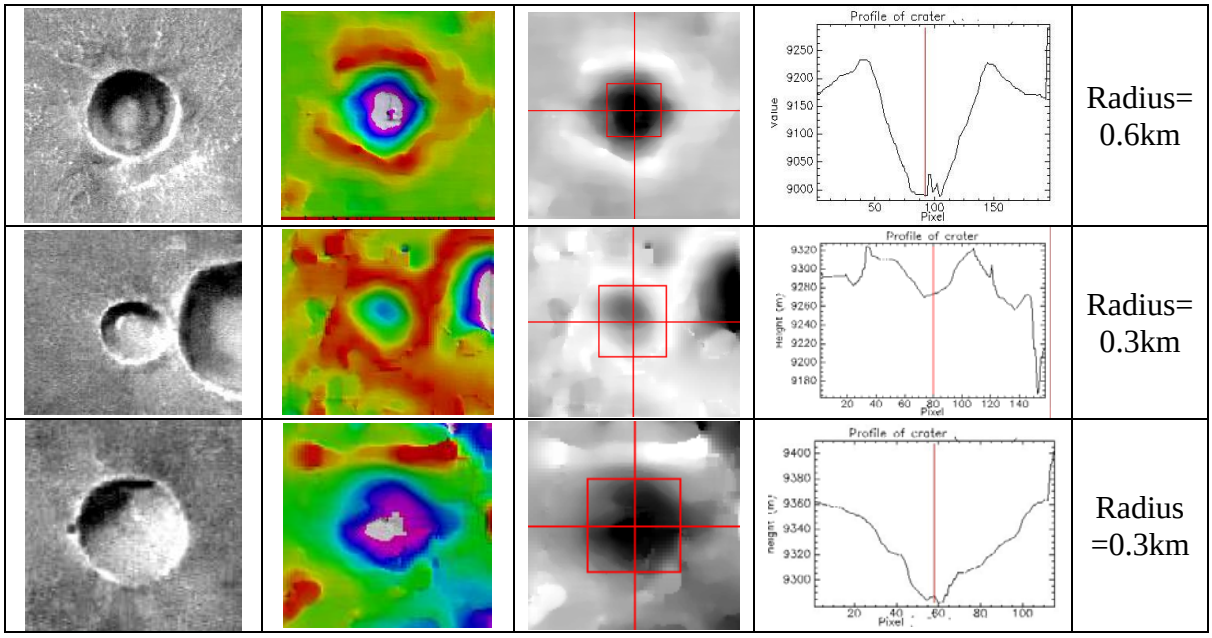

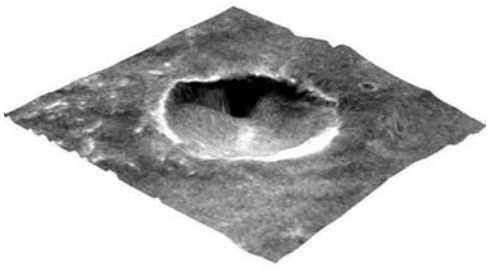

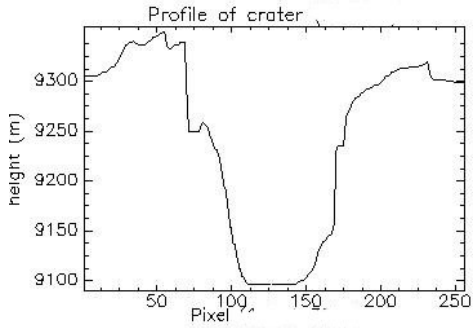

Radius= 0.87km

Figure 1. Stereo HRSC-derived DEMs of impact craters (HRSC orbit 68, nadir image, 12.5m)

References cited

Cook, T.C., T. Day, and J.-P. Muller, The UCL IUS-Tithonium Chasma Digital Elevation Model., in *ISPRS Workshop on "Mars Mapping" session of the 5th International Conference on Mars*, ISPRS WG on "Extra-terrestrial Mapping"/University of Arizona Press, 22-23 July 1999, Caltech, Pasadena, CA, USA, 1999.

Day, T., A.C. Cook, and J.-P. Muller, Automated Digital Topographic Mapping Techniques for Mars, in *International Archives of Photogrammetry and Remote Sensing*, edited by L.W. Fritz, and J.R. Lucas, pp. 801-808, American Society of Photogrammetry & Remote Sensing, Washington D.C., 1992.

Kim, J.-R. (2005), The detection and reconstruction of landscape objects using multi sensor fusion, PhD thesis, University of London

Kim, J.-R., Muller, J-P., Gasselt, S., Morley. J.G., Neukum, G., and the HRSC CoI team., Automated crater detection, quantitative assessment and some practical applications to Mars., *Photogramm. Eng. & Rem. Sens., (submitted 11/10/04)*, 2004.

Okutomi and Kanade (1994), A Stereo matching algorithm with an adaptive window : theory and experiment., IEEE PAMI, Vol.2(9), pp.920-932.

Mapping of Photometric Anomalies with HRSC: Demonstration of the Principal Possibility

Kreslavsky, M.; Bondarenko, N.; Raitala, J.; Korteniemi, J.; Pinet, P.; Neukum, G.

The bidirectional reflectance of the surface depends on the illumination / viewing geometry. This dependence ("photometric properties") is controlled by the surface structure at a wide range of scales from the wavelength to the resolution limit. Although the interpretation of the photometric properties is not simple, they certainly give some information, which is essentially complementary to information from all other remote sensing data like images, spectra, etc. Five channels of HRSC camera onboard Mars Express (the nadir channel, two stereo and two photometric channels) take images of the surface in the same wide-band filter under different viewing geometry. Thus, the HRSC images can potentially contain some information about photometric properties and hence about surface structure. As shown by Pinet et al., 2004 (see Ischia Mars International Conference), it is found that they do contain this information. Extracting of photometric properties from the five HRSC channels is not straightforward, first of all, due to non-negligible atmospheric scattering contribution. Rigorous separation of surface and atmospheric contributions is a very complex problem. Instead solving it, we applied an heuristic method, that allows us to map anomalies of the photometric behavior. Our approach makes use of the fact that the surface albedo contrasts are much higher than the contrasts due to photometric function variability. We use global correlation between images in different channels to derive the typical photometric behavior of the surface + atmosphere within given image under given illumination and atmospheric conditions. Then we map a parameter that quantifies small local deviation from this typical behavior. The mapped parameter characterizes relative deviation of the local phase function slope from the typical one. We applied this procedure to a number of HRSC images of Hesperia Planum. We found several anomalous areas that definitely are related to variations of the surface structure. For example, the floors of Dao Vallis, Niger Vallis, and several craters have anomalously gentle phase function indicating a very specific surficial deposit. There is an indication that the surface structure of dark and bright wind streaks is different.

The OMEGA Data Set

Langevin, Y.; Manaud, N.; Poulleau, G.; Bellucci, G-C.; Altierri, F.

In more than one year of operations, the OMEGA VIS/IR imaging spectrometer has obtained more than 200 tracks on the surface of Mars. It is constituted of 3 channels, 2 in the near-IR and 1 in the visible. The overall coverage should exceed 70% by the end of January. The data set is constituted of cubes, each corresponding to a single observation mode of the instrument. The dimensions of the cube are the length of the swath (16, 32, 64 or 128 pixels), the number of spectral channels (352 or 400, 256 in the near IR then 96 or 144 in the visible) and the number of swaths (typically 200 to 600 for swaths with 128 pixels, up to 8000 for swaths with 16 pixels). 16 pixels swaths are obtained close to the planet at resolutions of up to 300 m /pixels. Increasing swaths correspond to increasing altitudes and pixel size (2 to 4 km for 128 pixel swaths). The nominal exposure time is 5 msec (IR) and 50 msec (Vis). When bright terrains are observed close to the subsolar point, the IR exposure time can be reduced to 2.5 msec. The OMEGA data set is constituted of level 1B cubes in the PDS format. An auxiliary cube, also in the PDS format, provides useful geometrical information (longitude, latitude, slant distance, MOLA altitude, incidence, emergence, phase) for each of the three channels. Reduction software is provided in the SOFTWARE directory. It implements flat-fielding for the visible (which uses a 2-D CCD), then provides radiance and I/F data using the photometric function and the solar spectrum at the time of observations. This reduction software will be updated by new releases to the data set as understanding of the instrument improves. Only spectral features varying by 5% or more should be considered as fully reliable at this stage due to a non linear behaviour in part of the spectral range which varies from observation to observation. Further work should make it possible to provide correction software, hereby improving this confidence level constraint. For swaths with 128 pixels which were obtained after orbit 511, a perturbation is observed for 4 spectels every 32 from pixel 80 to pixel 95. For cubes with no spatial summation, this can be recovered with some loss of spatial resolution by considering the same pixel from the next swath, for which the perturbation is shifted by 16 spectels.

Statistical Interpretation of PFS Spectral Data

Fonti, S.; Marzo, G.A.; Formisano, V.; Giuranna, M.; Marra, A.C.; Maturilli, A.; Orofino, V.; Roush, T.L.

Many indications suggest that Martian paleoclimate allowed for the presence of liquid water on the surface. It is therefore reasonable to suppose that bodies of standing water were once present in basins or depressions where evaporite deposits (for example carbonates and sulphates) could have formed. The identification of such deposits, which might have survived in some regions of the planet, could confirm the present hypothesis about the ancient climate on Mars. However, no final evidence about such deposits has been reached, probably due to the difficult spectral detectivity of such evaporites. In this respect, the Astrophysics Group of Lecce University has started a statistical multivariate analysis program aimed to search for materials connected with the presence of water in the Martian spectral databases. This study is focused on geomorphological interesting areas such as the boundary zones between high- and low-lands and the outflow channels. The idea is to characterize each spectrum and associate it with the high-resolution image and topography of the footprint, linking the candidate water-connected surface features to the corresponding spectra. In this work we present the preliminary results of this procedure applied to some interesting Martian areas using PFS data in comparison with other spectral databases such as TES data.

Usage of Measured Mars Data for the Determination of the Field of View Orientation and Shape for the Planetary Fourier Spectrometer (PFS) Onboard the Mars Express Mission

Maturilli, A.; Formisano, V.; Grassi, D.

The precise misalignment between the line of sight in the PFS' Long and Short Wavelength Channels and the +Z axis of the MEX Spacecraft has never been measured on ground. Laboratory tests performed in the Instituto di Fisica dello Spazio Interplanetario (IFSI) in Rome show that such differences exist and influence the calculated geometries. The observing geometries calculated using this "nominal" misalignment show discrepancies with the measured spectra; this lead us to conclude that the exact pointing directions should be retrieved in comparison with special observations. Orbits moving from planet to limb are useful for this study, even though in the LWC the hot atmosphere is masking the precise instant when PFS loses the planet and the thermal part of the SWC is quite "blind" for night observations. For these reasons, bright Phobos observations were used to calibrate the viewing direction of the two channels of the PFS experiment. The result obtained have a great importance in the re-calculation of all the PFS observing geometries for the entire mission, giving a crucial information for the analysis of the measured spectra.

A Quantitative Assessment of Mars HRSC Stereo-Derived DTMS Using MOLA Profile Data and Experimental Results from the Operational VICAR Stereo-Photogrammetric System

Muller, J-P.; Van Gasselt, S.; Casley, S.; Kim, J.-R.; Spiegel, M.; Neukum, G.; HRSC Co-Investigator Team

Several stereo matching systems have been developed for the processing of HRSC multi-line stereo CCD line array data. The UCL Gotcha (Day et al., 1992) was the first stereo matching system developed and successfully applied to overlapping multi-resolution Viking Orbiter imagery (Cook et al., 1999). This was recently interfaced (Casley, 2004) to the operational HRSC stereo processing system (Scholten et al., 2004) and a comparison of results is shown in Albertz et al. (2004). A polar-coordinate based matcher developed by Kim and described in Kim et al. (2004) has also been developed primarily for obtaining very high resolution DTMs of craters on Mars. Using the improved orbit files from the Technical University of Munich (Schmidt et al., 2004), level 4 products have been created using these 3 different matchers and the results compared against MOLA profiles which have been adjusted to the same datums. In parallel, a systematic study has been conducted of the optimal parameters to employ with the operational VICAR stereo matcher to obtain the best possible DTMs and these have also been assessed against the MOLA profiles.

MEX:OMEGA-MRO: CRISM Cooperation: Testing the CRISM Global Mapping with Mars Express OMEGA Data

Mustard, J.; Bibring, J.P.; Pelkey, S.; Milliken, R.; Langevin, Y.; Gondet, B.; Gendrin, A.; Poulet, F.; Erard, S.; Kanner, L.; Hutchison, L.; Murchie, S.; Arvidson, R.; Gomez, C.

Over its first 9 months of operation, the OMEGA imaging spectrometer on Mars Express has sampled all major geologic and geographic areas and is approaching complete coverage of Mars. In August 2005, the CRISM imaging spectrometer will be launched on NASA's Mars Reconnaissance Orbiter. CRISM covers the wavelength range 0.4-4.0 µm, similar to OMEGA, but will sample down to 18 m/pixel spatial resolution. CRISM will cover up to 5% of the surface at full spectral and spatial resolution, and 100% of the surface in 60 spectral bands and 200 m/pixel spatial resolution. In anticipation of CRISM data, we have been analyzing OMEGA data to test the CRISM strategy of evaluating information obtained by mapping spectral parameters, which are derived from the multispectral bands. OMEGA spectra are sampled to approximate CRISM multispectral band passes. For parameters requiring atmospheric correction, the data are only corrected for atmospheric transmission. A total of 36 parameters related to atmospheric and surface properties have been calculated from the multispectral bands using OMEGA data. Detailed analysis of these parameters reveals that much of the spectral diversity of Mars is captured using this multispectral approach. However, several of the parameters do not show relevant variations on Mars as anticipated, while variations observed at the full OMEGA spectral resolution are not captured by any of the current parameters. We are refining the choice of spectral parameters based on this work and will present global mapping of spectral parameters related to mafic minerals (pyroxene, olivine), sulfates, and hydrated minerals. These results demonstrate that the CRISM strategy for multispectral mapping will achieve its goals for a) global mapping of the spectral diversity of Mars, b) provide critical inputs for targeting high spectral and spatial resolution observations, and c) provide high value products for integrated global science investigations.

The performance of HRSC's Super Resolution Channel (SRC)

J. Oberst, G. Schwarz, T. Behnke, H. Hirsch, K.-D. Matz, J. Flohrer, V. Mertens, F. Scholten, B. Brinkmann, T. Roatsch, H. Hoffmann, R. Jaumann, G. Neukum, and the HRSC Co-I Team

The SRC (Super Resolution Channel) is a 1024 x 1024 framing camera, equipped with a Matsutov-Cassegrain telescopic lens for imaging at highest resolution (up to 2.3 m/pix from the nominal pericenter height of 250 km), intended to show details within the large HRSC context frames. The operation of SRC is controlled by the HRSC digital unit. Normally, images are obtained as a series with approx. 5% overlap during an HRSC image sequence. The SRC images are mosaicked on the ground using nominal time tag and alignment data, and fall nicely into their predicted location within the HRSC context.

Using a digital image matcher as a tool for position measurement of features in the images, we estimate that the magnification factor of SRC with respect to HRSC is 4.33, corresponding to an SRC effective focal length of 974.5 mm. This value is in good agreement with the nominal focal length, but 1.5% lower than the value that has been directly measured on the ground.

However, the effective visibility of details in the SRC images is somewhat reduced over what one would expect: The MarsExpress mission constraints called for a low mass and low power instrument. These requirements resulted in an instrument design relying on thermally balanced conditions. In cases, where the thermal balance cannot be reached, imaging artifacts, such as blurring and “ghosts” have been observed. Camera models and image processing algorithms are currently being studied and tested to remove these artifacts.

By the time of writing (November, 2004) SRC has acquired more than 1300 frames. While the camera has a small field of view and cannot be pointed at specific targets as geologists may wish, the camera has very often incidentally captured fascinating details in surface morphology. The SRC has also proven to be very useful for statistics of small craters and for astrometric observations of Phobos.

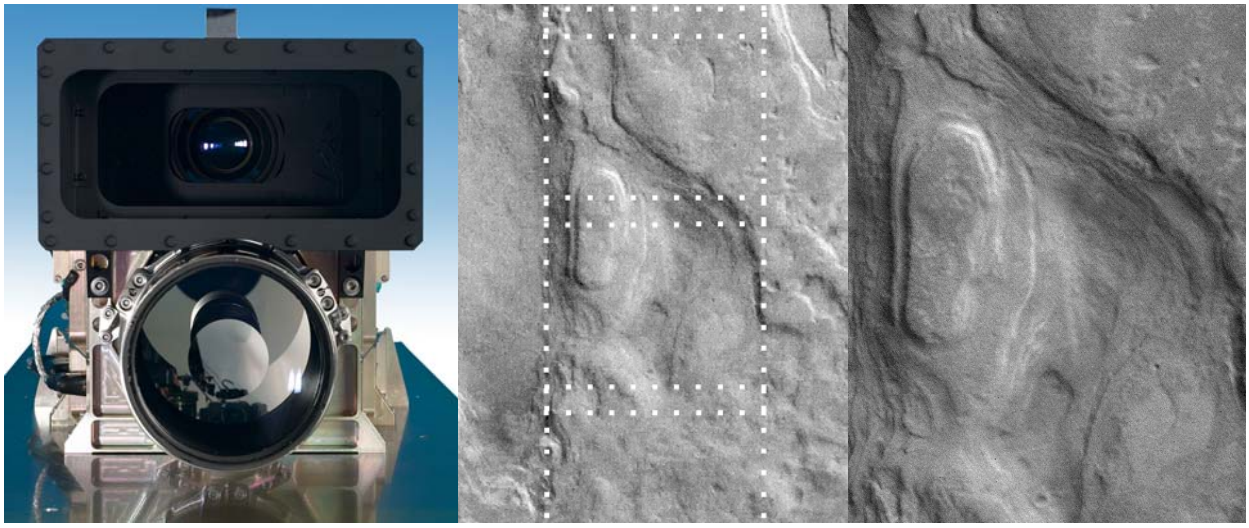

Fig. 1: Left: The HRSC/SRC assembly with the rectangle-shaped HRSC lens at the top and the circular SRC lens at the bottom. Center: Small portion of a HRSC frame showing the footprints of SRC images (note that the full HRSC swath –if in full resolution– is approx. 20 times wider than the SRC frame). Right: Corresponding SRC image mosaic.

Analysis and Automatic Feature Recognition on Images of the Surface of Mars

Pina, P.; Alves, I.; Barata, T.; Saraiva, J.; Vaz, D.; Bandeira, L.

As an offspring of project MAGIC (Mars Atmospherical, Geophysical and Exobiological Characterisation) [1], the present group of researchers has begun working on the processing and automatic recognition on images of the surface of Mars that were acquired by previous missions. This research line has already yielded some results in four areas:
- automatic recognition of craters;
- automatic recognition of fault systems;
- automatic recognition of sand dunes;
- automatic recognition and topological characterisation of patterned grounds.

In the area of automatic recognition of craters, the method that was developed consists of three main phases: in the first one the images are segmented through a principal components analysis of statistical texture measures, followed by the enhancement of the selected contours; in a second phase craters are recognised through a template matching approach [2]; in a third phase the rims of the plotted craters are locally fitted using the watershed transform [3]. An approach that has been attempted lately is the improvement of phase 2 through the use of the Hough transform.

Another endeavour of our group is the automatic recognition of fault systems by application of a method that is similar to the one that we have used on craters, but with shape recognition being performed by a bi-dimensional wavelet transform. This method has the advantage of revealing the orientation of the dip of fault planes and will henceforth constitute a useful tool for the interpretation of Martian palaeotectonics.

Our contribution to a better morphological characterisation of structures created by aeolian processes consists of a two-step algorithm to segment and recognize ripples. This image analysis procedure exploits simultaneously the brightness and morphological features of the ripples, which consist of elongated structures, exhibiting preferential alignments and occurring sequentially in patches with a certain periodicity [4].

The study of patterned or polygonal grounds is also being performed. Algorithms to segment automatically the polygons are based on previous studies on cellular materials [5]. The topological characterisation of polygonal grounds may be used to discriminate among different terrain types.

References

[1] Roos-Serote et al. (2005) MAGIC, the Portuguese participation in Mars Express (this conference).
[2] Alves, E. I. (2003), A new crater recognition method and its application to images of Mars. Geophys. Res. Abs. 5 (CD-ROM).
[3] Barata, T., et al. (2004) Automatic recognition of impact fcraters on the surface of Mars, in A. Campilho, M. Kamel (eds), Image Analysis and Recognition, Lecture Notes in Computer Science, 3213,Springer, Berlin, pp. 489-496.
[4] Pina, P., et al. (2004) Automatic recognition of aeolian ripples on Mars, Lunar and Planetary Science XXXV, Abstract #1621 (CD-ROM), Lunar and Planetary Institute, Houston.
[5] Pina P., Fortes M.A. (1996) Characterization of cells in cork, Journal of Physics D, 29: 1507-2514.

Joint Mars Science Opportunities using Mars Global Surveyor (MGS), Mars Odyssey (ODY), Mars Express (MEX) and the Mars Exploration Rovers (MER)

Plaut, J.; Thorpe, T.; Arvidson, R.; Chicarro, A.

A unique set of Mars science opportunities exist today with the presence for the first time of three operating orbiting spacecrafts (Mars Global Surveyor, Mars Odyssey, Mars Express) and two rovers (MER-A and MER-B). These orbiting and mobile in-situ analysis platforms provide orbiter–to-orbiter and orbiter to rover science opportunities never available before. Some of these opportunities have already successfully being exercise through the formation of collaborative science themes working groups with MGS, ODY and MER such as;

- Surface photometric properties, emission phase angle study,
- Wind-related features and processes, dust storms,
- Local / regional global weather the atmospheric aerosols (distribution, opacity, properties),
- Cloud and water vapor monitoring, Color calibration, and Thermo-physical properties

Present orbital characteristics of most of these spacecrafts have afternoon orbits, such as MGS (2:30 pm local time) and ODY (5:00pm local time) with twice a day passes over the MER sites (i.e. =2:30AM and 2:30PM). Emphasis in the synergistic science observations between the orbiters including the Mars Express spacecraft and its complementary payload will be discussed

Other joint opportunities to be explore would include data sets comparisons, cross calibrations, multi-spacecraft operation strategies, future missions planning, and joint scientific frameworks that could aid the exploration initiative.

First HRSC Archive in the Planetary Science Archive

Roatsch, T.; Matz, K-D.; Jaumann, R.; Neukum, G.

The High-Resolution Stereo Camera (HRSC) aboard Mars Express imaged Mars and Phobos in 127 orbits during the first 6 months of 2004. The data taken during these orbits were archived in the first seven HRSC datasets which were released in January 2005. The size of these datasets varies between 15 and 47 GByte.
The HRSC team archives the data as radiometrically calibrated data to allow easy use of the data for the scientific community. The datasets also contain the standard documentation and are supplemented by browse images for quick searches. Furthermore, software for the generation of map projected HRSC images and to display the data is distributed with the datasets.

Hypsometric Map of Mars

Rodionova, J.

Hypsometric map of hemispheres of Mars have issued in 2004 year. The MOLA data was used for mapping about elevation of 1º trapezium (64 800 points). A digital model of the relief was constructed with software ArcGIS. The digital model was constructed with the use of interpolation. An Equal Area Azimuth projection was chosen for maps of hemispheres. It was supposed to use these maps for measuring areas within different height levels. The names of terra, plateaus, mountains and lowlands – plains and also some big craters are labeled. An analysis of the heights of the martian relief was fulfilled. The areas between the contours were measured automatically. The results of the measurement are different from (Smith D.E. et al, 1999) about 4 - 6%. The total area of the plain (from -2 till -5 km) is 50 billion km or 34.5%. . 35% of the total area is occupied by the levels from 1 to 3 km. The mountains above 5 km occupy only 2.5% of the total surface of Mars (the highest of them above 10 km - only 1%). The transient zone from plains to the highland due to the level from -2 to 1 km and correspond 25%. The deepest depressions (less than 5 km) compose 2.5%. It is interesting that in the western and eastern hemispheres both maxima (-2 -5 km) and (1-3 km) are represented. The comparison of the heights of different regions obtained by MOLA with the previous investigations show that there are not systematic differences there.

MAGIC, the Portuguese Participation in Mars Express

Roos-Serote, M.; Alte Da Veiga, N.; Alves, E.I.; Assis Fernandes, V.; Bandeira, L.; Baptista, A.R.; Barata, T.; Conde, L.; Azevedo, J.; Fernandes, C.; Luz, D.; Monteiro, J.; Neves, L.; Pina, P.; Russo, P.; Saraiva, J.; Vaz, D.; Webb, M.

The Mars Atmospherical Geophysical and ExobIological Characterisation project (MAGIC) represents the Portuguese scientific participation in the Mars Express mission. MAGIC is an ESA Recognised Cooperative Laboratory (RCL) for the mission, approved in early 2002.
The project has received national funding of 160 kEuros, starting in July of 2004 for a three year period.
Half of the funds go to scholarships for students to participate in the project.

MAGIC is focused around seven tasks:

(1) Automatic Shape Recognition of surface feature.
(2) Mars Apparent Thermal Inertia map (ATI).
(3) Mars Lithospherical Map (MALI).
(4) Hydrogeology - Life Potential.
(5) Mars Atmospheric Minor Species.
(6) Magnetism and Surface Irradiation.
(7) Mars Orbital Movie (MOVIE).

Activities have started on tasks (1), (3), (4), (5) and (6). We plan to use data from the ASPERA, HRSC, OMEGA, PFS and MARSIS (when available) instruments. In this presentation, we will give an update on the ongoing activities and will introduce the MAGIC team.

This project is funded by the portuguese Foundation for Science and Technology (FCT) ref: PDCTE/CTA/49724/2003

Title: ArcGIS and GRASS GIS for planetary data

Authors: P. Saiger[1], M. Wählisch[1], F. Scholten[1], K.Gwinner[1], R. Jaumann[1], G. Neukum[2] , and the HRSC Co-Investigator Team

[1] Institute of Planetary Research, German Aerospace Center (DLR), Berlin.
[2] Institute of Geosciences, Remote Sensing of the Earth and Planets, Freie Universität Berlin.

Keywords: Planetary GIS with ArcGIS & GRASS 5.3

Geographic Information Systems (GIS) are powerful tools for integrating information from different planetary datasets e.g. images, spectral data and digital terrain models in different formats like vector and raster. Before analyzing these datasets within GIS it is necessary to relate them to a common reference system. However, while the regular standard GIS Systems are developed for terrestrial reference systems, additional efforts are required for the integration of planetary datasets into a GIS.

In this talk we describe the import of different datasets into ESRI`s commercial ArcGIS 9 and the open source project GRASS 5.3 (Geographic Resources Analysis Support System). We introduced several Mars datasets like MOLA (Mars Obiter Laser Altimeter), MDIM2.1 (Mars Digital Image Mosaic), MOC (Mars Orbiter Camera), TES (Thermal Emission Spectrometer), the Geologic Map of Mars and images of High Resolution Stereo Camera of ESA`s Mars Express mission. Before importing these datasets, we referenced all these data within the VICAR (Video Image Communication And Retrieval) software package to the MOLA reference sphere using our mapping tools. We developed scripts to automate these steps and to create the correct image formats for GRASS and ArcGIS, respectively. Some results will be presented at this conference.

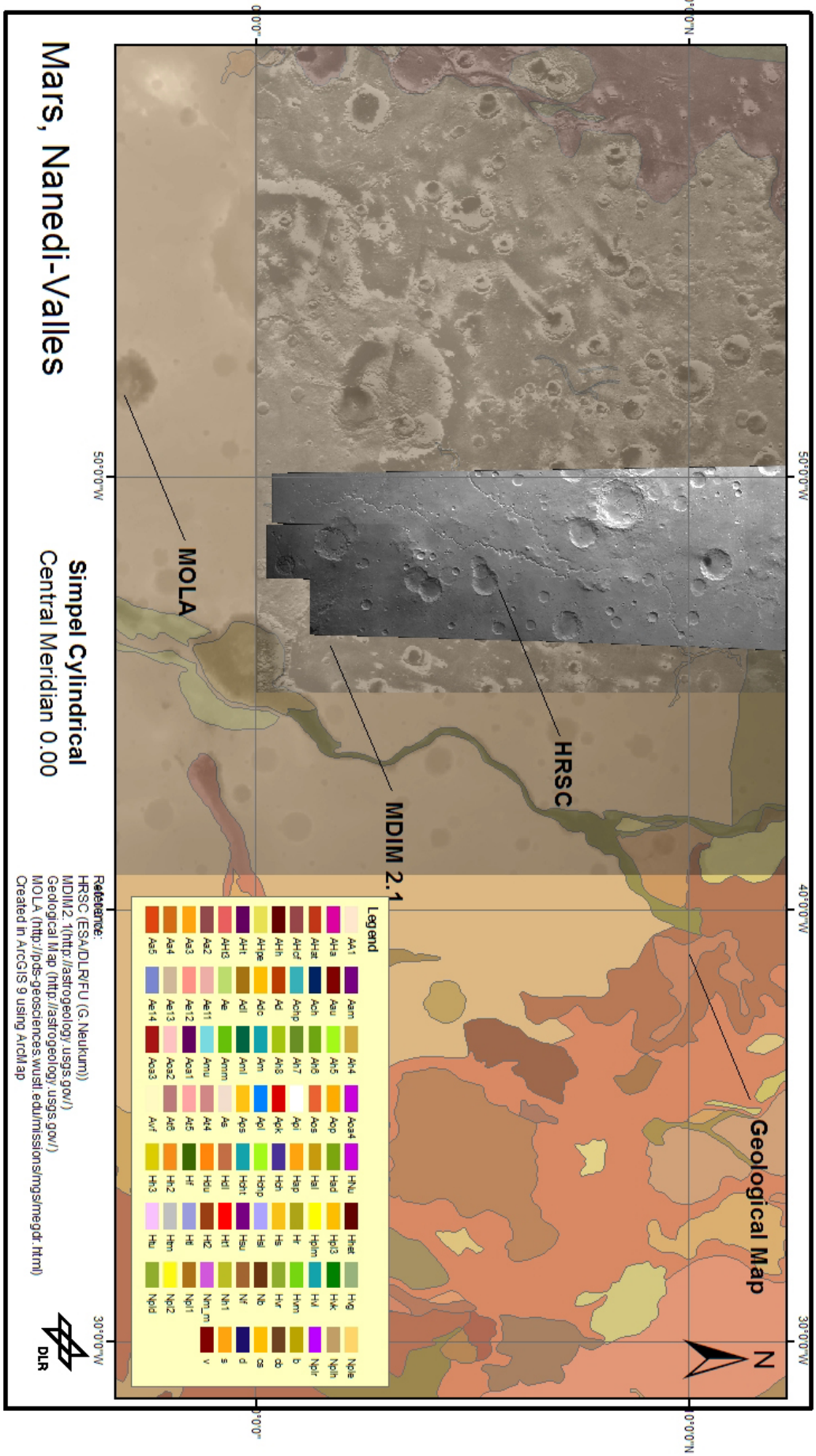
Mars, Nanedi-Valles
Simpel Cylindrical
Central Meridian 0.00
MOLA
HRSC
MDIM 2.1
Geological Map
N
Legend
Reference:
HRSC (ESA/DLR/FU (G. Neukum))
MDIM2. 1(http://astrogeology.usgs.gov/)
Geological Map (http://astrogeology.usgs.gov/)
MOLA (http://pds-geosciences.wustl.edu/missions/mgs/megdr.html)
Created in ArcGIS 9 using ArcMap
DLR
10°0'0"N
0°0'0"
50°0'0"W
40°0'0"W
30°0'0"W

Test of Statistical Methods for the Classification of Polar Terrains on Mars Observed by OMEGA

Schmidt, F.; Doute, S.; Schmitt, B.; OMEGA Team

INTRODUCTION

Since January 2004, the OMEGA spectrometer on Mars Express carried over 100 remote sensing observations in the visible and infra-red ranges in order to follow the seasonal variations of the volatiles (CO2, H2O) and dust. In each hyperspectral image, between 20 000 and 300 000 spectra are recorded to determine the spatial distribution of different types of terrains and to identify their constitutive materials. For that purpose, data reduction is required : reduction of the number of spectra and reduction of the spectral vector size by eliminating noise and redundant informations. This operation can be separated in two parts: First, the choice of the mathematical space where the data will be computed - for instance the usual spectral space but it can be its Fourier Transform (FT), its Wavelet Transform (WT), its Principal Component Analysis (PCA) transform...-
Second the definition of relevant information (endmembers, mean of spectral classes,...) and the choice of a method to extract it (Pixel Purity Index, Kmean,...). Focusing on the first step, I will evaluate the PCA space and the combination WT / PCA for the study of South Polar Cap NIR observations by OMEGA. The evaluation will be done in terms of component detection, physical meaning, noise dependence and reduction factor.

METHODS & RESULTS

i] Principal Component Analysis

The PCA is a very common linear transformation (translation, rotation and linear deformation) of spectral space which determines a new orthogonal referential with the following properties: all axis support a maximum of variance, the covariance between axis are null. The idea is to unravel physical processes by linking one axis to one effect (illumination conditions, albedo, nature of the surface, noise...).
Usually this new space possesses advantages to separate data from noise and at the same time to reduce the spectral dimension because about 10% of the axis store the essential information. Another advantage is to detect "hot spectels" which are spectral channels unusually noisy. There are still two main disadvantages: Firstly, instrument noise could induce a higher variance than signal but it could be partly corrected by removing "hot spectels" from the study. Secondly, the complexity of optical surface physics introduces non-linearity that is not compatible with linear orthogonalities of PCA (for instance between absorption band depths, albedo and composition). Therefore linking PCA axis and physical effects is difficult.

ii] Wavelet Filtering and Principal Component Analysis

We propose an improvement of PCA, which consists of applying a Daubechie wavelet filter before the PCA. The idea is to separate absorption bands from albedo and illumination effects only by the work at different spectral scales. At the scale of the whole spectrum, the only important effects are albedo and illumination. At the scale of individual channel, we must found only narrow absorption bands effects. At intermediate scale, we must found large absorption bands. Spectral reduction in this method is very high because the WT is adaptative to the scale and, after, the PCA apply another reduction.
Preliminary results on the same observation indicate that absorption band extraction by scale is quite efficient:
physical effects of albedo and spectral absorption can be efficiently unmixed. The disadvantages are: At high scale, albedo and illumination parameters are mixed, and at intermediate and low scale signal and noise have got the same energy. The noise can probably be partly removed by eliminating bad channels.

CONCLUSION

The usual choice of PCA space to analyse remote sensing data is relevant for southern polar cap observations by OMEGA because this method separates signal from noise, especially due to "hot spectels", and reduces data by a factor

of 10. However it is not efficient to discriminate albedo/illumination effects from absorption bands. Nevertheless this approach can be improved by a WT filtering.

Improving the Mars Express Orbit Using MOLA Data

Schmidt, R.; Spiegel, M.; Heipke, C.; Stilla, U.; Neukum, G.

In January 2004 the High Resolution Stereo Camera (HRSC) on board the ESA mission Mars Express started imaging the surface of planet Mars in colour and stereoscopically in high resolution. The Institute of Photogrammetry and GeoInformation (IPI) of the University of Hannover and the Department Photogrammetry and Remote Sensing (FPF) of the Technische Universitaet Muenchen are jointly processing the data of the HRSC: Using automatically extracted tie points and Mars Orbiter Laser Altimeter (MOLA) data, the exterior orientation of the Mars Express spacecraft is being calculated perpetually in a combined photogrammetric bundle adjustment during the two years of mission. The three-dimensional position and attitude of the spacecraft is constantly determined by the European Space Agency. These measurements are not accurate enough to generate high quality photogrammetric products like a digital terrain model or maps. But, the measurements can be considered as approximate exterior orientation in classical photogrammetry. However, these values are not consistent enough for high accuracy photogrammetric point determination. Therefore, a bundle adjustment has to be performed using these values as direct observations for the unknown exterior orientation parameters. As further input for the bundle adjustment automatically extracted tie points derived via digital image matching are being used. Additionally, ground control points are necessary to transform the results into a Mars-fixed coordinate system. Because on Mars very few classical GCPs exist, the globally available digital terrain model MOLA is applied.

Operational Processing of MEX HRSC Data

Scholten, F.; Roatsch, T.; Flohrer, J.; Giese, B.; Gwinner, K.; Hauber, E.; Hoffmann, H.; Jaumann, R.; Matz, K-D.; Mertens, V.; Neukum, G.; Oberst, J.; Waehlisch, M.; HRSC Co-Investigator Team

The HRSC onboard Mars Express is a multi-line pushbroom scanner which provides image data from 5 panchromatic stereo channels and 4 spectral bands (Neukum et al, 2004). A completely automated ground data processing line has been developed in the past years and is being applied on a routine base for each MEX orbit. It comprises the conversion of the original data stream transmitted to ground to de-compressed data (Level-1 data), the radiometric correction of the image data based on calibration information (Level-2 data) combined with orbit and pointing information for each image line, and a first rectification to standard scales of up to 12.5 m/pixel (Level-3 data) using a-priori topography information as defined by the MGS MOLA instrument. Level-2 and Level-3 data of HRSC's Super Resolution Channel (SRC) in scales of up to 2.5 m/pixel complete the HRSC capabilities. Thus, Level-2 and Level-3 are ready for distribution to the HRSC Co-Investigator team within one day after data acquisition.

A standard Level-4 generation is started after completion of Level-2 data in order to derive HRSC digital terrain models in a standard 200 m grid. These DTMs are finally used for the generation of orthoimages of all 4 spectral bands and the high-resolution nadir channel. This standardized processing provides 3D and image data products within a few days after data acquisition for first science analyses. Based on nominal pointing and reconstructed orbit information the standard Level-4 data products comprise a mean absolute accuracy of a few hundred meters for planimetry and of better than 100 m for height.

Reference:

Neukum, G., Jaumann, R. and the HRSC Co-Investigator Team, 2004. HRSC: The High Resolution Stereo Camera of Mars Express. ESA Special Publications SP-1240.

Height Measurements on HRSC Stereo-Image Data by Making Use of a High-Precision Stereo Comparator

Schreiner, B.; Neukum, G.; HRSC Co-I Team

Digital Terrain Models (DTMs) derived from Mars HRSC data are generated by automated area based matching and show significantly less spatial resolution (approx. 200m) than the stereo images they have been derived from. In the analog approach described here parallax differences between stereo images are measured using a high-precision stereo comparator (ZEISS) by making use of human 3D viewing capabilities. The measured parallax differences are calibrated with MOLA data to achieve absolute height information. By this method height information for discrete points with a spatial resolution comparable to that of stereo image (10-20m) data can be obtained, which enables height measurements on small features below DTM resolution. Results for a number of areas will be discussed.

Small Landers as a Tool to survey Mars for Life in Geology

Pillinger, C.; Sims, M.; Hurst, S.; Northey, D.; Taylor, P.; Bridges, J.

Based on lessons learned from Beagle 2, it is possible to produce a small lander of approximately 125 - 150 kg, which can be used to follow up lessons from Mars Express, in particular the methane water discovered combination in localised areas. Such landers can be deployed from orbit to ensure minimal risks in entry, descent and landing

Acton, Charles	NASA/Jet Propulsion Laboratory	US	+1 818 354-3869	charles.acton@jpl.nasa.gov
Altieri, F.	IFSI-INAF	IT	0039 06 4993 4373	francesca.altieri@ifsi.rm.cnr.it
Alves, Ivo	University of Coimbra	PT	+351239793420	e.ivo.alves@netc.pt
Amerstorfer, Ute	Space Research Institute, Austrian Academy of Scie	AT		ute.amerstorfer@stud.uni-graz.at
Andert, Thomas P.	Universität zu Köln	DE	+49 - 221 - 470 - 4035	andert@geo.uni-koeln.de
Arvidson, Raymond	Washington University in St. Louis	US	314 935 5609	arvidson@wunder.wustl.edu
Atreya, Sushil	University of Michigan	US	1-734-936-0489	atreya@umich.edu
Attwenger, Maria	Vienna University of Technology	AT	+43-1-58801-12243	ma@ipf.tuwien.ac.at
Barabash, Stas	Swedish Inst. of Space Physics	SE	+46-980-79122	stas@irf.se
Bellucci, G.	IFSI-INAF	IT	0039 06 4993 4373	giancarlo.bellucci@ifsi.rm.cnr.it
Bertaux, Jean-Loup	CNRS	FR	331 69 20 31 16	bertaux@aerov.jussieu.fr
Bibring, Jean-Pierre	IAS	FR	00 33 1 6985 8686	bibring@ias.fr
Billebaud, Francoise	UMR L3AB - OASU Bordeaux	FR	+33 (0) 5 57 77 61 29	billebaud@obs.u-bordeaux1.fr
BLECKA, MARIA I.	Space Research Centre PAS	PL	+48 22 737 09 94	mib@cbk.waw.pl
Boettger, Henning M.	ESTEC, ESA	NL	+31 (0)7156 55627	hboettge@rssd.esa.int
Bonello, Guillaume	CNR	IT	+39.0649934450	guillaume.bonello@rm.iasf.cnr.it
Bottger, Henning	ESTEC, ESA	NL	+0031715655627	hboettge@rssd.esa.int
Bougher, Stephen	U. of Michigan	US	734-647-3585	bougher@umich.edu
Boynton, William	University of Arizona	US	1-520-621-6941	wboynton@lpl.arizona.edu
Brain, David	University of California Berkeley	US	510 642-5442	brain@ssl.berkeley.edu
Breuer, Doris	DLR	DE	+49 30 67055 301	doris.breuer@dlr.de
Brückner, Johannes	Max-Planck-Instiut für Chemie	DE	+49-6131-305294	brueckner@mpch-mainz.mpg.de
Buchroithner, Manfred	Dresden University of Technology	DE	+49 351 463 34809	manfred.buchroithner@mailbox.tu-dresden.de
Catling, David	University of Washington	US	206-543-4576	davidc@atmos.washington.edu
Chicarro, Agustin	ESA / ESTEC	NL	071-5653613	agustin.chicarro@esa.int
Coates, Andrew	University College London	GB	+44-1493-204145	ajc@mssl.ucl.ac.uk
Cord, Aurélien	ESA	NL	+31 (0) 715658077	aurelien.cord@rssd.esa.int
D'Amore, Mario	Osservatorio Astronomico di Capodimonte	IT	0823/911813	damore@na.astro.it
Di Achille, Gaetano	IRSPS- Int'l Research School of Planetary Sciences	IT	+390854537506	gadiachi@irsps.unich.it
Diaz del Rio, Jorge	ESA	NL	+31-71-565-8391	jdiaz@rssd.esa.int
Dorninger, Peter	Vienna University of Technology	AT	+43-1-58801-12214	pdo@ipf.tuwien.ac.at
Dorrer, Egon	UniBw-München	DE	+45-089-6004-3448	egon.dorrer@unibw-muenchen.de
Doute, Sylvain	CNRS	FR	33 4 76514171	sylvain.doute@obs.ujf-grenoble.fr
Drossart, Pierre	Observatoire de Paris	FR	33 1 45 07 76 64	pierre.drossart@obspm.fr
Earl, Jon	LogicaCMG UK Ltd.	GB	+44-13723-69687	Jon.Earl@logicacmg.com
Encrenaz, Therese	Observatoire de Paris	FR	33 1 45 07 76 91	therese.encrenaz@obspm.fr
Erard, Stéphane	IAS- Université Paris-Sud	FR	33 1 69 85 86 41	erard@ias.fr
ESPOSITO, FRANCESCA	INAF-OAC	IT	+39.081.5575568	francesca.esposito@na.astro.it
Fedorov, Andrei	CESR/CNRS	FR	+33 561 55 64 82	Andrei.Fedorov@cesr.fr
Fedorova, Anna	IKI RAN	RU	+7(095) 333-10-67	fedorova@spectrum.iki.rssi.ru
Fels, Markus	University of Cologne	DE	0049-221-470-4035	fels@geo.uni-koeln.de
Fiorenza, Carlo	INAF	IT	00390649934373	carlo.fiorenza@ifsi.rm.cnr.it

Foing, Bernard	ESA	NL	+31-71565-4697	bfoing@rssd.esa.int
Forget, Francois	LMD, CNRS	FR	(+1) 650 604 25 29	forget@lmd.jussieu.fr
Formisano, Vittorio	IFSI-CNR/INAF	IT	00 39 06 4993 4362	formisan@nike.ifsi.rm.cnr.it
Forni, Olivier	IAS-CNRS	FR	+33 1 69858639	Olivier.Forni@ias.u-psud.fr
Fouchet, Thierry	Observatoire de Paris	FR	33 1 45 07 71 11	Thierry.Fouchet@obspm.fr
Fraenz, Markus	MPS	DE	0049 5556 979 441	fraenz@mps.mpg.de
Frahm, R.	Southwest Research Institute	US	+1 210 5223855	rfrahm@swri.edu
Fueten, Frank	Brock University	CA	1-905-688-5550xt 3856	FFueten@Brocku.ca
Galli, Andre	University of Bern	SZ	0041+ 31 631 85 34	galli@phim.unibe.ch
Gasnault, Olivier	CESR	FR	33 / 5 61 55 75 53	olivier.gasnault@cesr.fr
Gellert, Ralf	Max-Planck Institut für Chemie	DE	+49 6131 305342	gellert@mpch-mainz.mpg.de
Gendrin, Aline	IAS/Brown University	FR	00 1 401-863-9663	aline.gendrin@ias.fr
Gibson, Everett K.	NASA Johnson Space Center	US	281-483-6224	everett.k.gibson@nasa.gov
Giuranna, Marco	INAF	IT	+39-06-4993-4042	marco.giuranna@ifsi.rm.cnr.it
Glamoclija, Mihaela	Internacional School of Planetary Sciences	IT	+39-085-453-7506	mihaelag@irsps.unich.it
gondet, brigitte	IAS	FR	00 33 1 6985 8635	gondet@ias.u-psud.fr
González-Galindo, Francisco	CSIC	ES	+34 958121311	ggalindo@iaa.es
Grassi, Davide	Istituto Nazionale di Astrofisica	IT	+39-0649934034	grassi@ifsi.rm.cnr.it
Greeley, Ronald	Arizona State University	US	480-965-7029	greeley@asu.edu
Gunnlaugsson, Haraldur Páll	Aarhus University	DK	+45 89423723	hpg@ifa.au.dk
Gwinner, Klaus	German Aerospace Center (DLR)	DE		klaus.gwinner@dlr.de
Hanyk, Ladislav	Charles University	CZ	+420-2-21912544	ladislav.hanyk@mff.cuni.cz
Head, James	Brown University	US	401-863-2526	james_head_iii@brown.edu
Heather, Dave	ESA	NL	071 565 3388	dheather@rssd.esa.int
Helbert, Joern	DLR	DE	+493067055319	joern.helbert@dlr.de
Hoekzema, Nick	MPS	DE	+49 5556 979 438	hoekzema@linmpi.mpg.de
Hoffmann, Harald	German Aerospace Center (DLR)	DE	+49-30-67055327	harald.hoffmann@dlr.de
Ignatiev, Nikolay	Space Research Institute	RU	(+7 095) 333 34 66	Nikolay.Ignatiev@irn.iki.rssi.ru
Inada, Ai	Max-Planck-Institut fuer Sonnensystemforschung	DE	49-5556-979124	inada@linmpi.mpg.de
Ivanov, Anton	Jet Propulsion Laboratory	US	1-818-3549478	anton.ivanov@jpl.nasa.gov
Kaydash, Vadym	Kharkov National University	UA	+38-057-707-50-63	kvg@vk.kh.ua
Kazeminejad, Shahin	University Graz	AT	+43 (0) 650 / 66 38 368	Shahin.Kazeminejad@gmx.at
Kleinhans, Maarten	Utrecht University	NL	+31 30 2532405	m.kleinhans@geog.uu.nl
Klingelhöfer, Göstar	Johannes Gutenberg-University	DE	+49 6131 3923282	klingel@mail.uni-mainz.de
Kolb, Christoph	Space Research Institute	AT	00433164120642	christoph.kolb@oeaw.ac.at
Komatsu, Goro	IRSPS	IT	+39-085-453-7507	goro@irsps.unich.it
Korablev, Oleg	Space Research Institute (IKI)	RU	+7 095 3335434	oleg.korablev@irn.iki.rssi.ru
Kostrikov, Alexander	Vernadsky Institute	RU	(095) 137 14 84	akostrikov@obninsk.ru
Kozyrev, Alexander	Space Research Institute	RU	+7(095)333-41-23	kozyrev@rssi.ru
Kreslavsky, Mikhail	Brown University	US	+1 401 863 1437	misha@mare.geo.brown.edu
Laan, Erik	Universiteit van Amsterdam (UVA)	NL	+31-6-47974621	elaan@science.uva.nl

Lainey, Valéry	ROB	BE	+32 2 373 6772	Lainey@oma.be
Lammer, Helmut	Austrian Academy of Sciences	AT	0043 316 4120 641	helmut.lammer@oeaw.ac.at
Langevin, Yves	CNRS	FR	33-1-69-85-86-81	yves.langevin@ias.u-psud.fr
Leblanc, Francois	Service d'Aeronomie du CNRS/IPSL	FR	33 1 64 47 43 03	francois.leblanc@aerov.jussieu.fr
Lebonnois, Sebastien	Laboratoire de Meteorologie Dynamique / IPSL	FR	+33 1 44 27 23 14	sllmd@lmd.jussieu.fr
Lellouch, Emmanuel	Observatoire de Paris	FR	+33 1 45077110	emmanuel.lellouch@obspm.fr
Levrard, Benjamin	Laboratoire de Sciences de la Terre	FR	04-72-72-89-14	blevrard@ens-lyon.fr
liemohn, Michael	University of Michigan	US	734-763-6229	liemohn@umich.edu
Litvak, Maxim	Space Research Institute	RU	70953334123	max@cgrsmx.iki.rssi.ru
Lopez-Valverde, Miguel A.	Instituto de Astrofísica de Andalucía - CSIC	ES	+34 958 121 311	valverde@iaa.es
Lundin, Rickard	IRF	SE	+46 980 79063	rickard@irf.se
Maezawa, Kiyoshi	Japan Aerospace Exploration Agency	JP	+81-42-759-8172	maezawa@stp.isas.jaxa.jp
Mangold, Nicolas	CNRS	FR	33145360325	mangold@geol.u-psud.fr
Marinangeli, Lucia	IRSPS	IT	+39 085 453 7601	luciam@irsps.unich.it
Markiewicz, Wojciech	Max-Planck-Institute for Solar System Research	DE	[49]5556979294	markiewicz@linmpi.mpg.de
MARTIN, Patrick	European Space Agency - ESTEC	NL	+31 71 565 4927	patrick.martin@rssd.esa.int
Marzo, Giuseppe A.	University of Lecce	IT	+39 0832 297 479	giuseppe.marzo@le.infn.it
Masson, Philippe	University Paris-Sud	FR	33-1-6915-6149	masson@geol.u-psud.fr
Maturilli, Alessandro	DLR - IFSI	DE	+493067055313	alessandro.maturilli@dlr.de
McCord, Thomas	University of Hawaii	US	509 996 3933	mccordtb@aol.com
MELCHIORRI, Riccardo	Observatoire de Paris Meudon	FR	0033 1 45 07 76 73	riccardo.melchiorri@obspm.fr
Mitrofanov, Igor	Institute for Space Research	RU	7 095 333 34 89	imitrofa@space.ru
Montmessin, Franck	CNES/SA	US	+1 650 969 2628	fmontmessin@mail.arc.nasa.gov
Morgan, Geraint	The Open University	GB	01908 655180	g.h.morgan@open.ac.uk
Moroz, Lyuba	German Aerospace Center (DLR)	DE	+40(30)67055353	Ljuba.Moroz@dlr.de
Muller, Jan-Peter	University College	GB		jpmuller@ge.ucl.ac.uk
Mura, Alessandro	IFSI	IT	+39 06 49934386	mura@ifsi.rm.cnr.it
Murray, John B.	Open University	GB		J.B.Murray@open.ac.uk
Mustard, John	Brown University	US	401/863-2417	John_Mustard@brown.edu
Neukum, Gerhard	Freie Universitaet Berlin	DE	+49 30 83870579	gneukum@zedat.fu-berlin.de
Nornberg, Per	University of Aarhus	DK	+45 8942 3804	geopn@phys.au.dk
Nussbaumer, Juergen	The Natural History Museum	GB	+44 (0) 20 7942 5628	juergen_nussbaumer_2000@yahoo.de
Ori, G.G.	International Research School of Planetary Science	IT	+39 08 54537601	ggori@irsps.unich.it
Pacifici, Andrea	IRSPS	IT	+39-(0)85-453-7506	pacifici@irsps.unich.it
Palomba, Ernesto	INAF	IT	+39 0815575542	palomba@na.astro.it
Pätzold, Martin	Institut für Geophysik und Meteorologie	DE	+49-221-4703385	paetzold@geo.uni-koeln.de
Perrier, Séverine	Service d'Aéronomie du CNRS/IPSL	FR	33 (0)1 64 47 42 94	severine.perrier@aerov.jussieu.fr
Pina, Pedro	Instituto Superior Técnico	PT	+351-218417247	ppina@alfa.ist.utl.pt
Pinet, Patrick	OBSERVATOIRE MIDI-PYRENEES	FR	(33) 561 33 29 65	Patrick.Pinet@cnes.fr
Pischel, René	DLR	DE	+49 30 67055 338	rene.pischel@dlr.de
Plaut, Jeffrey	Jet Propulsion Laboratory	US	1-818-393-3799	plaut@jpl.nasa.gov
Politi, Romolo	Università degli Studi di Lecce	IT	+390832297479	romolo.politi@le.infn.it

Popa, I. Ciprian	IRSPS	IT	00398529735	ccipp@irsps.unich.it
Portyankina, Ganna	Max-Planck Institut für Sonnensystemforschung	DE	[49]05556 979 529	portyankina@linmpi.mpg.de
Poulet, Francois		FR	33169858582	francois.poulet@ias.fr
quantin, cathy	LST, UCBL, ENS-lyon	FR	(33) 04 72 44 62 40	cathy.quantin@univ-lyon1.fr
Quémerais, Eric	Service d'Aéronomie/CNRS	FR	01 64 47 43 17	quemerai@aerov.jussieu.fr
Raitala, Jouko	University of Oulu	FI	+358-8-553 1945	jouko.raitala@oulu.fi
Rannou, Pascal	Service d'Aeronomie	FR	(+33) 1 64 47 42 16	pra@aero.jussieu.fr
Richter, Lutz	DLR	DE	+49 2203 601 4568	lutz.richter@dlr.de
rinaldi, giovanna	IFSI	IT	06 4993 4042	giovanna.rinaldi@ifsi.rm.cnr.it
Roatsch, Thomas	German Aerospace Center (DLR)	DE	49-30-67055339	thomas.roatsch@dlr.de
Rodin, Alexander	Space Research Institute	RU	(7 095) 333-4067	rodin@irn.iki.rssi.ru
Rodionova, Janna	Sternberg State Astronomical Institute	RU	(095) 939 16 49	jeanna@sai.msu.ru
Roos-Serote, Maarten	Lisbon Astronomical Observatory	PT	+351 21 36 16 746	roos@oal.ul.pt
Rosenblatt, Pascal	Royal Observatory of Belgium	BE	00 32 2 373 67 30	rosenb@oma.be
Sanin, Anton	Space Research Institute	RU	70953334123	sanin@mx.iki.rssi.ru
SCHMIDT, Frédéric	Laboratoire de Planétologie de Grenoble	FR	0033 476 635 424	fschmidt@obs.ujf-grenoble.fr
Schmidt, Ralph	Uni Hannover	DE	++49-511/762-2484	schmidt@ipi.uni-hannover.de
Schmitt, Bernard	CNRS - UJF	FR	33 (0)476 51 41 50	Bernard.Schmitt@obs.ujf-grenoble.fr
Scholten, Frank	German Aerospace Center (DLR)	DE	+49-30-67055326	frank.scholten@dlr.de
Schreiner, Bjoern	Freie Universitaet Berlin	DE		schreine@zedat.fu-berlin.de
Schumacher, Sandra	WestfÃ¤lische Wilhelms-UniversitÃ¤t MÃ¼nster	DE	+49-251-8333557	sandra.schumacher@uni-muenster.de
Sims, Mark	University of Leicester	GB	+44 116 252 3513	mrs@star.le.ac.uk
Soobiah, Yasir	University College London	GB	01483 204146	yijs@mssl.ucl.ac.uk
Sprague, Ann	University of Arizona	US	520-621-2282	sprague@lpl.arizona.edu
Stanzel, Christina	University of Cologne	DE	+49-221-470-6131	stanzel@geo.uni-koeln.de
Szathmáry, Eörs	Collegium Budapest	HU	+36 1 224 8300	szathmary@colbud.hu
Tellmann, Silvia	Universität zu Köln	DE	+49-221-4704489	tellmann@geo.uni-koeln.de
Titov, Dmitry	MPS / IKI	DE	+49-5556-979-212	titov@mps.mpg.de
van den Berg, Arie	Utrecht University	NL	(+31) 30 - 253 5072	berg@geo.uu.nl
van Gasselt, Stephan	Freie Universitaet Berlin	DE		vgasselt@zedat.fu-berlin.de
van Thienen, Peter	Institut de Physique du Globe de Paris	FR	++33 1 45 11 41 23	thienen@ipgp.jussieu.fr
Vinatier, Sandrine	University Paris 6	FR	01.45.07.77.79	sandrine.vinatier@lmd.jussieu.fr
Wagner, Roland	German Aerospace Center (DLR)	DE	+49-30-67055-347	Roland.Wagner@dlr.de
Werner, Stephanie C.	Freie Universitaet Berlin	DE		swerner@zedat.fu-berlin.de
Williams, David	Arizona State University	US	480-965-7029	David.Williams@asu.edu
Witzke, Andreas	German Aerospace Center	DE	0049 (0)30 67055392	andreas.witzke@dlr.de
Zasova, Ludmila	IKI RAN	RU	+7-095-333-34-66	zasova@irn.iki.rssi.ru
Zegers, Tanja	ESA	NL	31-71-5656585	tzegers@rssd.esa.int
Zuschneid, Wilhelm	Freie Universitaet Berlin	DE		ewill@zedat.fu-berlin.de